

DIGITAL ACCESS TO SCHOLARSHIP AT HARVARD
DASH.HARVARD.EDU

HARVARD LIBRARY


The Contribution of Hippocampal Oxytocin Receptors to Social Memory Processing

Link
http://nrs.harvard.edu/urn-3:HUL.InstRepos:40050115

Terms of use
This article was downloaded from Harvard University's DASH repository, and is made available under the terms and conditions applicable to Other Posted Material (LAA), as set forth at
https://harvardwiki.atlassian.net/wiki/external/NGY5NDE4ZjgzNTc5NDQzMGIzZWZhMGFlOWI2M2EwYTg

Accessibility
https://accessibility.huit.harvard.edu/digital-accessibility-policy

Share Your Story
The Harvard community has made this article openly available.
Please share how this access benefits you. Submit a story

The contribution of hippocampal oxytocin receptors to social memory processing

A dissertation presented

by

Tara Raam

to

The Division of Medical Sciences

in partial fulfillment of the requirements

for the degree of

Doctor of Philosophy

in the subject of

Neurobiology

Harvard University

Cambridge, Massachusetts

April 2018

© 2018 Tara Raam

All rights reserved.

Dissertation Advisor: Professor Amar Sahay Tara Raam

The contribution of hippocampal oxytocin receptors to social memory processing

Abstract

Recent studies have highlighted growing evidence that the hippocampus assumes an underappreciated role in promoting social memories. However, the mechanisms by which discrimination of social and non-social stimuli are differentiated in the hippocampus are not known. The social hormone oxytocin has long been understood to promote discrimination of social stimuli. Remarkably, the physiological functions of oxytocin receptors (Oxtrs) in the mouse hippocampus are not known. Here, we demonstrate using genetic approaches that Oxtrs in the anterior dentate gyrus (aDG) of mice are necessary for discrimination of social, but not non-social, stimuli. In contrast, Oxtrs in pDG promote sociability without influencing social memory. We further demonstrate using genetic, pharmacological, and ensemble mapping strategies that Oxtrs in aCA2/CA3 recruit a population-based coding mechanism to mediate social stimuli discrimination. Optogenetic dissection of aCA2/CA3 outputs revealed a double dissociation by which social information in aCA2/CA3 is mediated to posterior CA1, while non-social information is mediated to aCA1. Collectively, these studies identify a role for an aDG-CA2/CA3 axis of *Oxtr* expressing cells in discrimination of social stimuli and delineate a pathway relaying social memory computations in the anterior hippocampus to the posterior hippocampus to guide social recognition.

Table of Contents

Abstract iii

Acknowledgements vi

1 Introduction. 1
1.1 The Social Hippocampus. 3
1.1.1 Hippocampal involvement in social memory. 3
1.1.2 Hippocampal dysfunction in disorders of social cognition. 5
1.1.3 Longitudinal axis segregation of hippocampal function. 6
1.1.4 Pattern separation as a potential substrate of behavioral discrimination. 8
1.2 Oxytocin: A Social Hormone. 10
1.2.1 The role of oxytocin in diverse social behaviors. 10
1.2.2 Implication of oxytocin in disorders of social cognition. 14
1.2.3 Oxytocin gates signal-to-noise processing. 15
1.3 Overarching Questions. 19

2 Functional dissociation of oxytocin receptors along the dentate gyrus longitudinal axis. . 21
2.1 Introduction. 23
2.1.1 The dentate gyrus as a pattern separator. 24
2.1.2 Local microcircuitry of the DG. 25
2.1.3 Segregation of function along the DG longitudinal axis. 29
2.1.4 Modulation of DG activity via oxytocin. 32
2.1.5 Involvement of DG in social behaviors. 34
2.2 Results. 38
2.3 Discussion. 58
2.4 Methods. 61
2.5 Author Contributions. 68
2.6 Acknowledgements. 68

3 Oxytocin receptors in CA2/CA3 promote discrimination of social stimuli. 69
3.1 Introduction. 71
3.1.1 Remapping mechanisms in CA subregions. 72
3.1.2 Behavioral significance of CA2/CA3. 73
3.1.3 Modulation of CA2/CA3 via oxytocin. 78
3.2 Results. 80
3.3 Discussion. 96
3.4 Methods. 100
3.5 Author Contributions. 108
3.6 Acknowledgments. 108

4 Optogenetic dissection of CA2/CA3 outputs mediating social memory. 109
4.1 Introduction. 111
4.1.1 aCA2/CA3 projections to aCA1. 112

4.1.2 aCA2/CA3 projections to the lateral septum. 114
4.1.3 aCA2/CA3 projections to pCA1. 117
4.2 Results. 119
4.3 Discussion. 132
4.4 Methods. 135
4.5 Author Contributions. 141
4.6 Acknowledgments. 141

5 The role of adult hippocampal neurogenesis in social behaviors 143
5.1 Introduction. 144
5.1.1 The DG is a locus for adult neurogenesis in the mammalian brain. 145
5.1.2 Adult-born neurons dictate population-based coding in the DG. 147
5.1.3 Modulation of Adult hippocampal neurogenesis by oxytocin. 149
5.1.4 The contribution of adult-born neurons to social behaviors. 150
5.2 Results. 153
5.3 Discussion. 155
5.4 Methods. 156

6 Conclusions and future directions 161
6.1 Conclusions. 162
6.2 Future Directions. 165
6.2.1 Mapping the inputs of Oxtr+ neurons in the hippocampus. 165
6.2.2 In vivo imaging of Oxtr+ neurons in the hippocampus. 165
6.2.3 Relating hippocampal oxytocin receptors to aggression and dominance. 166

References. 168

Appendix 1 (Raam *et al.*, 2017). 193

Acknowledgments

It would be terribly ironic to write a dissertation on the neurobiology of social interactions without acknowledging the contributions of the many individuals who, through their mentorship or friendship, have helped me advance over the past few years. The process of completing this degree was oscillatory in nature, and there are many people to thank for the momentum that propelled me from trough to peak.

First, I wish to thank my dissertation advisor, Dr. Amar Sahay, whose unwavering support, uncompromised standard of excellence, and ability to always see a few steps ahead propelled my forward movement at every milestone. Thank you for thinking with me and not for me, for teaching me to trust the scientific process, and for always answering my questions with a harder question. I feel I have transformed as a scientist over the last six years, and I have no doubt that my choice of advisor was the single most relevant factor in that. I would also like to thank my undergraduate advisor, Dr. Anirvan Ghosh, who took a chance on an inexperienced undergraduate who knew basically nothing, because he is a physicist by training and knew that acceleration says more about the trajectory of a moving object than does position or velocity.

Drs. Bradford Lowell, Mark Andermann, and Chris Cowan formed a fantastic dissertation committee who were generous with both time and reagents and asked incisive questions that enhanced the quality of my work. I am very grateful for their guidance and assistance, and regret being unable to benefit from their direct feedback in my future projects.

All the members of the Sahay lab, past and present, contributed to an environment that was rigorous, collaborative, and energetic. Postdoctoral fellows Nannan Guo, Kathleen McAvoy, Antoine Besnard, Hannah Twarkowski, and Cinzia Vicidomini have given me exceptional guidance at all stages, from things as simple as how to properly align the ear bars during a

stereotactic surgery, to decisions as significant as where to pursue my postdoctoral work. I cannot thank them enough for the additional layer of mentorship I have received from them, and I hope I can pay it forward to future mentees as a postdoc. Lab managers Tomer Langberg, Izzy Chu, and Michael Kim ensured that my work proceeded unhindered, and patiently responded to my many frantic last-minute requests to order a reagent with grace and efficacy. Finally, Hugo Vega-Ramirez, my classmate (littermate, rather) has been an unbounded source of friendship and understanding over the past few years, and was consistently the person who would bemoan my frustrations or celebrate my joy with me. Graduate school would have been a fundamentally different experience without you. The only unfortunate aspect of defending is realizing I will not get to see you all on a daily basis.

I would also like to acknowledge the efforts of the Institute for Studies in Global Prosperity for its unmatched efforts to create seminars for undergraduate and graduate students to examine the role of knowledge in the advancement of society. It was in these seminars that I was first exposed to any rigorous study of the philosophy of science at a very conceptual level, and its effects on my work and future goals are clear and tangible. I am deeply grateful to the coordinators and facilitators of this program, many of whom have become true friends and mentors in my life.

The last of the acknowledgements are often reserved for those closest to the author. I wish not to deviate from this tradition. To my older brother, the sail on my boat, who generously entertains all my aspirations, no matter how outlandish they are. To my father who instilled in me a curiosity and deep sense of wonder for the world. To my mother who taught me a machine-like diligence and never allowed me to believe that I should compromise anything in life. A thousand times, thank you. The three of you co-wrote all the chapters that led to this dissertation. This degree is as much yours as it is mine.

"Our ecological success, technology, and adaptation
to diverse environments is not due to our intelligence.
Alone and stripped of our culture, we are hopeless as a species…
The smartest among us could not in a single lifetime devise
even a small fraction of the techniques and technologies
that allow any foraging society to survive… It's the ability
to freely exchange information that sparks and accelerates
adaptive cultural evolution, and creates innovation.
At the population level,
it is much better to be social than it is to be smart."

Joseph Henrich

CHAPTER 1

Introduction

Social recognition is a complex biological process that necessitates, in part, communication between neural circuits subserving discrimination of socially relevant stimuli and those mediating expression of affiliation or avoidance. One general mechanism by which a variety of social behaviors are orchestrated is through the actions of the neuropeptide oxytocin. In the last several decades, a rich literature has elaborated on the role of oxytocin receptors (Oxtr) in limbic regions such as the nucleus accumbens, piriform cortex, lateral septum, and prefrontal cortex in social interactions. Additionally, recent studies have begun to shed light on a previously underappreciated role for the hippocampus in discrimination of social stimuli. Remarkably, the literature describing the contributions of oxytocin, on one hand, and the hippocampus on the other, to social recognition have largely developed in parallel, and no studies to date have probed the relevance of hippocampal Oxtrs to social memory. The aim of this dissertation is to bridge the gap between these two literatures which, until now, have existed as divergent subfields of neuroscience.

In this chapter, I will review the overarching literature that supports a role for both the hippocampus and oxytocin in regulating social memory and will expose the gaps in literature surrounding how oxytocin interacts with the hippocampus. In chapter two, I will explore the functions of the dentate gyrus, the primary input region of the hippocampus, and will examine a functional dissociation between oxytocin receptors along its longitudinal axis. Chapter three will present evidence supporting a role for oxytocin receptors in the CA2/CA3 subregion in social memories, and chapter four will delineate the segregation of social and non-social information to distinct downstream outputs of this area. Chapter five will examine the contribution of adult hippocampal neurogenesis to social behaviors. Finally, in chapter six I will discuss the implications of our studies and propose future experiments to address the questions that arise from our work.

1.1 The social hippocampus

1.1.1 Hippocampal involvement in social memory

The earliest human studies to elucidate the role of the hippocampus arose somewhat serendipitously through an accidental human experiment on a patient named Henry Molaison (H.M.). Born in 1926, H.M. suffered from severe, debilitating epilepsy, the focal point of which was in his medial temporal lobe (MTL), where the hippocampus resides. In the absence of suitable treatments at the time, his physicians recommended at the age of 27 that he undergo a bilateral resection of his medial temporal lobe, including the hippocampus and adjacent cortices. At a time when the basic functions of the hippocampus were not understood, this may have seemed like a promising treatment, but H.M. emerged from this surgery with irreversible impairments in memory function. From then forward, he became the subject of intense behavioral study that lasted throughout the course of his life, as physicians and scientists tried to understand what exactly the hippocampus does.

Notably, studies of H.M.'s symptoms led to an understanding of the hippocampus as critical for episodic memories (memories of what, when and where), and allowed scientists to dissociate between, for example, H.M.'s motor memory to learn complex tasks that required finely tuned motor skills, and his recollection of having ever performed the task before. From then forward, the field of neuroscience experienced an explosion of studies in species ranging from rodents to humans that attempted to continue chipping at the black box that was the hippocampus. The vast majority of this work has been focused on understanding how the hippocampus processes spatial and contextual cues, as a rodent model for understanding the storage and retrieval of unique "episodes." However, one of the most understated symptoms of H.M.'s pathology was a profound deficit in social recognition memory, to the extent that Dr. Brenda Milner, the scientist who spent

most of her time working with him, noted in his obituary: “He was a very gracious man, very patient, always willing to try these tasks I would give him. And yet every time I walked in the room, it’s like we’d never met…” (Carey, New York Times, 2008).

Over the past 10 years since that statement, hippocampal theory has expanded to include its functions in social behaviors (Montagrin et al. 2017). Human brain imaging studies have indicated changes in hippocampal activation in diverse social tasks such as face recognition (Paller et al. 2003; Rametti et al. 2009; Trinkler et al. 2009), empathy (Beadle et al. 2013), and navigation of complex social spaces composed of dynamically changing social relationships (Tavares et al. 2015). Additionally, amnesic patients with sustained MTL damage report fewer relationships with neighbors and community groups, and difficulty sustaining relationships (Davidson et al. 2012).

Rodent studies of hippocampal circuitry have reinforced the emerging evidence from human literature. In depth discussion of this literature will be revisited in chapters 2, 3, and 4. Briefly, recent attention has converged on CA2, a unique and understudied hippocampal subregion, in social behaviors (Dudek et al. 2016). In vivo recordings of CA2 pyramidal cells indicates global remapping of place fields in response to familiar and novel social stimuli, the first evidence to demonstrate responsiveness of CA2 to social information *in vivo* (Alexander et al. 2016). Furthermore, loss of function manipulations of CA2 reinforce this finding. Excitotoxic lesions of CA2 produce loss of both sociability and social memory (Stevenson and Caldwell 2014), and silencing of CA2 neuron output via tetanus toxin light chain impairs habituation to a familiar social stimulus (Hitti and Siegelbaum 2014). Furthermore, targeted stimulation of inputs to CA2 arising from the PVN enhances social memory (Smith et al. 2016). In addition to CA2, recent work in which the NR1 subunit of the NMDA receptor is conditionally deleted from the adjacent CA3

also demonstrates a deficit in social memory, suggesting that the general CA2/CA3 subregion may be important for discrimination of social stimuli (Chiang et al. 2018).

In addition to the CA2 subregion, recent work has identified posterior CA1 (pCA1) as an additional locus for social memories. A landmark study by Okuyama and colleagues demonstrated that pCA1, via its projections to the nucleus accumbens (but not projections to the basolateral amygdala or olfactory bulbs) is necessary for discrimination of social stimuli (Okuyama et al. 2016). Furthermore, pCA1 neurons undergo population-based coding of social stimuli, whereby animals re-exposed to the same stimulus show elevated reactivation of ensembles in pCA1, whereas animals exposed to two different stimuli show very little reactivation of ensembles. Collectively these two studies suggest a role for both CA2/CA3 and pCA1 in social memories, however how these regions may be linked to each other is not understood.

1.1.2 Hippocampal dysfunction in disorders of social cognition

Individuals with autism struggle with a number of tasks directly mediated by the hippocampus, such as episodic memory, facial recognition, and cognitive flexibility. Due to difficulty in directly probing brain function in human patients with autism, our understanding of hippocampal function in autism is generally sparse. However, a few studies offer initial insights into the mechanisms underlying hippocampal dysfunction in autism spectrum disorders (ASD), and how the hippocampus may be harnessed as a therapeutic target to alleviate symptoms.

Initial studies of hippocampal size and shape in patients with ASD indicate significant perturbations in hippocampal morphology in ASD. Structural imaging of the brain in these patients shows significant enlargement of the hippocampus in children and adolescents with ASD, as compared to controls (Schumann et al. 2004; Groen et al. 2010). Additionally, further studies analyzing hippocampal shape in 3-4 year olds with ASD found that the degree to which the

hippocampus was characterized by abnormalities in shape strongly predicted performance in hippocampus-dependent tasks (Dager et al. 2007). Analysis of post-mortem tissue of individuals with autism indicates increased density of cells in hippocampal subregions (Bauman and Kemper 1985; Bauman et al. 1995). Functional imaging studies indicate that the hippocampus of individuals with ASD is characterized by hyper-reactivity in response to aversive sensory stimuli (Green et al. 2013). While the hippocampus has been loosely implicated in ASD, whether or not hippocampal dysfunction underlies pathologies of social behaviors in ASD remains under-explored, in large part because the hippocampus has been overlooked in this field, in pursuit of more typically studied limbic and social regions, such as the amygdala and temporoparietal junction.

1.1.3 Longitudinal axis segregation of hippocampal function

The hippocampus is a substantially large structure that extends along the septo-temporal axis. It is composed of anterior and posterior poles and is suggested to be anatomically and functionally differentiated along its longitudinal axis (Fanselow and Dong 2010; Strange et al. 2014). It should be noted here that typically the two poles of the hippocampus are referred to as "dorsal" and "ventral." However, for the purpose of this thesis, I will refer to these two poles as "anterior" and "posterior" respectively (reasons for this are described in greater detail in Chapter 4). "Anterior" and "posterior" in this context are not to be confused with "anterior" and "posterior" in the primate brain which, in contrast to the rodent brain, correspond to "ventral" and "dorsal" respectively. The dissociation in function along the longitudinal axis implicates the posterior hippocampus in emotional processing and regulation of anxiety states, while the anterior hippocampus is implicated in predominantly cognitive functions, such as memory and spatial navigation. For example, pharmacological lesions to the posterior, but not anterior hippocampus,

have an anxiolytic effect, exhibited by increased time spent in the open arms of an elevated plus maze (Kjelstrup et al. 2002). In contrast, lesions to the anterior, but not posterior hippocampus result in impaired ability to locate a hidden platform in the Morris water maze spatial learning task (Moser et al. 1995). While these initial studies were carried out using lesions, a more recent study by Kheirbek *et al.* demonstrated that optogenetic inhibition of the anterior, but not posterior, dentate gyrus (DG) impairs encoding of contextual fear (Kheirbek et al. 2013). Conversely, stimulation of anterior DG increases exploratory behavior, while stimulation of posterior DG induces a strong anxiolytic effect (Kheirbek et al. 2013). In addition to posterior DG, posterior CA1 is also thought to be closely linked to anxiety states in mice. Optogenetic inhibition of basolateral amygdala (BLA) inputs to pCA1 decreases anxiety in the open field and elevated plus maze, while activation of these terminals increases anxiety (Felix-Ortiz et al. 2013). In vivo calcium imaging of aCA1 and pCA1 cell bodies demonstrates that nearly 50% of pCA1 pyramidal neurons are allocated to encoding the open-arm of the elevated plus maze, whereas a preferential recruitment is not observed in aCA1 (Jimenez et al. 2018). Furthermore, pCA1 anxiety representations are relayed to the lateral hypothalamus, while those representing contextual fear are relayed to the BLA (Jimenez et al. 2018).

The functional dissociation along hippocampal longitudinal axis is thought to be supported in part by unique projection patterns in and out of the anterior and posterior poles (Fanselow and Dong 2010; Strange et al. 2014). The hippocampus sends and receives diffuse projections to various parts of the brain. However, these connections are segregated along the longitudinal axis, rendering distinct topographical patterns. The anterior hippocampus receives highly processed sensory information from multiple cortical areas, via the postrhinal, perirhinal, and entorhinal cortices. Projections out of dorsal CA1 and subiculum (the primary outputs of the hippocampus)

project to the retrosplenial and anterior cingulate cortices, which process visuospatial information (Cenquizca and Swanson 2007). The posterior hippocampus, however, connects extensively with limbic areas. Posterior CA1 and subiculum share a large network of bidirectional connections with the amygdala, nucleus accumbens, lateral hypothalamus, lateral septum, as well as olfactory and prefrontal cortices (Felix-Ortiz et al. 2013; Ciocchi et al. 2015; Padilla-Coreano et al. 2016; Aqrabawi and Kim 2018; Jimenez et al. 2018). Interestingly, both the anterior and posterior poles of hippocampus, through the activity of aCA2 and pCA1 respectively, have been implicated in social recognition (Hitti and Siegelbaum 2014; Okuyama et al. 2016). However, whether these subregions function synergistically to promote social memories or function independently of each other is not understood.

1.1.4 Pattern separation as a potential substrate for behavioral discrimination

A computational characteristic of the hippocampus is its ability to robustly segregate overlapping inputs into distinct outputs, a process referred to as pattern separation (O'Reilly and McClelland 1994; Yassa and Stark 2011; Knierim and Neunuebel 2016). Pattern separation is critical to the fidelity of any mnemonic process—without it, interference between similar representations arises, which can lead to generalization or forgetting, and can therefore promote inappropriate behavioral responses to contextual cues (Besnard and Sahay 2016). Critically, the hippocampus is specifically engaged in resolving interference between stimuli that are similar or ambiguous, but not between stimuli that are sufficiently dissimilar, suggesting a role for mediating fine, but not gross, discrimination (Besnard and Sahay 2016). For example, targeted manipulations of the DG impair spatial learning in radial arm maze task in trials when the degree of separation between arms is small (e.g. animals must discriminate between two arms that are very close to each other), but not when the spatial separation is sufficiently large (Clelland et al. 2009; Morris

et al. 2012). Furthermore, studies of contextual fear indicate that the DG is only engaged when the animal must discriminate between a fearful context A and a similar context B, which contains some environmental cues in common with context A (McHugh et al. 2007). When behavioral tasks demand the animal to discriminate between context A and a very different context C, the DG is dispensable (McAvoy et al. 2016).

Within the hippocampus, anatomical and physiological properties of distinct subregions renders them more or less suitable to mediating pattern separation. These properties will be discussed at length in Chapter 2 (regarding the DG) and Chapter 3 (regarding CA2 and CA3). Briefly, the DG, which is the primary input structure of the hippocampus, is characterized by sparse coding schemes that minimize overlap in ensembles encoding similar stimuli (Barnes et al. 1990; Jung et al. 1994; Aimone et al. 2011). In addition, DG neurons outweigh those projecting from the entorhinal cortex (EC) by a ratio of 10:1, and these projections from the EC are thought to be random, which facilitates effective orthogonalization of entorhinal inputs (West et al. 1991; O'Reilly and McClelland 1994). Additionally, the conjunctive nature of these projections allows diverse sensory stimuli to be associated in a single representation (O'Reilly and McClelland 1994). The CA3 and CA2 subregions follow a gradient-like pattern by which the regions of CA3 most proximal to the DG robustly pattern separate, whereas CA2 and the regions of CA3 most distal to the DG, more readily perform pattern completion computations (Lee et al. 2015). *In vivo* recordings of proximal and distal CA3 during exploration of a spatial arena demonstrates that during modest rotations of the arena, CA3 distal maintains coherent representations of the spatial context, whereas CA3 proximal shows degraded representations (Lee, Wang et al. 2015). Although these properties have been well characterized within the framework of encoding spatial and contextual cues, only two studies to date have examined the physiological characteristics of

hippocampal neurons during exposure to social stimuli. Alexander et al. used *in vivo* recordings to demonstrate that aCA2 pyramidal neurons undergo remapping of place fields in response to exposure to social stimuli, whereas aCA1 pyramidal neurons do not (Alexander et al. 2016). Additionally, Okuyama et al. used *in vivo* calcium imaging of aCA1 and pCA1 pyramidal neurons to show that pCA1 responds more robustly to social stimuli than aCA1, and the ensemble encoding a single social stimulus expands several days after initial exposure (Okuyama et al. 2016). These studies suggest compelling initial evidence that the hippocampus engages population-based coding mechanisms in response to social stimuli. However, the contribution of additional hippocampal subfields to population-based coding of social stimuli is not well understood and is in need of further investigation.

1.2 Oxytocin: A social hormone

1.2.1 The role of oxytocin in diverse social behaviors

Oxytocin (OT) is a nonapeptide hormone produced in the paraventricular nucleus of the hypothalamus (PVN), stored in the posterior pituitary, and best known for the critical role it plays in social interactions (Bargmann and Scharrer 1951; Lee et al. 2009; Dölen 2015; Marlin and Froemke 2017), although it also plays a role in basic physiological functions such as regulation of water in-take and body temperature (Pirnik et al. 2004; da Silveira et al. 2007; Kasahara et al. 2007). It can exert its influence either through direct projections throughout the brain, or through release into the bloodstream and cerebrospinal fluid (Lee et al. 2009; Dölen 2015; Marlin and Froemke 2017). Oxytocin has only one known receptor (Oxtr), a Gq-protein coupled receptor, although it does retain some affinity for the vasopressin-1b receptor as well (Hoyle 1999; Busnelli et al. 2013). When bound to its receptor, oxytocin induces a depolarizing, excitatory effect on hippocampal neurons (Pagani et al. 2015). The Oxtr gene and its protein is widely expressed

throughout the mouse brain, including the hippocampus, however many techniques used to characterize the expression pattern of Oxtrs have relied on techniques of varying resolution (radioligand binding, antibodies, and reporter mouse lines) and an understanding of the precise cell-types and regions in which Oxtr is expressed is still lacking.

Measures of neural activity utilizing c-Fos immunoreactivity and *in vivo* photometry imaging of calcium signals in the PVN demonstrates that oxytocin neurons are specifically active during exploration of social stimuli, but not inanimate objects (Cservenak et al. 2017; Hung et al. 2017). Similarly, optogenetic stimulation of these neurons is sufficient to enhance social behaviors such as maternal pup retrieval (Marlin et al. 2015), social exploration (Oettl et al. 2016; Hung et al. 2017), odor-driven social learning (Choe et al. 2015) and social recognition (Oettl et al. 2016), while chemogenetic activation of these neurons via DREADDS enhances socially learned fear (Pisansky et al. 2017). Here, I will review the involvement of oxytocin and its receptor in circuits mediating a variety of social behaviors.

Oxytocin is perhaps best known for its role in social bonding, such as mating and parenting behaviors. Pioneering studies identified that central administration of oxytocin antagonist dramatically impairs pair bonding in prairie voles (Insel and Hulihan 1995). Whereas normally prairie voles will exhibit prolonged mating relationships with a single partner characterized by repeated bouts of sexual contact, oxytocin antagonist prevents the long-term bond, while leaving copulation itself intact. Pair bonding is thought to be mediated by Oxtrs in the nucleus accumbens, the gene for which is epigenetically primed by histone acetylation upon first sexual exposure to promote enduring bonds (Wang et al. 2013). In mice, Oxtrs in a class of prefrontal cortical interneurons are thought to mediate social approach towards males in females, in an estrous-cycle dependent manner (Nakajima et al. 2014). Furthermore, oxytocin is thought to promote effective

parenting behaviors. Its release promotes the biological processes associated with lactation and parturition (Soloff et al. 1979). In addition, it is critical for both the generation of ultrasonic vocalizations by pups (Winslow et al. 2000), and maternal pup retrieval in response to these vocalization (Marlin et al. 2015).

Oxytocin is also understood to play a role in sociability, the preference that most animals display for social exploration, rather than isolation. While initial studies utilizing whole brain knock out of the oxytocin gene demonstrated no effect on sociability (Crawley et al. 2007), a more recent study utilizing acute optogenetic stimulation of oxytocin neurons in the PVN of adults shows increase in both the number and duration of sniffing events (Oettl et al. 2016). The lack of an effect on sociability in the oxytocin whole brain knockout animals may be due to compensatory effects that arise over the course of development (these animals lack oxytocin throughout the developmental time course). Recent studies have begun to untangle the circuit and synaptic mechanisms underlying sociability. Work by Dölen and colleagues (2013) demonstrated that the nucleus accumbens is a critical site for the expression of social reward (the preference for social, rather than isolate, environments). Pharmacological infusion of Oxtr antagonist in the nucleus accumbens is sufficient to block social reward, however conditional deletion of Oxtrs in NAc cell bodies is insufficient to recapitulate this effect (Dölen et al. 2013). Instead, rabies virus (RbV) Cre that induces deletion of Oxtrs in inputs onto the NAc indicates that presynaptic Oxtrs arising from the dorsal raphe nucleus are responsible for social reward. Critically, it is the coordination of oxytocin and serotonin release in the NAc that induces the long-term depression associated with social reward. Follow up studies indicate a similar intersection in neurotransmitter systems, whereby direct oxytocin release from the PVN onto dopamine-producing neurons in the ventral tegmental area (VTA) is essential for social reward (Hung et al. 2017).

One of the critical functions of oxytocin and its receptors lies in mediation of social recognition memory. Early studies utilizing knockout mouse lines demonstrate social memory impairments in mice lacking genes for either oxytocin, or Oxtr. Mice lacking the oxytocin gene demonstrate a deficit in social memory habituation tests (Ferguson et al. 2000). Whereas control animals will demonstrate loss of interest in exploring a familiar mouse after several exposures, mice lacking the oxytocin gene show persistent interest in exploring familiar social stimuli (Ferguson et al. 2000). Local infusion of oxytocin into the medial amygdala (MeA) is sufficient to restore these deficits (Ferguson et al. 2001). Similarly, mice lacking the *Oxtr* gene also show deficits in social memory, wherein $Oxtr^{-/-}$ mice show no preference for a novel animal over a familiar animal (Takayanagi et al. 2005). While these studies were performed in whole-brain knockout mice that lack the *Oxt* or *Oxtr* gene throughout development, more recent developments have allowed for the generation of *Oxtr* conditional knockout mice (*Oxtr f/f*) which allow both for temporal specificity, as well as spatial restriction to a cell-type or region of interest (Lee et al. 2008). When crossed with a CamKIIα-Cre line that specifically targets excitatory neurons of the forebrain (also referred to as Oxtr FB deletion mice), these animals show pronounced deficits in social memory that recapitulate whole-brain knockout animals (Lee et al. 2008; Macbeth et al. 2009). Critically, however, these animals only show a deficit for discrimination of two animals of the same strain, but perform the same as controls when discriminating between social stimuli of two different strains (Macbeth et al. 2009). This critical yet often overlooked finding indicates that forebrain Oxtrs are necessary for "fine" discrimination of genetically identical social stimuli, and dispensable for "gross" discrimination of social stimuli of different strains, which may be more readily distinguished through visual or olfactory cues (mice of different strains may have different fur pigmentation or more readily distinguishable pheromones). Interestingly, these mice lack Oxtrs

in the hippocampus, but retain them in other areas that are also involved in social memory, such as the olfactory bulbs and medial amygdala (Lee et al. 2008). Given the explicit role of the hippocampus in mediating fine discrimination of spatial and contextual cues, this study suggests that oxytocin may harness a similar mechanism to promote fine discrimination of similar social stimuli.

The generation of these *Oxtr f/f* conditional deletion mice has also allowed for region specific manipulation of Oxtrs in adulthood. Conditional deletion of Oxtrs in the lateral septum impairs discrimination of social stimuli but not sociability (Mesic et al. 2015). Additionally, conditional deletion of Oxtrs in ensembles of the piriform cortex impairs learned associations that link otherwise neutral odors with socially-mediated valence. Optogenetic stimulation of piriform cortex ensembles during pairing of an odor with a social stimulus results in post-training place preference for a chamber that contains the odor versus a neutral chamber, indicative of a learned positive valence association (Choe et al. 2015). Conditional deletion of Oxtrs in the same neurons being stimulated abolishes this effect. Importantly, piriform Oxtrs are not important for non-social odor learning tasks (Choe et al. 2015). The importance of Oxtrs in the olfactory system have also been recapitulated by studies indicating that conditional deletion of Oxtrs in the anterior olfactory nucleus (AON) is sufficient to impair performance in a social discrimination task, but not a non-social odor discrimination task (Oettl et al. 2016). Collectively, these studies suggest an important role for Oxtrs in diverse brain regions in rodent social recognition, however much work remains to be done in determining the contribution of additional circuits.

1.2.2 Implication of oxytocin in disorders of social cognition

Given the critical role that oxytocin places in various aspects of social cognition, its function or dysfunction may confer greater understanding of disease etiology underlying disorders

of social cognition, such as autism spectrum disorders (ASD) (Dölen 2015). Neurobiological mechanisms that promote healthy social interactions may also serve as potential therapeutic targets to address social deficits in these ASD. While longstanding theories have hypothesized that oxytocin pathology may underlie social deficits of ASD, evidence regarding plasma oxytocin levels in ASD has been conflicting, with some human studies indicating that individuals with ASD may have lower plasma oxytocin levels than neurotypical controls (Modahl et al. 1998; Al-Ayadhi 2005; Andari et al. 2010) and other studies indicating no difference (Miller et al. 2013; Parker et al. 2014). How these variations in plasma OXT may correlate with CSF and brain oxytocin is unclear, and whether or not brain oxytocin or Oxtr dysfunction underlies deficits in social function in ASD remains an unresolved question. Lack of clarity regarding oxytocin dysfunction in ASD withstanding, several studies have aimed to determine whether OXT nasal administration can improve social deficits in individuals with ASD. Many such studies have indicated positive effects of OXT administration on social communication (Watanabe et al. 2015; Parker et al. 2017), emotion recognition (Guastella et al. 2010), facial recognition (Anagnostou et al. 2012), and social learning (Andari et al. 2010). However, the precise circuit mechanisms underlying these improvements are not clear. Further research dissecting out oxytocin circuit function in animal models may be necessary to achieve clarity in this area.

1.2.3 Oxytocin gates signal-to-noise processing

Many of the earliest studies elucidating the function of oxytocin have relied on pharmacological and knockout studies during various behavioral states. Recently, however, additional studies utilizing *in vivo* recordings and slice physiology have elucidated the circuit mechanisms by which oxytocin promotes social behaviors. Notably, many of these studies have

converged on the notion that oxytocin promotes enhanced signal-to-noise processing broadly throughout the brain by carefully mediating excitation-inhibition balance.

Two studies have suggested that oxytocin enhances signal-to-noise in sensory circuits that promotes behavioral responses to social cues. A seminal study by Marlin and colleagues (2015) identified that pup calls reliably evoke spiking in the left, but not right, auditory cortex of maternal females. Interestingly, the expression of Oxtrs in auditory cortex is also lateralized to the left auditory cortex, and maternal pup retrieval is blunted by local infusion of oxytocin antagonist into left auditory cortex (Marlin et al. 2015). Physiologically, oxytocin acts to disinhibit layer II/III A1 pyramidal neurons and enhances the temporal correlation of excitation and inhibition, promoting the salience of auditory social cues (Marlin et al. 2015). Similarly, Oettl and colleagues demonstrated that top-down cortical inhibition from the anterior olfactory nucleus (AON) promotes odor cue saliency in the main olfactory bulb (MOB). Activation of Oxtrs in the AON drives robust excitation of AON regular-firing neurons, which increases excitatory drive onto GABAergic granule cells of the MOB (Oettl et al. 2016). Granule neurons form synapses onto mitral cells, and oxytocin release in the AON therefore drives inhibition of mitral cells. Local release of oxytocin agonist in the AON increases the signal-to-noise ratio of MOB mitral cells in response to olfactory cues by increasing the odor-evoked firing rate and decreasing the baseline firing rate. This mechanism is proposed underlie discrimination of social, but not non-social odors (Oettl et al. 2016).

In addition to modulation of sensory circuits, oxytocin also modifies synaptic properties in limbic regions. Oxytocin neurons in the PVN send direct projections to the ventral tegmental area (VTA), the locus for dopamine production in the brain (Hung et al. 2017). Local application of (Thr^4,Gly^7)-Oxytocin (TGOT, oxytocin agonist) in the VTA induces spiking specifically in VTA

DA neurons that project to the nucleus accumbens medial shell, but not in those which do not project to the accumbens (Hung et al. 2017). TGOT application increases evoked EPSCs and decreases IPSCs, an effect thought to be mediated presynaptically by inhibitory neurons (Hung et al. 2017). This mechanism is thought to regulate socially-mediated release of dopamine into the nucleus accumbens in order to mediate the intrinsically rewarding valence of social interactions (Hung et al. 2017). Oxytocin also mediates encoding of diverse social cues in the medial amygdala (MeA). Whereas in control animals MeA neurons will disambiguate cues representing males, females, pups, and predators by minimizing overlap in neuronal populations encoding them, animals injected with an Oxtr antagonist show disruption of this coding scheme, and greater overlap between these ensembles (Li et al. 2017). It is not clear if modulation of excitation-inhibition balance specifically mediates this effect, however these effects are suggestive of disrupted signal-to-noise balance that may lead to convergence of these populations.

Finally, oxytocin has also been shown to mediate excitation-inhibition balance in the hippocampus, a topic to be discussed at greater length in Chapters 2 and 3. Briefly, however, treatment of cultured hippocampal neurons with oxytocin stunts the development of glutamatergic dendrites and reduces both spontaneous and evoked synaptic transmission of these cells, suggesting an overall bias towards decreased excitation, which may shift the excitation-inhibition (E-I) balance towards inhibition (Ripamonti et al. 2017). Slice experiments have indicated that bath application of TGOT in hippocampal slices reliably induce activation of fast-spiking interneurons (FSIs) in both the DG (Harden and Frazier 2016), and in CA1 (Owen et al. 2013). In the DG, these FSIs mediate the excitability of dentate granule neurons via direct projections to the granule cell layer and promote sparse coding schemes. In CA1, TGOT release promotes higher fidelity spike transmission from incoming Schaffer collaterals arising in CA3. Additionally,

oxytocin also induces depolarization and synaptic potentiation of pyramidal neurons in CA2/CA3 (Pagani, Zhao et al. 2015, Lin, Hsieh et al. 2018). Together, these studies suggest an important role for Oxtrs in mediating network activity and encoding mechanisms such as pattern separation in the hippocampus.

1.3 Overarching Questions

The hippocampus is emerging as a significant locus for the discrimination of social stimuli. Whether and how the hippocampus utilizes common mechanisms for social and non-social learning are poorly understood, however. The neuropeptide oxytocin has long been understood to facilitate social memory, and in recent years has also gained additional appreciation in promoting signal-to-noise ratio in the hippocampus and elsewhere in the brain. However, despite the enrichment of oxytocin receptors in the hippocampus, studies of neuromodulatory systems and hippocampal circuitry have yet to converge on a single unified model elucidating how oxytocin receptors may promote discrimination of social stimuli through hippocampal computations that minimize interference between stimuli. The work presented in this thesis will aim to bridge these gaps by:

1) using multiplex fluorescence in situ hybridization to comprehensively map the expression pattern and cellular identity of Oxtrs along the hippocampal longitudinal axis.

2) using virally-mediated deletion of Oxtrs in hippocampal subregions to determine the functional role they play in social and non-social behaviors.

3) using ensemble mapping techniques to determine what coding schemes the hippocampus uses to segregate social stimuli into distinct neuronal populations, and whether these coding schemes are dependent on the action of oxytocin.

4) using *in vivo* optogenetics to delineate the outputs that may relay representations of social and non-social stimuli to distinct downstream regions.

Page intentionally left blank.

CHAPTER 2

Functional dissociation of oxytocin receptors along the dentate gyrus longitudinal axis

Parts of this chapter are adapted from a manuscript published in *Nature Communications* (Dec 8, 2017), included as Appendix 1

Hippocampal oxytocin receptors are necessary for discrimination of social stimuli

Tara Raam[1,2,3,4], Kathleen M. McAvoy[1,2,3], Antoine Besnard[1,2,3], Alexa Veenema[5], Amar Sahay[1,2,3,4,6]

[1]Center for Regenerative Medicine, Massachusetts General Hospital, Boston, MA 02114, USA

[2]Harvard Stem Cell Institute, Cambridge, MA 02138, USA

[3]Department of Psychiatry, Massachusetts General Hospital, Harvard Medical School, Boston, MA 02114 USA

[4]Department of Psychology, Michigan State University, East Lansing, MI, 48824

[5]Broad Institute of Harvard and MIT, Cambridge, MA 02142, USA

[6]Program in Neuroscience, Harvard Medical School, Boston, MA 02115, USA

Corresponding Author: Amar Sahay, asahay@mgh.harvard.edu

2.1 Introduction

Decades worth of work on the hippocampus has demonstrated that the dentate gyrus (DG) is critical for pattern separation, a process by which very similar representations can be segregated into non-overlapping ensembles of neurons, thereby minimizing interference and confusion between them. Work in both rodents and humans has widely implicated the DG in resolution of memory interference underlying spatial and contextual memory and has formed the foundation of the modern framework for learning and memory. Analysis of connectivity patterns and electrophysiological properties of dentate granule neurons (the primary encoding unit of the DG) suggests that the DG governs pattern separation through sparse coding schemes that minimize the likelihood of overlap between similar representations. This sparseness is thought to be mediated in part by potent control of granule neuron activation by inhibitory interneurons and glutamatergic mossy cells of the hilus. Recent studies in the past five years have begun to elucidate a role for the dentate gyrus in the representation of social experiences, a previously underappreciated function, however its role in discriminating between social stimuli is unclear. Interestingly, compelling evidence from multiple groups suggests that the DG is a locus for the expression of receptors for the social hormone, oxytocin (Oxtr). However the expression pattern of Oxtrs in the DG has been poorly characterized, and their behavioral function has not been elucidated. Given the critical role of the DG in minimizing overlap between similar stimuli, and the specific role of oxytocin in social behaviors, we hypothesized that Oxtrs in the DG are critical for discrimination of social stimuli. Here, we utilized multiplex fluorescence *in situ* hybridization to map the distribution of Oxtrs along the DG long axis, and characterize their cellular identity. We then harnessed viral genetics in combination with behavioral assays of social behaviors to demonstrate, for the first time, a functional dissociation of oxytocin receptor function along the DG longitudinal axis.

2.1.1 The dentate gyrus as a pattern separator.

The dentate gyrus is the primary input region of the hippocampus. It receives its main inputs in the form of excitatory afferents from the entorhinal cortex (EC) and sends its main output in the form of strong excitatory synapses onto CA3 pyramidal neurons, known as the mossy fiber synapse. A vast literature composed of anatomical, electrophysiological, and behavioral studies have converged on the notion that the DG mediates pattern separation, a term that generally refers to the computational function that facilitates orthogonalization: the segregation of overlapping inputs into divergent outputs (Marr 1971; Amit et al. 1987; Treves and Rolls 1994; Santoro 2013).The DG is also thought to promote resolution of memory interference, the cognitive and/or behavioral state of discriminating between very similar stimuli, such as similar contexts, objects, or spatial cues. Critically, these two processes may be linked: it is precisely the segregation of inputs into distinct outputs at the level of connectivity and cellular activity that is thought to mediate effective discrimination at the behavioral level (Treves and Rolls 1992; McClelland and Goddard 1996; Colgin et al. 2008; Neunuebel and Knierim 2014; Besnard and Sahay 2016; McAvoy et al. 2016).

A number of features of the dentate gyrus render it an effective pattern separator. First, the sheer density of cells in the DG that receive input from the EC is such that the number of dentate granule neurons outnumbers the number of EC pyramidal neurons by nearly tenfold, a ratio that facilitates divergence of entorhinal inputs into ensembles of neurons that have a low probability of overlap with each other (Schmidt et al. 2012). Simply put, the more units of storage that are available in the DG, the more opportunity there is to distribute similar representations in a manner that minimizes overlap between them. Second, the electrophysiological properties of granule neurons also support pattern separation. The activity of the DG is remarkably sparse: at any given

moment, roughly 3% of the 1,000,000+ cells are active (Jung and McNaughton 1993; Neunuebel and Knierim 2012). Granule neurons therefore tend to fire very selectively at restricted locations in the environment, a mechanism which promotes precise encoding of environmental stimuli with minimal interference with other very similar stimuli (GoodSmith et al. 2017; Senzai and Buzsaki 2017). Indeed, disruptions in DG function impairs behavioral discrimination. Rats with colchicine-induced lesions to the DG (which kills roughly 90% of granule neurons) demonstrate impaired spatial working memory in both the Morris water maze and the radial arm maze (Jeltsch et al. 2001). Additionally, conditional deletion of the NMDA receptor NR1 subunit in granule neurons does not impair conditioned fear, but does impair discrimination between two very similar contexts (McHugh et al. 2007). These rodent studies are corroborated by human fMRI studies. When human subjects are viewing images of either objects or scenes, greater activation of the DG or DG/CA3 subregion is observed during perception of 'lure' images, images that are very similar to objects or scenes that have already been seen, but are not exactly the same (Bakker et al. 2008; Berron et al. 2016). Despite lure images being very similar to those of images already seen before, blood oxygenation levels in the DG are comparable to those of novel objects and scenes, suggesting that the DG is distinguishing very similar stimuli. Additionally, the DG displays repetition suppression, a decrease in BOLD signal in response to a familiar stimulus, when the subject is presented with repeat images. Although the DG has been extensively implicated in pattern separation mediating discrimination of contexts, objects, and spatial location, it is poorly understood whether this same mechanism mediates discrimination of social stimuli. Understanding this underappreciated role of the DG in social memories is therefore the focus of this chapter.

2.1.2 Local microcircuitry of the DG.

The sparse activity of the DG that is thought to underlie effective pattern separation can be understood by examining the local microcircuitry of the DG. While the cytoarchitecture of the DG is made up of a variety of cells, its main units of function can be summarized as three main cell types: dentate granule cells (DGCs), inhibitory interneurons, and mossy cells. Here I will briefly review the connectivity patterns and general function of these three cell types, as depicted in **Figure 2.1** (Scharfman and Bernstein 2015).

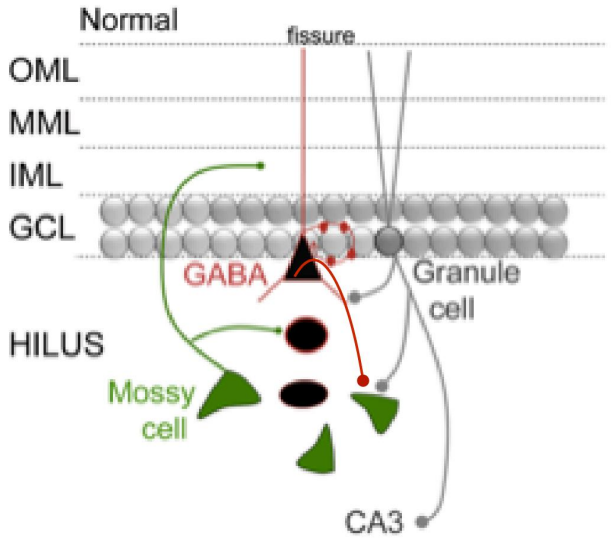


Figure 2.1 (*adapted from Scharfman and Bernstein., 2015)*

Depiction of local DG microcircuitry including granule cell, mossy cell, and basket cell interneuron reciprocal synapses.

GCL: Granule Cell Layer, IML: Inner Molecular Layer, MML: Middle Molecular Layer

OML: Outer Molecular Layer

The granule cell layer is overwhelmingly made up of tightly packed dentate granule cells (DGCs), the primary encoding unit of the DG. DGCs are thought to be predominantly glutamatergic, and, in rodents, send afferents to only one subregion: the CA2/CA3 subregion of the hippocampus, a dense projection known as the mossy fiber synapse. The density of cells in the DG-CA3 axis is variable along the longitudinal axis such that DGCs are much more densely

packed than in the posterior pole (Amaral et al. 2007). Conversely, CA3 shows the opposite pattern—CA3 pyramidal neurons are much more densely packed in the posterior pole than in the anterior pole (Amaral et al. 2007). Taken together, these variations in cell density render a ratio of DGCs to CA3 pyramidal neurons that is approximately 10:1 in the anterior pole but only 2:3 in the posterior pole, a connectivity pattern that is thought to underlie the differences in pattern separation function along the longitudinal axis (Amaral et al. 2007). In addition to projections to CA2/CA3, DGCs also make strong en passant contacts with mossy cells of the hilus, a cell type to be discussed below.

The sparse activity of DGCs is due in large part to potent gating by local inhibitory interneurons that regulate the firing of DGCs. DG interneurons are located in both the hilus as well as sparsely in the GCL. A commonly studied interneuron in the DG is the basket cell, which are parvalbumin (PV) positive interneurons. Due to their unique, rapidly firing properties, these cells are also commonly referred to as fast-spiking interneurons. A critical feature of these cells is that they form synapses directly onto the cell bodies of DGCs, conferring more direct control of DGC activity, whereas other interneuron cell types such as somatostatin (SST) positive interneurons, mostly form synapses onto distal dendrites. These differences are true not only in the hippocampus, but broadly throughout the neocortex (Hayut et al. 2011; Hattori et al. 2017). Additionally, basket cell axons are characterized by many branch points that extend along both the hippocampal transverse and longitudinal axes, rendering a single basket cells capable of inhibiting up to 1% of DGCs, despite there being upwards of one hundred times as many DGCs as basket cells (Amaral et al. 2007). The disruption of interneuron activity in the hippocampus, and its subsequent disturbance of excitation-inhibition balance is thought to underlie a variety of psychiatric and neurodevelopmental disorders, such as schizophrenia, autism, and depression (Hu et al. 2014).

An additional cell type located in the hilus of the DG is the mossy cell, a peculiar cell type that modulates the excitation and disynaptic inhibition of DGCs. Mossy cells are large, glutamatergic cells of the hilus that send both direct and indirect connections to granule neurons. In addition to their direct projections onto DGC apical dendrites located in the inner molecular layer of the DG, mossy cells also indirectly innervate DGCs via inhibitory interneurons in the hilus. Thus, a single mossy cell can potentially either excite or inhibit DGCs, depending on which projection dominates at a given time. For decades, much controversy existed about whether or not mossy cells had a net excitatory or net inhibitory effect on DGCs, a question that was not readily testable due do a lack of technical strategies to selectively target mossy cells. A study by Jinde and colleagues resolved this question by developing a Cre mouse line that specifically targets mossy cells and utilizing a Cre-dependent diphtheria toxin to silence them (Jinde et al. 2012; Jinde et al. 2013). This manipulation led to a net excitatory effect on DGC activity, an effect that was accompanied by increased anxiety-like behavior and impaired contextual discrimination, suggesting that the normal physiological role of mossy cells is primarily to inhibit DGCs and promote sparse coding underlying pattern separation (Jinde et al. 2012; Jinde et al. 2013). *In vivo* recordings of mossy cells during spatial navigation tasks suggests that mossy cells are characterized by promiscuous firing properties and can form multiple place fields in a single environment, as well as across environments (GoodSmith et al. 2017; Senzai and Buzsaki 2017), suggesting that mossy cells are less spatially tuned than DGCs themselves, which generally have only a single place field. Additionally, a unique property of mossy cells is that they form synapses less so onto proximal DGCs (those that are closer to the mossy cell itself), and send denser and stronger projections to DGCs further along the longitudinal axis (from anterior to posterior, and vice versa). Given that mossy cells receive strong inputs from local DGCs, this unique projection

pattern of mossy cells may underlie relaying of information between DGCs in anterior and posterior DG (Amaral et al. 2007).

2.1.3 Segregation of function along the DG longitudinal axis.

As discussed in Chapter 1, much of the thinking within hippocampal literature has been carried out within the framework of a dissociation in function along the longitudinal axis, whereby the most anterior pole of the hippocampus is thought to mediate spatial and contextual learning, and the posterior pole is thought to give rise to unconditioned emotional responses such as the expression of fear (Fanselow and Dong 2010; Strange et al. 2014). The earliest functional and anatomical studies that identified these differences utilized lesions of large swaths of tissue and did not differentiate between hippocampal subregions (such as the DG vs CA3 or CA1). More recent studies that have restricted the lesion site to smaller subregions of the hippocampus, as well as the emergence of genetic technologies, such as mouse lines that specifically target desired subregions, however, have enabled an initial understanding of the functional dissociation of the DG along its long axis.

A landmark paper by Kheirbek and colleagues was among the first to systematically interrogate the contribution of anterior (dorsal) vs posterior (ventral) DG to a variety of behavioral states. Utilizing a genetic driver line that specifically targets the granule cell layer of the dentate gyrus (POMC-Cre) to drive the expression of excitatory (ChR2) or inhibitory (eNpHR3.0) opsins, Kheirbek and colleagues demonstrated a segregation in function whereby granule neurons in the anterior, but not posterior, DG control the encoding of a contextual fear memory (Kheirbek et al. 2013). Conversely, stimulating granule neurons in the posterior DG results in a potent anxiolytic effect in the elevated plus maze (EPM) and open field test (OFT). Stimulation of granule neurons in the anterior DG resulted in an increase in locomotor activity, but not in innate anxiety (Kheirbek

et al. 2013). These effects on innate anxiety obtained via optogenetic manipulations of posterior DG mimic those of cytotoxic lesions that specifically target pDG in measures of OFT and EPM (Weeden et al. 2015). Together, these experiments support a long-axis dissociation in DG function that recapitulates much of the earlier lesion studies that implicated the posterior hippocampus in limbic function and the anterior hippocampus in spatial and contextual learning.

Classic experiments support a notion that spatial and contextual pattern separation in general are more robust in anterior hippocampus and less robust in posterior hippocampus. For example, classical studies utilizing *in vivo* recordings have demonstrated that fewer pCA1 pyramidal cells contained place fields than in aCA1, and those that do have place fields that are significantly larger and less spatially selective than those in aCA1 (Jung et al. 1994). Similarly, electrophysiological recordings of aDG granule neurons have demonstrated that these cells are sparsely active, and typically only have one place field (GoodSmith et al. 2017; Senzai and Buzsaki 2017). The firing properties and place fields of pDG granule neurons have not been well characterized *in vivo*. However, studies of contextual representations along the DG long axis via activity-dependent measures of ensemble overlap indicate that aDG more efficiently minimizes overlap between ensembles encoding two very similar contexts (McAvoy et al. 2016). Conversely, overlap in ensembles encoding similar contexts is significantly greater in posterior DG, a result suggestive of less efficient population-based coding (McAvoy et al. 2016). Although these studies may suggest that spatial pattern separation is more robustly performed by computations in aDG, some initial lesion studies indicate that pDG is also engaged in behavioral tasks of olfactory discrimination (Weeden et al. 2015) and discrimination of reward value (Kirk et al. 2017). Thus, the notion that posterior DG does not segregate similar inputs as readily as aDG may reflect a limited view that has probed its role in spatial tasks only, whereas pDG may be more engaged in

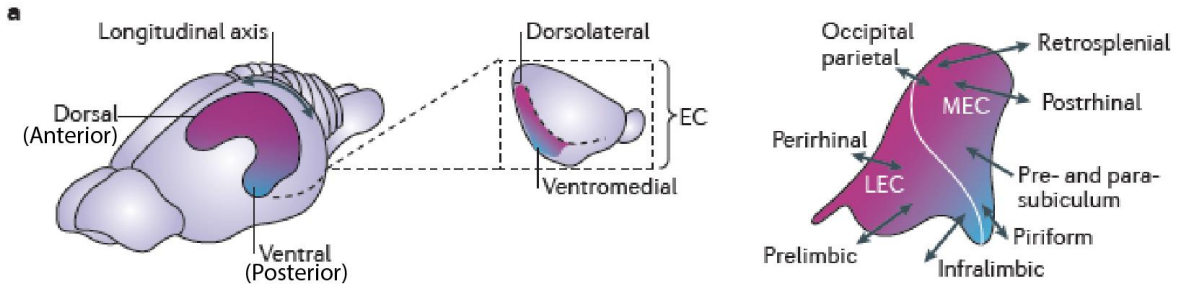
discrimination of cues that have strong sensory or limbic valence. Future studies utilizing *in vivo* recordings or calcium imaging during exposure to emotionally salient stimuli may give clarity to these ideas.

The functional dissociation in DG function along the longitudinal axis is thought to be in part mediated by topographic differences in connectivity patterns. The primary input into the DG is through the medial and lateral entorhinal cortices. Through them, the DG receives a large amount of indirect, highly processed sensory information from broadly distributed cortical and subcortical regions. However, projections from the entorhinal cortices (EC) into the DG are characterized by an anatomical gradient, whereby the anterior DG receives input from the dorsolateral EC and the posterior DG receives input from the ventromedial EC (**Figure 2.2**, adapted from (Strange et al. 2014). A further level of analysis reveals that inputs onto EC are also topographically organized, whereby limbic regions such as the piriform cortex, prefrontal cortex, and BLA preferentially target the ventromedial EC, which communicates with the posterior DG. Conversely, regions such as the retrosplenial, postrhinal, and perirhinal cortices project to the dorsolateral EC, which communicates with the anterior DG (**Figure 2.2**, adapted from (Strange et al. 2014). In addition to inputs from the EC, the anterior and posterior DG also receive direct input from subcortical regions such as the medial septum and supramammillary nucleus, and the projection patterns of these two regions are also organized in a gradient-like manner along the DG long-axis (Ohara et al. 2013).

Figure 2.2 (*adapted from Strange et al., 2014)*
Left: Schematic depicting gradient-like topographical organization of entorhinal cortex (EC) inputs to anterior and posterior hippocampus.

Right: Schematic depicting gradient-like topographical organization of diverse cortical inputs to EC regions projecting into hippocampus.

Figure 2.2 (Continued)



2.1.4 Modulation of DG activity via oxytocin.

A number of studies in recent years have converged upon the intriguing observation that the DG is a locus for the expression of the oxytocin receptor. Pioneering studies utilizing radioligand binding of Oxtr demonstrate enriched expression in the DG of the mouse hippocampus (Lee et al. 2008; Hammock and Levitt 2013). These observations have been corroborated by the development of antibodies that bind Oxtr protein, yielding expression in both the hilus and the granule cell layer (Mitre et al. 2016). Complimentary approaches utilizing mouse genetics to generate a knock-in reporter line expressing Venus-EYFP under the control of the regulatory region of the *Oxtr* gene demonstrate specific expression in the polymorphic layer (hilus) of the DG, but little to no expression in the granule cell layer (Yoshida et al. 2009; Lin et al. 2017). mRNA labeling in macaque monkeys suggests a similar enrichment in non-human primates (Freeman et al. 2014). Importantly, this enrichment in the hippocampus seems to be evolutionarily conserved between rodents, primates, and humans—*Oxtr* mRNA expression mapping in human post-mortem tissue indicates elevated expression in the hippocampus and parahippocampal gyrus (Quintana, Rokicki et al., BioRxiv, 2017). These data are supported by post-mortem human microarray data that suggests *Oxtr* enrichment in the DG and CA2 subregions of the hippocampus

(Allen Brain Atlas, human.brain-map.org). Interestingly, all of these studies only include reports of the anterior DG, and to date no reports of Oxtr expression in the posterior hippocampus have been mentioned. In light of previous reports that indicate differential patterns of gene expression along the long-axis of the hippocampus generally (Thompson et al. 2008; Strange et al. 2014), and also within the DG specifically (Sun et al. 2015; Zhang et al. 2018), the distribution of *Oxtr* mRNA along the DG long axis stands out as a significant gap in the literature.

Physiologically, oxytocin is thought to play a critical role in modulation of signal-to-noise in diverse networks across the brain, as outlined in Chapter 1. Evidence from the few papers examining oxytocin in the hippocampus suggests that this principle seems to remain consistent in the DG. Early studies utilizing c-Fos immunoreactivity as a readout for activity demonstrate robust hyperactivation of the DG granule cell layer in oxytocin whole-brain knockout animals following a social exposure, but not at baseline (Ferguson et al. 2001). Conversely, local infusion of OT in the DG of male rats during *in vivo* field potential recordings results in decreases EPSPs in dentate granule neurons, a result that is dependent upon tetanization of perforant pathway afferents (Dubrovsky et al. 2002). Together, these two studies suggest that the presence of oxytocin may promote sparse activity in the granule cell layer, and its absence may disrupt sparse coding schemes, however the mechanism underlying these effects have remained elusive until recently. An in-depth slice physiology study conducted by Harden and colleagues determined that bath application of the Oxtr agonist TGOT reliably induces activation of GABA-ergic fast-spiking interneurons in the hilus, which functionally form synapses onto and inhibit neighboring mossy cells, and also extend dendrites into the granule cell layer (Harden and Frazier 2016). Thus, oxytocin may harness local mechanisms to regulate the inhibitory tone of the granule cell layer by

co-opting the potent gating of GCL activity by hilar interneurons and mossy cells, an intriguing mechanism by which oxytocin may influence encoding in the DG.

2.1.5 Involvement of the DG in social behaviors.

In addition to the role of the DG in storing spatial and contextual representations, recent studies have begun to dissect the function of ensembles of neurons that encode social experiences in the DG. Groundbreaking studies from the laboratory of Susumu Tonegawa have identified an inducible, activity-dependent system for the tagging of memory-bearing ensembles of neurons that encode distinct mnemonic events, also known as engrams (Tonegawa et al. 2015). This system takes advantage of the immediate early gene promoter, *c-Fos*, and the tetracycline transactivator (tTA) system, to indelibly tag neurons active during a particular experience with target proteins, such as reporters that allow the visualization of engram-bearing cells (mcherry, EYFP etc.), and light-sensitive opsins that allow their subsequent manipulation (ChR2). The earliest studies utilizing this system demonstrated that the freezing associated with fear memories can be optogenetically induced in the absence of any sensory cue that would naturally induce freezing, simply by optogenetically stimulating the engram-bearing cells associated with the fear memory (Liu et al. 2012). Furthermore, these representations can be updated with new sensory information to create "false" memories by optically stimulating the representation of a safe context while shocking the animal, such that it now associates fear with a context in which a footshock was never experienced (Ramirez et al. 2013). Having begun to elucidate some of the characteristics of fear memory engrams, subsequent studies from the Tonegawa lab began probe the flexibility and therapeutic utility of social ensembles in the DG (Redondo et al. 2014; Ramirez et al. 2015). Redondo and colleagues demonstrated that social engrams in the DG (tagged during the experience of a male mouse affiliating with female mice in its homecage) carry a positive valence and, when

stimulated, drive conditioned place preference. Furthermore, stimulating these positive social engrams during delivery of a footshock reverses the valence of the engram, such that subsequent stimulation induces conditioned place aversion (Redondo et al. 2014). The subsequent study by Ramirez and colleagues harnessed the same strategy to tag social engrams in the DG and demonstrated that optical stimulation of these ensembles rescues depression-like phenotypes that develop after chronic restraint stress, as measured in the tail suspension test and sucrose preference test (Ramirez et al. 2015). These therapeutic effects were not recapitulated when stimulating engrams of negative or neutral valence.

While both of these studies were carried out primarily with the aim of understanding the flexibility and therapeutic potential of engrams of positive valence (as reflected in the language used in both manuscripts), the significance of the social nature of these positive engrams should not be minimized. The extent to which a positive engram that is rewarding but not socially mediated (e.g. cocaine consumption), may drive similar effects on conditioned place preference, or rescue of depression-like phenotypes remains unclear. Additionally, these studies represent some of the first direct evidence that social experiences 1) are represented in ensembles in the DG and 2) seem to be physiologically distinguishable from engrams of negative valence, through mechanisms that are still unknown. While these differences may potentially be mediated through distinct connectivity patterns, an additional intriguing hypothesis is that social ensembles are preferentially modulated by social hormones such as oxytocin or vasopressin.

Subsequent studies have also identified the DG as a locus for the effects of social stress and social buffering of stress. In mice chronically reared in isolate housing, the intrinsic firing properties of DG granule neurons, measured via whole-cell patch clamp in slice, is dramatically altered such that DGCs have lower resting membrane potentials in adolescence (Talani et al. 2016).

However, action potential properties (threshold voltage, duration, and amplitude) remain unchanged, and therefore a greater minimum current is required for an action potential to fire, rendering these DGCs less excitable than group housed animals. Interestingly, these effects seem to be modulated by the hormone progesterone, and bath application of progesterone is sufficient to restore these deficits (Talani et al. 2016). In addition to being sensitive to stress during the developmental period, the DG is also sensitive to social stressors during adulthood. A recent study utilizing the tandem stressor paradigm, in which animals are first subjected to several randomly delivered footshocks followed by a period of restraint stress, demonstrated a deficit in novel object recognition in animals subjected to the stress paradigm as compared to controls (Tzeng et al. 2016). This deficit is correlated with perturbations in dendritic morphology in granule neurons of the anterior DG, such that animals subjected to stress demonstrate stunted dendritic length, fewer dendritic branches, and fewer dendritic crossings. However, when animals undergo the tandem stress paradigm in social groups rather than in isolate, the behavioral and morphological effects of stress are prevented (Tzeng et al. 2016). *In vivo* multi-electrode recordings of local field potential (LFP) in hippocampal subregions corroborate synaptic-level findings from both of these studies. LFP power of theta and gamma oscillations is significantly lower in DG granule neurons, but not in CA3 or CA1 pyramidal neurons, of mice exposed to chronic 12-day social defeat stress (Aoki et al. 2017). Finally, the DG has been implicated in the expression of aggressive behavior that leads to ascent in rank in social groups (Williamson, Klein et al., BioRxiv, 2018). When an alpha male is removed from a group of co-housed animals that has established a stable dominance hierarchy, a period of social plasticity occurs in which subordinate betas begin competing via aggressive behaviors for a more dominant rank. Brain-wide c-Fos analysis in betas that have undergone rank ascent following alpha removal, versus betas living in a stable hierarchy,

demonstrates increased cFos immunoreactivity in the DG (Williamson, Klein et al., BioRxiv, 2018). This result is suggestive of the involvement of the DG in processing social changes in the contextual environment, however the precise stimulus that results in these changes is unclear. Increased activation of the DG may reflect network engagement in social recognition of the absence of the alpha male, or, may alternatively reflect the effects of stress induced by exposure to aggression or simply rapid and substantial changes in the environment.

Although a number of studies outlined above have demonstrated a role for the DG in social exploration and social stress, few studies have directly probed the role of the DG in social recognition memory. The first study to broadly implicate the rodent hippocampus in social memory is the paper published by Kogan and colleagues, discussed in greater detail in Chapter 1. This study utilized ibotenic acid to lesion the hippocampus along the long axis and observed a deficit in habituation to a social stimulus 30 minutes after the first exposure (Kogan et al. 2000). However, while lesion studies are useful in broadly implicating a brain region in a behavior, this approach does not allow us to draw conclusions about the role of distinct hippocampal subregions (DG, CA2/3, CA1), or to dissociate the contributions of anterior vs posterior hippocampus. A recent study utilizing conditional deletion of the NMDA receptor NR1 subunit in the DG, via POMC-Cre driver line, does not impair habituation to a familiar social stimulus one hour after initial exposure, suggesting that if the DG does contribute to social memory, it may be through other receptors or cell types (Chiang et al. 2018). Indeed, silencing of PV+ interneurons in the DG using DREADDS is sufficient to impair social novelty seeking, but not social exploration (Zou et al. 2016). Interestingly, this manipulation also led to a deficit in novel object recognition at both 1-hour and 24-hour time points. To date, only one group has directly probed the contribution of oxytocin in the hippocampus to social behaviors, and found that local infusion of anti-oxytocin

sera in posterior, but not anterior, DG produces a decrease in social exploration (van Wimersa Greidanus and Maigret, 1996). The distribution of oxytocin receptors along the DG longitudinal axis, their relevance to social behaviors, and their effects on GCL activity, therefore, remain outstanding questions to be addressed.

2.2 Results

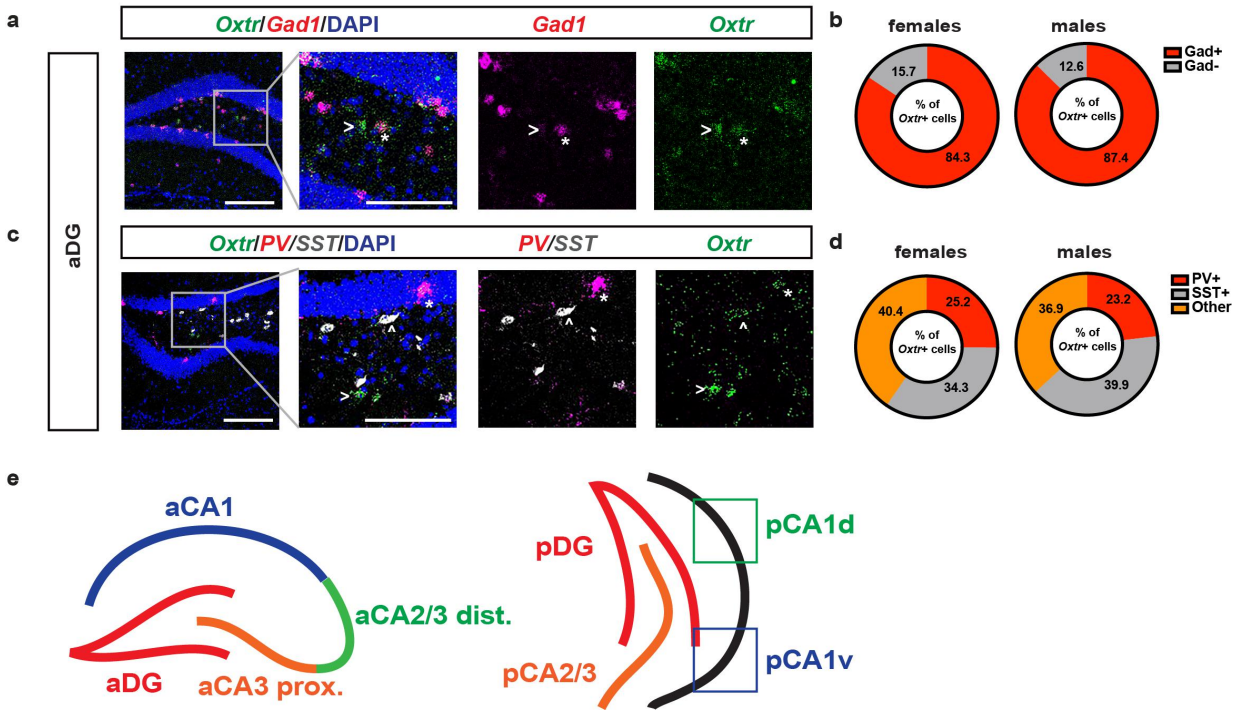
2.2.1 Characterization of Oxtr expression in the anterior DG.

In order to comprehensively map the expression pattern and cellular identity of *Oxtr* in the hippocampus, I performed multiplex fluorescence *in situ* hybridization (FISH) using riboprobes directed against *Oxtr*, Glutamate Decarboxylase 1 (*Gad1),* a marker for GABAergic inhibitory neurons, and markers of interneuron subpopulations, Parvalbumin (*PV*), and Somatostatin (*SST)* in age-matched male and female mice. Within aDG, *Oxtr* expression colocalized primarily with *Gad1* (84.3% in females and 87.4% in males), indicating the identity of these neurons primarily as inhibitory interneurons (**Figure 2.3a,b**). A small population of $Oxtr^{+}$ cells in the hilus did not colocalize with *Gad1* (**Figure 2.3a**), suggesting that these cells are most likely excitatory mossy cells. Oxtr expression was absent from $Gad1^{-}$ cells in the granule cell layer of the DG, indicating that *Oxtr* is not expressed in dentate granule neurons. Analysis of *Oxtr*, *PV* and *SST* expression in aDG showed greater colocalization of *Oxtr* with *SST* than with *PV* (**Figure 2.3c,d**). Further, a significant percentage of *Oxtr* cells in aDG were negative for both *PV* and *SST,* indicating the presence of additional subclasses of $Oxtr^{+}$ interneurons that are not captured in *PV* and *SST* only expressing populations. I did not detect any sexual dimorphism in the distribution or identity of *Oxtr* in the anterior DG.

Figure 2.3 | Characterization of *Oxtr* distribution in anterior DG.

(**a**) Representative low-magnification (left) and high-magnification (right) images of *Oxtr* and *Gad1* mRNA expression in anterior DG by FISH (n=4 males, 3 females). Asterisk (*) denotes $Oxtr^{+}/Gad1^{+}$ interneuron. Arrowhead (>) denotes $Oxtr^{+}/GAD1^{-}$ mossy cell. Scale bar denotes 100 μm. Inset scale bar denotes 50 μm. (**b**) Quantification of *Gad1* and *Oxtr* colocalization for males and females, expressed as a percentage of $Gad1^{+}$ cells over total $Oxtr^{+}$ cells. (**c**) Representative images of low-magnification (left) and high-magnification (right) images of *Oxtr*, *PV*, and *SST* mRNA expression in anterior DG by FISH (n=4 males, 3 females). Asterisk (*) denotes $PV^{+}/Oxtr^{+}$ interneuron. Right-facing arrowhead (>) denotes $Oxtr^{+}$ mossy cell. Upward facing arrowhead (^) denotes $Oxtr^{+}/SST^{+}$ interneuron. Scale bar denotes 100 μm. Inset scale bar denotes 50 μm. (**d**) Quantification of *Oxtr* colocalization with *PV* and *SST*, expressed as a percentage of total *Oxtr* cells. (**e**) Schematics indicating boundaries of aDG, $aCA3_{proximal}$, and $aCA2/CA3_{distal}$, and aCA1 in anterior hippocampus and pDG, pCA2/3, pCA1d, and pCA1v in posterior hippocampus.

Figure 2.3 (Continued)



2.2.2 aDG hilar Oxtrs are necessary for social discrimination.

To determine the behavioral contributions of *Oxtr* in aDG hilar neurons, we utilized a conditional knockout mouse line of the oxytocin receptor, *Oxtr*$^{f/f}$ (Lee *et al.*, 2008), which permits Cre recombinase-dependent deletion of *Oxtr*. I employed an AAV_9 Cre expressing virus expressed under the control of a human Synapsin promoter in order to target both inhibitory interneurons and excitatory mossy cells in aDG (**Figure 2.4a,b**). Although previous reports indicate that the AAV_9 serotype is anterogradely transported from some cell types, I did not observe any transport to CA2/CA3 (**Figure 2.5a**) or retrograde trafficking to brain regions projecting to the DG (**Figure 2.5b,c,d,e**), as has also been previously reported with high titre AAV_9 viruses (Aschauer et al. 2013; Cook-Snyder et al. 2015). In order to determine virally mediated recombination of *Oxtrs*, we quantified the percentage of DAPI+ cells expressing *Oxtr* mRNA in aDG hilar neurons of *Oxtr* $^{+/+}$ vs. *Oxtr* $^{f/f}$ mice injected with AAV_9-hSyn-Cre. *Oxtr*+ cells comprised 11% of all DAPI+ cells in *Oxtr* $^{+/+}$ mice and 6% of all DAPI+ cells in *Oxtr* $^{f/f}$ mice, demonstrative of *Oxtr* recombination (**Figure 2.5f,g**).

Bilateral infection of Cre-expressing virus in aDG resulted in an increased number of *c-fos*-expressing dentate granule neurons following exposure to a social stimulus suggesting a loss of inhibition onto dentate granule neurons (unpaired t-test, GFP vs Cre: $p = .0158$, **Figure 2.4c**). aDG *Oxtr* deletion did not significantly affect performance in tests of object exploration, novel object recognition, or social exploration (**Figure 2.4d,e,f**). Habituation to a social stimulus trended towards impairment (trend, two-way ANOVA, interaction: $F_{(2,30)} = 2.613$, $p = .0899$). However, aDG *Oxtr* deletion resulted in a robust deficit in the social discrimination task. Whereas control animals strongly preferred a novel animal to a familiar animal, Cre-injected animals did not show a preference (two-way ANOVA, treatment: $F_{(1,15)} = .8955$, $p = .3590$, stimulus: $F_{(1,15)} = 25.78$, $p =$

Figure 2.4 | Viral recombination of *Oxtr* in anterior DG hilar neurons of adult mice impairs discrimination of social, but not non-social, stimuli.

(**a**) Schematic illustrating viral injection and behavioral testing timeline. (**b**) Representative images of Cre and GFP virus infection in aDG. Scale bar denotes 200 μm. (**c**) Representative images and quantifications of cFos immunoreactivity in granule cell layer of aDG (GFP: n=7, Cre: n = 4). Scale bar denotes 75 μm. (**d**) Behavioral schematic (top) and quantification (bottom) of single object exploration (GFP: n=11, Cre: n=6). (**e**) Behavioral schematic (top) and quantification (bottom) of novel objection recognition (GFP: n=11, Cre: n=6). Quantifications are displayed as Habituation (trials 1-3), Test (trial 4), and discrimination ratio (trial 4). (**f**) Behavioral schematic (top) and quantification (bottom) of social exploration test (GFP: n=11, Cre: n=6). (**g**) Behavioral schematic (top) and quantification (bottom) of social discrimination task (GFP: n=11, Cre: n=6). Quantifications are displayed as Habituation (trials 1-3), Test (trial 4), and discrimination ratio (trial 4). All data are displayed as mean ± SEM.

Figure 2.4 (Continued)

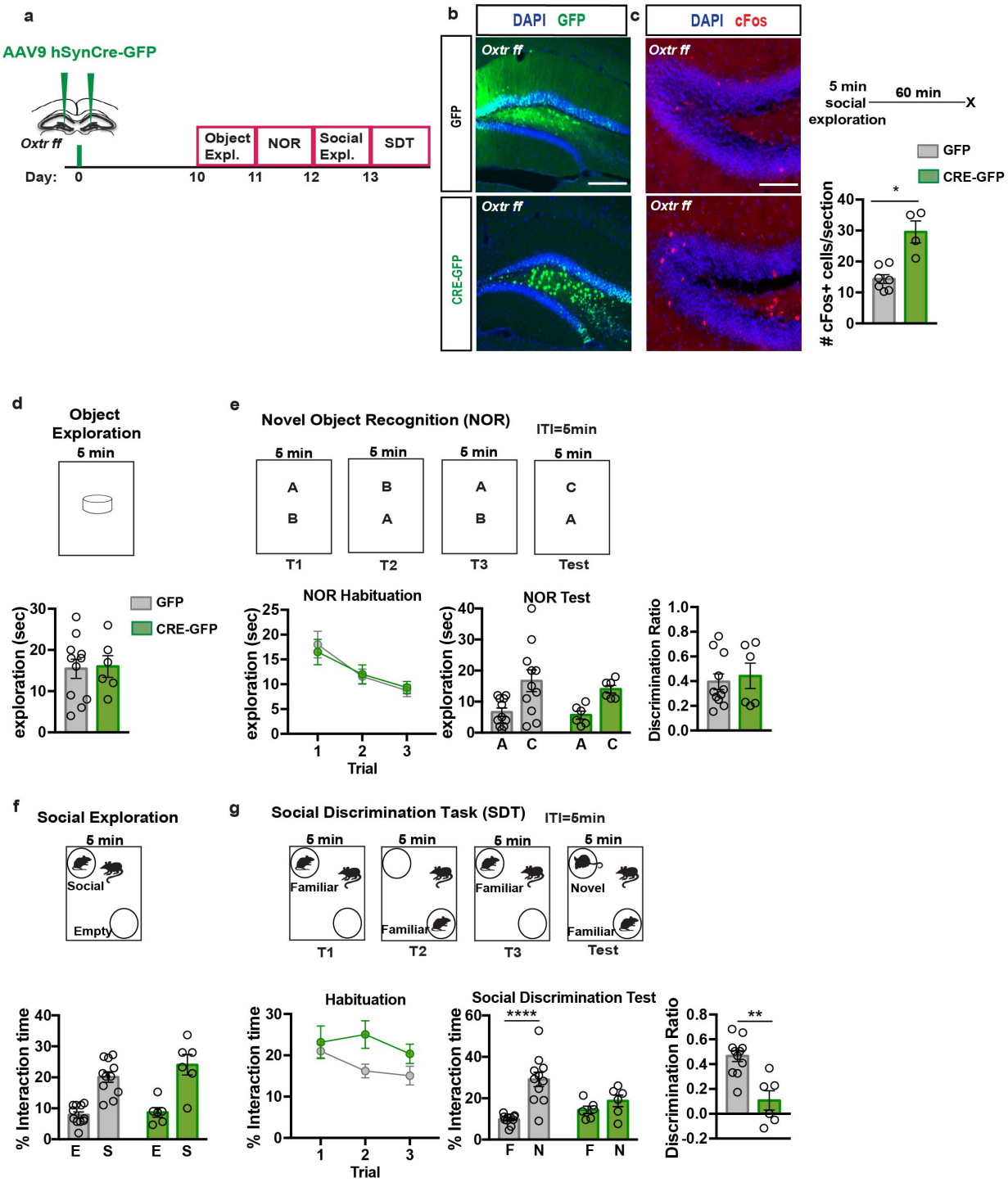
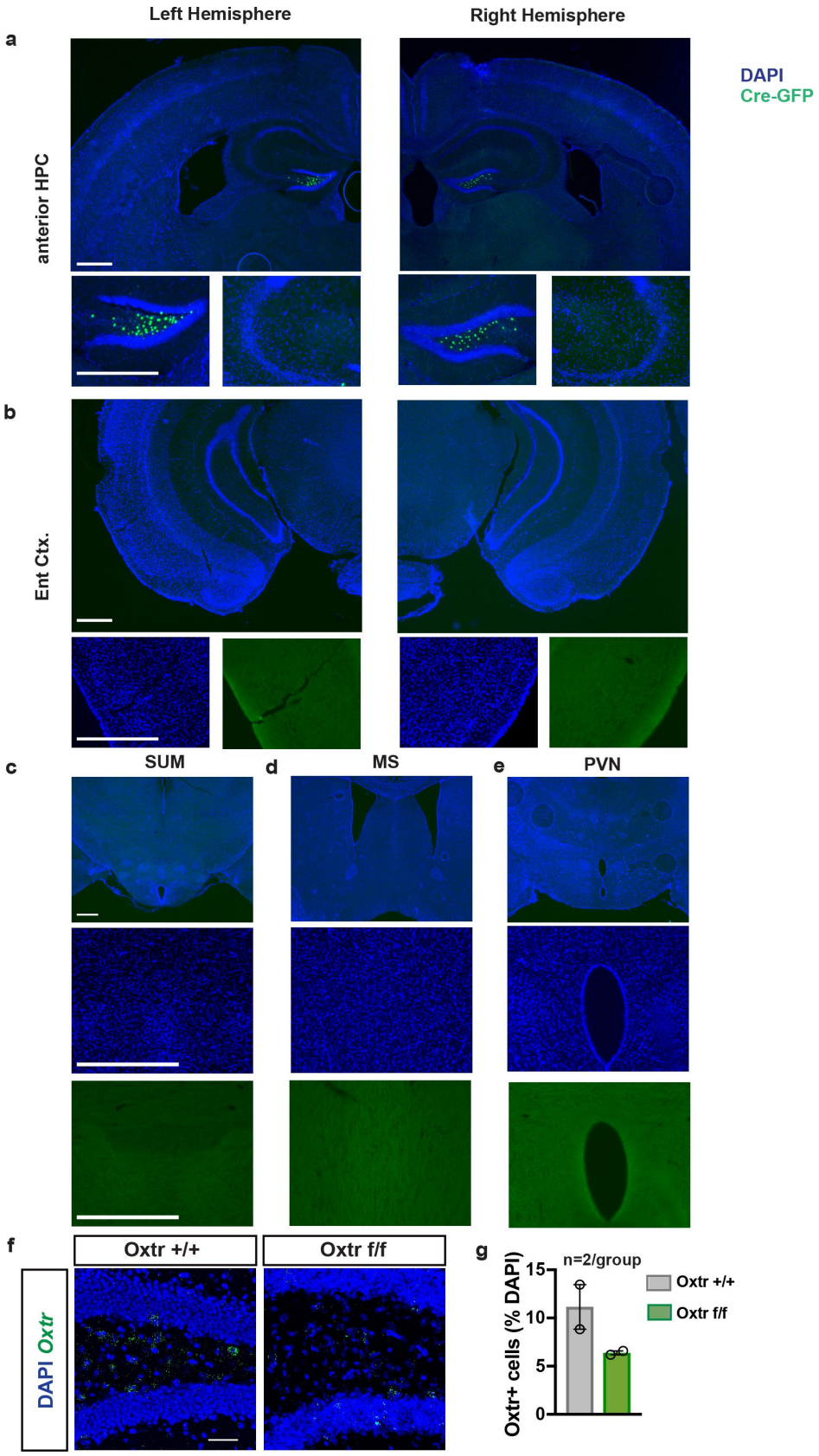


Figure 2.5 | Viral expression of AAV$_9$-hSyn-Cre-GFP in anterior DG is not retrogradely or anterogradely trafficked.

(**a**) Low magnification (top) and high magnification (bottom) images of anterior hippocampus at the site of injection in aDG. Scale bars denote 500 μm (top) and 600 μm (bottom). (**b**) Low magnification (top) and high magnification (bottom) images of Entorhinal Cortex depicting lack of retrograde labeling from aDG. Scale bars denote 500 μm (top) and 600 μm (bottom). (**c**) Low magnification (top) and high magnification (bottom) images of SUM depicting lack of retrograde labeling from aDG. Scale bars denote 500 μm (top) and 600 μm (bottom). (**d**) Low magnification (top) and high magnification (bottom) images of MS depicting lack of retrograde labeling from aDG. (**e**) Low magnification (top) and high magnification (bottom) images of PVN depicting lack of retrograde labeling from aDG. (**f)** Representative images of aDG hilus *Oxtr* mRNA expression in Oxtr +/+ and Oxtr f/f animals injected with hSyn-Cre virus. Scale bar denotes 50 μm. (**g**) Quantification of *Oxtr* mRNA in aDG expressed as a percentage of total DAPI+ cells in Oxtr +/+ and Oxtr f/f animals injected with hSyn-Cre virus.

Figure 2.5 (continued)



.0001, interaction: $F_{(1,15)}$ = 10.32, p = .0058; Multiple comparisons, Familiar vs. Novel, GFP: p<.0001, Cre: p = .5294, **Figure 2.4g**). Discrimination ratios were also significantly lower in Cre animals than in GFP animals (unpaired t-test, GFP vs Cre: p = .0036, **Figure 2.4g**). Unilateral injection of Cre into aDG was insufficient to reproduce this effect (GFP n= 11, Cre n =7, unpaired t-test GFP vs. Cre: p = .2976). Deletion of Oxtrs in aDG did not affect measures of innate anxiety in the open field test (OFT) or elevated plus maze (EPM) (**Figure 2.6b,c**). Together, these data demonstrate a critical role for Oxtrs in the aDG in mediating discrimination of social, but not non-social, stimuli.

2.2.3 Characterization of Oxtr expression in the posterior hippocampus.

Within the posterior hippocampus, I observed dense *Oxtr* expression in the hilus of pDG (**Figure 2.7a**). In contrast to aDG where the majority of *Oxtr* cells were GABA-ergic interneurons, greater than 50% of *Oxtr* expressing cells in pDG were *Gad1*$^{-}$ putative mossy cells (**Figure 2.7a,b**). Similar to aDG, *Oxtr*$^{+}$ dentate granule neurons were not observed in pDG. Additionally, further characterization of *Oxtr*+ cells revealed a mixed population of *PV*$^{+}$ and *SST*$^{+}$ cells, with a larger fraction of *Oxtr*+ cells colocalizing with *SST* than with *PV* (**Figure 2.7c,d**).

Next, I analyzed *Oxtr* expression within posterior CA subfields (pCA2/3 and the dorsal and ventral segments of pCA1, schematic shown in **Figure 2.3e**). I observed enriched expression of *Oxtr* in pCA2/3, and pCA1v, however *Oxtr* expression was comparable to background in pCA1d (**Figure 2.7e,i,j,k**). Within pCA2/3, *Oxtr* is predominantly expressed in excitatory neurons of the pyramidal cell layer, with 15-20% overlap between *Oxtr* and *Gad1* (**Figure 2.7e,f**). These cells are a mixed population of *PV* and *SST* expressing cells, with a larger fraction of *PV*+ cells expressing *Oxtr* than *SST*+ cells (**Figure 2.7g,h**). *Oxtr* expression was dense in the pyramidal layer of the ventral segment of pCA1 (**Figure 2.7k,l**). A small fraction of *Oxtr*+

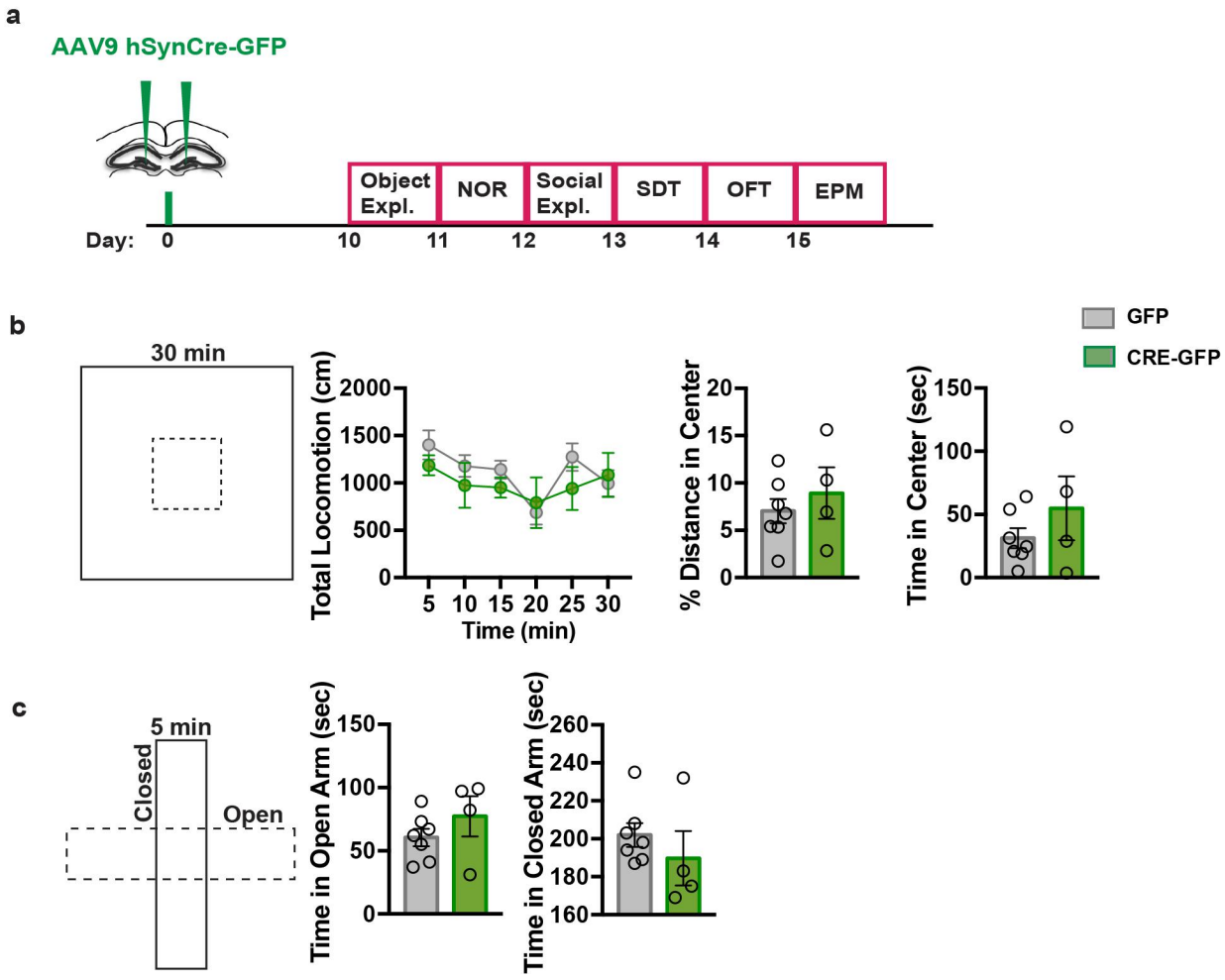


Figure 2.6 | Viral recombination of Oxtrs in anterior DG hilar neurons does not affect behavioral measures of innate anxiety.

(**a**) Schematic illustrating viral injection and behavioral testing timeline. (**b**) Schematic illustrating open field test (left) and quantification of total locomotion, percent distance in center, and time in center (right, GFP: n=7, Cre: n=4). (**c**) Schematic illustrating elevated plus maze (left) and quantification of time in open arm and time in closed arm (right, GFP: n=7, Cre: n=4). All data are displayed as mean ± SEM.

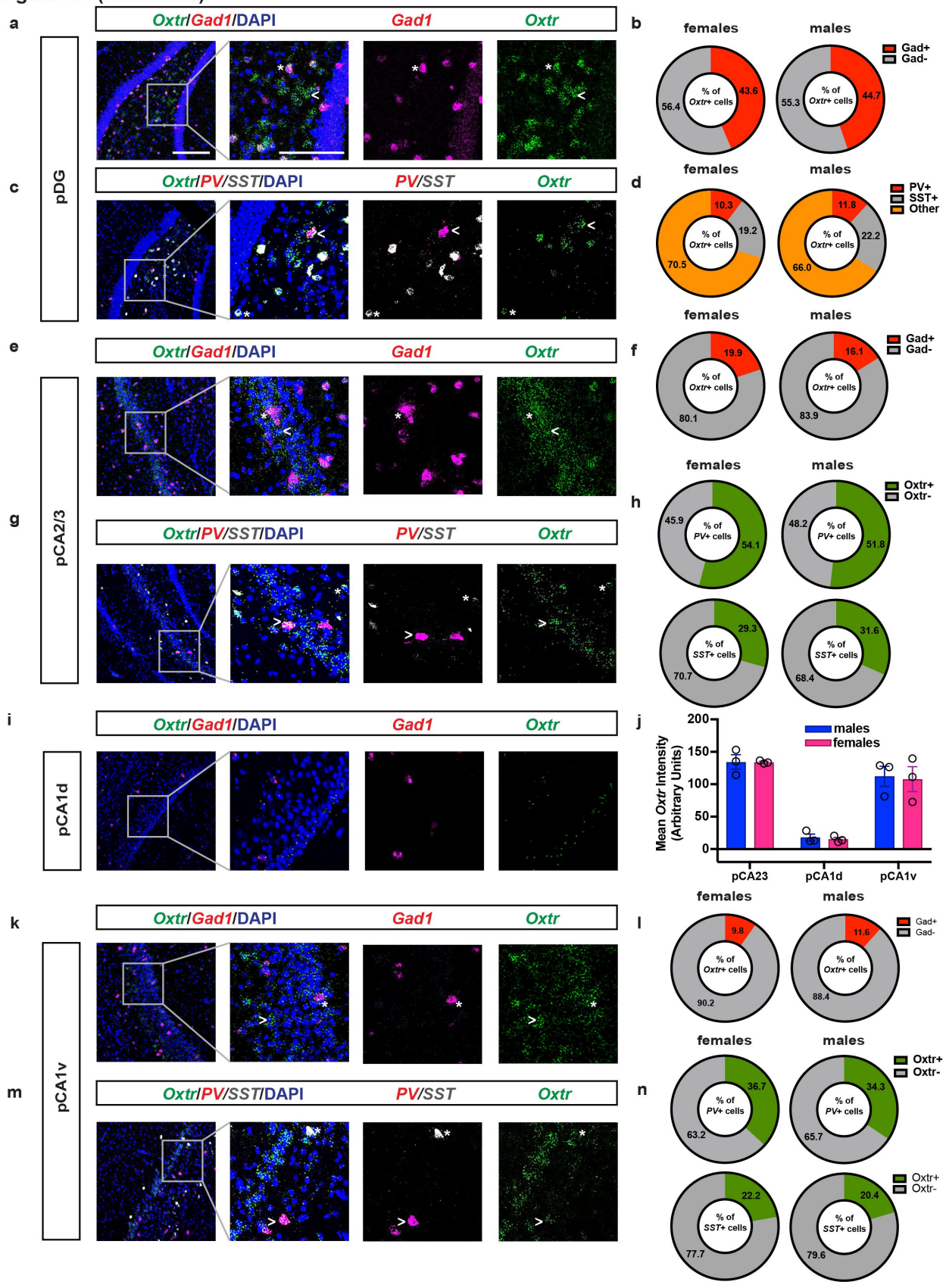
Figure 2.7 | Characterization of *Oxtr* distribution in posterior hippocampus.

(**a**) Representative low-magnification (left) and high-magnification (right) images of *Oxtr* and *Gad1* mRNA expression in posterior DG by FISH (n=3 males, 3 females). Asterisk (*) denotes $Oxtr^+/GAD1^+$ interneuron. Arrowhead (<) denotes $Oxtr^+/GAD1^-$ mossy cell. Scale bar denotes 100 μm. Inset scale bar denotes 50 μm. (**b**) Quantification of *Gad1* and *Oxtr* colocalization for males and females, expressed as a percentage of $Gad1^+$ cells over total $Oxtr^+$ cells. (**c**) Representative low-magnification (left) and high-magnification (right) images of *Oxtr*, *PV*, and *SST* mRNA expression in posterior DG by FISH (n=3 males, 3 females). Arrowhead (<) denotes $Oxtr^+/PV^+$ interneuron. Asterisk (*) denotes $Oxtr^+/SST^+$ interneuron. (**d**) Quantification of *Oxtr* colocalization with *PV* and *SST* for males and females, expressed as a percentage of total *Oxtr* cells. (**e**) Representative low-magnification (left) and high-magnification (right) images of *Oxtr* and *Gad1* mRNA expression in pCA2/3 by FISH (n=3 males, 3 females). Asterisk (*) denotes $Oxtr^+/GAD1^+$ interneuron. Arrowhead (<) denotes $Oxtr^+/GAD1^-$ pyramidal neuron. (**f**) Quantification of *Gad1* and *Oxtr* colocalization for males and females, expressed as a percentage of $Gad1^+$ cells over total $Oxtr^+$ cells. (**g**) Representative low-magnification (left) and high-magnification (right) images of *Oxtr*, *PV*, and *SST* mRNA expression in pCA2/3 by FISH (n=3 males, 3 females). Arrohead (>) denotes $Oxtr^+/PV^+$ interneuron. Asterisk (*) denotes $Oxtr^+/SST^+$ interneuron. (**h**) Quantification of *Oxtr* colocalization with *PV* and *SST* in pCA2/3, expressed as a percentage of total *PV* cells (top) or *SST* cells (bottom). (**i**) Representative low-magnification (left) and high-magnification (right) images of *Oxtr* and *Gad* mRNA expression in pCA1d by FISH (n=3 males, 3 females). (**j**) Quantification of mean *Oxtr* intensity for CA regions expressed in arbitrary units, normalized for background.

Figure 2.7 (Continued)

(**k**) Representative low-magnification (left) and high-magnification (right) images of *Oxtr* and *Gad1* mRNA expression in pCA1v by FISH (n=3 males, 3 females). Asterisk (*) denotes *Oxtr*$^+$*/GAD1*$^+$ interneuron. Arrowhead (>) denotes *Oxtr*$^+$*/GAD1*$^-$ pyramidal neuron. (**l**) Quantification of *Gad1* and *Oxtr* colocalization for males and females, expressed as a percentage of *Gad1*$^+$ cells over total *Oxtr*$^+$ cells. (**m**) Representative low-magnification (left) and high-magnification (right) images of *Oxtr*, *PV*, and *SST* mRNA expression in pCA1v by FISH (n=3 males, 3 females). Arrowhead (>) denotes *Oxtr*$^+$/PV$^+$ interneuron. Asterisk (*) denotes PV+/SST+ interneuron. (**n**) Quantification of *Oxtr* colocalization with *PV* and *SST* in pCA2/3, expressed as a percentage of total *PV* cells (top) or *SST* cells (bottom).

Figure 2.7 (continued)



cells colocalized with *Gad1*, with a larger fraction of these cells being PV^+ rather than *SST*+ cells (**Figure 2.7m,n**). I did not detect any sexual dimorphism in *Oxtr* expression within any subregion of posterior hippocampus.

2.2.4 pDG hilar Oxtrs modulate social exploration.

Having established the role of aDG Oxtr in modulating discrimination of social stimuli, I next sought to probe the behavioral function of Oxtrs. I employed an AAV_1 Cre expressing virus expressed under the control of a CAG promoter in order to target both inhibitory interneurons and excitatory mossy cells in pDG, and part of CA2/CA3 most proximal to the hilus (**Figure 2.8a,b**). Although previous reports indicate that the AAV_1 serotype can be retrogradely transported from some cell types, I did not observe any retrograde trafficking to brain regions projecting to the pDG (**Figure 2.9**).

Unlike aDG, bilateral infection of Cre-expressing virus in pDG hilus did not result in an altered number of *c-fos*-expressing dentate granule neurons following exposure to a social stimulus (unpaired t-test, Dead-Cre vs Cre: p = .1188, **Figure 2.8c**). During behavioral assays, pDG *Oxtr* deletion did not significantly affect performance in tests of object exploration or novel object recognition (**Figure 2.8d,e**). However, pDG *Oxtr* deletion resulted in a robust decrease in social exploration. Whereas control animals strongly preferred a wire cup containing a social stimulus to an empty cup, Cre-injected animals did not show a preference for the social cup (two-way ANOVA, treatment: $F_{(1,13)} = .911$, p = .3573, stimulus: $F_{(1,13)} = 25.52$, p = .0002, interaction: $F_{(1,13)} = 6.822$, p = .0215; Multiple comparisons, Social vs. Empty, DeadCre: p =.0002, Cre: p = .2373, **Figure 2.8f**). Measures of social exploration were also significantly lower during trials 1-3 of the social discrimination test in the Cre-injected animals (two-way ANOVA, treatment: $F_{(1,13)} = .8.689$, p = .0113, time: $F_{(2,26)} = 2.877$, p = .0743, interaction: $F_{(2,26)} = 2.662$, p = .0888), however

Figure 2.8 | Viral recombination of *Oxtr* in posterior DG hilar neurons of adult mice impairs social exploration.

(**a**) Schematic illustrating viral injection and behavioral testing timeline. (**b**) Representative images of Cre and Dead-Cre virus infection in pDG. Scale bar denotes 200 μm. (**c**) Representative images and quantifications of cFos immunoreactivity in granule cell layer of pDG (GFP: n=8, Cre: n = 6). Scale bar denotes 75 μm. (**d**) Behavioral schematic (top) and quantification (bottom) of single object exploration (GFP: n=8, Cre: n=8). (**e**) Behavioral schematic (top) and quantification (bottom) of novel objection recognition (GFP: n=8, Cre: n=6). Quantifications are displayed as Habituation (trials 1-3), Test (trial 4), and discrimination ratio (trial 4). (**f**) Behavioral schematic (top) and quantification (bottom) of social exploration test (GFP: n=8, Cre: n=7). (**g**) Behavioral schematic (top) and quantification (bottom) of social discrimination task (GFP: n=8, Cre: n=7). Quantifications are displayed as Habituation (trials 1-3), Test (trial 4), and discrimination ratio (trial 4). All data are displayed as mean ± SEM.

Figure 2.8 (Continued)

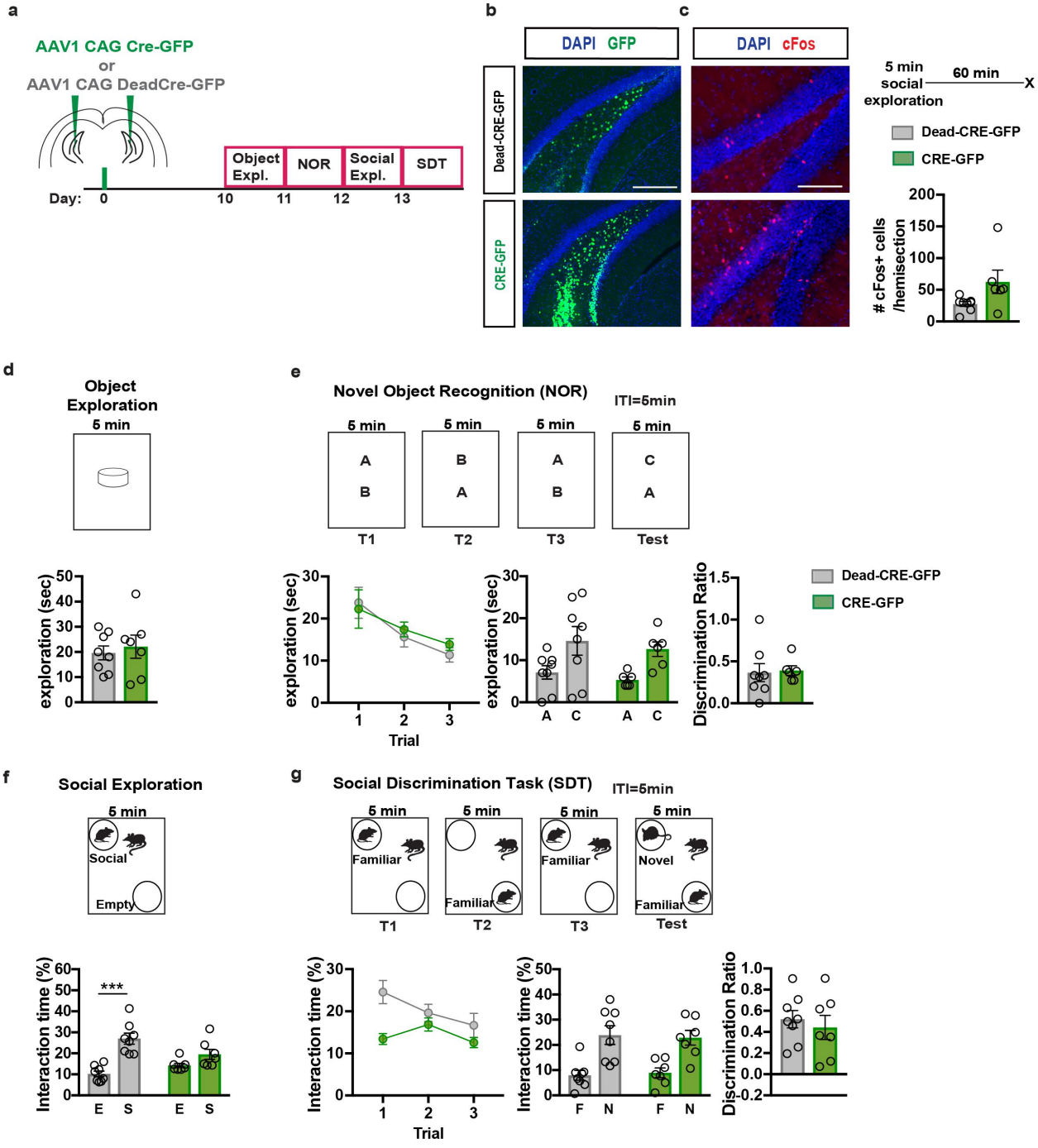
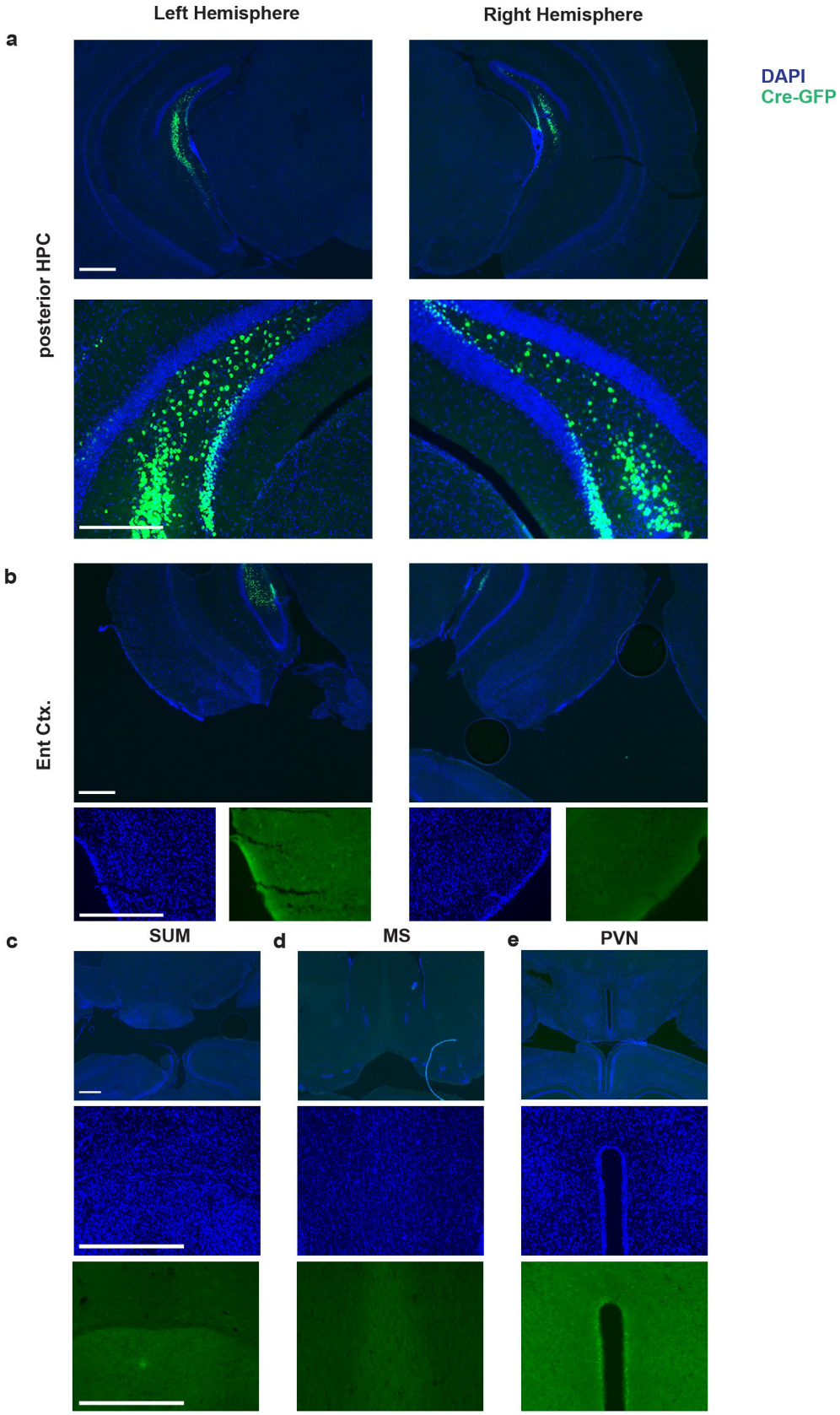


Figure 2.9 | Viral expression of AAV_1-CAG-Cre-GFP in posterior DG is not retrogradely trafficked.

(**a**) Low magnification (top) and high magnification (bottom) images of posterior hippocampus at the site of injection in pDG. Scale bars denote 500 μm (top) and 300 μm (bottom). (**b**) Low magnification (top) and high magnification (bottom) images of Entorhinal Cortex depicting lack of retrograde labeling from pDG. Scale bars denote 500 μm (top) and 600 μm (bottom). (**c**) Low magnification (top) and high magnification (bottom) images of SUM depicting lack of retrograde labeling from aDG. Scale bars denote 500 μm (top) and 600 μm (bottom). (**d**) Low magnification (top) and high magnification (bottom) images of MS depicting lack of retrograde labeling from pDG. (**e**) Low magnification (top) and high magnification (bottom) images of PVN depicting lack of retrograde labeling from pDG.

Figure 2.9 (continued)



discrimination between familiar and novel social stimuli in trial 4 was unchanged (**Figure 2.8g**). Deletion of Oxtrs in pDG did not affect measures of innate anxiety in the open field test (OFT), but resulted in a trend towards increased time spent in open arms in the elevated plus maze (EPM, unpaired t-test, DeadCre vs Cre: $p = .0860$) (**Figure 2.10b,c**). Together, these data demonstrate a critical role for Oxtrs in the pDG in mediating motivation to explore social stimuli, but not ability to discriminate between them.

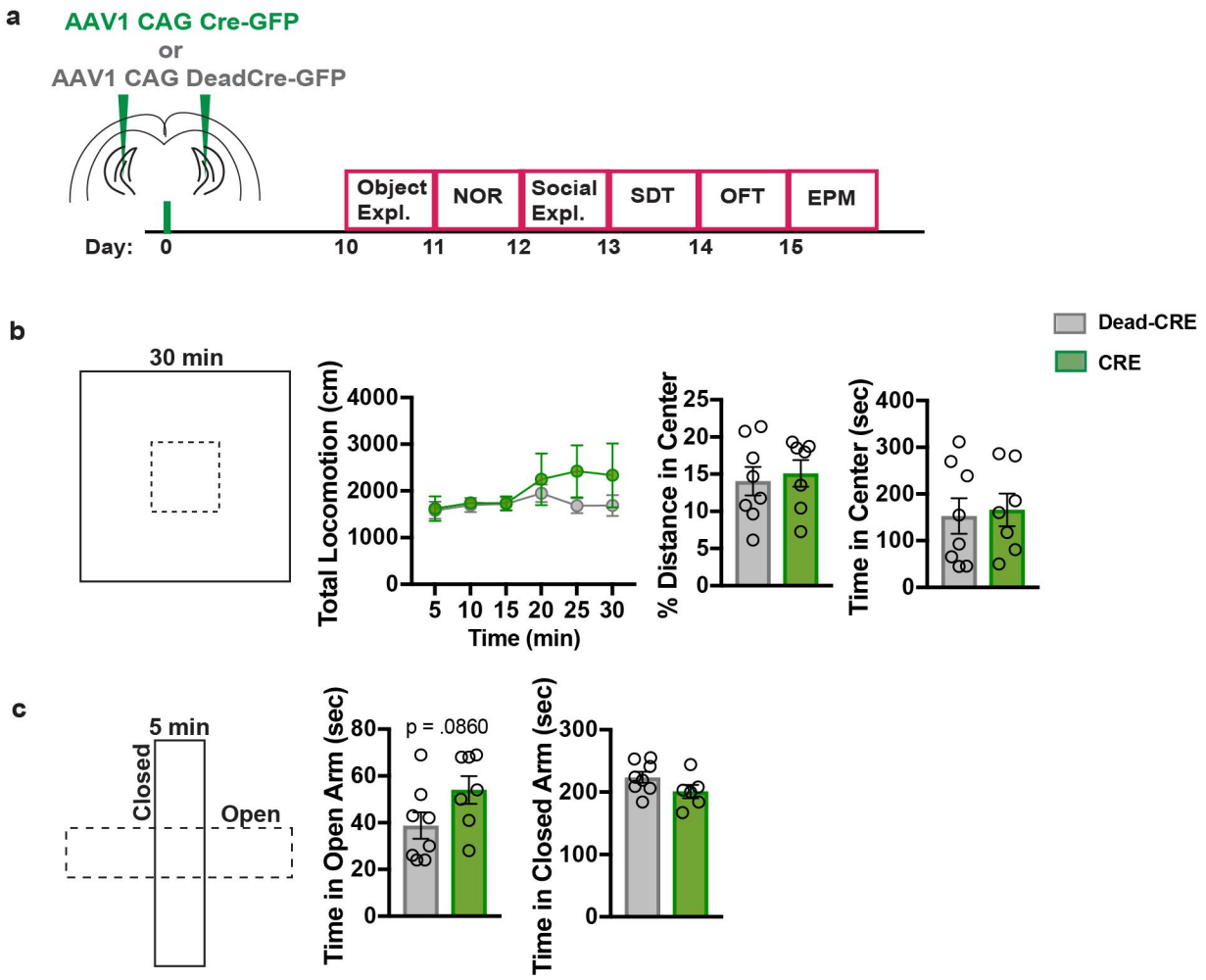


Figure 2.10 | Viral recombination of Oxtrs in posterior DG hilar neurons does not affect behavioral measures of innate anxiety.

(**a**) Schematic illustrating viral injection and behavioral testing timeline. (**b**) Schematic illustrating open field test (left) and quantification of total locomotion, percent distance in center, and time in center (right, DeadCre: n=8, Cre: n=7). (**c**) Schematic illustrating elevated plus maze (left) and quantification of time in open arm and time in closed arm (right, DeadCre: n=8, Cre: n=7). All data are displayed as mean ± SEM.

2.3 Discussion

Several studies over the last several years have utilized radioligand binding, antibody labeling, and reporter mouse lines to provide compelling evidence (to varying degrees of resolution) that the DG is a locus for the expression of the oxytocin receptor. Remarkably, until now, no studies have assessed the expression pattern of Oxtr in the DG, whether or not there may be a dissociation in expression along the DG long axis, and what the cellular identity of Oxtr-expressing neurons is. Additionally, no studies have directly probed the behavioral function of Oxtrs along the DG long axis, during social and non-social behaviors. Here, we utilize a combination of multiplex FISH, conditional deletion of the *Oxtr* gene, and behavioral assays for object, social, and anxiety-related behaviors to demonstrate, for the first time, a DG long-axis dissociation in Oxtr function whereby those in aDG mediate the discrimination of social stimuli, and those in pDG mediate social exploration.

Utilizing multiplex FISH to determine the expression pattern of the *Oxtr* gene yielded some consistencies in distribution of *Oxtr* expressing neurons in both the anterior and posterior DG. In both poles, *Oxtr* was restricted to hilar interneurons and mossy cells, and was conspicuously absent from dentate granule neurons in the GCL. However, differences existed at the level of cellular identity. In aDG hilus, the majority of cells were GABAergic interneurons, whereas in pDG hilus, greater than 50% of the cells were putative mossy cells. Previous reports utilizing the Oxtr-Venus knock-in reporter mouse line have indicated that Oxtr-expressing neurons in the aDG hilus are only 25% inhibitory interneurons, and are therefore predominantly excitatory mossy cells (Lin et al. 2017). This result stands in contrast to our data, which suggests that up to 90% of *Oxtr* expressing neurons in aDG were inhibitory interneurons, and only 10% were GAD1 negative putative mossy cells. These differences may be explained by a possible temporal turnover in Oxtr

expression in hilar neurons, whereby cells that previously expressed Oxtrs no longer do. Because EYFP protein and *Oxtr* mRNA may have different half-lives, persistent expression of EYFP may be observed in mossy cells that no longer express the *Oxtr* gene. Therefore, *Oxtr* mRNA distribution seems to be a more conservative readout for *Oxtr* expression. In contrast to aDG, Oxtr-expressing cells in the pDG hilus were comprised of a greater proportion of mossy cells (approximately 55%). The functional significance of this enrichment in *Oxtr* expression in mossy cells in the pDG will need to be further delineated in future studies, however some insights may be gleaned from the behavioral dissociation observed in our studies.

Given the explicit role of hilar interneurons and mossy cells as gatekeepers of DGC activity, this distribution pattern is suggestive that oxytocin may harness local DG microcircuitry to promote sparse representations of social stimuli. Indeed, mice lacking Oxtrs in anterior DG showed increased cFos activation in the GCL 60 minutes after a social exposure, as compared to controls. This result is reminiscent of the aDG hyperactivation observed in animals lacking *Oxtr* broadly in the forebrain (Ferguson et al. 2001). It is also consistent with slice physiology studies in the anterior DG demonstrate that Oxtr agonist potently activates GABAergic interneurons and mossy cells, thereby potentially inhibiting DGCs (Harden and Frazier 2016), a potential mechanism by which Oxtrs may promote pattern separation in the aDG. I did not observe a difference in pDG GCL cFos activation in the cohort of mice in which pDG Oxtrs were deleted, a result that is initially surprising. However, given that greater than 50% of these cells are mossy cells, which project more to DGCs distally along the longitudinal axis, rather than those more proximal, it is possible that pDG conditional Oxtr deletion may mediate activation of DGCs in aDG.

Behavioral assays of object and social behaviors demonstrate a specific role for aDG Oxtrs in mediating discrimination of social stimuli, but not non-social stimuli. Given that previous reports have implicated the aDG in object and context recognition, this result suggests that oxytocin adds an additional layer of neuromodulatory control to co-opt this circuit for social recognition. This result cannot be explained by any general effects on sociability or innate anxiety, and is consistent with previous literature implicating oxytocin in a variety of social, but not non-social tasks. In addition to the dissociation between object and social recognition in the aDG, I also observed a dissociation between aDG and pDG Oxtr function, wherein animals lacking Oxtrs in the pDG hilus did not demonstrate interest in engaging with a social stimulus during the test of social exploration, or upon initial exposure during the four-trial social discrimination test. Impressively, these animals retain the ability to discriminate between familiar and novel social stimuli during the fourth trial, suggesting that social exploration and social recognition may be mediated by distinct hippocampal circuitry. While all of these behavioral studies were only carried out in male subjects, I did not observe any sexual dimorphism in distribution pattern or cellular identity of Oxtr neurons anywhere along the DG long axis, suggesting that hippocampal Oxtrs may mediate similar functions in both males and females.

Collectively, these experiments suggest a double dissociation between DG Oxtr function along the hippocampal longitudinal axis, whereby those in the posterior DG gate social affiliation with conspecifics, and those in the anterior DG mediate discrimination between familiar and novel social stimuli. Such a dissociation is consistent with hippocampal long-axis theory in general, which proposes that the posterior pole is more engaged in unconditioned limbic responses such as fear and anxiety, and the anterior pole is more engaged in fine discrimination of contextual cues (Strange, Witter et al. 2014). These results suggest that oxytocin harnesses basic hippocampal

circuit mechanisms to mediate both affiliation with and discrimination between social stimuli. Because the act of discriminating between social stimuli innately requires preference for some social stimuli and not others (a form of sociability in itself), communication between anterior and posterior DG seems highly likely, and may be mediated by the large number of mossy cells in pDG that project longitudinally to aDG. Future studies utilizing *in vivo* calcium imaging of Oxtr-expressing cells in aDG and pDG in response to familiar and novel social stimuli may begin to elucidate a more nuanced mechanism of how these regions communicate with each other to subserve social cognition.

2.4 Methods

Mouse Lines and Animal Care

Two strains of mice were used in these experiments. Multiplex FISH experiments were carried out in C57Bl/6J mice. Oxytocin receptor conditional knock-out mice (*Oxtr* $^{f/f}$) rederived at Jackson Labs were utilized for viral mediated recombination of Oxtrs (Jackson Laboratories stock #008471). All experiments were carried out in adult male mice (8 weeks old). All mice were housed 3-5 per cage in standard laboratory conditions under a 12-hour light-dark cycle (7:00 a.m. to 7:00 p.m.) with ad libitum access to food and water. Behavioral testing occurred during the light cycle. All experiments were carried out in accordance with procedures approved by the Institutional Animal Care and Use Committee at the Massachusetts General Hospital in accordance with NIH guidelines.

Multiplex Fluorescence *in situ* Hybridization

FISH was carried out using ACDBio RNAscope multiplex fluorescence assay. Probes were obtained as following: C1: *PV* (Mm-Pvalb: 421931)*, Cre* (CRE: 312281), C2: *Oxtr* (Mm-Oxtr-C2: 402651-C2), C3: *Gad1* (Mm-Gad1-C3: 400951-C3)*, SST* (Mm-Sst-C3: 404631-C3). Brain tissue

was obtained from age-matched 8-10 week old male and female C57Bl/6J mice and immediately fresh-frozen in OCT on dry ice. 20 um sections were obtained using a cryostat (Leica, Germany) and stored at -80°C. Prior to RNAscope protocol, sections were incubated at -20°C for 1hour. RNAscope protocol was followed as indicated in user manual with adjustments as mentioned here. Briefly, sections were fixed with 4% chilled PFA for 30 or 60 minutes minutes and rinsed in 1X PBS for 5 minutes. Sections were then dehydrated in four 5 min dehydration steps in 50%, 75%, 100% and 100% ethanol respectively. Tissue was digested with Protease III for 30 min at room temperature and rinsed in 1X PBS. *Oxtr* and *Gad1* probes were diluted 1:50 in probe diluent and pipetted onto each slide. *Oxtr* and *SST* probes were diluted 1:50 in *PV* C1 probe and pipetted onto each slide. For assessment of OxtR knockout, *Oxtr* probe was diluted 1:50 in *Cre* C1 probe. Probe hybridization took place for 2 hours at 40°C and slides were then rinsed in 1X wash buffer. Sections were then incubated at 40°C in Amp1 for 30 min, Amp 2 for 15 min, and Amp3 for 30 min, and Amp4 for 15 min, with 1x Wash Buffer rinses between each incubation. Sections were finally mounted with DAPI Fluoromount and stored at -20°C.

For the assessment of Oxtr knockout, *Oxtr* $^{+/+}$ and *Oxtr* $^{f/f}$ mice were injected in aDG with AAV-CRE (AAV-hSyn Cre-GFP, diluted 1:100, .3ul bilaterally, in aDG).

Adeno-associated Viruses (AAV)

AAV_9-CamKIIα-GFP (6.27 x 10^{13} particles/mL) and AAV_9-hSyn-Cre-GFP (11.7 x 10^{13} particles/mL) were generated by and obtained from the University of Pennsylvania Vector Core (Philadelphia, Pennsylvania). AAV_1-CAG-Cre-GFP and AAV_1-CAG-DeadCre-GFP were generously donated by the laboratory of Dr. Larry Zweifel at the University of Washington.

Stereotactic Surgery

Viral Injections: Adult mice (8 week-old) were maintained under standard housing conditions. Mice were given carprofen (5mg kg^{-1} s.c.) prior to surgery and 24h later to minimize discomfort. Mice were anaesthetized with ketamine and xylazine (10mg mL^{-1} and 1.6mg mL^{-1} , i.p.) and placed in a stereotaxic frame (Stoelting). Small holes were drilled at each injection location and injected with a Hamilton microsyringe at a rate of 0.1 µl/min. For aDG KO experiment, .3 µl 1:1000 AAV9-hSyn-Cre-GFP or 1:50 AAV9-CamKIIα-GFP was injected bilaterally (AP -1.9 mm, ML +/- 1.1 mm, DV -2.6 mm from Bregma) into *Oxtr f/f* mice. For pDG KO experiment, .4 µl of AAV1-CAG-Cre-GFP or AAV1-CAG-deadCre-GFP was injected bilaterally (AP -3.0 mm, ML +/- 2.7 mm, DV -4.0 mm from Bregma). After completion of the injection, the needle was left on the site of injection for 5 min, raised 0.2 mm and left on the site for an additional 5 min to allow diffusion of virus at the injection site and then slowly withdrawn. The skin incision was closed carefully using nylon sutures. Animals were monitored during recovery.

Single Object Exploration

Mice were placed an arena filled with bedding (45cm long, 15cm high and 30cm wide) with a single novel object for 5 minutes. Sessions were video-recorded, and videos were manually scored for object exploration (when an animal's snout was 2cm or less from the object) by an investigator blind to animal treatment identity.

Novel Object Recognition

Mice were placed in an arena filled with bedding (45cm long, 15cm high and 30cm wide) with two distinct objects (A and B) for three 5 min sessions, with a 5 minute intertrial interval. Mice habituated to the objects during the three training sessions, and one of the objects was subsequently replaced with a novel object (C) in session four. Objects were counterbalanced across subjects and

object positions were counterbalanced across trials. The objects that were selected for testing elicited comparable levels of exploration based on exploration levels in pilot experiments. Sessions were video-recorded, and videos were manually scored for object exploration (when an animal's snout was 2cm or less from the object) by an investigator blind to object identity and animal treatment identity.

Social Exploration

Mice were placed in an open plexiglass arena (41cm x 41 cm, Kinder Scientific) for 5 minutes with two pencil-wire cups placed on opposing corners of the arena. Habituation to the chamber took place one day prior to start of behavioral testing. One cup remained empty while the other contained a novel adult male C57Bl/6J mouse. Sessions were video-recorded, and videos were manually scored for exploration of the social cup and empty cup (direct snout-to-cup contact, with at least two paws on the ground--time spent climbing on the cup was not included) by an investigator blind to animal treatment identity. Stimulus mice were trained to sit in pencil-wire cups for three 15 minute sessions several days prior to behavioral testing.

Social Recognition (Habituation, Discrimination)

The same plexiglass arena and pencil-wire cup set-up as described for social exploration was used. Mice were placed in the arena for three 5 min sessions with an empty cup and a novel adult male C57Bl/6J mouse, with a 5 minute intertrial interval. Mice habituated to the stimulus during the first three sessions, rendering it "familiar." During trial 4, a novel adult male mouse was placed in the opposing cup, and subjects were tested for discrimination between the novel and familiar mouse. Social stimuli were counterbalanced across subjects, and the position of the familiar social stimulus was counterbalanced across trials. Sessions were video-recorded, and videos were manually scored for interaction with the novel vs familiar mouse (direct snout-to-cup contact, with

at least two paws on the ground--time spent climbing on the cup was not included) by an investigator blind to animal treatment identity. Stimulus mice were trained to sit in pencil-wire cups for three 15 minute sessions several days prior to behavioral testing. Videos were scored by two different investigators.

Open Field Test

Locomotor behavior was recorded for 30 min divided in six 5 min epochs in a Plexiglas open-field (OF) box of 41 x 41cm (Kinder Scientific) with 16 sets of double stacked pulse-modulated infrared photobeams (SmartFrame Open Field System; Kinder Scientific, Poway, CA) equally spaced on every wall (128 total) to record x-y ambulatory movements. MotorMonitor Software (Kinder Scientific, Poway,CA) defined grid lines that divided the open field into center (25% of total area) and periphery (75% of total area), with the periphery consisting of the 10 cm closest to the wall around the entire perimeter. Dependent measures were the overall motor activity quantified as the total locomotion (in centimeters), the distance traveled in the center divided by total distance traveled (percentage distance in center), and the time spent in the center (seconds). For *Oxtr f/f* DG cohort, two cohorts were used in order to increase Ns, and tests for innate anxiety (OFT and EPM) were performed only on the first cohort.

Elevated Plus Maze

Innate anxiety was recorded in the elevated plus maze (EPM) for 5 min. The maze consisted of a black Plexiglas apparatus placed 1m above the floor, with two open arms (67 cm x 7 cm) perpendicular to two enclosed arms (67 x 7 x 17 cm). The four arms were separated by a neutral transition central square (5 x 5 cm) in which mice were placed at the beginning of the experiment and their behavior was recorded for 5 min with a video camera system (ViewPoint, Lyon, France) located above the maze. Cumulative time spent in the open, closed, and center arms was scored

manually by an investigator blind to the treatment conditions and data were expressed as the time spent in open arms (seconds) and time spent in closed arms (seconds). An arm visit was recorded when the mouse moved its forepaws into the arm. For *Oxtr* $^{f/f}$ DG cohort, two cohorts were used in order to increase Ns, and tests for innate anxiety (OFT and EPM) were performed only on the first cohort.

aDG genetic deletion cohorts

For Figure 2 and the corresponding Figure S3, number of animals is variable across behaviors because two different cohorts were used. The first cohort (n=7,4) was used for all behaviors and cFos analysis. The second cohort (n=4,2) was used to increase the N for the four behaviors in the main Figure, but was not used for anxiety (OFT, EPM) or cFos analysis.

Histology and Immunohistochemistry

Mice were anesthetized with ketamine (100 mg kg^{-1} i.p.) and xylazine (3 mg kg^{-1} i.p.) and transcardially perfused with 10mM phosphate buffer saline (PBS), pH 7.5 at 4°C, followed by a fixative solution containing 4% paraformaldehyde (PFA) in PBS. Brains were post-fixed in 4% PFA overnight at 4°C and cryo-protected for 72 hours in 30% sucrose at 4°C prior to freezing in OCT on dry ice. Coronal sections were obtained at 35 μm using a cryostat (Leica, Germany) in six matched sets. Sections were stored in 1X PBS with 0.01% Azide at 4°C. Floating sections were used to perform immunohistochemical labeling. Briefly, sections were washed in 1X PBS, incubated for 15 min at room temperature in 1X PBS containing .3% Triton X-100, blocked in 1X PBS containing .3% Triton X-100 and 10% NDS for 1 hour at room temperature, and incubated in primary antibodies in blocking buffer with shaking overnight at 4°C. Primary antibodies were used as follows: GFP (rabbit anti-GFP, Life Technologies A11122, 1:500, Antibodyregistry.org: AB_221569); goat anti-GFP, Novus Biologicals, NB100-1770, 1:500, (Antibodyregistry.org:

AB_10128178), cFos (Rabbit, Santa Cruz, 1:2000, Santa Cruz SC52, Antibodyregistry.org: AB_2106783). The following day, sections were washed 3 times in 1X PBS and incubated with fluorescent-label-coupled secondary antibodies (Jackson Immunoresearch, Donkey anti-Rabbit, Goat, or Mouse, 488-, Cy3-, or Cy5- coupled, 1:500) for 2 hours at room temperature.

cFos and Perfusion

Mice were exposed to a novel social stimulus in a novel arena filled with bedding for 5 minutes, and promptly returned to home cage. Mice were then anesthetized with ketamine (100 mg kg^{-1} i.p.) and xylazine (3mg kg^{-1} i.p.) and transcardially perfused 60 minutes post exposure, as described above in "Histology and Immunohistochemistry."

Image Acquisition and Analysis

For RNAscope Multiplex FISH: 20x, 40x, or 60x Confocal z-stack images were obtained with a Nikon A1R Si confocal laser. Images were acquired at 1024 resolution as 10μm z-stacks with a step size of 2μm. For colocalization analysis, cells were manually identified as *Oxtr*$^+$, *Gad1*$^+$, *SST*$^+$, and/or *PV*$^+$ or double positive and expressed as a percentage of *Oxtr*$^+$ cells (for DG) or as a percentage of *SST*$^+$, or *PV*$^+$ cells (for pCA2/CA3). For *Oxtr* mean intensity calculated for CA regions, mean intensity was measured for the region comprised by the principal layer. A similar sized region from background area was measured for intensity and subtracted from mean *Oxtr* intensity in order to control for differences in background. For *Oxtr* knockdown analysis, all DAPI nuclei per image were counted (for DG injections: cells in the hilus, excluding granule cell layer and CA3 were counted) and cells were manually identified as *Oxtr*$^+$, *Cre*$^+$, and/or *OxtR*$^+$*CRE*$^+$ double positive. The *Oxtr*$^+$ population was expressed as a percentage of total DAPI cells.

For cFos analysis: 10x bilateral images were acquired using a Nikon epifluorescence microscope. cFos+ cells were manually quantified as those with intensity higher than background in the aDG

or pDG granule cell layer. Both blades were assessed. Data was expressed as # cFos+ cells per section or hemi-section. All quantifications and analyses were completed by an experimenter blind to treatment condition.

Statistics

Statistical analysis was carried out using GraphPad Prism v7 software. Data (mean ± SEM). Discrimination ratios, cFos analysis, and measures of object exploration were analyzed using unpaired two-tailed student's t-test to compare two groups. Measures of NOR, social exploration, and social discrimination were analyzed using mixed factor two-way ANOVA with repeated measure followed by Bonferroni's multiple comparisons test when the interaction, p value was < .05. In all cases, significance was set at $p < 0.05$.

2.5 Author Contributions

T.R. carried out experiments and analyzed data with help from K.M.M., and A.B.

A.V. contributed reagents and shared resources.

T.R. and A.S. co-developed the concept and wrote the manuscript.

A.S. conceived and supervised all aspects of the project.

2.6 Acknowledgments

We thank members of the Sahay lab for their comments on the manuscript. A.S. acknowledges support from US National Institutes of Health Biobehavioral Research Awards for Innovative New Scientists (BRAINS) 1-R01MH104175, NIH-NIA 1R01AG048908-01, NIH-NIMH 1R01MH111729-01, Ellison Medical Foundation New Scholar in Aging, Whitehall Foundation, Inscopix Decode award, NARSAD Independent Investigator Award, Ellison Family Philanthropic support, Blue Guitar Fund, Harvard Neurodiscovery Center/MADRC Center Pilot Grant Award, HSCI Development grant, and HSCI seed grant

CHAPTER 3

Oxytocin receptors in CA2/CA3 promote discrimination of social stimuli

This chapter is adapted from a manuscript published in *Nature Communications* (Dec 8, 2017), included as Appendix 1

Hippocampal oxytocin receptors are necessary for discrimination of social stimuli

Tara Raam[1,2,3,4], Kathleen M. McAvoy[1,2,3], Antoine Besnard[1,2,3], Alexa Veenema[5], Amar Sahay[1,2,3,4,6]

[1]Center for Regenerative Medicine, Massachusetts General Hospital, Boston, MA 02114, USA

[2]Harvard Stem Cell Institute, Cambridge, MA 02138, USA

[3]Department of Psychiatry, Massachusetts General Hospital, Harvard Medical School, Boston, MA 02114 USA

[4]Department of Psychology, Michigan State University, East Lansing, MI, 48824

[5]Broad Institute of Harvard and MIT, Cambridge, MA 02142, USA

[6]Program in Neuroscience, Harvard Medical School, Boston, MA 02115, USA

Corresponding Author: Amar Sahay, asahay@mgh.harvard.edu

3.1 Introduction

The primary output region of the dentate gyrus is generally thought to be CA3, an adjacent hippocampal subregion which receives direct, powerful synapses from the DG called mossy fibers. Traditional theories of the hippocampus have depicted CA3 as a pattern completion region, owing to its dense recurrent collaterals that facilitate the recall of a whole representation from a partial cue. However, recent studies have allowed for a more nuanced understanding of CA3 computations by depicting it as a functionally heterogeneous structure in which regions closest to the DG perform pattern separation computations, and those furthest from the DG mediate pattern completion. Just beyond CA3 lies the peculiar hippocampal subregion CA2, which has remained underappreciated in hippocampal literature. In the last few years, CA2 (and to some extent CA3) has gained increasing attention due its unique role in mediating social recognition memory. Interestingly, CA2 and CA3 receive direct input from the PVN of the hypothalamus, and densely express receptors for the social hormones arginine-vasopression and oxytocin in the pyramidal cell layer (Avpr1b and Oxtr). While the contribution of Avpr1b to social memory has been delineated by multiple groups, no studies to date have examined the contribution of CA2/CA3 Oxtrs to social memory, and whether or not they may also mediate non-social memory. Further, despite the unique role that oxytocin plays in enhancing signal to noise processing in diverse regions of the brain, including the hippocampus, it is also not known whether CA2/CA3 Oxtrs mediate population-based coding of social stimuli that promotes effective discrimination at the behavioral level. Here, we utilize a combination of FISH, viral genetics, pharmacology, behavioral assays for social and object recognition, and ensemble mapping to demonstrate that Oxtrs in CA2/CA3 specifically promote social, but not non-social memory. Furthermore, we demonstrate for the first time, an Oxtr-dependent hippocampal mechanism that segregates social stimuli into unique ensembles.

3.1.1 Remapping mechanisms in CA subregions.

The discrimination of similar stimuli requires cellular mechanisms by which similar or overlapping information is uncoupled, a process that when disrupted can result in interference or generalization (Besnard and Sahay 2016). One such mechanism is remapping in the hippocampus, which falls under two general categories: rate remapping and global remapping (Colgin et al. 2008). Rate remapping occurs when a single ensemble of neurons alters its firing rate in order to encode changes in the environment. In contrast, global remapping is primarily characterized by distinct populations of neurons encoding these changes, but may also involve changes in firing rate. Within the framework of discrimination of contextual cues, it is thought that rate remapping may occur as a result of subtle changes in the environment, while global remapping may occur as a result of more drastic changes in the environment, such as altering contexts or spatial locations altogether (Colgin et al. 2008).

Within the hippocampus, division of labor renders different structures suitable for different functions. A recent electrophysiological study by Lee and colleagues demonstrates that along the transverse axis, remapping in CA3 follows a functional gradient-like organization. The region of CA3 most proximal to the DG ($CA3_{proximal}$) functions most akin to the DG as a pattern separator, and the region of CA3 most distal to the DG ($CA3_{distal}$) functions more as a pattern completion region (Lee et al. 2015). Firing rates and place field size gradually increase along this axis from $CA3_{proximal}$ to $CA3_{distal}$, suggesting that $CA3_{proximal}$ encodes spatial and contextual information with greater specificity (Lee et al. 2015).

This functional heterogeneity may be mediated by a number of anatomical gradients. One possible mechanism by which $CA3_{distal}$ may more readily pattern complete is through its highly interconnected recurrent collateral pathway in which CA3 pyramidal neurons form synapses onto

neighboring CA3 neurons (Miles and Wong 1983; Miles and Wong 1986; Ishizuka et al. 1990; Witter 2007). This network is thought to facilitate pattern completion by mediating rapid retrieval of a complete memory by a partial cue (McNaughton and Morris 1987; Treves and Rolls 1994; Le Duigou et al. 2014; Neunuebel and Knierim 2014). While these collaterals do extend back along the transverse axis, their projections to $CA3_{proximal}$ are weakest. In addition, $CA3_{proximal}$ receives mossy fiber input from both blades of the DG, while $CA3_{distal}$ receives input only from the suprapyramidal (upper) blade, suggesting less input from the DG, which is the primary pattern separation region of the hippocampus (Witter 2007).

Just beyond $CA3_{distal}$, immediately before the transition to CA1, lies a sliver of pyramidal neurons referred to as CA2, that had been largely neglected within hippocampal literature until the past few years (Dudek et al. 2016). Originally discovered by Rafael Lorente de Nó, CA2 was thought to lack input from the DG due to its absence of thorny excrescences, the enlarged dendritic spines associated with mossy fiber terminals (Lorente de Nó, 1934). However, more recent studies utilizing genetic strategies to target DG output have determined functional monosynaptic mossy fiber input that extend into CA2 (Kohara et al. 2014). Additionally, CA2 also preferentially targets the deep layer of CA1, whereas CA3 targets the superficial layer of CA1 (Kohara et al. 2014). Curiously, CA2 pyramidal neurons are unusual in that they are highly resistant to LTP induction and cell death, however the functional significance of these properties is not well understood (Sloviter and Damiano 1981; Zhao et al. 2007; Chevaleyre and Siegelbaum 2010).

3.1.2 Behavioral significance of CA2/CA3.

Functionally, the CA2 subregion is thought to mediate a diverse range of behaviors, that seem to at least partially overlap with behaviors mediated by CA3, such as spatial learning, temporal encoding, immobility, object recognition, and most notably, social behaviors.

While the role of the hippocampus in forming the brain's internal navigation system has been well defined by John O'Keefe and Edvard and May-Britt Moser and colleagues over the past few decades, few studies had determined what role, if any, CA2 may play in processing spatial information. An early study that knocked out the gene *RGS14*, which is commonly used as a marker to demark the anatomical boundaries of CA2, demonstrate enhanced spatial memory performance in the Morris water maze, and allows for induction of LTP (Lee et al. 2010). The first study to perform *in vivo* recordings of CA2, by Mankin and colleagues, found that CA2 is characterized by increased peak firing rate and greater number of place fields than CA3 and CA1. Additionally, these place fields were larger in size and carried less spatial information than CA3 and CA1 (Mankin et al. 2015), suggesting that CA2 does encode some spatial information, but not as robustly as its neighboring regions. In contrast, CA2 activity patterns reliably change over time, even when the animal is located in the same context, suggesting that CA2 place fields are less stable than those of CA3, and that CA2 may encode temporal information with greater fidelity than spatial information (Mankin et al. 2015). These results corroborate older findings that mice lacking the Avpr1b gene (which is most densely expressed in CA2 in the mouse brain) show normal memory for the identity of objects, and the spatial location in which the objects were encountered, but showed impaired recognition for the temporal order in which the objects were learned (DeVito et al. 2009).

There is also some evidence that the CA2/CA3 subregion may play a role in locomotion. *In vivo* single unit records of hippocampal CA subregions indicate that a subset of CA2 pyramidal neurons fire at high rates during periods of immobility as an animal navigates a W-shaped maze, and that this firing pattern is not correlated with the timing of sharp-wave ripples (Kay et al. 2016). In this sense, CA2 stands out from CA3 and CA1 in that pyramidal neurons of the latter two regions

generally exhibit firing patterns that align with the timing of sharp-wave ripples (Kay et al. 2016). CA3 has also previously been shown to regulate state-dependent increases in running speed via its projections to the lateral septum, however whether or not CA2 also performs this function is not known (Bender et al. 2015).

A number of studies have also converged on the notion that the activity of CA2 is sensitive to objects and may mediate novel object recognition. Very subtle changes in a context induced by swapping out one object for another leads to dramatic changes in ensemble overlap in CA2, as measured by fluorescence *in situ* for *Arc1* mRNA (Wintzer et al. 2014). A similar study utilizing *in vivo* recordings of CA2 cell bodies demonstrate that CA2 place fields undergo global remapping when exposed to a novel object (Alexander et al. 2016). The original loss of function study by Lee and colleagues mentioned above, demonstrated that deletion of *RGS14* in CA2 enhanced object recognition as compared to control animals, and this was associated with induction of LTP at CA2 synapses (Lee et al. 2010). Together, these studies suggest that CA2 may play an important role in promoting appropriate behavioral responses to contextual cues by encoding object-related information, a function that closely mimics the functions of CA3 and CA1 (Kesner 2007; Cohen et al. 2013).

Perhaps the most intriguing function of CA2 (and to some extent, CA3) that has garnered much attention in systems and behavioral neuroscience in the past few years is its unique role in promoting social memories. In a study using *in vivo* recordings of rats, Alexander and colleagues show altered place fields in response to familiar and novel social stimuli, suggestive of global remapping, in aCA2 cell bodies but not aCA1 (Alexander et al. 2016). These reductions in spatial correlation of aCA2 place fields were not accompanied by an overall change in peak firing rate, indicating that the effects on global remapping were not simply due to a general increase or

decrease of network activity (Alexander et al. 2016). Loss of function strategies have yielded further evidence to support a role for CA2 in social memory. Bilateral excitotoxic lesion of CA2 produced deficits in both sociability and discrimination of familiar and novel social stimuli (Stevenson and Caldwell 2014), however the extent to which the lesioned area is restricted to CA2 versus CA3, and its spread along the longitudinal axis, is difficult to control in lesion studies. The emergence of novel genetic strategies to isolate CA2 and drive Cre-dependent expression of tetanus toxin to prevent excitation of CA2 pyramidal neurons yields greater specificity. In a landmark paper using this strategy, Hitti and Siegelbaum demonstrate deficits in a rigorous 5-trial assay of habituation and dis-habituation to familiar social stimuli (Hitti and Siegelbaum 2014). In contrast to other observations, this manipulation did not suggest a role for CA2 in other hippocampus-dependent measures of memory, such as novel object recognition, contextual fear conditioning, and spatial memory, suggesting that this genetic strategy may have targeted a specific sub-set of CA2 neurons that, through either neuromodulatory mechanisms or connectivity patterns may specifically modulate social memory (Hitti and Siegelbaum 2014). A further study study by Boehringer and colleagues using the same manipulation demonstrated that CA2 output to CA3 is primarily inhibitory (Boehringer et al. 2017). CA2 recruits feed-forward inhibition to dampen CA3 network excitability, such that animals in which CA2 is chronically silenced show increased CA3 recurrent activity and a higher likelihood of co-activation of CA3 neurons (Boehringer et al. 2017). Thus, CA2 may serve as a modulator of social ensembles in CA3, and may regulate the probability of coincidence between representations of two social stimuli.

Interestingly, CA2 receives direct vasopressin releasing terminals from the paraventricular nucleus of the hypothalamus (PVN) (Cui et al. 2013; Zhang and Hernandez 2013; Smith et al. 2016), and expression of the receptor for arginine-vasopressin (Avpr1b) throughout is almost

entirely confined to CA2 (Young et al. 2006). Avpr1b knockout mice show robust deficits in both sociability and social novelty seeking, which is likely to be mediated by Avpr1b in CA2 (DeVito et al. 2009). Furthermore, direct optical stimulation of vasopressin-releasing terminals from the PVN onto CA2 pyramidal neurons is sufficient to enhance social memory (Smith et al. 2016). In addition to social approach and social novelty seeking behaviors, vasopressin is also thought to mediate attack behavior indicative of aggression. Avpr1b knockout mice show a reduction in aggressive-like behavior (Wersinger et al. 2002), and lentiviral mediated delivery of Avpr1b to aCA2 alone is sufficient to restore this reduction (Pagani et al. 2015).

The study of social interactions may be one of the few subfields of hippocampal function in which CA2 has received more attention than CA3. Little is known about the contributions of CA3 to social behaviors and how they may recapitulate or differ from than the contributions of CA2. However, a few initial studies do offer some evidence for engagement of CA3 in social behaviors, yet the data is sparse and disparate. Conditional deletion of BDNF, a key regulator of synaptic plasticity, in CA3 neurons using a KA1-Cre mouse line, increases attack behaviors associated with aggression, but does not affect measures of social recognition (Ito et al. 2011). Two studies of NMDA NR1 subunit function in CA2/CA3 also provide insight. One study relied upon viral injection of Cre into aCA2/CA3 of adult NR1-floxed mice and showed reduced sociability, but no effect on discrimination of social stimuli (Finlay et al. 2015). However, a more recent study utilizing chronic deletion of NR1 in CA3 via KA1-Cre mice shows the opposite result: a deficit in discrimination of social stimuli, but no effect on sociability (Chiang et al. 2018). Discrepancies in these two studies may arise from the fact that the experiments carried out by Finlay and colleagues employed virally injected Cre virus into aCA2/CA3 in adult mice, whereas the manipulation carried out by Chiang and colleagues employed chronic silencing throughout

development, and may also reflect effects of KA1-Cre positive cells in pCA2/CA3. Attenuation of aCA3 and pCA3 cell bodies via DREADDS showed a specific role for pCA3, but not aCA3 in social memory (Chiang et al. 2018), an intriguing result given the role of pCA1 in social memory (Okuyama et al. 2016). Collectively, these studies suggest that CA3 encodes social information that may be relevant to social affiliation or social novelty seeking, however further studies will need to be carried out that more specifically regulate the site of manipulation to CA3 specifically, without effects on CA2.

3.1.3 Modulation of CA2/CA3 via oxytocin.

While the contribution of oxytocin receptors to social memory has long been understood through pioneering studies utilizing whole-brain and forebrain conditional deletion of oxytocin receptors, only recently have several groups converged on CA2/CA3 as a specific site of action of oxytocin. Within the hippocampus, the CA2/CA3 subregion is a privileged recipient of direct projections from the paraventricular nucleus of the hypothalamus (PVN), where the social hormones oxytocin and arginine-vasopressin are synthesized. Anterograde mapping of outputs from the PVN results in illumination of terminals in aCA2/CA3 (Cui et al. 2013; Mitre et al. 2016; Smith et al. 2016), while retrograde mapping of inputs onto aCA2/CA3 via CTB injection results in cell body labeling in the PVN that colocalizes with antibodies for oxytocin (Lin et al. 2017). Additionally, aCA2/CA3 also expresses receptors for oxytocin. Early studies utilizing radioligand binding of Oxtr demonstrate enriched expression in aCA2/CA3 of mice (Lee et al. 2008; Hammock and Levitt 2013). These observations have been corroborated by the development of antibodies that bind Oxtr protein, also yielding dense expression in aCA2/CA3 (Mitre et al. 2016). Complimentary approaches utilizing mouse genetics have also converged on similar findings. Knock-in reporter lines that express Venus-EYFP under the regulatory region of the *Oxtr* gene

also demonstrate expression in the pyramidal cell layer of aCA2/CA3 (Yoshida et al. 2009; Lin et al. 2017). Similarly, injection of AAV-FLEX-mCherry in aCA2/CA3 of *Oxtr-Ires-Cre* knock-in mice that drive the expression of Cre-recombinase under the control of the *Oxtr* demonstrates enriched expression of mCherry in aCA2/CA3 (Hidema et al. 2016). Additional studies that have fluorescently labeled *Oxtr* mRNA also converges on the above findings (Smith et al. 2016; Lin et al. 2017; Lin et al. 2018). Interestingly, many of these studies have additionally noted a sharp dissociation between aCA2/CA3 and aCA1, wherein aCA1 shows little to no expression of Oxtrs. This selective enrichment of Oxtrs in the CA2/CA3 subregion appears to be consistent across rodent species such as prairie voles (Freeman et al. 2014). However, no studies to date have delineated Oxtr expression in specific CA3 subregions, and the particular CA2/CA3 cell types in which Oxtrs are expressed is not known (Yoshida et al. 2009; Lin et al. 2017).

Despite our knowledge that aCA2/CA3 is a locus for Oxtr expression, we know very little about what function oxytocin performs in this circuit. Physiologically, bath application of OXT induces membrane depolarization of aCA2/CA3 pyramidal neurons, as well as rapid firing of action potentials in response to a postsynaptic current injection, effects that are not observed in knockout mice lacking the *Oxtr* gene (Lin, Chen et al. 2017). This excitatory response is specific to CA2 and CA3, but absent in CA1, where expression of Oxtr is absent (Pagani et al. 2015). Conditional deletion of aCA2/CA3 *Oxtr* also impairs the induction of LTP at direct entorhinal cortex (EC) inputs to CA2/CA3, such that twice as much presynaptic stimulation is required to achieve the same amount of postsynaptic potentiation as control animals (Lin et al. 2018). Bath application of OXT also induces synaptic potentiation of EC inputs to aCA2/CA3, while application of OXT antagonist decreases EPSC amplitude at EC synapses onto aCA2/CA3 (Lin et al. 2018).

In addition to mediating synaptic strength of inputs onto aCA2/CA3 pyramidal neurons, oxytocin is also thought to enhance spike transmission in aCA2/CA3 outputs to aCA1 (Owen et al. 2013), a finding consistent with broader theories that oxytocin may modulate signal-to-noise in widespread circuits throughout the brain. Bath application of the Oxtr-agonist TGOT during stimulation of aCA2/CA3 input to aCA1 enhances the probability of evoked, but not spontaneous spiking in aCA1 pyramidal neurons (Owen et al. 2013). This effect is mediated by GABAergic fast-spiking interneurons (FSIs), but not regular-spiking (RS) interneurons—application of TGOT strongly depolarizes FSIs that exert perisomatic inhibition onto CA1 pyramidal neurons, but does not influence RSIs (Owen et al. 2013). Additionally, examination of CA1 pyramidal neurons under voltage clamp mode while stimulating Schaeffer Collaterals, enabling isolation of EPSCs and IPSCs, reveals that TGOT reduces the evoked disynaptic IPSC, but does not affect the monosynaptic EPSC, shifting the excitation-inhibition balance to promote greater spike fidelity. Together, these studies suggest that oxytocin may play a role in regulating synaptic strength and promoting excitation-inhibition balance in aCA2/CA3 circuitry. However, no studies to date have tested the behavioral relevance of Oxtrs in aCA2/CA3, therefore whether these physiological properties are engaged in promoting social memories is not known. Here, we begin to probe the role of Oxtrs in aCA2/CA3 in social behaviors.

3.2 Results

3.2.1 Characterization of Oxtr expression in aCA2/CA3 and aCA1.

To comprehensively map the expression of *Oxtr* in aCA2/CA3 subregions and aCA1, I performed multiplex fluorescence *in situ* hybridization (FISH) using riboprobes directed against *Oxtr*, Glutamate Decarboxylase 1 (*Gad1),* a marker for GABAergic inhibitory neurons, and markers of interneuron subpopulations, Parvalbumin (*PV*), and Somatostatin (*SST)* in age-matched

male and female mice. I analyzed *Oxtr* expression within anterior CA subfields: $aCA3_{proximal}$, $aCA2/CA3_{distal}$, and aCA1 (schematic shown in **Figure 3.1h**). Quantification of *Oxtr* intensity revealed enrichment of *Oxtr* expression in the $aCA2/CA3_{distal}$ region while *Oxtr* levels in $aCA3_{proximal}$ and aCA1 were comparable to that of background (**Figure 3.1a,b,c,g**). Colocalization analysis of *Oxtr* and *Gad1* in $aCA2/CA3_{distal}$ subregion revealed low overlap (10.1% in females and 8.9% in males, **Figure 3.1c,d**) suggesting that the vast majority of *Oxtr* expressing cells in $aCA2/CA3_{distal}$ are excitatory. Assessment of overlap between *Oxtr*, *PV* and *SST* in $aCA2/CA3_{distal}$ revealed a larger fraction of PV cells than SST cells that were double positive for the *Oxtr* gene (**Figure 3.1e,f**). I did not detect sexual dimorphism in *Oxtr* expression within any subregion of aCA2/CA3 or aCA1.

3.2.2 $aCA2/CA3_{distal}$ Oxtrs are necessary for social discrimination.

Because CA2/CA3 is the primary output of the DG, and aDG *Oxtrs* are critical for social memory, I next sought to assess the contributions of Oxtr in $aCA2/CA3_{distal}$ to object and social recognition. I preferentially targeted the principal layer of $aCA2/CA3_{distal}$ of *Oxtr* $^{f/f}$ mice by employing a virus that drives expression of Cre-recombinase under a CamKIIα promoter (**Figure 3.2a,b**). Cre virus was expressed predominantly in pyramidal neurons (92.8%), and a small percentage of GABA-ergic interneurons (7.3%) (**Figure 3.4b**). I did not observe any retrograde or anterograde transport of Cre virus to inputs or outputs of $aCA2/CA3_{distal}$ in sections immunolabeled for GFP (**Figure 3.3a-c**). To determine recombination of *Oxtrs* in $aCA2/CA3_{distal}$, we quantified the percentage of DAPI+ cells expressing *Oxtr* mRNA in $aCA2/CA3_{distal}$ of *Oxtr* $^{+/+}$ vs. *Oxtr* $^{f/f}$ mice injected with AAV_9- CamKIIα-Cre. *Oxtr*+ cells comprised 50% of all DAPI+ cells in *Oxtr*$^{+/+}$ mice, and 25% of all DAPI+ cells in *Oxtr* $^{f/f}$ mice (**Figure 3.3d,e**). Interestingly, while we observed fewer total DAPI+ cells that were positive for *Oxtr* in *Oxtr* $^{f/f}$ mice, we observed larger *Oxtr* puncta

Figure 3.1 | Characterization of *Oxtr* expression in anterior CA2/3 and CA1.

(**a**) Representative low-magnification (left) and high-magnification (right) images of *Oxtr* and *Gad1* mRNA expression in $aCA3_{proximal}$ by FISH (n=4 males, 3 females). Scale bar denotes 100 μm. Inset scale bar denotes 50 μm. (**b**) Quantification of mean *Oxtr* intensity for CA regions expressed in arbitrary units, normalized for background. (**c**) Representative low-magnification (left) and high-magnification (right) images of *Oxtr* and *Gad1* mRNA expression in $aCA2/CA3_{distal}$ by FISH (n=4 males, 3 females). Asterisk (*) denotes $Oxtr^+/GAD1^+$ interneuron. Scale bar denotes 100 μm. Inset scale bar denotes 50 μm. (**d**) Quantification of *Gad1* and *Oxtr* colocalization in $aCA2/CA3_{distal}$ for males and females, expressed as a percentage of $Gad1^+$ cells over $Oxtr^+$ cells. (**e**) Representative images of *Oxtr*, *PV*, and *SST* mRNA expression in $aCA2/CA3_{distal}$ by FISH (n=4 males, 3 females). Asterisk (*) denotes $PV^+/Oxtr^+$ interneuron. Scale bar denotes 50 μm. Inset scale bar denotes 25 μm. (**f**) Quantification of *Oxtr* colocalization with *PV* and *SST* in $aCA2/CA3_{distal}$, expressed as a percentage of total *PV* cells (top) or *SST* cells (bottom). (**g**) Representative low-magnification (left) and high-magnification (right) images of *Oxtr* and *Gad1* mRNA expression in aCA1 by FISH (n=4 males, 3 females). Scale bar denotes 100 μm. Inset scale bar denotes 50 μm. (**h**) Schematic of anterior hippocampal subregion boundaries.

Figure 3.1 (Continued)

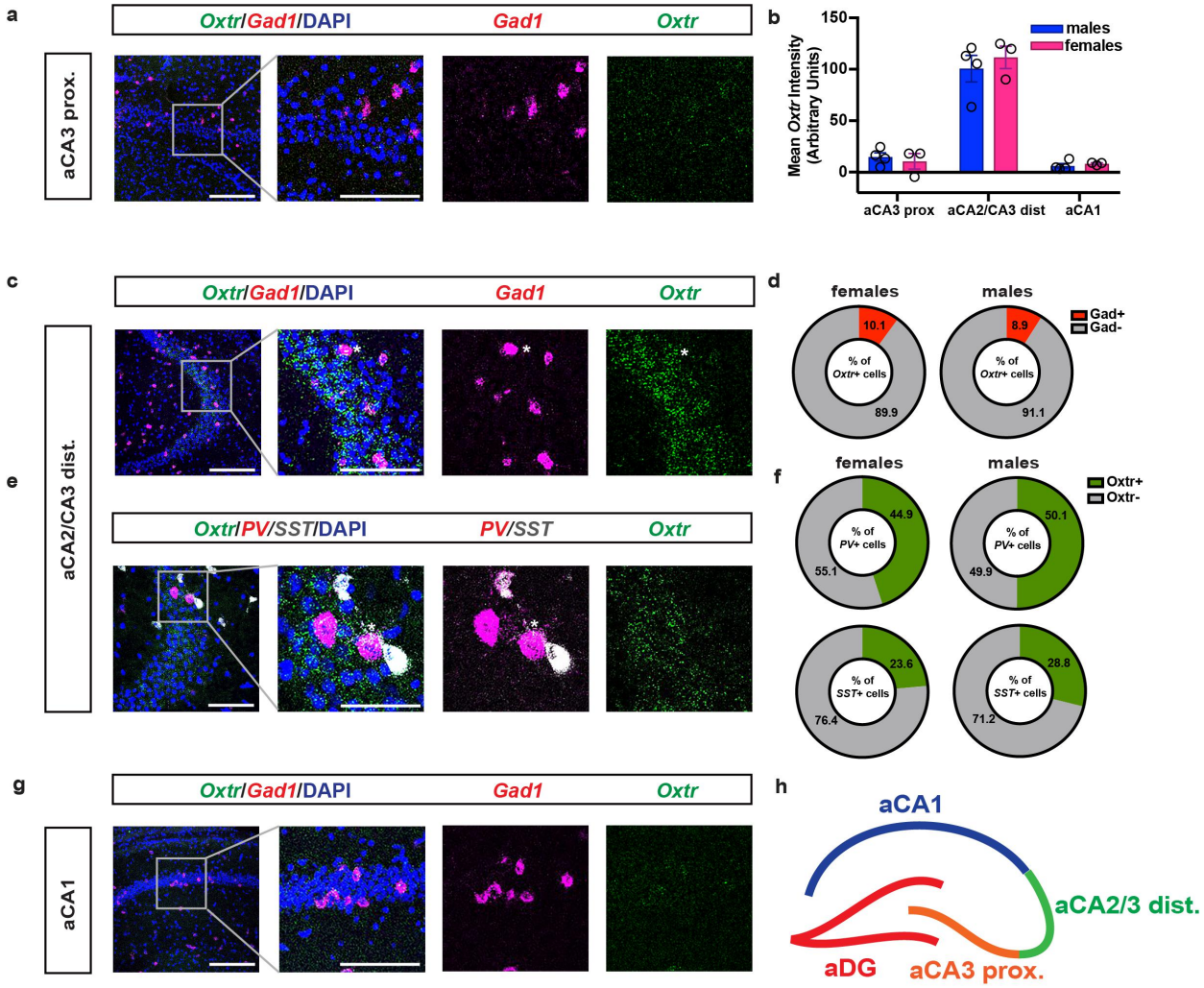


Figure 3.2 | Viral recombination of *Oxtr* in aCA2/CA3$_{distal}$ impairs discrimination of social, but not non-social, stimuli.

(**a**) Schematic illustrating viral injection and behavioral testing timeline. (**b**) Representative images of Cre and GFP virus infection in aCA2/CA3. Scale bar denotes 200 μm. (**c**) Behavioral schematic (top) and quantification (bottom) of single object exploration (GFP: n=7, Cre: n=10). (**d**) Behavioral schematic (top) and quantification (bottom) of novel objection recognition (GFP: n=7, Cre: n=10). Quantifications are displayed as Habituation (trials 1-3), Test (trial 4), and discrimination ratio (trial 4). (**e**) Behavioral schematic (top) and quantification (bottom) of social exploration test (GFP: n=7, Cre: n=10). (**f**) Behavioral schematic (top) and quantification (bottom) of social discrimination task (GFP: n=7, Cre: n=10). Quantifications are displayed as Habituation (trials 1-3), Test (trial 4), and discrimination ratio (trial 4). All data are displayed as mean ± SEM.

Figure 3.2 (Continued)

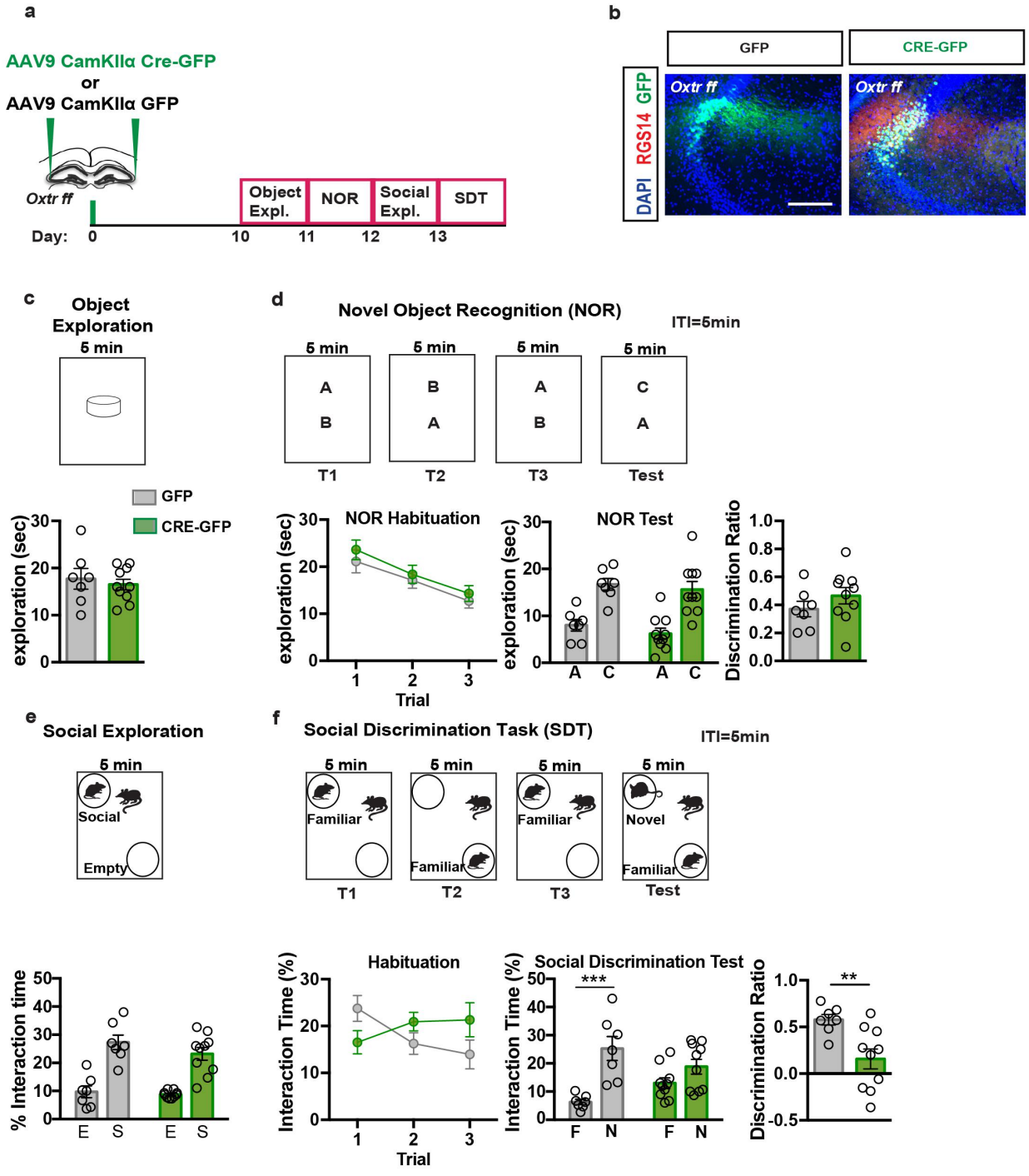
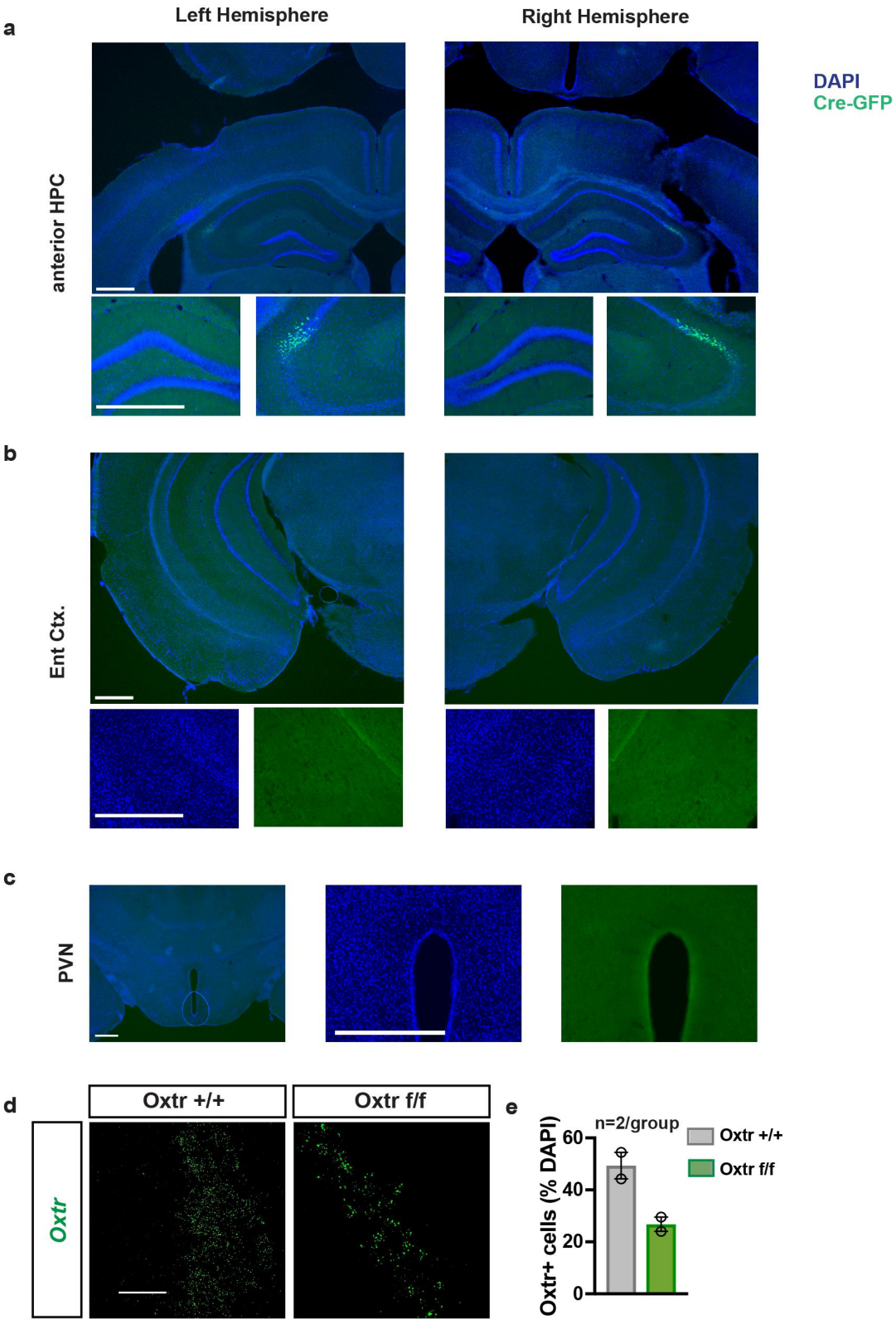


Figure 3.3 | AAV_9-CaMKIIα-Cre-GFP injected into aCA2/$CA3_{distal}$ is not retrogradely or anterogradely trafficked.

(**a**) Low magnification (top) and high magnification (bottom) images of anterior hippocampus at the site of injection in aCA2/$CA3_{distal.}$ Scale bars denote 500 μm (top) and 600 μm (bottom). (**b**) Low magnification (top) and high magnification (bottom) images of Entorhinal Cortex depicting lack of retrograde labeling from aCA2/$CA3_{distal}$. Scale bars denote 500 μm (top) and 600 μm (bottom). (**c**) Low magnification (left) and high magnification (right) images of PVN depicting lack of retrograde labeling from aCA2/$CA3_{distal}$. Scale bars denote 500 μm (left) and 600 μm (right). (**d)** Representative images of aCA2/$CA3_{distal}$ *Oxtr* mRNA expression in Oxtr +/+ and Oxtr f/f animals injected with CaMKIIα-Cre virus. Scale bar denotes 50 μm. (**e**) Quantification of *Oxtr* mRNA in aCA2/$CA3_{distal}$ expressed as a percentage of total DAPI+ cells in Oxtr +/+ and Oxtr f/f animals injected with CaMKIIα-Cre virus.

Figure 3.3 (Continued)



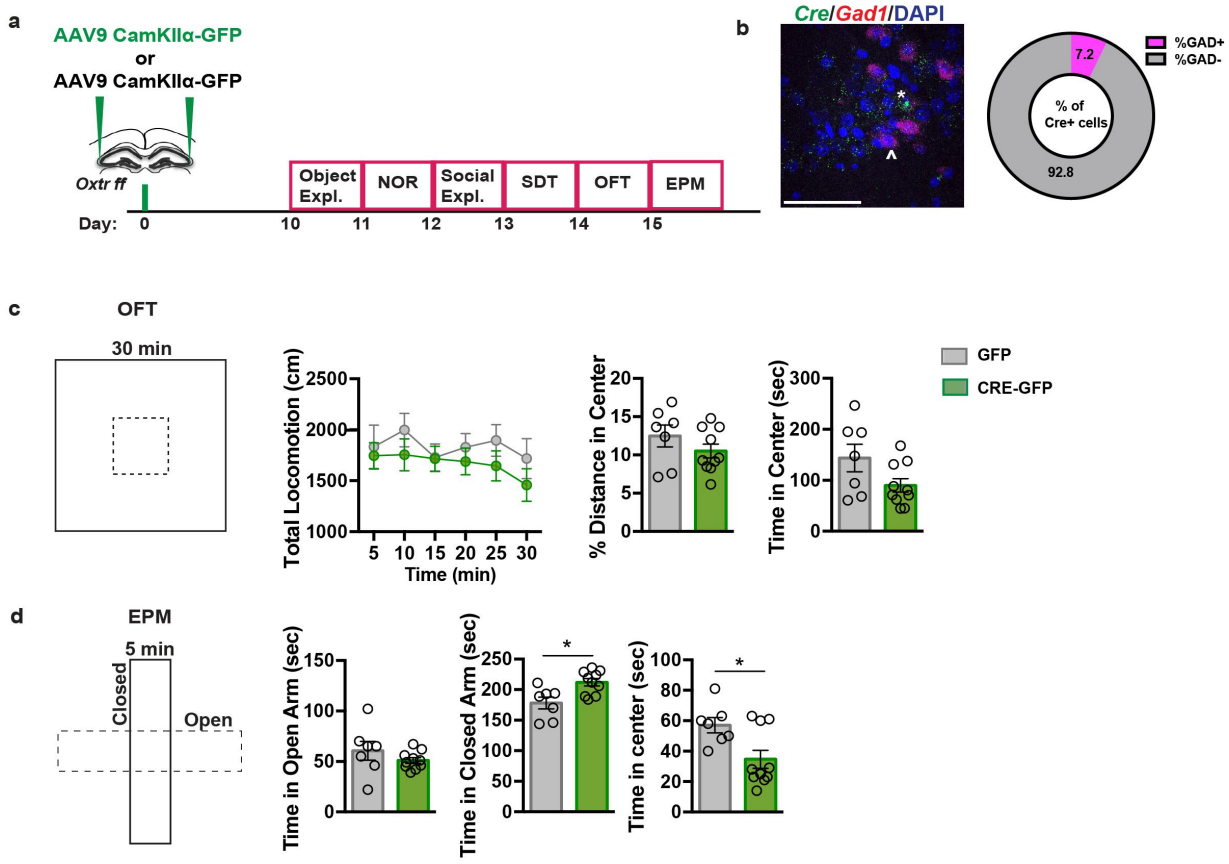


Figure 3.4 | Assessment of behavioral measures of innate anxiety following viral recombination of *Oxtrs* in aCA2/CA3$_{distal}$.

(**a**) Schematic illustrating viral injection and behavioral testing timeline. (**b**) Representative image (left) and quantification (right) of overlap of *Cre* mRNA with *Gad1* mRNA. Scale bar denotes 50 μm. (**c**) Schematic illustrating open field test (left) and quantification of total locomotion, percent distance in center, and time in center (right, GFP: n=7, Cre: n=10). (**d**) Schematic illustrating elevated plus maze (left) and quantification of time in open arm, time in closed arm, and time in center (right, GFP: n=7, Cre: n=10). All data are displayed as mean ± SEM.

in cells that retained *Oxtr* mRNA, suggestive of potential redistribution of transcripts. *Oxtr* deletion in aCA2/CA3$_{distal}$ neurons did not affect object exploration, novel object recognition, or social exploration (**Figure 3.2c,d,e**). However, although control virus (GFP) injected mice habituated to the familiar animal over trials 1 through 3, Cre-injected animals failed to show this habituation (two-way ANOVA, treatment: $F_{(1,15)} = .2574$, $p = .6193$, trial: $F_{(2,30)} = .6646$, $p = .5219$, interaction: $F_{(2,30)} = 6.282$, $p = .0053$; Multiple comparisons, Trial 1 vs Trial 3, GFP: $p < .05$, Cre: $p > .05$, **Figure 3.2f**). Furthermore, control animals demonstrated a strong preference for the novel animal, while Cre-injected animals failed to show a preference (two-way ANOVA, treatment: $F_{(1,15)} = .00185$, $p = .9663$, stimulus: $F_{(1,15)} = 19.98$, $p = .0004$, interaction: $F_{(1,15)} = 5.597$, $p = .0319$; Multiple comparisons, Familiar vs Novel, GFP: $p = .0009$, Cre: $p = .2439$, **Figure 3.2f**). Discrimination ratios were also significantly lower in Cre animals than in GFP animals (unpaired t-test, GFP vs. Cre: $p = .0038$, **Figure 3.2f**). Deletion of *Oxtrs* in aCA2/CA3$_{distal}$ did not affect measures of innate anxiety in the open field (**Figure 3.4c**). In the elevated plus maze, I observed a decrease in time spent in the center, a decision-making point in the maze, at the expense of time spent in the closed arm, but not time spent in open arms (**Figure 3.4d**).

To distinguish between the potential contribution of Oxtrs to habituation (or acquisition) versus retrieval in the social discrimination task, I employed pharmacological blockade of Oxtrs *in vivo* only during the retrieval phase of this task. Adult male C57BL/6J mice received a bilateral guide cannulae placed over aCA2/CA3 10 days prior to behavior (**Figure 3.5a,b**). Following habituation and acquisition, I infused sterile saline or Oxtr antagonist, Oxtr-A, (L-368,899 Hydrochloride, Tocris) bilaterally into aCA2/CA3$_{distal}$ after Trial 3 and immediately before Trial 4. Under conditions in which subjects have sufficiently encoded the familiar stimulus, acute blockade of Oxtrs during retrieval was sufficient to impair discrimination of social stimuli (two-

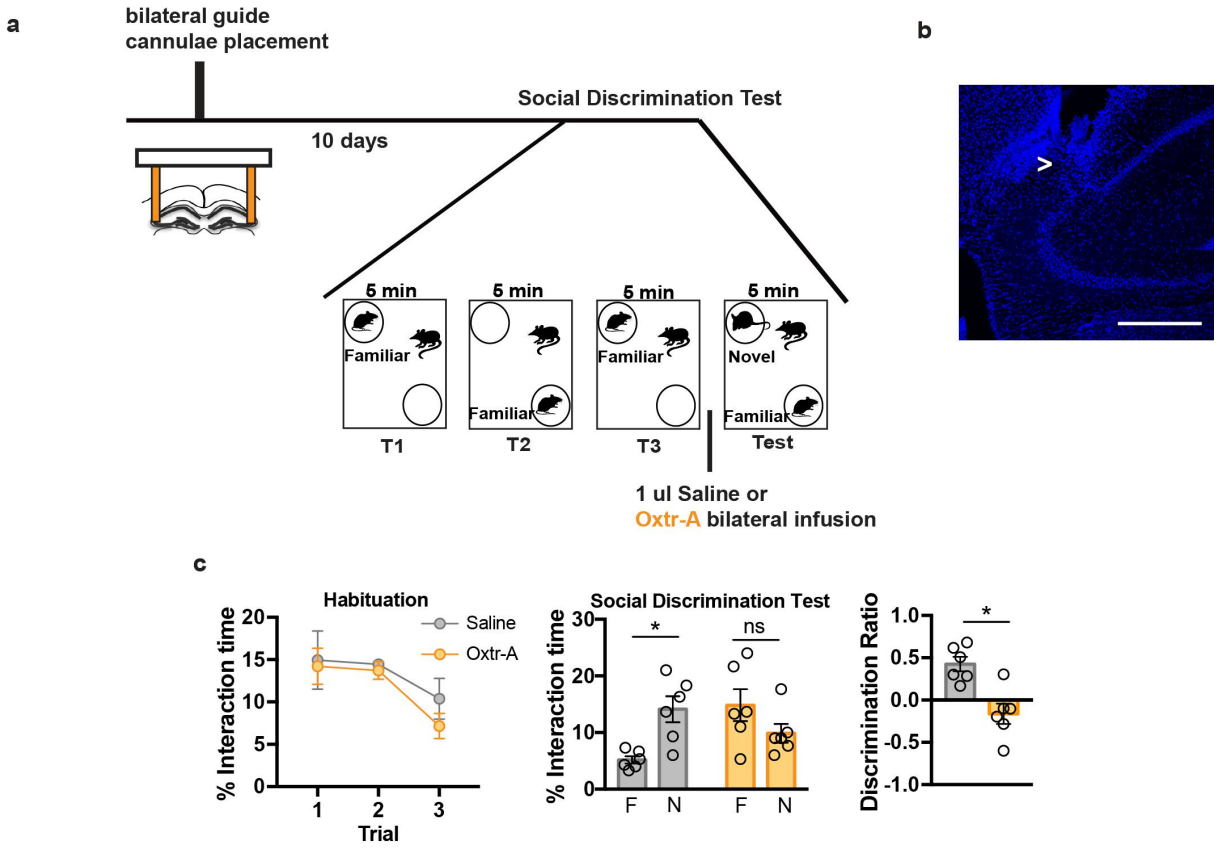


Figure 3.5 | Pharmacological blockade of Oxtrs in aCA2/CA3$_{distal}$ after acquisition is sufficient to impair retrieval.

(**a**) Schematic illustrating placement of guide cannulae and behavioral testing timeline. (**b**) Representative image of guide cannula placement above *aCA2/CA3$_{distal}$*. Arrowhead represents tract of cannula. Scale bar denotes 200 μm. (**c**) Quantification of social discrimination task (n=6). Quantifications are displayed as Habituation (trials 1-3), Test (trial 4), and discrimination ratio (trial 4). All data are displayed as mean ± SEM.

way ANOVA, treatment: $F_{(1,5)} = 2.373$, p = .1841, stimulus, $F_{(1,5)} = 1.509$, p = .2739, interaction, group x stimulus: $F_{(1,5)} = 9.802$, p = .0259; paired t-test Familiar vs Novel, Saline: p = .0148, Oxtr-A: p = .1672, **Figure 3.5c**). Similarly, discrimination ratios were significantly lower during Oxtr-A infusion than during saline infusion (paired t-test, p = .0109, **Figure 3.5c**).

Together, these experiments suggest through genetic deletion that Oxtrs in aCA2/$CA3_{distal}$ are critical for social discrimination, but not object discrimination. Furthermore, our pharmacological blockade studies suggest that Oxtr function is necessary during the retrieval window to mediate discrimination of social stimuli.

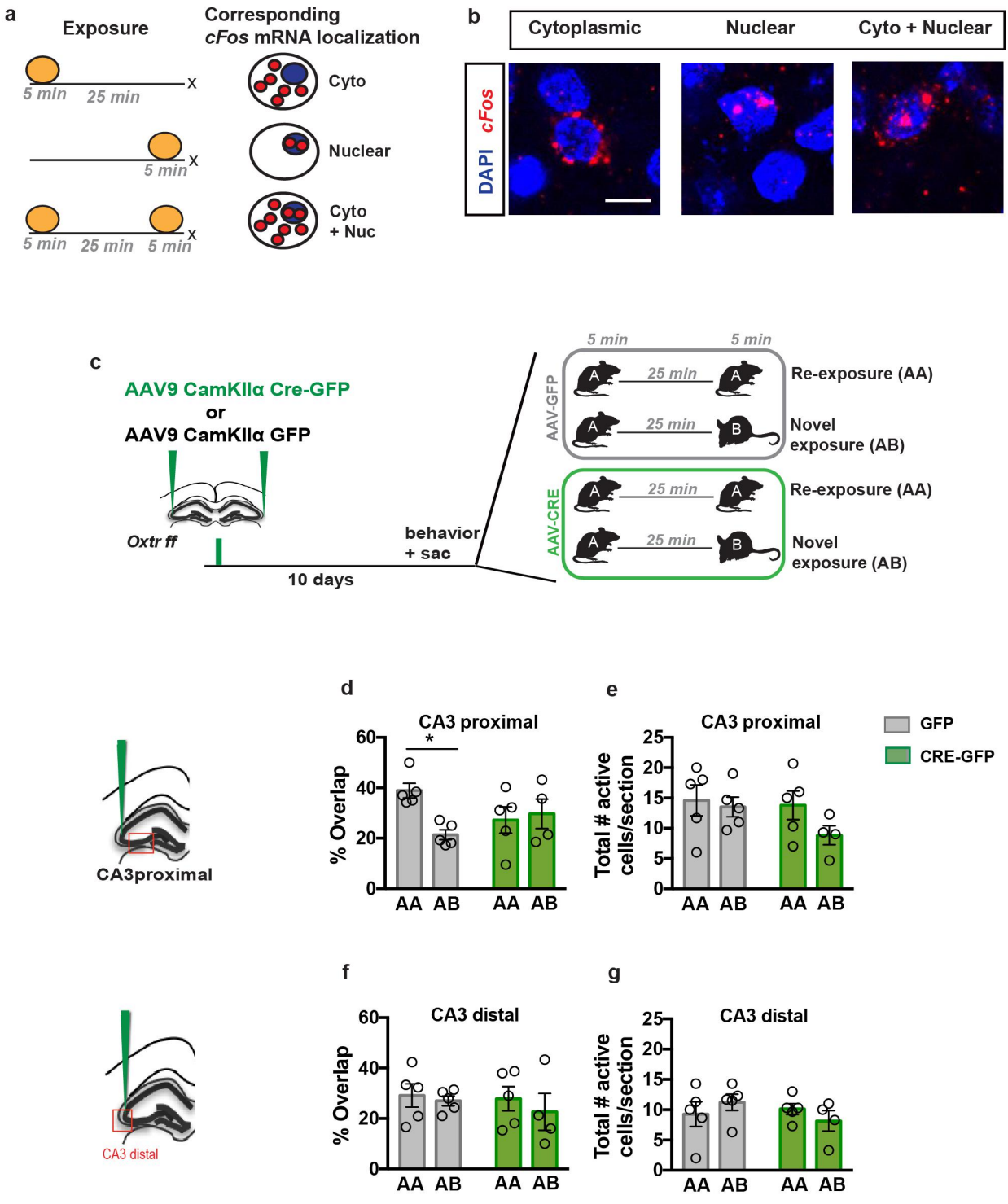
3.2.3 aCA2/$CA3_{distal}$ Oxtrs mediate population-based social coding

The DG-CA3 circuit recruits population-based coding to encode similar memories in non-overlapping ensembles thereby minimizing interference between similar memories during storage. Such a mechanism has been extensively demonstrated to underlie navigation and discrimination of similar contexts, and more recently has been shown in CA2 of rats in response to social stimuli (Alexander et al. 2016). We therefore asked whether Oxtrs in aCA2/$CA3_{distal}$ recruit population based coding mechanisms to distinguish between similar social stimuli by utilizing catFISH (cellular compartment analysis of temporal activity using fluorescence in situ hybridization) in combination with viral deletion of *Oxtrs* in aCA2/$CA3_{distal}$. This approach allows us to visualize ensembles of neurons activated in response to social stimuli at distinct temporal windows based on sub-cellular localization of *cFos* mRNA transcripts in either the nucleus or the cytoplasm (Guzowski and Worley 2001; Lin et al. 2011) (**Figure 3.6a,b**). Adult male *Oxtr* $^{f/f}$ mice were injected with AAV CamKIIα-GFP or CamKIIα-Cre-GFP in aCA2/$CA3_{distal}$ one week prior to exposure to two social stimuli: re-exposure to a single mouse (A-A), or new exposure to a novel mouse (A-B) (four groups in total, **Figure 3.6c**). Analysis of cellular ensembles in $CA3_{proximal}$ of

Figure 3.6 | Viral recombination of *Oxtr* in aCA2/CA3$_{distal}$ impairs population based coding of social stimuli.

(**a**) Schematic illustrating conceptual design of catFISH using *c-fos* intronic and full-length mRNA localization as readouts for ensembles of neurons activated at distinct behavioral windows. (**b**) Representative images of *CA3* pyramidal neurons exhibiting cytoplasmic, nuclear, or cytoplasmic and nuclear localization of *c-fos* mRNA transcripts. Scale bar denotes 10 μm. (**c**) Schematic illustrating viral injection and behavioral exposure timelines (GFP AA: n=5, GFP AB: n=5, Cre AA: n=5, Cre AB: n=4). (**d**,**f**) Percent overlap between ensembles of neurons encoding first and second stimulus for CA3$_{proximal}$ (top) and CA3$_{distal}$ (bottom) respectively. (**e**,**g**) Total number of active cells per section for CA3$_{proximal}$ (top) and CA3$_{distal}$ (bottom) respectively. All data are displayed as mean ± SEM.

Figure 3.6 (Continued)



control animals revealed higher percentage overlap (cells positive for both nuclear and cytoplasmic *cFos* transcript are indicative of reactivation) in the A-A condition relative to the A-B condition (**Figure 3.6d**). In contrast, Cre-injected animals exhibited comparable levels of re-activation (overlap) in A-A and A-B conditions (two-way ANOVA, treatment: $F_{(1,15)} = .1703$, $p = .6856$, exposure: $F_{(1,15)} = 3.335$, $p = .0878$, interaction: $F_{(1,15)} = 5.917$, $p = .0280$; Multiple comparisons, AA vs AB, GFP: $p = .0145$, Cre: $p > .9999$, **Figure 3.6d**). Interestingly, analysis of sub-cellular transcript localization in $CA3_{distal}$ of controls and experimental groups revealed comparable levels of ensemble reactivation in response to A-A and A-B conditions, consistent with reports that $CA3_{proximal}$ and $CA3_{distal}$ are functionally distinct (**Figure 3.6f**). We did not observe differences in the total number of activated cells for either $CA3_{proximal}$ or $CA3_{distal}$ (**Figure 3.6e,g**, **Figure 3.7a,b**).

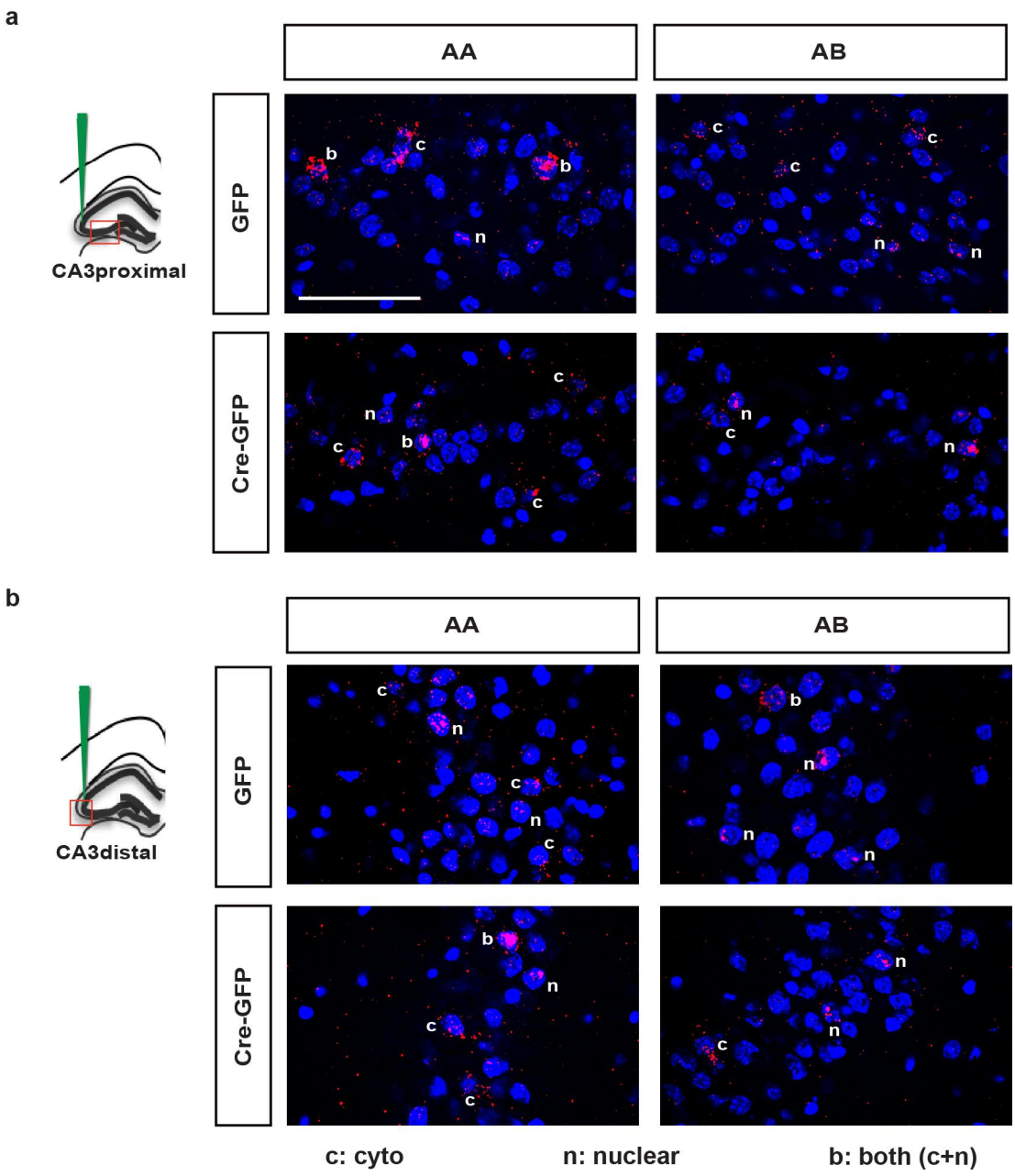


Figure 3.7 | Representative catFISH images.

Representative confocal images of $CA3_{proximal}$ (**a**) and $CA3_{distal}$ (**b**) exhibiting cytoplasmic, nuclear, or both (cytoplasmic and nuclear) localization of *cFos* transcripts. Scale bar denotes 50 μm.

3.3 Discussion

Recent studies in the past few years have generated compelling evidence for CA2 and CA3 as a locus for social recognition memory, an underappreciated function of the hippocampus. However, the mechanisms by which CA2/CA3 mediates this unique role, and whether the same mechanisms govern non-social memories such as object and context recognition, have remained poorly understood. In addition, the computations by which very similar social stimuli are rendered distinct in order to minimize interference between them, has not been delineated. Collectively, the experiments presented in this chapter demonstrate a mechanism by which the neuromodulatory hormone, oxytocin, promotes population-based coding of social stimuli in CA3 that promotes effective social recognition.

Utilizing multiplex FISH to determine the expression pattern of the *Oxtr* gene yielded an enrichment of *Oxtr* in the pyramidal cell layer of CA2 and $CA3_{distal}$, and an absence in $CA3_{proximal}$ and CA1. The distribution of *Oxtr* mRNA in CA2/CA3distal is quite dense, but notably inconsistent with cell body labeling, and may suggest a role for presynaptic Oxtrs residing on the terminals of afferents arriving from the DG, PVN, or elsewhere (Dölen et al. 2013). The vast majority of *Oxtr* expressing cells are pyramidal neurons, with only 10% colocalizing with GAD1, a curious result given that in many cortical and subcortical regions, including our own findings in aDG in Chapter 2, the action of oxytocin is biased towards inhibitory interneurons (Owen et al. 2013; Nakajima et al. 2014; Marlin et al. 2015). The significance of this deviation may lie in that excitatory pyramidal neurons represent the primary outputs of the CA2/CA3 subregion, and oxytocin may therefore harness these cells to route social information to particular downstream regions, a topic to be explored in depth in Chapter 4. Though expression in interneurons is sparse, the presence of even a small percentage of interneurons can exert great influence on local circuit

activity. I therefore sought to characterize the particular identity of *Oxtr* neurons in CA2/CA3 and found biased expression in PV interneurons, although expression does also exist in SST interneurons. PV interneurons are generally enriched in CA2, but show age-dependent reduction in density in the 22q11.2 mouse model of schizophrenia, which is also correlated with deficits in social recognition (Piskorowski et al. 2016). The biased expression of *Oxtr* in PV interneurons may therefore reflect a potential disruption in Oxtr functioning in psychiatric disorders of social cognition, and may open up new avenues to target oxytocin signaling pathways in disorders such as autism and schizophrenia.

Conditional deletion of *Oxtr* in aCA2/CA3$_{distal}$ resulted in a specific deficit in social memory, and yielded remarkably no behavioral phenotypes in measures of sociability, novel object recognition, or innate anxiety. This effect on social memory was recapitulated by pharmacological approaches that acutely blocked Oxtr function in aCA2/CA3$_{distal}$ after habituation to a social stimulus, and directly before the discrimination trial. These data suggest that the role of Oxtrs is temporally specific to the real-time discrimination of social stimuli, and the deficits in discrimination observed via conditional deletion are not simply due to lack of effective encoding of the familiar during the first three trials. Furthermore, ensemble mapping via catFISH determined a role for CA3$_{proximal}$, but not CA3$_{distal}$ in population based coding of social stimuli, an effect reminiscent of studies elucidating a functional hetereogeneity along the CA3 transverse axis wherein CA3$_{proximal}$ mediates pattern separation and CA3$_{distal}$ mediates pattern completion of spatial information (Lee et al. 2015). Critically, population-based coding of social stimuli in CA3$_{proximal}$ depends on the presence of Oxtrs in CA2/CA3$_{distal}$. That the locus for remapping of social stimuli is in CA3$_{proximal}$ despite the absence of Oxtrs in that subregion suggests local circuitry that relays information from CA2/CA3$_{distal}$ back along the transverse axis to CA3$_{proximal}$. Two

potential candidates for this transfer of information may be the CA3 recurrent collateral which directly projects from distal to proximal CA3, or, a polysynaptic connection via local CA3 interneurons. While these experiments suggest that remapping of social stimuli assumes a transverse axis gradient similar to that of remapping of spatial locations, it is also possible that ensemble mapping of *cFos* transcripts does not provide the resolution to detect potentially subtle changes ensemble remapping in $CA3_{distal}$ and CA2. Further experiments utilizing *in vivo* recordings or calcium imaging of these subregions imaging may provide greater clarity to these circuit mechanisms.

The deficits in social novelty seeking observed in animals lacking Oxtrs in aCA2/CA3 were recently recapitulated in a study that was published shortly after our own. In this study, a deficit in social discrimination was observed in mice lacking CA2/CA3a Oxtrs, although only at long-term time points (7 days) rather than immediately (Lin et al. 2018). Comparison of methods in this study and our own yielded few significant differences in approach, however one difference observed is that social stimuli used in this study were juvenile males, while the stimuli used in our study were adult males. Given that juvenile animals secrete unique pheromones in their tears that suppresses sexual behavior of adult animals (Ferrero et al. 2013), these differences may be attributed to the pheromones of juvenile animals being more readily discriminated than those of adult animals, which may underlie the lack of an effect at short term memory time points in the study by Lin and colleagues.

Given the diverse roles CA2 and CA3 are thought to play in spatial navigation, object recognition, locomotion, temporal encoding, and social memories, our studies shed light on a mechanism by which these diverse functions may be segregated at the circuit level. Previous studies manipulating CA2/CA3 in social behavior have often relied on chronic manipulation of

the activity of these neurons over the course of development, which may lead to activity-dependent circuit remodeling over time, or have nonspecifically silenced pyramidal neurons using strategies such as NR1 deletion or tetanus toxin. The significance of our work lies in that pyramidal neurons are not chronically and irreversibly prevented from firing action potentials, rather they are simply rendered insensitive to the actions of oxytocin, thereby preserving their non-social functions (such as object recognition and promotion of innate anxiety). These studies therefore identify a mechanism by which an evolutionarily conserved neuromodulatory hormone such as oxytocin, harnesses a basic hippocampal circuit scaffold to promote appropriate behavioral responses to social stimuli, without influencing approach to non-social cues. Our work raises broader questions about the roles that other neuromodulatory systems, such as serotonin, dopamine, and norepinephrine, may play in other hippocampus-dependent behaviors, and how these systems may even interact with each other to promote finer aspects of social interactions. For example, the oxytocin system in the hippocampus may interact with dopamine to promote approach associated with rewarding social encounters such as sexual exposure, and may interact with norepinephrine to promote avoidance associated with threatening social stimuli, such as aggressors. Future experiments that unravel the cross-talk between these systems may prove to be a compelling line of work.

3.4 Methods

Mouse Lines and Animal Care

Two strains of mice were used in these experiments. Multiplex FISH experiments were carried out in C57Bl/6J mice. Oxytocin receptor conditional knock-out mice (*Oxtr* $^{f/f}$) rederived at Jackson Labs were utilized for viral mediated recombination of Oxtr (Jackson Laboratories stock #008471). All experiments were carried out in adult male mice (8 weeks old). All mice were housed 3-5 per cage in standard laboratory conditions under a 12-hour light-dark cycle (7:00 a.m. to 7:00 p.m.) with ad libitum access to food and water. Behavioral testing occurred during the light cycle. All experiments were carried out in accordance with procedures approved by the Institutional Animal Care and Use Committee at the Massachusetts General Hospital in accordance with NIH guidelines.

Multiplex Fluorescence *in situ* Hybridization

FISH was carried out using ACDBio RNAscope multiplex fluorescence assay. Probes were obtained as following: C1: *PV* (Mm-Pvalb: 421931)*, Cre* (CRE: 312281), C2: *Oxtr* (Mm-Oxtr-C2: 402651-C2), C3: *Gad1* (Mm-Gad1-C3: 400951-C3)*, SST* (Mm-Sst-C3: 404631-C3). Brain tissue was obtained from age-matched 8-10 week old male and female C57Bl/6J mice and immediately fresh-frozen in OCT on dry ice. 20 um sections were obtained using a cryostat (Leica, Germany) and stored at -80°C. Prior to RNAscope protocol, sections were incubated at -20°C for 1hour. RNAscope protocol was followed as indicated in user manual with adjustments as mentioned here. Briefly, sections were fixed with 4% chilled PFA for 30 or 60 minutes minutes and rinsed in 1X PBS for 5 minutes. Sections were then dehydrated in four 5 min dehydration steps in 50%, 75%, 100% and 100% ethanol respectively. Tissue was digested with Protease III for 30 min at room temperature and rinsed in 1X PBS. *Oxtr* and *Gad1* probes were diluted 1:50 in probe diluent and

pipetted onto each slide. *Oxtr* and *SST* probes were diluted 1:50 in *PV* C1 probe and pipetted onto each slide. For assessment of OxtR knockout, *Oxtr* probe was diluted 1:50 in *Cre* C1 probe. Probe hybridization took place for 2 hours at 40°C and slides were then rinsed in 1X wash buffer. Sections were then incubated at 40°C in Amp1 for 30 min, Amp 2 for 15 min, and Amp3 for 30 min, and Amp4 for 15 min, with 1x Wash Buffer rinses between each incubation. Sections were finally mounted with DAPI Fluoromount and stored at -20°C.

For the assessment of Oxtr knockout, *Oxtr* $^{+/+}$ and *Oxtr* $^{f/f}$ mice were injected in aCA2/CA3 with AAV-CRE (AAV_9- CamKIIα-Cre, diluted 1:5, .3 ul bilaterally in $aCA2/CA3_{distal}$).

Adeno-associated Viruses (AAV)

AAV_9-CamKIIα-GFP (6.27 x 10^{13} particles/mL) and AAV_9-CamKIIα-GFP (6.27 x 10^{13} particles/mL) were generated by and obtained from the University of Pennsylvania Vector Core (Philadelphia, Pennsylvania).

Stereotactic Surgery

Viral Injections: Adult mice (8 week-old) were maintained under standard housing conditions. Mice were given carprofen (5mg kg^{-1} s.c.) prior to surgery and 24h later to minimize discomfort. Mice were anaesthetized with ketamine and xylazine (10mg mL^{-1} and 1.6mg mL^{-1} , i.p.) and placed in a stereotaxic frame (Stoelting). Small holes were drilled at each injection location and injected with a Hamilton microsyringe at a rate of 0.1 µl/min. For $aCA2/CA3_{distal}$ KO experiments, .3 µl 1:50 AAV9-CamKIIα-Cre-GFP or 1:50 AAV9-CamKIIα-GFP was injected bilaterally (AP -2.0 mm, ML +/- 2.5 mm, DV -2.3 mm from Bregma) into *Oxtr f/f* mice. After completion of the injection, the needle was left on the site of injection for 5 min, raised 0.2 mm and left on the site for an additional 5 min to allow diffusion of virus at the injection site and then slowly withdrawn.

The skin incision was closed carefully using nylon sutures. Animals were monitored during recovery.

Single Object Exploration

Mice were placed an arena filled with bedding (45cm long, 15cm high and 30cm wide) with a single novel object for 5 minutes. Sessions were video-recorded, and videos were manually scored for object exploration (when an animal's snout was 2cm or less from the object) by an investigator blind to animal treatment identity.

Novel Object Recognition

Mice were placed in an arena filled with bedding (45cm long, 15cm high and 30cm wide) with two distinct objects (A and B) for three 5 min sessions, with a 5 minute intertrial interval. Mice habituated to the objects during the three training sessions, and one of the objects was subsequently replaced with a novel object (C) in session four. Objects were counterbalanced across subjects and object positions were counterbalanced across trials. The objects that were selected for testing elicited comparable levels of exploration based on exploration levels in pilot experiments. Sessions were video-recorded, and videos were manually scored for object exploration (when an animal's snout was 2cm or less from the object) by an investigator blind to object identity and animal treatment identity.

Social Exploration

Mice were placed in an open plexiglass arena (41cm x 41 cm, Kinder Scientific) for 5 minutes with two pencil-wire cups placed on opposing corners of the arena. Habituation to the chamber took place one day prior to start of behavioral testing. One cup remained empty while the other contained a novel adult male C57Bl/6J mouse. Sessions were video-recorded, and videos were manually scored for exploration of the social cup and empty cup (direct snout-to-cup contact, with

at least two paws on the ground--time spent climbing on the cup was not included) by an investigator blind to animal treatment identity. Stimulus mice were trained to sit in pencil-wire cups for three 15 minute sessions several days prior to behavioral testing.

Social Recognition (Habituation, Discrimination)

The same plexiglass arena and pencil-wire cup set-up as described for social exploration was used. Mice were placed in the arena for three 5 min sessions with an empty cup and a novel adult male C57Bl/6J mouse, with a 5 minute intertrial interval. Mice habituated to the stimulus during the first three sessions, rendering it "familiar." During trial 4, a novel adult male mouse was placed in the opposing cup, and subjects were tested for discrimination between the novel and familiar mouse. Social stimuli were counterbalanced across subjects, and the position of the familiar social stimulus was counterbalanced across trials. Sessions were video-recorded, and videos were manually scored for interaction with the novel vs familiar mouse (direct snout-to-cup contact, with at least two paws on the ground--time spent climbing on the cup was not included) by an investigator blind to animal treatment identity. Stimulus mice were trained to sit in pencil-wire cups for three 15 minute sessions several days prior to behavioral testing. Videos were scored by two different investigators.

Open Field Test

Locomotor behavior was recorded for 30 min divided in six 5 min epochs in a Plexiglas open-field (OF) box of 41 x 41cm (Kinder Scientific) with 16 sets of double stacked pulse-modulated infrared photobeams (SmartFrame Open Field System; Kinder Scientific, Poway, CA) equally spaced on every wall (128 total) to record x-y ambulatory movements. MotorMonitor Software (Kinder Scientific, Poway,CA) defined grid lines that divided the open field into center (25% of total area) and periphery (75% of total area), with the periphery consisting of the 10 cm closest to the wall

around the entire perimeter. Dependent measures were the overall motor activity quantified as the total locomotion (in centimeters), the distance traveled in the center divided by total distance traveled (percentage distance in center), and the time spent in the center (seconds).

Elevated Plus Maze

Innate anxiety was recorded in the elevated plus maze (EPM) for 5 min. The maze consisted of a black Plexiglas apparatus placed 1m above the floor, with two open arms (67 cm x 7 cm) perpendicular to two enclosed arms (67 x 7 x 17 cm). The four arms were separated by a neutral transition central square (5 x 5 cm) in which mice were placed at the beginning of the experiment and their behavior was recorded for 5 min with a video camera system (ViewPoint, Lyon, France) located above the maze. Cumulative time spent in the open, closed, and center arms was scored manually by an investigator blind to the treatment conditions and data were expressed as the time spent in open arms (seconds) and time spent in closed arms (seconds). An arm visit was recorded when the mouse moved its forepaws into the arm.

Pharmacological Blockade of Oxtrs

Cannula implantation for drug delivery to CA2/3 was carried out as described previously (McAvoy *et al.*, 2016). Cannula were purchased from Plastics One (Roanoke, VA) and consisted of bilateral guide cannula (center to center 5.0mm, custom depth 1.8 mm) and removable dummy cannula. Adult (8-10 week-old) C57Bl/6J male mice were maintained under standard housing conditions, and anaesthetized with ketamine / xylazine (10mg/mL and 1.6mg/mL, i.p.). Mice were placed in the stereotaxic apparatus and small hole was drilled at each bilateral injection location (AP = -2.0mm from bregma; ML = ± 2.5mm) and cannula slowly lowered to the appropriate depth. The cannula was secured to the skull with two cranial screws and dental cement. After allowing ten days for the mice to recover, the dummy cannula was removed, and the injection cannula was

inserted through the guide cannula, from which it projected 0.5mm. Animals were allowed to recover for 10 days post surgery. On the day of behavioral testing, the injection cannula was attached to PE50 tubing and a New Era Syringe pump. 1μl bilateral sterile saline or Oxtr antagonist, Oxtr-A, (L-368,899 Hydrochloride, Tocris #2641, dose 10 mM) was infused at a rate of 1μl/minute bilaterally. Infusion occurred directly after trial 3 and before trial 4 of the social discrimination task (inter-trial interval 10 min). This experiment followed a within-animal comparison design in which half the animals received saline treatment and half received Oxtr-A on the first day, and were subsequently counterbalanced for treatment on the following day.

CatFISH

The catFISH assay was performed as previously described (McAvoy *et al.*, 2016). Briefly, adult male *Oxtr f/f* mice received bilateral stereotactic injections of AAV_9-CamKIIα-Cre-GFP or AAV_9-CamKIIα-GFP diluted at 1:50 into aCA2/$CA3_{distal}$ ten days prior to behavior, as described above. Animals experienced two 5 min behavioral episodes 25 min apart and brains were isolated and flash frozen in isopentane on dry ice immediately after the second episode. Sections containing anterior hippocampus were cryosectioned at 20 μm on a Leica Cryostat, immediately mounted on Fisherbrand Superfrost Plus Slides, and stored at -80C until use. An intronic *c-fos* probe containing the entire first intron of the Fos gene (Lin *et al.*, 2011; generous gift of Dr. Dayu Lin) and a full-length *c-fos* cRNA probe were used to detect nuclear and cytoplasmic c-fos transcripts, respectively. Nuclear c-fos was defined as puncta colocalizing with DAPI labeling, whereas cytoplasmic labeling was defined as c-fos-positive labeling surrounding the nucleus. $CA3_{proximal}$ comprised an ROI with a volume of 788,546 cubic microns per section and contained on average 521.67 $DAPI^+$ cells (n=3). $CA3_{distal}$ comprised an ROI with a volume of 1,216,503 cubic microns per section and contained an average of 554.67 $DAPI^+$ cells (n=3). CA2 was not quantified due to too few $cFos^+$ foci for analysis (on average 2 $cFos^+$ cells per section).

Histology and Immunohistochemistry

Mice were anesthetized with ketamine (100 mg kg^{-1} i.p.) and xylazine (3 mg kg^{-1} i.p.) and transcardially perfused with 10mM phosphate buffer saline (PBS), pH 7.5 at 4°C, followed by a fixative solution containing 4% paraformaldehyde (PFA) in PBS. Brains were post-fixed in 4% PFA overnight at 4°C and cryo-protected for 72 hours in 30% sucrose at 4°C prior to freezing in OCT on dry ice. Coronal sections were obtained at 35 μm using a cryostat (Leica, Germany) in six matched sets. Sections were stored in 1X PBS with 0.01% Azide at 4°C. Floating sections were used to perform immunohistochemical labeling. Briefly, sections were washed in 1X PBS, incubated for 15 min at room temperature in 1X PBS containing .3% Triton X-100, blocked in 1X PBS containing .3% Triton X-100 and 10% NDS for 1 hour at room temperature, and incubated in primary antibodies in blocking buffer with shaking overnight at 4°C. Primary antibodies were used as follows: GFP (rabbit anti-GFP, Life Technologies A11122, 1:500, Antibodyregistry.org: AB_221569); goat anti-GFP, Novus Biologicals, NB100-1770, 1:500, (Antibodyregistry.org: AB_10128178), RGS14 (Mouse, UC Davis/NIH NeuroMab, 1:400). The following day, sections were washed 3 times in 1X PBS and incubated with fluorescent-label-coupled secondary antibodies (Jackson Immunoresearch, Donkey anti-Rabbit, Goat, or Mouse, 488-, Cy3-, or Cy5-coupled, 1:500) for 2 hours at room temperature.

Image Acquisition and Analysis

For RNAscope Multiplex FISH: 20x, 40x, or 60x Confocal z-stack images were obtained with a Nikon A1R Si confocal laser. Images were acquired at 1024 resolution as 10μm z-stacks with a step size of 2μm. For colocalization analysis, cells were manually identified as *Oxtr*$^+$, *Gad1*$^+$, *SST*$^+$, and/or *PV*$^+$ or double positive and expressed as a percentage of *Oxtr*$^+$, *SST*$^+$, or *PV*$^+$ cells (for CA2/CA3). For *Oxtr* mean intensity calculated for CA regions, mean intensity was measured

for the region comprised by the principal layer. A similar sized region from background area was measured for intensity and subtracted from mean *Oxtr* intensity in order to control for differences in background. For *Oxtr* knockdown analysis, all DAPI nuclei per image were counted (only cells in the CA2/CA3$_{distal}$ principal cell layer were counted) and cells were manually identified as *Oxtr*$^{+}$, *Cre*$^{+}$, and/or *OxtR*$^{+}$*CRE*$^{+}$ double positive. The *Oxtr*$^{+}$ population was expressed as a percentage of total DAPI cells.

For catFISH: Confocal z-stack images using a 60x oil objective (1.0 μm step size) were acquired along the aCA2/CA3 pyramidal layer using a Nikon A1R Si confocal laser, a TiE inverted research microscope, and NIS Elements software. Image analysis was performed with NIS Elements software. Four to eight hemisections were scanned per mouse. Images were manually counted for c-fos transcript labeling. Data are presented as cells/section. Quantifications were performed by an investigator blind to treatment condition and two different investigators.

Statistics

Statistical analysis was carried out using GraphPad Prism v7 software. Data (mean ± SEM). Discrimination ratios, cFos analysis, and measures of object exploration were analyzed using unpaired two-tailed student's t-test to compare two groups. Measures of NOR, social exploration, and social discrimination were analyzed using mixed factor two-way ANOVA with repeated measure followed by Bonferroni's multiple comparisons test when the interaction, p value was < .05. In all cases, significance was set at $p < 0.05$.

3.5 Author Contributions

T.R. carried out experiments and analyzed data with help from K.M.M., and A.B.

A.V. contributed reagents and shared resources.

T.R. and A.S. co-developed the concept and wrote the manuscript.

A.S. conceived and supervised all aspects of the project.

3.6 Acknowledgments

We thank members of the Sahay lab for their comments on the manuscript. A.S. acknowledges support from US National Institutes of Health Biobehavioral Research Awards for Innovative New Scientists (BRAINS) 1-R01MH104175, NIH-NIA 1R01AG048908-01, NIH-NIMH 1R01MH111729-01, Ellison Medical Foundation New Scholar in Aging, Whitehall Foundation, Inscopix Decode award, NARSAD Independent Investigator Award, Ellison Family Philanthropic support, Blue Guitar Fund, Harvard Neurodiscovery Center/MADRC Center Pilot Grant Award, HSCI Development grant, and HSCI seed grant.

CHAPTER 4

Optogenetic dissection of CA2/CA3 outputs mediating social memory

This chapter is adapted from a manuscript published in *Nature Communications* (Dec 8, 2017), included as Appendix 1

Hippocampal oxytocin receptors are necessary for discrimination of social stimuli

Tara Raam[1,2,3,4], Kathleen M. McAvoy[1,2,3], Antoine Besnard[1,2,3], Alexa Veenema[5], Amar Sahay[1,2,3,4,6]

[1]Center for Regenerative Medicine, Massachusetts General Hospital, Boston, MA 02114, USA

[2]Harvard Stem Cell Institute, Cambridge, MA 02138, USA

[3]Department of Psychiatry, Massachusetts General Hospital, Harvard Medical School, Boston, MA 02114 USA

[4]Department of Psychology, Michigan State University, East Lansing, MI, 48824

[5]Broad Institute of Harvard and MIT, Cambridge, MA 02142, USA

[6]Program in Neuroscience, Harvard Medical School, Boston, MA 02115, USA

Corresponding Author: Amar Sahay, asahay@mgh.harvard.edu

4.1 Introduction

A comprehensive model that seeks to put forth a circuit-based mechanism underlying hippocampal contributions to social memory would necessarily address the question of hippocampal outputs. The discrimination of social stimuli is a unique mental process that represents the convergence of both the cognitive and the limbic—well-characterized, historically studied hippocampal computations that segregate very similar stimuli into distinct ensembles of neurons, thereby minimizing interference between them, must be communicated to reward circuitry that drives affiliation with or avoidance of conspecifics. However, while the importance of the aCA2/CA3 locus to social memories has been demonstrated by multiple groups, and the importance of oxytocin signaling in this subregion clearly delineated in the previous chapter, the outputs of aCA2/CA3 that mediate social discrimination, and render it a distinct process from non-social discrimination, remain poorly understood. Fortunately, the rapid development of novel technologies in systems neuroscience over the past decade, particularly the emergence of *in vivo* optogenetics, renders these experiments tractable and amenable to clean interpretation. Here, I utilize anterograde viral mapping to first identify three dense, predominantly excitatory outputs from aCA2/CA3—aCA1, the dorsolateral septum (DLS), and pCA1. I then harness the power of *in vivo* terminal specific silencing by injecting a virally mediated, light-sensitive opsin (halorhodopsin, NpHR) into the cell bodies of aCA2/CA3 and selectively placing a chronically dwelling fiber optic implant over the terminals of aCA1, the DLS, and pCA1 in three distinct cohorts of mice. By combining this strategy with behavioral assays that probe object and social discrimination, I identify, for the first time, clearly dissociable outputs of aCA2/CA3 that selectively and specifically modulate social and non-social memory.

4.1.1 aCA2/CA3 projections to aCA1.

The most commonly studied, canonical output of the aCA3 subregion is known as aCA1. The synapse that links aCA3 to aCA1 is often referred to as the "Schaffer Collateral" pathway, named after the Hungarian neuroanatomist who discovered it, Károly Schaffer. Schaffer collaterals form the final synapse in the hippocampal trisynaptic loop, and represent the single most widely studied excitatory synapse in the rodent brain. Many classical rodent models of learning and memory, and the synaptic plasticity that underlies it, rest on our understanding of this pathway.

Classical studies utilizing *in vivo* and slice physiology combined with behavior have converged on a significant involvement of aCA1 in spatial and contextual learning. Pioneering studies by John O'Keefe have demonstrated that cells in aCA1 fire when the animal is positioned at specific spatial locations within an arena, which led cells of this nature to be referred to as "place cells" (O'Keefe and Dostrovsky 1971; O'Keefe 1976). These studies have been corroborated by additional studies using larger arenas to demonstrate that aCA1 place cells respond to multiple locations when an animal is placed in a larger environment (Park et al. 2011). More recent work utilizing calcium imaging has also found that aCA1 ensembles show increased activity in response to a particular spatial environment when that environment is associated with a nicotine reward, and chemogenetic silencing of aCA1 using hM4Di DREADDS is sufficient to block preference for reward-associated environments (Xia et al. 2017). In addition to spatial and contextual learning, aCA1 has been heavily implicated in novel object recognition in many studies utilizing both mice and rats (Cohen et al. 2013; Cohen and Stackman 2015). Interestingly, the importance of aCA1 to object discrimination seems to be independent from inputs arising from the medial entorhinal cortex (Robinson et al. 2017).

While a highly detailed literature has come to a degree of consensus regarding the role of aCA1 and its inputs via the Schaffer collateral in both spatial and object learning, much less evidence exists to suggest the same degree of certainty about its role in social memory. Surprisingly, few studies have directly tested this question, and those that have do not necessarily converge. Studies utilizing local infusion of the protein-synthesis inhibitor anisomycin into aCA1 of male mice and rats demonstrated that protein synthesis in aCA1 is necessary for 24-hour retention of a social stimulus (Zinn et al., 2016, Pena et al., 2014). Furthermore, pharmacological manipulation of adrenergic, dopaminergic, and histaminergic pathways in aCA1 recapitulated this effect (Zinn et al., 2016). However, more nuanced studies utilizing *in vivo* electrophysiological recordings, calcium imaging, and optogenetics suggest otherwise. Single unit recordings in adult male mice suggest that aCA1 may encode spatial information more robustly than social information, while nearby, the upstream aCA2 region is characterized by larger place fields and encodes social information more faithfully than spatial information (Alexander et al. 2016). Furthermore, aCA1 does not undergo global remapping in response to social stimuli (Alexander et al. 2016). This study is corroborated by evidence from freely moving calcium imaging experiments demonstrating that aCA1 population dynamics do not evolve in response to familiarization to a social stimulus, whereas those in pCA1 do (Okuyama et al. 2016). Finally, optogenetic terminal specific silencing of aCA1 cell bodies does not impair discrimination of social stimuli (Okuyama et al. 2016).

Discordant observations among these studies may reflect differences in species (mouse versus rat), strain, or behavioral task protocols. Alternatively, the effects observed by the aforementioned pharmacological manipulations, but not optogenetic or recording techniques, may be explained by technical limitations due to nonspecific localization of antagonists that spread

away from cannula site to nearby CA2 and CA3 areas, or the underlying DG. Alternatively, pharmacological manipulations may act on presynaptic receptors on local axon terminals rather than those residing in cell bodies of the region of interest. Technical considerations notwithstanding, all of these studies have probed the role of aCA1 cell bodies directly, and not the function of inputs arriving from aCA3 onto CA1. Causally probing the contribution of Schaffer collaterals to social memory, therefore remains to be tested.

As the CA2 subregion has only recently claimed its rightful place in hippocampal literature, very few studies have examined the circuitry intrinsic to aCA2, including inputs and outputs. The presence of aCA2 projections that form synapses directly onto aCA1 cell bodies was only recently established, albeit this pathway is thought to terminate on the deep layer of aCA1, rather than the superficial layer, where aCA3 synapses are thought to terminate (Kohara et al. 2014). Therefore, the behavioral relevance of this pathway, and how it may functionally differ from Schaffer collaterals originating in aCA3 is not understood. Given the central role of aCA2/CA3 to social memory, testing the role of aCA2/CA3 projections to aCA1 stands out as a critical experiment.

4.1.2 aCA2/CA3 projections to the lateral septum.

While aCA1 and the subiculum are often considered the primary output of the anterior hippocampus, there are other potential extra-hippocampal outputs that may represent more rapid transfer of information to limbic regions. For example, the aCA2/CA3 subregion also sends a dense, yet highly understudied, projection to the lateral septum.

Functionally, the lateral septum is thought to regulate a diverse array of limbic behaviors, including fear, anxiety, and reward (Sheehan et al. 2004). Early studies utilizing lesions and electrical stimulation led to a general model of the lateral septum as an inhibitor of fear. A classical study that induced damage to the lateral septum of rats resulted in “septal rage”, the expression of

exaggerated fear responses to innocuous environmental cues (Brady and Nauta 1953). High frequency stimulation (HFS)-induced LTP in the lateral septum significantly reduced fear responses to contextual cues paired with a foot shock, while subsequent lesions of the lateral septum resulted in potentiated fear responses (Vouimba et al. 1998). In contrast, more recent studies utilizing genetic and optogenetic tools identified a specific population of *Crfr2+* lateral septal neurons that, via their projections to the anterior hypothalamus, enhance stress-induced anxiety (Anthony et al. 2014). The lateral septum is also thought to mediate reward-seeking behaviors such as cocaine-seeking through its connections to the ventral tegmental area and lateral hypothalamus (Luo et al. 2011; Sartor and Aston-Jones 2012).

In addition to its critical role in fear, anxiety, and reward, the lateral septum has also been implicated in a variety of social behaviors and their pathological states. Early pharmacological studies demonstrated that serotonin and dopamine act on the lateral septum to modulate dominance and subordinance in male rats (Clarke and File 1982), a result corroborated by recent observations that male aggressive behaviors are associated with increased vasopressin release in the lateral septum (Veenema et al. 2010). Furthermore, increased anxiety produced by social defeat is also thought to be partially modulated by glucocorticoid receptors in the lateral septum (Calfa et al. 2006). Yet in addition to aggressive behaviors, the lateral septum is also thought to modulate affiliative social interactions. For example, pharmacological blockade of GABA and glutamate transmission in the lateral septum of rats promotes social play (Bredewold et al. 2015), while conditional deletion of mGluR5 receptors in the lateral septum impairs sociability (Mesic et al. 2015). A recent study suggests that the negative effects of early life social deprivation on adult sociability are attributable to dopamine receptors in the lateral septum (Shin et al. 2018). Interestingly, studies utilizing radioligand binding, antibody labeling, and knock-in reporter lines

suggest that the lateral septum is also a locus for the dense expression of Oxtrs (Yoshida et al. 2009; Hammock and Levitt 2013; Mitre et al. 2016). Oxytocin signaling pathways in the lateral septum are recruited for social fear conditioning, in which subjects learn to associate a social stimulus with a footshock (Zoicas et al. 2014), while pharmacological and genetic deletions indicate that Oxtrs in the lateral septum are critical for discrimination of social stimuli (Lukas et al. 2013; Mesic et al. 2015). These studies suggest that distinct inputs to the lateral septum may be critical modulators of a variety of social behavior.

Anatomically, the lateral septum sits at the crossroads of diverse and widely distributed neural networks. It both sends and receives projections to several cortical and subcortical areas such as the prefrontal cortex, amygdalar nuclei, hypothalamus, thalamus, nucleus accumbens, supramammillary nucleus, and VTA (Risold and Swanson 1997; Sheehan et al. 2004). This diverse connectivity pattern positions the lateral septum as a potentially effective relay integrating both cognitive computations that dissociate social stimuli from each other, with limbic computations that drive affiliation or avoidance behavior. However, in addition to these projections, strong bilateral, predominantly glutamatergic inputs from the CA2/CA3 subregion of the hippocampus project to the lateral septum (Swanson et al. 1981; Witter 2007; Cui et al. 2013). Projections from anterior CA2/CA3 project to the most dorsal region of the lateral septum (dorsolateral septum, DLS) while those from poster CA2/CA3 project to the more ventral portion of the lateral septum. While this projection had been anatomically characterized as early as the 1980s, its behavioral significance remained unknown until the past decade, when a small but growing number of pharmacological, genetic, and optogenetic studies began to probe its function.

The earliest study to interrogate this pathway utilized pharmacological lesions and electrophysiology to identify a functional circuit that conveys contextual information from dorsal

CA3, via its projection to the DLS, to VTA dopaminergic neurons in order to promote context-dependent cocaine seeking (Luo, Tahsili-Fahadan et al. 2011). Follow-up studies from the same group demonstrated that this pathway was specifically recruited for context-, but not cue-, dependent cocaine seeking (McGlinchey and Aston-Jones 2018). Additionally, dorsal CA3 projections to the DLS promote state-dependent transitions in running speed via downstream projections to the hypothalamus (Bender et al. 2015). In contrast, projections from ventral CA3 to the lateral septum appear to have no effect on locomotor activity as measured in the open field test, but instead regulate feeding behavior (Sweeney and Yang 2015). Despite the established role of both CA2/CA3 and the DLS in social memory, and the growing literature elucidating the function of the pathways connecting them, no studies to date have probed the role of the CA2/CA3 projection to the DLS in social behaviors, a compelling candidate for social memory.

4.1.3 aCA2/CA3 projections to posterior CA1.

In addition to the projections from aCA2/CA3 to aCA1 and the DLS, I also observed a dense and somewhat spatially large projection from aCA2/CA3 to the most dorsal segment of posterior CA1 (pCA1). The segregation of hippocampal poles is usually differentiated by the terms "dorsal" and "ventral", however for anatomical reasons that render this specific projection outside the range of what is typically considered vCA1, I have chosen to adopt "anterior" and "posterior nomenclature.

pCA1, and the posterior hippocampus in general, have been well studied in the context of anxiety and fear, but are somewhat understudied in their relation to social behavior. Early lesion studies lead to circumstantial and conflicting evidence. One of the first studies to loosely implicate pCA1 in social behaviors is the original work by Kogan and colleagues using ibotenic acid to lesion the hippocampus in mice, and observing a deficit in long-term social recognition memory

(Kogan et al. 2000). However, because this study lesioned both the anterior and posterior poles of the hippocampus, it is not clear whether the effect observed is due to contributions from anterior hippocampus, posterior hippocampus, or both. Alternatively, follow-up studies utilizing ibotenic acid early in development showed that in contrast to the amygdala, lesions of the posterior hippocampus did not affect measures of social play during adulthood, suggesting that if the posterior hippocampus is involved in social play behavior, its presence during development is negligible (Daenen et al. 2002).

However, more recent studies utilizing more specific tools clearly implicate posterior hippocampus in social behaviors. A clear set of experiments utilizing both *in vivo* optogenetic terminal-specific activation and silencing demonstrate that outputs from the BLA to the posterior hippocampus (which largely terminate in pCA1), bidirectionally modulate social affiliation, such that activating these terminals decreases social exploration, and silencing them increases social exploration (Felix-Ortiz and Tye 2014). Furthermore, a recent study investigating how hippocampal pathology relates to susceptibility following social defeat stress demonstrated that posterior hippocampus seems to be the locus for susceptibility. Animals that demonstrated passive coping mechanisms (indicative of susceptibility) following social defeat stressed demonstrated increased cFos activity, increased activity of markers for neuroinflammatory responses, and increased blood vessel density in the posterior, but not anterior, hippocampus (Pearson-Leary et al. 2017). A convergent study also implicates pCA1 in susceptibility to social defeat stress by showing decreased IEG expression in animals resilient to defeat stress (Bagot et al. 2015). Further, optogenetic induction of long-term depression (LTD) at glutamatergic synapses from pCA1 to the nucleus accumbens (NAcc) was sufficient to induce resilient-like behavior (Bagot et al. 2015).

The pCA1-NAcc circuit has also received recent attention in the realm of social recognition. A seminal study carried out by Okuyama and colleagues utilized *in vivo* optogenetic silencing to implicate pCA1 as a critical locus for social memory, for the first time (Okuyama et al. 2016). In contrast to aCA1 cell bodies, silencing pCA1 cell bodies was sufficient to disrupt discrimination between novel and familiar mice (Okuyama et al. 2016). Additionally, terminal-specific silencing of pCA1 outputs determined that social information in pCA1 is relayed via projections to the NAcc, but not to the BLA or olfactory bulbs (Okuyama et al. 2016). Further, experiments utilizing *in vivo* calcium imaging demonstrate that the ensemble of neurons that encodes a particular social stimulus undergoes a four-fold expansion three days following initial social contact (Okuyama et al. 2016).

Critically, while aCA2/CA3 and pCA1 are both indispensable for social recognition memory, it is not understood whether and how computations from aCA2/CA3 are linked to those in pCA1. Interestingly, few reports have demonstrated that a projection does exist from aCA2/CA3 to pCA1 that may link the two (Kohara et al. 2014; Okuyama et al. 2016).but whether or not this pathway is functionally relevant to social discrimination is not clear. This pathway therefore stands out as an intriguing candidate to relay computations from anterior to posterior hippocampus, and eventually to reward circuits such as the nucleus accumbens.

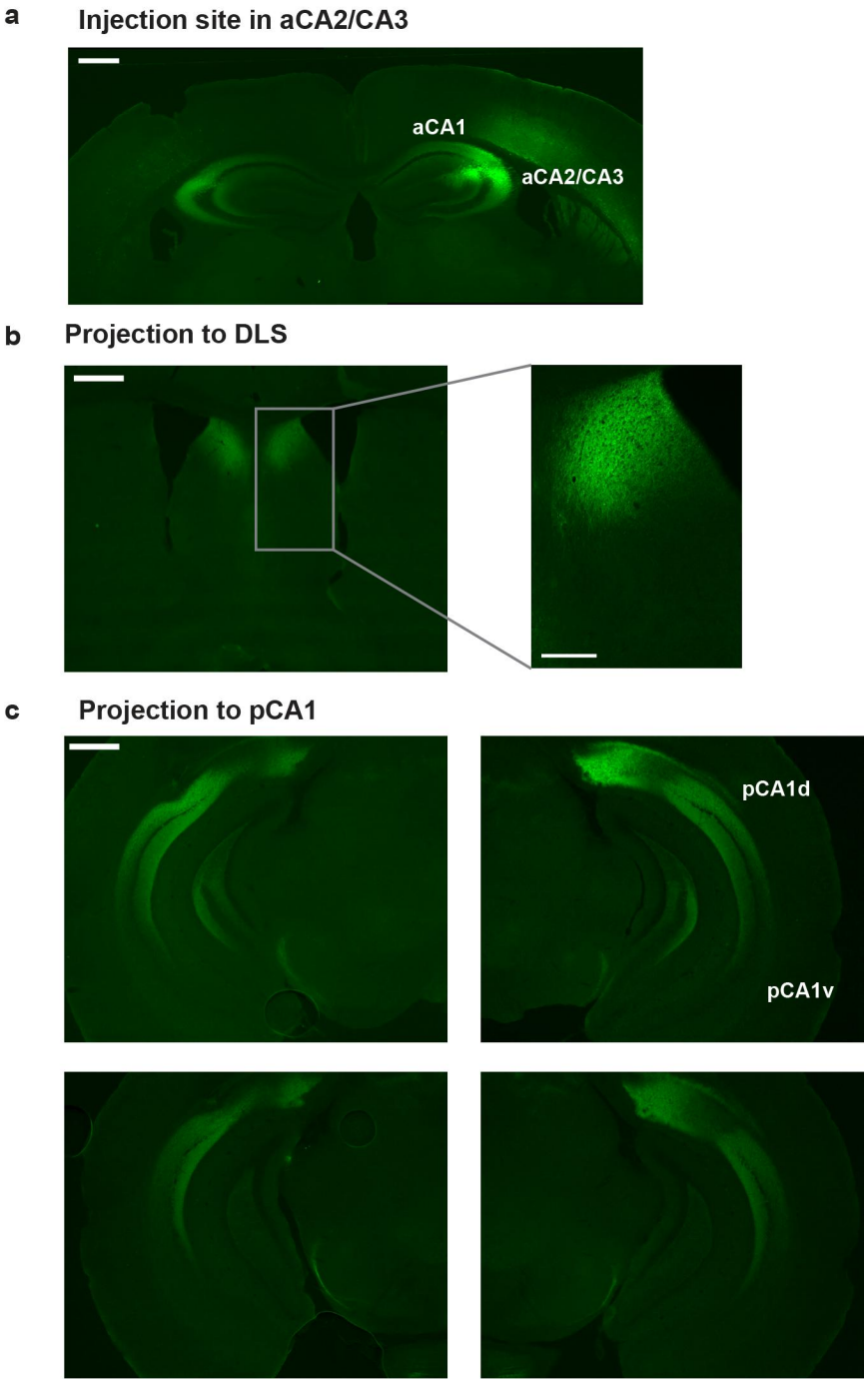
4.2 Results

Given the variety of outputs of aCA2/CA3$_{distal}$, social information may be relayed via projections to aCA1, DLS, and/or pCA1 to subcortical and prefrontal circuits to guide social behavior (**Figure 4.1**). To begin to understand how Oxtr-dependent computations underlying social recognition performed in aCA2/CA3$_{distal}$ are relayed out of the anterior hippocampus to limbic circuits that mediate social behavior, I utilized *in vivo* terminal-specific optogenetic

Figure 4.1 | Representative images of projection pattern from aCA2/CA3$_{distal}$ to aCA1, pCA1, and DLS.

(**a**) Representative low magnification image of injection of NpHR virus in aCA2/CA3$_{distal}$ and corresponding terminals in aCA1. Scale bar denotes 500 μm. (**b**) Representative low magnification (left) and high magnification (right) images of NpHR terminals in dorsolateral septum (DLS). Scale bars denote 500 μm (left) and 100 μm (right). (**c**) Representative low magnification images of NpHR terminals in posterior CA1. Scale bar denotes 500 μm.

Figure 4.1 (Continued)



silencing to attenuate aCA2/CA3$_{distal}$ outputs to these three downstream targets.

I first targeted the pathway from aCA2/CA3$_{distal}$ to aCA1 (**Figure 4.2a,b**). I injected the light-sensitive chloride pump halorhodopsin, AAV$_5$-CamKIIα-eNpHR-EYFP, or control virus, AAV$_5$-CamKIIα-EYFP bilaterally into aCA2/CA3$_{distal}$ of adult male mice. Three weeks post-injection, bilateral optogenetic implants were placed above aCA1. Mice were then tested for both object behavior and social behavior. Optogenetic illumination of aCA2/CA3$_{distal}$ terminals in aCA1 during the test phase of novel object recognition task robustly impaired discrimination between the familiar and novel object in NpHR animals relative to controls (two-way ANOVA, treatment: $F_{(1,14)} = 3.783$, $p = .0721$, object: $F_{(1,14)} = 28.67$, $p = .0001$, interaction: $F_{(1,14)} = 15.88$, $p = .0014$; Multiple comparisons, Object A vs C, EYFP: $p < .0001$, NpHR: $p = .6985$, **Figure 4.2d**). Discrimination ratios of NpHR mice were significantly lower than controls (unpaired t-test $p = .0029$, **Figure 4.2d**). I did not observe any effects on object exploration, social exploration, or discrimination of social stimuli (**Figure 4.2c,e,f**). These data suggest that aCA2/CA3$_{distal}$ outputs to aCA1 are critical for object recognition but are dispensable for discrimination of social stimuli. I next asked if aCA2/CA3$_{distal}$ outputs to the DLS mediate social discrimination. AAV$_5$-CamKIIα-eNpHR-EYFP or AAV$_5$-CamKIIα-EYFP viruses were bilaterally injected into aCA2/CA3$_{distal}$ of adult male mice and bilateral optogenetic implants were placed above the DLS (**Figure 4.3a,b**). Optogenetic attenuation of terminals was confirmed by quantifying the number of cFos+ cells in the termination area (unpaired t-test, $p = .0006$, **Figure 4.3c**). I observed a modest enhancement in social discrimination (two-way ANOVA, treatment: $F_{(1,30)} = .2753$, $p = .6037$, stimulus: $F_{(1,30)} = 52.65$, $p < .0001$, interaction: $F_{(1,30)} = 4.861$, $p = .0353$; Multiple comparisons, Familiar vs Novel, EYFP: $p = .0018$, NpHR: $p < .0001$, **Figure 4.3g**). Discrimination ratios were significantly higher

Figure 4.2 | Optogenetic attenuation of aCA2/CA3$_{distal}$ outputs to aCA1 impairs discrimination of object, but not social stimuli.

(**a**) Schematic illustrating viral injection, optogenetic implants and behavioral testing timeline. (**b**) Representative images of site of injection of eNpHR3.0 virus in *aCA2/CA3$_{distal}$* cell bodies (top) and corresponding axon terminals in aCA1 (bottom). Scale bar denotes 200 μm. (**c**) Behavioral schematic (top) and quantification (bottom) of single object exploration (EYFP: n=9, NpHR: n=7). (**d**) Behavioral schematic (top) and quantification (bottom) of novel objection recognition (EYFP: n=8, NpHR: n=8). Quantifications are displayed as Habituation (trials 1-3), Test (trial 4), and discrimination ratio (trial 4). Laser was on during trial 4 only. (**e**) Behavioral schematic (top) and quantification (bottom) of social exploration test (EYFP: n=10, NpHR: n=7). (**f**) Behavioral schematic (top) and quantification (bottom) of social discrimination task (EYFP: n=6, NpHR: n=6). Quantifications are displayed as Habituation (trials 1-3), Test (trial 4), and discrimination ratio (trial 4). Laser was on during trial 4 only. All data are displayed as mean ± SEM.

Figure 4.2 (Continued)

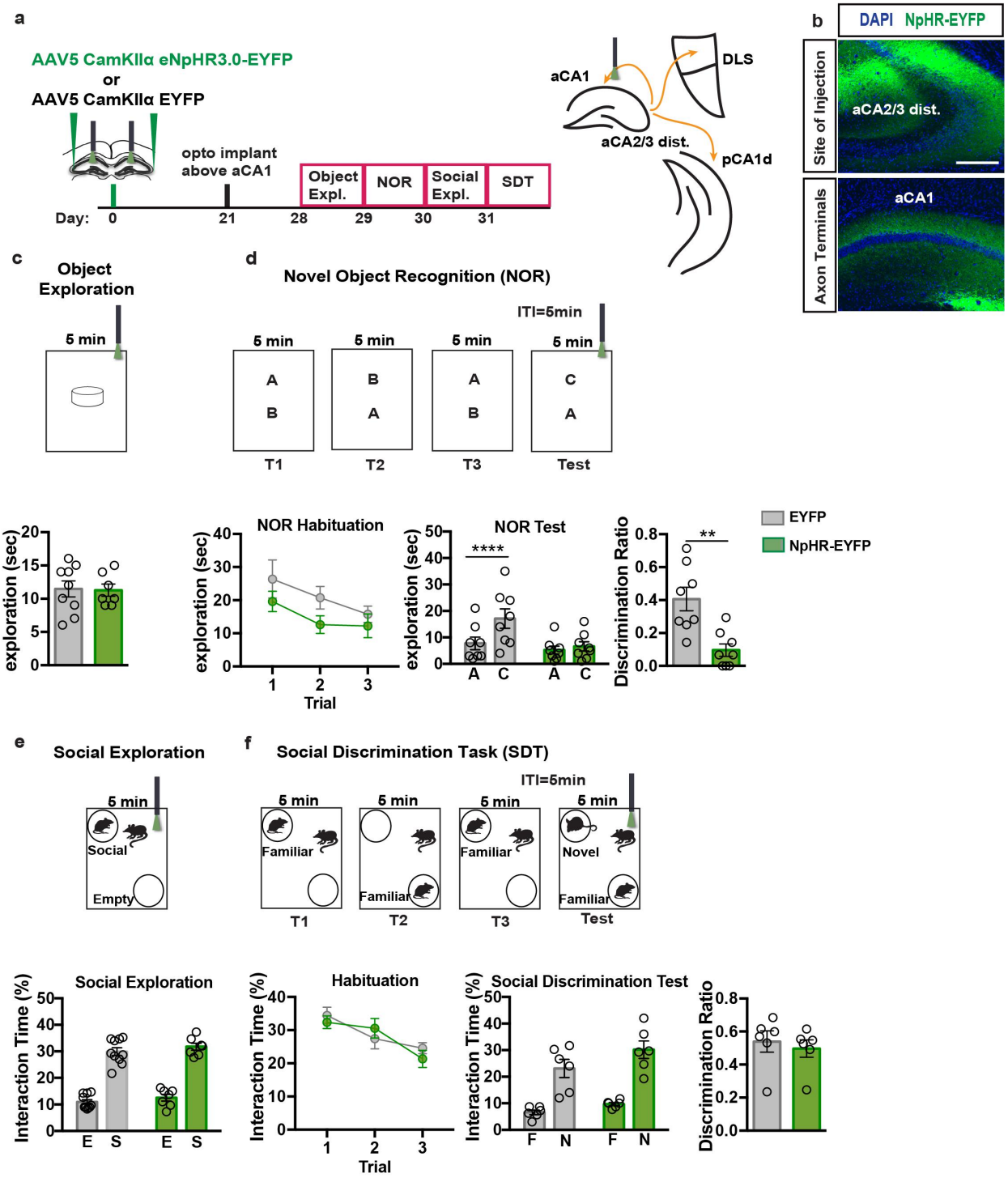
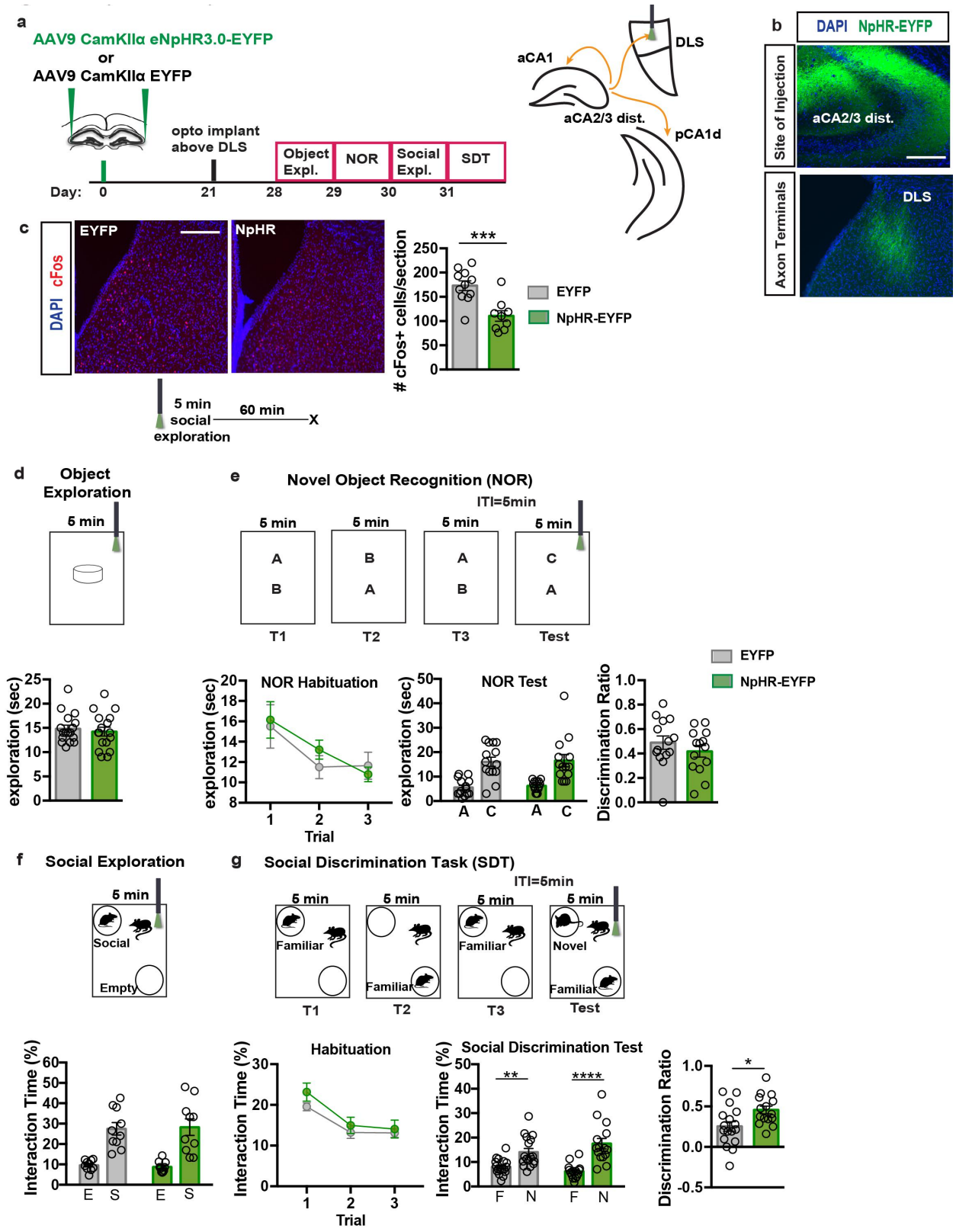


Figure 4.3 | Optogenetic attenuation of aCA2/CA3$_{distal}$ outputs to DLS modestly enhances discrimination of social stimuli.

(**a**) Schematic illustrating viral injection, optogentic implant and behavioral testing timeline. (**b**) Representative images of site of injection of eNpHR3.0 virus in aCA2/CA3$_{distal}$ cell bodies (top) and corresponding axon terminals in DLS (bottom). Scale bar denotes 200 μm. (**c**) Representative images and quantifications of cFos immunoreactivity in termination zone of DLS during optogenetic silencing (EYFP: n=11, NpHR: n=9). Scale bar denotes 200 μm. (**d**) Behavioral schematic (top) and quantification (bottom) of single object exploration (EYFP: n=17, NpHR: n=17). (**e**) Behavioral schematic (top) and quantification (bottom) of novel objection recognition (EYFP: n=14, NpHR: n=14). Quantifications are displayed as Habituation (trials 1-3), Test (trial 4), and discrimination ratio (trial 4). Laser was on during trial 4 only. (**f**) Behavioral schematic (top) and quantification (bottom) of social exploration test (EYFP: n=10, NpHR: n=10). (**g**) Behavioral schematic (top) and quantification (bottom) of social discrimination task (EYFP: n=17, NpHR: n=15). Quantifications are displayed as Habituation (trials 1-3), Test (trial 4), and discrimination ratio (trial 4). Laser was on during trial 4 only. All data are displayed as mean ± SEM.

Figure 4.3 (Continued)



for NpHR animals than control animals (unpaired t-test, p = .0121, **Figure 4.3g**). I did not observe any effects on object exploration, NOR, or social exploration (**Figure 4.3d,e,f**). These data suggest that attenuation of aCA2/CA3$_{distal}$-DLS projections may modestly promote discrimination of social stimuli.

Recent studies have demonstrated a role for pCA1-NAcc circuit in social discrimination (Okuyama et al. 2016). I observed direct outputs from aCA2/CA3$_{distal}$ to the dorsal segment of pCA1 (**Figure 4.4a,b**) (Kohara et al. 2014) and confirmed the colocalization of these terminals with the CA1 marker, WFS1 (**Figure 4.5**). I attenuated these outputs by injecting AAV$_5$-CamKIIα-eNpHR-EYFP or AAV$_5$-CamKIIα-EYFP into bilateral aCA2/CA3$_{distal}$ of adult male mice, and placing a bilateral optogenetic implant above pCA1 (**Figure 4.4a**). Effective silencing was confirmed by quantifying the number of cFos+ cells in pCA1 below the optogenetic implant (unpaired t-test, p = .0223, **Figure 4.4c**). Optogenetic attenuation of aCA2/CA3$_{distal}$ terminals in pCA1 did not affect performance in tests of single object exploration, novel object recognition, or social exploration (**Figure 4.4d,e,f**). In contrast, optogenetic illumination of aCA2/CA3$_{distal}$ terminals in pCA1 during the test phase of social discrimination task markedly impaired discrimination in NpHR animals as compared to controls (two-way ANOVA, treatment: $F_{(1,12)}$ = .82, p = .3830, stimulus: $F_{(1,12)}$ = 64.71, p < .0001, interaction: $F_{(1,12)}$ = 13.4, p = .0033; Multiple comparison, Familiar vs Novel, EYFP: p < .0001, NpHR: p = .0184, **Figure 4.4g**). Discrimination ratios were also significantly lower for NpHR animals as compared to controls (unpaired t-test, p = .0006, **Figure 4.4g**). Together, these data suggest that aCA2/CA3$_{distal}$ projections to pCA1 may relay social memory computations to subcortical and prefrontal circuits to guide social behavior.

Figure 4.4 | Optogenetic attenuation of aCA2/CA3$_{distal}$ outputs to pCA1 impairs discrimination of social, but not non-social, stimuli.

(**a**) Schematic illustrating viral injection, optogenetic implants and behavioral testing timeline. (**b**) Representative images of site of injection of eNpHR3.0 virus in *aCA2/CA3$_{distal}$* cell bodies (top) and corresponding axon terminals in pCA1 (bottom). Scale bars denote 200 μm (top) and 500 μm (bottom). (**c**) Representative images and quantifications of cFos immunoreactivity in pyramidal layer of pCA1 during optogenetic silencing (EYFP: n=7, NpHR: n=7). Scale bar denotes 100 μm. (**d**) Behavioral schematic (top) and quantification (bottom) of single object exploration (EYFP: n=7, NpHR: n=7). (**e**) Behavioral schematic (top) and quantification (bottom) of novel objection recognition (EYFP: n=6, NpHR: n=7). Quantifications are displayed as Habituation (trials 1-3), Test (trial 4), and discrimination ratio (trial 4). Laser was on during trial 4 only. (**f**) Behavioral schematic (top) and quantification (bottom) of social exploration test (EYFP: n=6, NpHR: n=7). (**g**) Behavioral schematic (top) and quantification (bottom) of social discrimination task (EYFP: n=6, NpHR: n=7). Quantifications are displayed as Habituation (trials 1-3), Test (trial 4), and discrimination ratio (trial 4). Laser was on during trial 4 only. All data are displayed as mean ± SEM.

Figure 4.4 (continued)

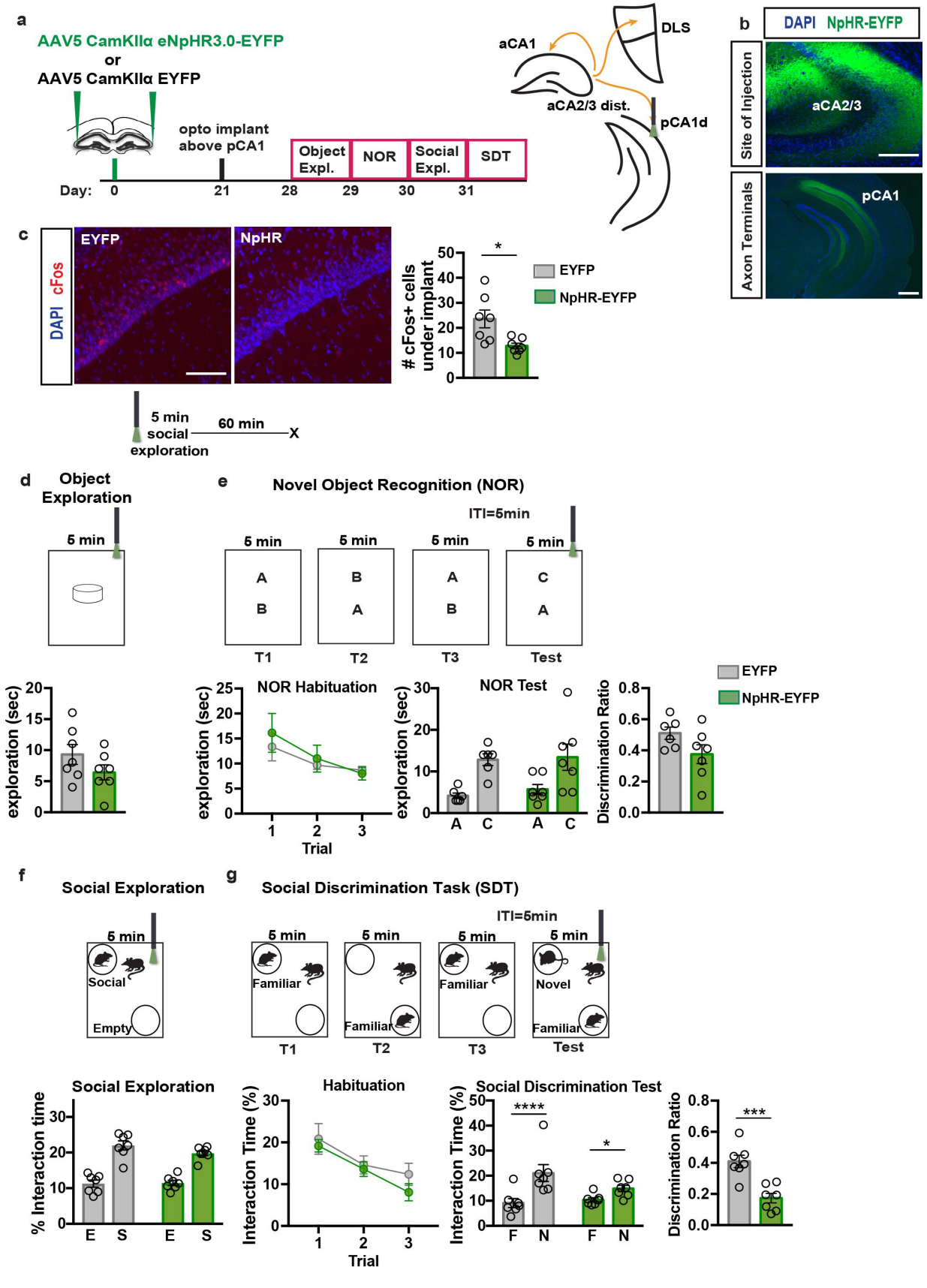
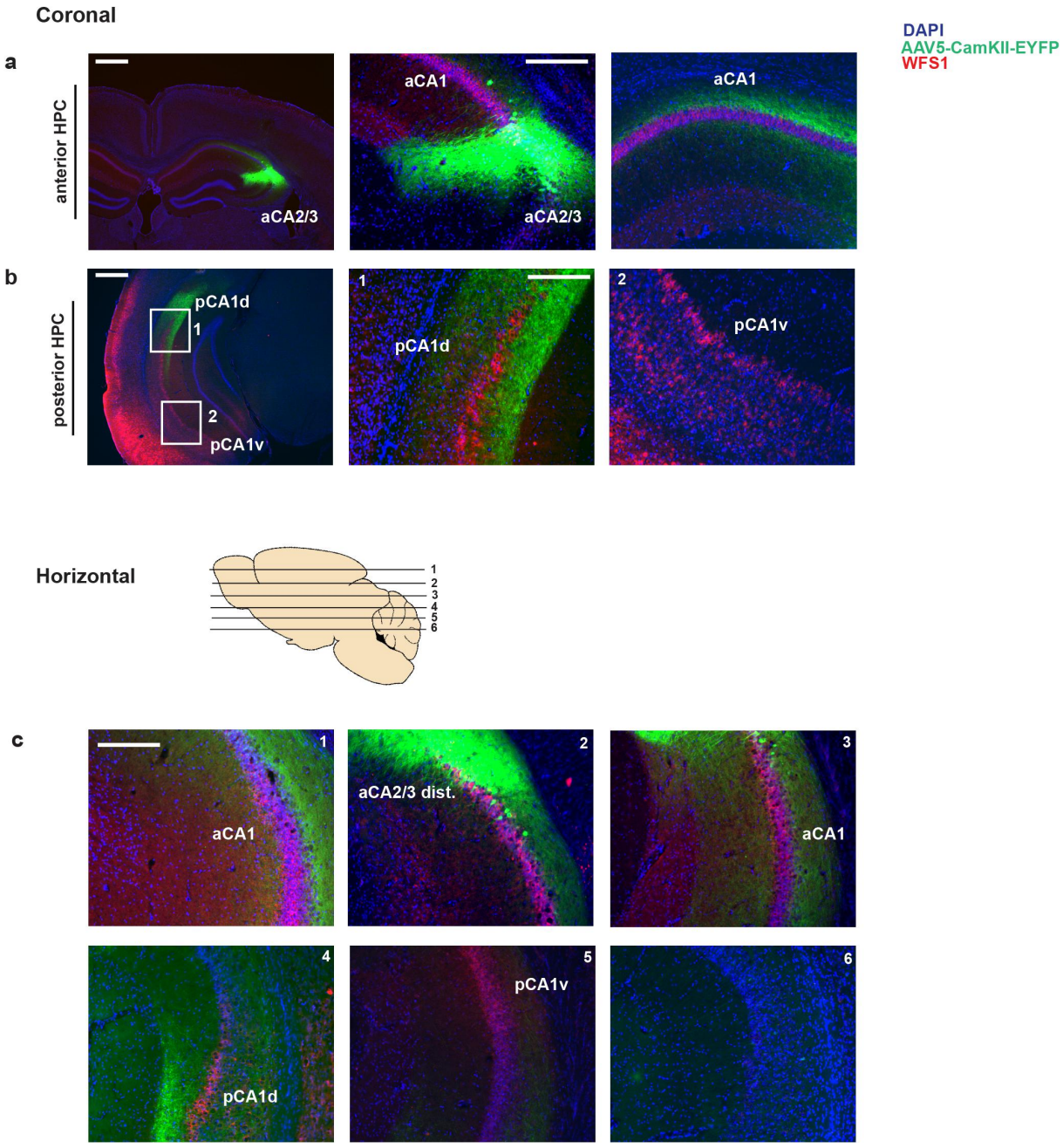


Figure 4.5 | Projections from aCA2/CA3$_{distal}$ colocalize with CA1 marker WFS1 in both anterior and posterior CA1.

(**a**) Low magnification (left) and high magnification (right) images of coronal sections depicting projections from aCA2/CA3$_{distal}$ to aCA1. Scale bars denote 500 μm (left) and 200 μm (right). (**b**) Low magnification (left) and high magnification (right) images of coronal sections depicting projections from aCA2/CA3$_{distal}$ to pCA1. Scale bars denote 500 μm (left) and 200 μm (right). (**c**) Representative images of horizontal sections from most superficial (1) to most deep (6), depicting projections from aCA2/CA3$_{distal}$ to aCA1 and pCA1d. Scale bar denotes 200 μm.

Figure 4.5 (Continued)



4.3 Discussion

Until recently, it was poorly understood how the hippocampus subserves a variety of discrimination-related behaviors across many modalities, whether or not the same circuits were involved for both social and non-social discrimination tasks, and if so, how the hippocampus functionally segregates them. Studies from our group and others have converged on the idea that the aCA2/CA3 subregion may mediate both social discrimination and object discrimination; yet how these computations are rendered distinct and relayed to appropriate circuits is not understood. Collectively, the experiments delineated in this chapter demonstrate, for the first time, unique sets of projections out of aCA2/CA3 that functionally and anatomically dissociate social discrimination from object discrimination.

That optogenetic silencing of aCA2/CA3 outputs to the DLS did not impair social discrimination was an initially perplexing result, given the critical role of both structures to social recognition, and the explicit role of oxytocin in mediating social discrimination in the DLS (Lukas et al. 2013; Mesic et al. 2015). Indeed, not only was this pathway unnecessary for social discrimination, optogenetic silencing in fact modestly enhanced discrimination. We propose a number of possible explanations that may underlie this result. First, given that the DLS is made up almost entirely of GABAergic interneurons (Zhao et al. 2013), one possible mechanism underlying the modest enhancement observed is that optogenetically silencing this population led to the opposite effect—rather than a net effect of silencing, we may have disinhibited downstream limbic regions that receive input from the DLS. Additionally, given the previously demonstrated role of the aCA2/CA3—DLS pathway in regulating state-dependent transitions in running speed (Bender et al. 2015), the result obtained may represent an artifact induced by increased locomotor activity. Finally, given hippocampal literature on sparse activity being essential to minimizing interference

through non-overlapping ensembles of neurons, attenuation of aCA2/CA3 outputs to the DLS may have artificially mimicked a physiological state which resembles sparse activity in aCA2/CA3, thereby mildly facilitating discrimination. Technical considerations aside, however, it remains clear that this projection is not necessary for social discrimination. Future research may uncover a role for the DLS in other social behaviors such as aggression, or sexual behaviors.

Within the hippocampus I observed that optogenetically attenuating aCA2/CA3 outputs to aCA1 robustly impaired object discrimination, but did not affect social discrimination. Conversely, attenuating outputs to pCA1 revealed the opposite—this pathway is critical for social discrimination, and dispensable for object discrimination. These results are concordant with previous observations that activity in pCA1 cell bodies, but not aCA1 cell bodies is critical for social discrimination, but not object discrimination (Okuyama et al. 2016), and activity in aCA1 cell bodies is critical for object recognition (Cohen et al. 2013; Cohen and Stackman 2015). Given that *in vivo* single unit recordings in aCA2 reveal responsiveness to both social stimuli and objects (Alexander et al. 2016), such a neatly separable double dissociation suggests that aCA2/CA3 acts as a divergence point that integrates a variety of sensory information via inputs from the DG, entorhinal cortices, and paraventricular nucleus of the hypothalamus (among others) and routes them to appropriate downstream outputs depending on modality and sensory cues.

This double dissociation is also particularly interesting in light of the long-axis dissociation discussed in Chapters 1 and 2. Evolving models of the hippocampus in both rodents and humans largely depict a polarized structure in which “cognitive” and “limbic” features are neatly separated into anterior and posterior poles, respectively. The anterior pole is primarily thought to govern “cognitive” tasks such as spatial navigation, contextual learning, and object recognition through the utilization of spatially localized place fields that tightly encode specific elements of the sensory

environment (Fanselow and Dong 2010; Strange et al. 2014). The posterior pole, on the other hand, is thought to be a locus that subserves limbic functions such as anxiety, susceptibility to stress, and social behaviors, and is characterized by place fields with much less spatial specificity (Fanselow and Dong 2010; Strange et al. 2014). This behavioral dissociation is thought to be partially mediated by unique projection patterns in and out of the anterior and posterior hippocampus, as well as molecular differences in gene and protein expression (Fanselow and Dong 2010; Strange et al. 2014). However, social discrimination as a mental phenomenon seems to defy simple dichotomies between the cognitive and the limbic—recognition in a broad sense is a traditionally cognitive process that, through growing evidence, seems to draw on pattern separation via either population-based encoding or rate coding to effectively minimize overlap and interference between stimuli. However, the drive to seek interaction with some social stimuli and not others is thought to be mediated by a variety of limbic circuits. That aCA2/CA3 sends a longitudinal projection to pCA1 that mediates social discrimination represents the convergence of the cognitive and limbic demands of the task, and stands in stark contrast to traditional theories of hippocampal intrinsic circuitry, which often define the hippocampus in terms of parallel trisynaptic comparator loops along the anterior-posterior axis. That this circuit facilitates direct communication between anterior and posterior hippocampus raises valuable questions about how separable cognitive and limbic processes are from each other, whether or not additional underappreciated longitudinal circuits may exist in the hippocampus, and how hippocampal theory may begin to evolve in the coming years to place greater emphasis on cross-talk between anterior and posterior poles.

4.4 Methods

Mouse Lines and Animal Care

Optogenetic terminal-specific silencing experiments were carried out in adult male C57Bl/6J mice (8 weeks old). All mice were housed 3-5 per cage in standard laboratory conditions under a 12-hour light-dark cycle (7:00 a.m. to 7:00 p.m.) with ad libitum access to food and water. Behavioral testing occurred during the light cycle. All experiments were carried out in accordance with procedures approved by the Institutional Animal Care and Use Committee at the Massachusetts General Hospital in accordance with NIH guidelines.

Adeno-associated Viruses (AAV)

AAV_5-CaMKIIα-eYFP (6 x 10^{12} particles/mL) and AAV_5-CaMKIIα-eNpHR3.0-eYFP (3 x 10^{12} particles/mL) viruses were generated by and obtained from the University of North Carolina Vector Core (Chapel Hill, NC).

Stereotactic Surgery

Viral injection: Mice were given carprofen (5mg kg^{-1} s.c.) prior to surgery and 24h later to minimize discomfort. Mice were anaesthetized with ketamine and xylazine (10mg mL^{-1} and 1.6mg mL^{-1} , i.p.) and placed in a stereotaxic frame (Stoelting). Small holes were drilled at each injection location and injected with a Hamilton microsyringe at a rate of 0.1 µl/min. For optogenetic silencing experiments, .3 µl undiluted AAV5-CaMKIIα-eNpHR3.0-eYFP or AAV5-CaMKIIα-eYFP was injected bilaterally into $aCA2/CA3_{distal}$ (AP -2.0 mm, ML +/- 2.5 mm, DV -2.3 mm from Bregma). After completion of the injection, the needle was left on the site of injection for 5 min, raised 0.2 mm and left on the site for an additional 5 min to allow diffusion of virus at the injection site and then slowly withdrawn. The skin incision was closed carefully using nylon sutures. Animals were monitored during recovery.

Optogenetic Implants: Mice were surgically implanted with fiber optic cannulas 3 to 4 weeks following injection of AAV5-CaMKIIα-eYFP or AAV5-CaMKIIα-eNpHR3.0-eYFP and behavioral experiments started 1 week after surgery. Mice were implanted bilaterally with chronically dwelling optical fibers targeted to the anterior CA1 (AP -1.9 mm, ML +/- 1.5 mm, DV -1.2 mm from Bregma), posterior CA1 (AP -3.35 mm, ML +/- 3.1 mm, DV -1.7 mm from Bregma), or dorsolateral septum (AP +1.15 mm, ML +/- 1.0 mm angle +/- 10°, DV -2.5 mm from Bregma). Optical fibers were secured with one cranial screw and dental cement. After surgery, mice were returned to their home cage and monitored until recovery from surgery.

Construction of Optical Fibers

200um core, 0.37 numerical aperture (NA) multimode fiber (ThorLabs) was threaded through and glued with epoxy to a 230um core stainless steel or zirconia multimode ferrule (Fiber Instrument Sales and Precision Fiber Products), polished and cut for implantation. Optical patch cables were generated the same way, with the free end connected to a multimode FC ferrule assembly for connecting to a 1X2 Optical rotary joint (Doric lenses). The other end of the rotary joint was connected via a patch cable to a 561 nm laser diode (OEM laser systems) via a non-contact style laser to fiber coupler (OZ optics).

***In vivo* Laser Delivery**

Age-matched, genotyped-matched male mice (3-4 months old) were used for all behavioral experiments. Mice were kept in a quiet room for at least 1 h before testing. Behavioral tests took place under bright lighting conditions (700 lux) and performed in the following order: single object exploration (day 1), novel object recognition (day 2), social exploration (day 3) and social discrimination (day 4). Prior to each experiment, mice were bilaterally attached to the patch cables via a zirconia sleeve, and allowed to recover for 2-3 min in a transition cage similar to their home

cage. The patch cables were interfaced to an FC/PC rotary joint (Doric lenses), which was attached on the other end to a laser diode (561nm). The light power at the end of the fiber tip was 10-15mW. At the end of each behavioral experiment (5-7 weeks following viral surgery), mice were analyzed for viral and fiber optics placement and mis-targeted animals were excluded from the analysis. In aCA2/CA3-CA1 attenuation experiment, animal numbers varied across behavioral tasks because of loss of optogenetic implants during course of testing, and two behavioral cohorts were utilized, with second cohort being used for a context-updating task instead of social discrimination after social exploration. Randomly selected videos were scored by two different investigators.

Single Object Exploration

Mice were placed an arena filled with bedding (45cm long, 15cm high and 30cm wide) with a single novel object for 5 minutes. Sessions were video-recorded, and videos were manually scored for object exploration (when an animal's snout was 2cm or less from the object) by an investigator blind to animal treatment identity. For optogenetic experiments, light of 561 nm was turned on for the full duration of the session.

Novel Object Recognition

Mice were placed in an arena filled with bedding (45cm long, 15cm high and 30cm wide) with two distinct objects (A and B) for three 5 min sessions, with a 5 minute inter-trial interval. Mice were allowed to habituate to the objects during the three training sessions, and one of the objects was subsequently replaced with a novel object (C) in session four. Objects were counterbalanced across subjects and object positions were counterbalanced across trials. The objects that were selected for testing elicited comparable levels of exploration based on exploration levels in pilot experiments. Sessions were video-recorded, and videos were manually scored for object exploration (when an animal's snout was 2cm or less from the object) by an investigator blind to

object identity and animal treatment identity. For optogenetic experiments, light of 561 nm was turned on only during trial 4.

Social Exploration

Mice were placed in an open plexiglass arena (41cm x 41 cm, Kinder Scientific) for 5 minutes with two pencil-wire cups placed on opposing corners of the arena. Habituation to the chamber took place one day prior to start of behavioral testing. One cup remained empty while the other contained a novel adult male C57Bl/6J mouse. Sessions were video-recorded, and videos were manually scored for exploration of the social cup and empty cup (direct snout-to-cup contact, with at least two paws on the ground--time spent climbing on the cup was not included) by an investigator blind to animal treatment identity. Stimulus mice were trained to sit in pencil-wire cups for three 15 minute sessions several days prior to behavioral testing. For optogenetic experiments, light of 561 nm was turned on for the full duration of the session.

Social Recognition (Habituation, Discrimination)

The same plexiglass arena and pencil-wire cup set-up as described for social exploration was used. Mice were placed in the arena for three 5 min sessions with an empty cup and a novel adult male C57Bl/6J mouse, with a 5 minute intertrial interval. Mice habituated to the stimulus during the first three sessions, rendering it "familiar." During trial 4, a novel adult male mouse was placed in the opposing cup, and subjects were tested for discrimination between the novel and familiar mouse. Social stimuli were counterbalanced across subjects, and the position of the familiar social stimulus was counterbalanced across trials. Sessions were video-recorded, and videos were manually scored for interaction with the novel vs familiar mouse (direct snout-to-cup contact, with at least two paws on the ground--time spent climbing on the cup was not included) by an investigator blind to animal treatment identity. Stimulus mice were trained to sit in pencil-wire

cups for three 15 minute sessions several days prior to behavioral testing. For optogenetic experiments, light of 561 nm was turned on only during trial 4. Videos were score by two different investigators.

Histology and Immunohistochemistry

Mice were anesthetized with ketamine (100 mg/kg i.p.) and xylazine (3 mg/kg i.p.) and transcardially perfused with 10mM phosphate buffer saline (PBS), pH 7.5 at 4°C, followed by a fixative solution containing 4% paraformaldehyde (PFA) in PBS. Brains were post-fixed in 4% PFA overnight at 4°C and cryo-protected for 72 hours in 30% sucrose at 4°C prior to freezing in OCT on dry ice. Coronal sections were obtained at 35 μm using a cryostat (Leica, Germany) in six matched sets. Sections were stored in 1X PBS with 0.01% Azide at 4°C. Floating sections were used to perform immunohistochemical labeling. Briefly, sections were washed in 1X PBS, incubated for 15 min at room temperature in 1X PBS containing .3% Triton X-100, blocked in 1X PBS containing .3% Triton X-100 and 10% NDS for 1 hour at room temperature, and incubated in primary antibodies in blocking buffer with shaking overnight at 4°C. Primary antibodies were used as follows: GFP (rabbit anti-GFP, Life Technologies A11122, 1:500, Antibodyregistry.org: AB_221569); goat anti-GFP, Novus Biologicals, NB100-1770, 1:500, (Antibodyregistry.org: AB_10128178), cFos (Rabbit, Santa Cruz, 1:2000, Santa Cruz SC52, Antibodyregistry.org: AB_2106783), RGS14 (Mouse, UC Davis/NIH NeuroMab, 1:400). The following day, sections were washed 3 times in 1X PBS and incubated with fluorescent-label coupled secondary antibodies (Jackson Immunoresearch, Donkey anti-Rabbit, Goat, or Mouse, 488-, Cy3-, or Cy5- coupled, 1:500) for 2 hours at room temperature.

cFos and Perfusion

Mice were exposed to a novel social stimulus in a novel arena filled with bedding for 5 minutes, and promptly returned to home cage. Mice were then anesthetized with ketamine (100 mg/kg i.p.) and xylazine (3mg/kg i.p.) and transcardially perfused 60 minutes post exposure, as described above in "Histology and Immunohistochemistry." For optogenetic silencing cFos experiments, mice were given 3-5 minutes to acclimate after being bilaterally attached to a laser patch cord, before the laser was turned on and social exposure began.

Image Acquisition and Analysis

For cFos analysis: 10x bilateral images were acquired using a Nikon epifluorescence microscope. cFos+ cells were manually quantified as those with intensity higher than background in the aDG granule cell layer, pCA1 pyramidal cell layer directly under the implant, and DLS. For aDG, both blades were assessed. Six hemisections were analyzed for aDG and pCA1, while four hemisections were captured for the DLS. Data was expressed as # cFos+ cells per section. All quantifications and analyses were completed by an experimenter blind to treatment condition.

Statistics

Statistical analysis was carried out using GraphPad Prism v7 software. Data (mean ± SEM). Discrimination ratios, cFos analysis, and measures of object exploration were analyzed using unpaired two-tailed student's t-test to compare two groups. Measures of NOR, social exploration, and social discrimination were analyzed using mixed factor two-way ANOVA with repeated measure followed by Bonferroni's multiple comparisons test when the interaction, p value was < .05. In all cases, significance was set at $p < 0.05$.

4.5 Author Contributions

T.R. carried out experiments and analyzed data with help from K.M.M., and A.B.

A.V. contributed reagents and shared resources.

T.R. and A.S. co-developed the concept and wrote the manuscript.

A.S. conceived and supervised all aspects of the project.

4.6 Acknowledgments

We thank members of the Sahay lab for their comments on the manuscript. A.S. acknowledges support from US National Institutes of Health Biobehavioral Research Awards for Innovative New Scientists (BRAINS) 1-R01MH104175, NIH-NIA 1R01AG048908-01, NIH-NIMH 1R01MH111729-01, Ellison Medical Foundation New Scholar in Aging, Whitehall Foundation, Inscopix Decode award, NARSAD Independent Investigator Award, Ellison Family Philanthropic support, Blue Guitar Fund, Harvard NeurodiscoveryCenter/MADRC Center Pilot Grant Award, HSCI Development grant, and HSCI seed grant.

Page intentionally left blank.

CHAPTER 5

The role of adult hippocampal neurogenesis in social behaviors

5.1 Introduction

The 20th century saw an explosion of foundational work establishing the presence of new neurons in the adult brain. Such a notion was entirely antithetical to historical assumptions of the brain as being hardwired, mechanistic, and unchangeable beyond early stages of development. Initial studies by Joseph Altman and others were therefore inflexibly dismissed in favor of studies that supported the prevailing model. However, after more than 40 years of work that slowly chipped away at a stubborn dogma, neuroscience experienced what philosopher Thomas Kuhn may have referred to as a paradigm shift, and adult neurogenesis in both the dentate gyrus and subventricular zone became accepted as a credible phenomenon in organisms across many stages of the evolutionary tree. Adult hippocampal neurogenesis is now one of the most prolific and rapidly evolving subfields of neuroscience, and its potentially wide-reaching impact as a therapeutic strategy for disorders of memory and mood is promising. Functionally, adult-born neurons are critical for spatial and contextual discrimination—animals lacking adult-born neurons show deficits in these behaviors, while those with increased neurogenesis show enhancements. This is thought to be at least partially mediated by governance of inhibitory tone in local DG microcircuitry, whereby adult-born neurons potently regulate the excitability of mature granule neurons, promoting sparse activity that supports pattern separation. However, while the role of adult-born neurons in spatial and contextual discrimination has been well defined, much less is known about whether or not these neurons also promote social discrimination. Interestingly, adult neurogenesis is tightly regulated by both social exposure and oxytocin, suggesting that these neurons may represent an understudied substrate for social memory. Here I demonstrate the use of a loss-of-function mouse line, GFAP-TK, in order to probe the role of adult-born neurons in both object and social discrimination.

5.1.1 The DG is a locus for adult neurogenesis in the mammalian brain.

The first examples of mammalian adult neurogenesis were reported by Joseph Altman in the 1960s in two studies using tritiated (radioactive) thymidine in the rat and cat brain to label actively proliferating cells (Altman 1963; Altman and Das 1965). In these studies, intraperitoneal injection of ^{3}H-thymidine resulted in labeling of putative adult-born neurons in the subgranular zone (SGZ) of the dentate gyrus, as well as the subventricular zone (SVZ) of the lateral ventricles. Although these studies offered compelling initial evidence for the presence of adult neurogenesis, they challenged dogmatic and unquestioned notions that the generation of new neurons was strictly confined to early postnatal development (Ramón y Cajal, 1928), and were confounded by the inability to unequivocally distinguish neurons from glia. Much of Altman's pioneering work was therefore at best ignored, and at worst aggressively attacked by skeptics who sought to disprove his work and tarnish his reputation as a scientist. Follow-up work by Michael Kaplan combined ^{3}H-thymidine labeling and electron microscopy to demonstrate that ^{3}H-thymidine labeled cells in the SGZ of adult rats had the structural characteristics of neurons (as opposed to glia), yet adult hippocampal neurogenesis continued to remain controversial and disputed (Kaplan and Hinds 1977). Altman's courage in publishing such studies did not come without cost—he was denied tenure at MIT where he had established his lab, moved to Purdue University in order to continue his work, and was met with subsequent rejection by funding agencies and journals.

Over two decades later, adult neurogenesis was "rediscovered" in the 1980s and 1990s by a series of studies that corroborated Altman's initial findings. Pioneering studies by Fernando Nottebohm identified adult neurogenesis in the brain of songbirds. This work was initiated by the observation that the size of the high-level vocal nucleus (HVc) of canaries was subject to variation due to season, hormonal changes, and sexual experience (Nottebohm 1985). Hypothesizing that

this variation may be due to increase or decrease in the number of neurons, Nottebohm and colleagues demonstrated that the HVc contained proliferating ^{3}H-thymidine positive cells (Goldman and Nottebohm 1983), that these cells had the structural characteristics of neurons (Burd and Nottebohm 1985), and that they fired action potentials in response to auditory stimuli (Paton and Nottebohm 1984). By the 1990s, the development of molecular markers to differentiate neurons from glia, as well as mitotic cells from cells at rest, had advanced enough that adult neurogenesis in the rodent hippocampus had been corroborated several times (Cameron et al. 1993; Kuhn et al. 1996). Additional studies have also confirmed the presence of adult neurogenesis in the hippocampus of non-human primates (Gould et al. 1998; Gould et al. 1999). The presence of adult-born neurons in the human hippocampus is a phenomenon that has received similar debate. Studies utilizing BrdU labeling and carbon-14 dating have recapitulated rodent and primate studies and demonstrated adult neurogenesis in the hippocampus and striatum of humans (Eriksson et al. 1998; Spalding et al. 2013; Ernst et al. 2014). However recent analyses utilizing immunostaining for DCX and PSA-NCAM (two frequently used markers of neurogenesis in rodents) demonstrate that hippocampal neurogenesis rapidly declines in the first year of life in human infants and is nearly absent beyond the age of seven (Sorrells et al. 2018). Further studies that delineate differences in markers between rodent and human tissue may resolve these conflicting results.

The proliferation of neural stem cells and their subsequent survival is regulated by a number of biological and experience-dependent factors. Stress (Gould et al. 1998) and aging (Kuhn et al. 1996; McAvoy et al. 2016) lead to decreased neurogenesis, while running (van Praag et al. 1999), enriched environments (Kempermann et al. 1997), and antidepressant drugs (Malberg et al. 2000) can all lead to increased neurogenesis. The proliferation of adult-born neurons is regulated by the pro-apoptotic gene *Bax*, such that 60-80% of adult-born neurons undergo programmed cell

death within one month of their birth (Sun et al. 2004). Survival is also dependent upon NMDA-mediated functional integration into local hippocampal networks (Tashiro et al. 2006), and is governed by synaptic competition with mature DGCs (McAvoy et al. 2016). Following survival, adult-born neurons undergo a two-month process of maturation, reaching their peak plasticity at four weeks of age (Gu et al. 2012), and becoming morphologically and physiologically indistinguishable from mature neurons at eight weeks of age (Zhao et al. 2006).

5.1.2 Adult-born neurons dictate population-based coding in the DG.

Functionally, adult-born neurons are critical for pattern separation (Deng et al. 2010). This is thought to be mediated via distribution of entorhinal cortical inputs into sparse, orthogonalized ensembles within the DG (Yassa and Stark 2011). Studies manipulating either the size or activity of the adult-born DGC population support the role of neurogenesis in this function. Several studies have demonstrated that ablating neurogenesis leads to impaired spatial or contextual discrimination. Mice lacking hippocampal neurogenesis due to focal x-irradiation showed impaired spatial discrimination in a radial arm maze task when differentiating between spatial locations that were close to each other, but not those that were far apart (Clelland et al. 2009), and impaired contextual fear discrimination (Nakashiba et al. 2012). Genetic ablation of adult-born neurons up to nine weeks of age is also sufficient to impair context discrimination (Tronel et al. 2012). Interestingly, impairment of LTP in perforant pathway input via selective deletion of NR2B NMDA receptors in adult-born neurons is sufficient to impair context discrimination, despite the size of the adult-born neuron population remaining unchanged (Kheirbek et al. 2012). In the reverse direction, increasing neurogenesis via conditional deletion of the proapoptotic gene *Bax*, resulting in increased survival and integration of adult-born DGCs, is sufficient to enhance context discrimination (Sahay et al. 2011).

Studies probing the behavioral relevance of adult-born DGCs to discrimination tasks are supported by additional studies suggesting a role in population-based encoding of contextual cues. An initial study utilizing *Arc* activity as a readout for ensemble activation demonstrated that chemical depletion of neurogenesis using TMZ (Temozolomide, a chemotherapy drug) or genetic deletion of adult-born neurons using GFAP-TK mice is sufficient to impair population-based coding of very similar, but not distinct contexts in CA3 (Niibori et al. 2012). Conversely, enhancement of neurogenesis is sufficient to reduce overlap between ensembles encoding similar contexts in DG granule neurons, in both young adulthood and aging (McAvoy et al. 2016).

Mechanistically, multiple theories have been postulated as to how adult-born neurons mediate population-based coding at the cellular level. Given strong mossy fiber projections from adult-born neurons to pyramidal neurons of CA3 (Gu et al. 2012), one possibility is that adult-born neurons may themselves be the sparsely active units of the DG and directly "carry the message" from the DG to CA3 pyramidal neurons (Piatti et al. 2013). However, an alternate hypothesis is that adult-born neurons may modulate the excitation-inhibition balance of mature DGCs via local inhibitory interneurons, thereby promoting sparse activity of the DG GCL, which then sends robust mossy fiber projections to CA3 (Piatti et al. 2013). This second hypothesis seems to hold more promise in light of recent findings. For example, *in vivo* calcium imaging of adult-born DGCs shows that adult-born neurons are generally more active (as measured by frequency of calcium transients), and are less spatially tuned than mature DGCs (Danielson et al. 2016). Similarly, studies utilizing *in vivo* electrophysiological recordings demonstrate that focal irradiation of adult-born DGCs is sufficient to increase the amplitude of spontaneous gamma frequency bursts (Lacefield et al. 2012). Moreover, increasing neurogenesis in the presence of a voltage-sensitive dye is sufficient to decrease DG excitability and increases synaptic contacts of adult-born neurons

with hilar interneurons (Ikrar et al. 2013). Conversely, ablation of neurogenesis increases DG excitability (Ikrar et al. 2013). These studies are corroborated by slice physiology experiments indicating that optogenetic activation of adult-born DGCs results in robust polysynaptic inhibition of mature DGCs via local inhibitory interneurons, and decreased activity of mature DGCs during exploration of a novel context (Drew et al. 2016). Collectively, these studies suggest that neurogenesis mediates pattern separation in the DG-CA3 network by activating hilar interneurons that then promote sparse activation of mature DGCs. These sparse coding schemes promote non-overlapping traces in CA3, minimizing interference and cross-talk between similar representations.

5.1.3 Modulation of adult hippocampal neurogenesis by oxytocin

Hippocampal neurogenesis is highly sensitive to the activity of neuromodulators, including corticosterone, dopamine, and serotonin (Schoenfeld and Gould 2012; Takamura et al. 2014; Alenina and Klempin 2015). While a substantial literature has emerged around the role of these neuromodulators in promoting or suppressing neurogenesis, much less is known about the effects of oxytocin in regulating neurogenesis. A few initial studies offer insight. Measures of neuronal proliferation in the SVZ (indicated by BrdU labeling) indicate that peripheral administration of oxytocin via intraperitoneal injection and central administration via local infusion is sufficient to enhance proliferation in the ventral, but not dorsal, DG (Leuner et al. 2012; Opendak et al. 2016). However, in addition to the ventral hippocampus, more specific manipulations also demonstrate oxytocinergic modulation of neurogenesis in the dorsal DG. Conditional deletion of Oxtrs in CA2/CA3 by injection CamKii-Cre virus into Oxtr f/f mice does not affect proliferation, but does result in decreased survival of 2- and 4-week old adult-born neurons (Lin et al. 2017). Furthermore, deletion of Oxtrs in CA2/CA3 results in delayed morphological maturation of adult-born neurons,

as measured by dendritic length, branch point, and crossings. These results are particularly intriguing in light of classical hippocampal theory which often portrays CA2/CA3 as downstream of the DG. However, in order to modulate adult neurogenesis, oxytocin appears to harness an excitatory CA3 back-projection to the DG, as the negative effects on adult-born neuron survival induced by Oxtr conditional deletion is reversed by hM4Di-induced silencing of CA3 pyramidal neurons, suggesting that these effects are activity dependent (Lin et al. 2017).

5.1.4 The contribution of adult-born DGCs to social behaviors

In addition to their role in spatial and contextual learning, adult-born DGCs also appear to have a bi-directional relationship with social behaviors—the regulation of neurogenesis is sensitive to social contact of both positive and negative valence, and adult-born neurons also directly promote social behaviors (Opendak et al. 2016). Initial studies in marmosets have demonstrated that a single exposure to resident intruder stress is sufficient to significantly reduce the number of BrdU+ proliferating cells in the DG just 2 hours post stress (Gould et al. 1998). Additional studies have recapitulated this finding in mice and have shown that neurogenesis may be important for susceptibility-dependent avoidance of social contact after social defeat stress. Proliferation in the SGZ is transiently blunted in animals exposed to defeat stress, and those animals that are most susceptible (indicated by social avoidance post-stress) show greater survival and integration of adult-born neurons four weeks after the stress paradigm has completed (Lagace et al. 2010). Furthermore, irradiation of adult-born neurons prior to onset of social defeat stress is sufficient to block susceptibility-dependent social avoidance (Lagace et al. 2010). Adult-born neurons are also negatively regulated by social isolation stress (Stranahan et al. 2006), subordinate social rank (Gould et al. 1997), and dominance hierarchy reorganization (Opendak et al. 2016). In addition to social interactions of negative valence, hippocampal neurogenesis is also modulated by

interactions of positive valence. Sexual exposure boosts proliferation in the SGZ and is sufficient to restore levels of neurogenesis in aging animals to those of young adults (Leuner et al. 2012; Glasper and Gould 2013). Furthermore, chronic optogenetic stimulation of ensembles in the DG that represent sexual experience, but not neutral or fearful experiences, is sufficient to increase neurogenesis (Ramirez et al. 2015).

While many studies have elucidated the role of neurogenesis in social stress, dominance and aggression, and sexual behaviors, very few studies have directly assessed whether increasing or decreasing neurogenesis may modulate discrimination of social stimuli. Preliminary studies have indicated that disruption of dominance hierarchies in rats leads to decreased hippocampal neurogenesis and deficits in social memory, however these data are correlative only and may reflect separate mechanisms by which dominance hierarchy reorganization influences neurogenesis and social memory independently (Opendak et al. 2016). A separate study that directly ablated adult-born neurons by targeting diphtheria toxin specifically to DCX-positive cells in the hippocampus did show deficits in the social discrimination assay (Garrett et al. 2015). However, behavioral cohorts used in this study were comprised of both male and female mice and may reflect differences induced by sexual dimorphism. The question of whether or not adult-born neurons modulate social discrimination therefore remains an open question. If so, it also begs the question whether such a mechanism is at least partially mediated by oxytocin receptors in CA2/CA3. Given the role of hippocampal neurogenesis in both pattern separation and social behaviors, this largely unexplored question stands out as fundamental to understanding social memory.

5.2 Results

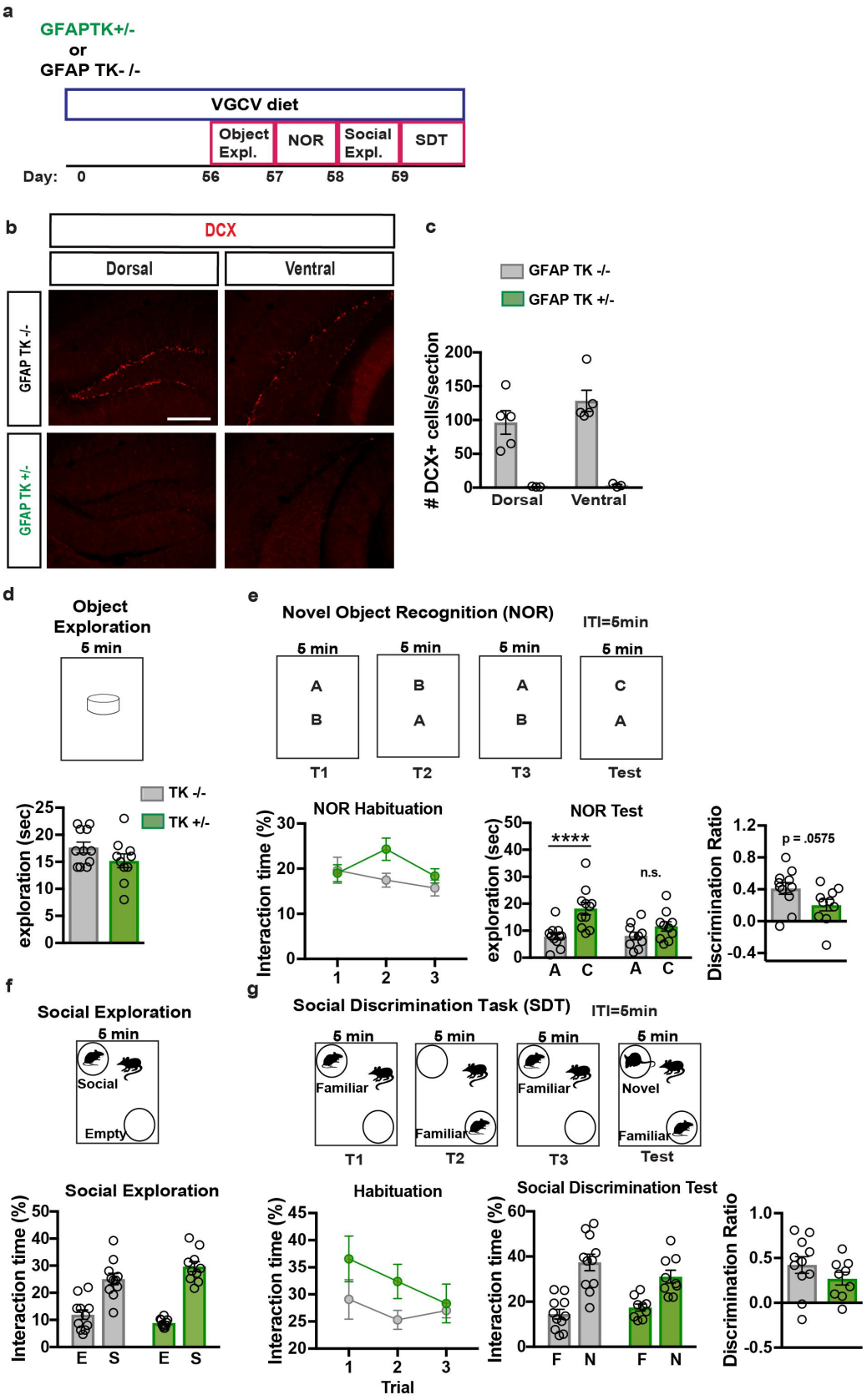
Given concordant findings that adult-born dentate granule neurons are modulated by oxytocin, and may contribute to a variety of social behaviors, I sought to determine whether or not loss of these cells affects behavioral measures of object and social recognition. I utilized a transgenic loss-of-function mouse line that selectively ablates neural precursors by expressing a herpes simplex virus thymidine kinase (TK) under a glial fibrillary acidic protein (GFAP) promoter. TK renders cells sensitive to the antiviral drug valganciclovir (VGCV, administered via diet), resulting in cell death. While the GFAP promoter drives TK expression in both radial cell precursors and stellate astrocytes, only mitotic cells are affected, and stellate astrocytes are spared (Snyder et al. 2011).

I placed GFAP-TK+/- and age-matched GFAP-TK-/- adult males on VGCV diet for eight weeks (56 days) prior to behavioral testing (**Figure 5.1a**). Eight weeks of VGCV treatment was sufficient to induce complete loss of doublecortin (DCX) expressing cells, cells between 2-3 weeks of age), in the subgranular zone of both the dorsal and ventral DG **(Figure 5.1b,c**). Behavioral testing began on day 56 of VGCV administration. While I did not observe any difference in time spent exploring a single object (unpaired t-test, $p = .1490$, **Figure 5.1d**), I did observe a deficit in novel object recognition. As compared to controls, GFAP-TK+/- animals did not show a preference for the novel object C during trial 4 of the NOR test (two-way ANOVA, *treatment:* $F_{(1,19)} = 2.601$, $p = .1233$, object: $F_{(1,19)} = 23.94$, $p = .0001$, interaction: $F_{(1,19)} = 5.788$, $p = .0265$; Multiple comparisons, Object A vs C, GFAP-TK-/- : $p<.0001$, GFAP-TK+/- : $p = .2041$, **Figure 5.1e**). Discrimination ratios of GFAP-TK+/- animals were much lower than controls, although significance was not attained in this measure (unpaired t-test, $p = .0575$). I observed a trend towards a deficit in the habituation of these animals across trials 1-3, as noted in a modest increase in

Figure 5.1 | Genetic ablation of adult-born neurons in adult male mice impairs object discrimination, but not social discrimination.

(**a**) Schematic illustrating VGCV diet administration (8 wks) and behavioral testing timeline. (**b**) Representative images of doublecortin (DCX) staining in dorsal (left) and ventral (right) DG in control animals and GFAP TK +/- animals. Scale bar denotes 200 μm. (**c**) Quantification of DCX staining in dorsal and ventral DG indicative of effective ablation of adult-born neurons (GFAP TK -/-: 5, GFAP TK +/-: 3) (**d**) Behavioral schematic (top) and quantification (bottom) of object exploration (GFAP TK -/-: 11, GFAP TK +/-: 10). (**e**) Behavioral schematic (top) and quantification (bottom) of novel objection recognition (GFAP TK -/-: 11, GFAP TK +/-: 10). Quantifications are displayed as Habituation (trials 1-3), Test (trial 4), and discrimination ratio (trial 4). (**f**) Behavioral schematic (top) and quantification (bottom) of social exploration test (GFAP TK -/-: 11, GFAP TK +/-: 10). (**g**) Behavioral schematic (top) and quantification (bottom) of social discrimination task (GFAP TK -/-: 11, GFAP TK +/-: 9). Quantifications are displayed as Habituation (trials 1-3), Test (trial 4), and discrimination ratio (trial 4). All data are displayed as mean ± SEM.

Figure 5.1 (continued)



exploration time in trial 2 for the GFAP-TK +/- animals, however this measure also remained a strong trend (two-way ANOVA, *treatment:* $F_{(1,19)} = 1.564$, $p = .2263$, time: $F_{(2,38)} = 3.179$, $p = .0529$, interaction: $F_{(2,38)} = 3.039$, $p = .0597$). I did not observe any differences in social exploration (**Figure 5.1f**) or social discrimination (**Figure 5.1g**), however I did observe increased exploration of the familiar animal during trials 1-3 of the social discrimination task. Together, these results suggest that adult-born neurons of 0-8 weeks of age may modulate object recognition, but not social recognition.

5.3 Discussion

That ablation did not result in impaired discrimination of social stimuli was contrary to our initial hypothesis based on disparate observations that neurogenesis promotes social affiliation and is modulated by oxytocin in CA2/CA3. However, a few possible explanations may underlie this result. First, our strategy nonspecifically ablated adult-born neurons from zero to eight weeks of age, a decision made based on the evidence that at eight weeks of age adult-born neurons become functionally indistinguishable from mature neurons (Nakashiba et al. 2012). However, given the critical nature of social recognition to the stability and maintenance of social dominance hierarchies, it is possible that such a prolonged manipulation may have promoted the recruitment of hippocampus-independent pathways such as cortical or olfactory circuits that compensate for the loss of adult-born neurons. Instead, a more acute manipulation, such as selectively targeting four-week old neurons at the peak of their plasticity (Gu et al. 2012) may have revealed a behavioral phenotype and may explain the deficit observed by Garrett and colleagues, in which behavioral testing took place only 3 weeks after onset of the manipulation (Garrett et al. 2015). In addition, in comparison to the study by Garrett and colleagues, our behavioral design included more time for encoding and habituation to the familiar social stimulus—whereas Garrett *et al.*

included only one habituation trial of four minutes, I performed three habituation trials of 5 minutes each, nearly four times as much exposure time to the familiar stimulus. Under these conditions, social stimuli may have been more easily discriminated, and may have engaged pathways that bypass the active engagement of adult-born neurons.

The variation in results across studies and sparse investigation into this question points to a need for additional experiments to establish the conditions under which adult-born neurons may participate in social discrimination. For example, increasing neurogenesis in mice that lack Oxtrs in CA2/CA3 may determine whether adult-born neurons are recruited under conditions where oxytocin signaling is not present. Additionally, utilizing *in vivo* calcium imaging of the DG GCL during exploration of familiar and unfamiliar conspecifics under conditions of decreased or increased neurogenesis may elucidate whether neurogenesis modulates the responsiveness of the DG to social stimuli, in addition to its previously established roles in spatial and contextual cues. Finally, delineating the role of adult-born neurons in male and female mice in order to determine whether or not sexual dimorphism may have contributed to the discrepancy observed would be a useful area of research. Future work by additional groups may give clarity to these questions.

5.4 Methods

Mouse Lines and Animal Care

GFAP TK mice were maintained as crosses between heterozygous GFAP-TK females and wildtype C57/B6J males. Mice were genotyped for the TK transgene between ages P10 and P13 and, upon weaning at P28, were housed in mixed genotype cages (TK-/- and TK+/-). At 8 weeks of age, all mice were placed on 8 weeks of valganciclovir diet (VGCV) prior to onset of behavioral testing and were kept on VGCV diet during the full duration of behavioral testing. All mice were housed 3-4 per cage in standard laboratory conditions under a 12-hour light-dark cycle (7:00 a.m.

to 7:00 p.m.) with ad libitum access to food and water. Behavioral testing occurred during the light cycle. All experiments were carried out in accordance with procedures approved by the Institutional Animal Care and Use Committee at the Massachusetts General Hospital in accordance with NIH guidelines.

Single Object Exploration

Mice were placed an arena filled with bedding (45cm long, 15cm high and 30cm wide) with a single novel object for 5 minutes. Sessions were video-recorded, and videos were manually scored for object exploration (when an animal's snout was 2cm or less from the object) by an investigator blind to animal treatment identity.

Novel Object Recognition

Mice were placed in an arena filled with bedding (45cm long, 15cm high and 30cm wide) with two distinct objects (A and B) for three 5 min sessions, with a 5 minute inter-trial interval. Mice were allowed to habituate to the objects during the three training sessions, and one of the objects was subsequently replaced with a novel object (C) in session four. Objects were counterbalanced across subjects and object positions were counterbalanced across trials. The objects that were selected for testing elicited comparable levels of exploration based on exploration levels in pilot experiments. Sessions were video-recorded, and videos were manually scored for object exploration (when an animal's snout was 2cm or less from the object) by an investigator blind to object identity and animal treatment identity.

Social Exploration

Mice were placed in an open plexiglass arena (41cm x 41 cm, Kinder Scientific) for 5 minutes with two pencil-wire cups placed on opposing corners of the arena. Habituation to the chamber took place one day prior to start of behavioral testing. One cup remained empty while the other

contained a novel adult male C57Bl/6J mouse. Sessions were video-recorded, and videos were manually scored for exploration of the social cup and empty cup (direct snout-to-cup contact, with at least two paws on the ground--time spent climbing on the cup was not included) by an investigator blind to animal treatment identity. Stimulus mice were trained to sit in pencil-wire cups for three 15 minute sessions several days prior to behavioral testing.

Social Recognition (Habituation, Discrimination)

The same plexiglass arena and pencil-wire cup set-up as described for social exploration was used. Mice were placed in the arena for three 5 min sessions with an empty cup and a novel adult male C57Bl/6J mouse, with a 5 minute intertrial interval. Mice habituated to the stimulus during the first three sessions, rendering it "familiar." During trial 4, a novel adult male mouse was placed in the opposing cup, and subjects were tested for discrimination between the novel and familiar mouse. Social stimuli were counterbalanced across subjects, and the position of the familiar social stimulus was counterbalanced across trials. Sessions were video-recorded, and videos were manually scored for interaction with the novel vs familiar mouse (direct snout-to-cup contact, with at least two paws on the ground--time spent climbing on the cup was not included) by an investigator blind to animal treatment identity. Stimulus mice were trained to sit in pencil-wire cups for three 15 minute sessions several days prior to behavioral testing. Videos were score by two different investigators.

Histology and Immunohistochemistry

Mice were anesthetized with ketamine (100 mg/kg i.p.) and xylazine (3 mg/kg i.p.) and transcardially perfused with 10mM phosphate buffer saline (PBS), pH 7.5 at 4°C, followed by a fixative solution containing 4% paraformaldehyde (PFA) in PBS. Brains were post-fixed in 4% PFA overnight at 4°C and cryo-protected for 72 hours in 30% sucrose at 4°C prior to freezing in

OCT on dry ice. Coronal sections were obtained at 35 μm using a cryostat (Leica, Germany) in six matched sets. Sections were stored in 1X PBS with 0.01% Azide at 4°C. Floating sections were used to perform immunohistochemical labeling. Briefly, sections were washed in 1X PBS, incubated for 15 min at room temperature in 1X PBS containing .3% Triton X-100, blocked in 1X PBS containing .3% Triton X-100 and 10% NDS for 1 hour at room temperature, and incubated in Goat anti-Doublecortin (DCX) primary antibody (sc-8066, Santa Cruz, 1:500) in blocking buffer with shaking overnight at 4°C. The following day, sections were washed 3 times in 1X PBS and incubated with fluorescent-label coupled secondary antibodies (Jackson Immunoresearch, Donkey anti-Rabbit, Goat, or Mouse, Cy3-coupled, 1:500) for 2 hours at room temperature. Sections were finally washed 3 times in 1X PBS and mounted using DAPI Fluoromount medium.

Image Acquisition and Analysis

For DCX quantification: 10x bilateral images of dorsal and ventral DG were acquired using a Nikon epifluorescence microscope. DCX+ cells were manually quantified and both blades of the DG were assessed. Six hemisections were analyzed for dDG and vDG respectively. Data was expressed as # DCX+ cells per section. All quantifications and analyses were completed by an experimenter blind to treatment condition.

Statistics

Statistical analysis was carried out using GraphPad Prism v7 software. Data (mean ± SEM). Discrimination ratios and measures of object exploration were analyzed using unpaired two-tailed student's t-test to compare two groups. DCX analysis and measures of NOR, social exploration, and social discrimination were analyzed using mixed factor two-way ANOVA with repeated measure followed by Bonferroni's multiple comparisons test when the interaction, p value was < .05. In all cases, significance was set at $p < 0.05$.

Page intentionally left blank.

CHAPTER 6

Conclusions and Future Directions

6.1 Conclusions

Social recognition, the ability to recognize and distinguish between conspecifics, is essential to the formation and stability of social interactions across species. As such, it is not surprising that cortical and subcortical circuits must communicate to support efficient social recognition. Remarkably, despite several studies implicating Oxtrs in diverse brain regions in social recognition, the role of Oxtrs in the hippocampus, the primary region for the consolidation of memories, has remained unaddressed. Here, we identify a role for the aDG-CA2/CA3 axis of Oxtr expressing cells in discrimination of social, but not non-social, stimuli. Further, Oxtr deletion in aDG and $aCA2/CA3_{distal}$ did not affect object behaviors or social interaction suggesting a specific role for Oxtrs in fine discrimination of social stimuli, consistent with phenotype of mice lacking Oxtrs in the forebrain (Macbeth et al. 2009). Our findings are consistent with a general role of the aDG-CA3 circuit of the hippocampus in resolving interference between similar memories (Frankland et al. 1998; Fanselow and Dong 2010; Yassa and Stark 2011; Besnard and Sahay 2016). The lack of an effect of Oxtr deletion in aDG-CA2/CA3 in object recognition suggests that the same aDG-CA2/CA3 memory circuit scaffold has been co-opted by an ancient evolutionarily conserved neuromodulatory system, oxytocin-Oxtr, to permit encoding when oxytocin is released, such as during encounter of social stimuli (Hung et al. 2017). Furthermore, we demonstrate a dissociation in Oxtr function along the DG longitudinal axis, whereby those in aDG promote discrimination of social stimuli, and those in pDG promote social approach.

Recent studies have suggested that CA2 links social information with space or contextual information (Alexander et al. 2016). However, whether CA2/CA3 exhibits population-based coding in response to similar social stimuli, and whether oxytocin engages such population-based coding mechanisms to promote social discrimination is not known. Using activity-dependent

ensemble mapping I found that the $CA3_{proximal}$, but not $CA3_{distal}$, subregion exhibits population-based coding when mice encountered novel, yet genetically identical, social stimuli. The lack of population-based coding in $CA3_{distal}$ may be explained by changes in firing rate that are not detectable with catFISH. Caveats notwithstanding, these findings are consistent with growing evidence that under conditions of high input similarity, as is the case here with mice of the same genetic background, $CA3_{proximal}$, but not $CA3_{distal}$, undergoes global remapping (Lee et al. 2015; Knierim and Neunuebel 2016). Preferential removal of Oxtrs of aCA2/CA3 pyramidal neurons impaired population-based coding in $CA3_{proximal}$, suggesting that oxytocin recruits basic circuit mechanisms normally used by $CA3_{proximal}$ to support orthogonalization of similar inputs into divergent outputs (pattern separation) to minimize overlap between social stimuli. These findings are consistent with previous reports that identify functional heterogeneity among CA3 subregions, with $CA3_{proximal}$ behaving as a pattern separator, much like the DG, and $CA3_{distal}$, strongly influenced by its auto-associative networks, functioning as a pattern completion network (Lee et al. 2015; GoodSmith et al. 2017). However, that I see a disruption in population based coding in $CA3_{proximal}$, despite low Oxtr expression in this region, suggests a role for local microcircuits within CA3 that communicate social information mediated by oxytocin signaling in aCA2/$CA3_{distal}$ to pattern separation networks in $CA3_{proximal}$.

Oxtrs in the auditory cortex, olfactory bulbs, and hippocampus have been shown to enhance signal-to noise-processing through the modulation of excitatory and inhibitory neurons (Owen et al. 2013; Marlin et al. 2015; Harden and Frazier 2016; Oettl et al. 2016). Interestingly, I observed increased activation of the DG following recombination of Oxtr in the hilus, suggestive of decreased sparseness, and reminiscent of potentiated social stimulus-induced DG activation in mice lacking oxytocin (Ferguson et al. 2001). Clarification of the functions of Oxtr in aCA2/CA3

excitatory neurons and within distinct GABAergic populations (SST, PV and other subtypes) and non-GABAergic putative mossy cells cells in the hilus will further edify the contributions of Oxtrs to DG-CA2/CA3 circuit properties.

Our optogenetic terminal-specific attenuation studies revealed a critical role for aCA2/CA3 outputs to pCA1, but not aCA1, for discrimination of social stimuli. The modest levels of discrimination of social stimuli that were persistent following optogenetic attenuation of aCA2/CA3 projections to pCA1 may reflect insufficient illumination of the large termination zone in pCA1d, incomplete silencing, or non-specific targeting of aCA2/CA3 neurons that do not express Oxtr. Nevertheless, these results are consistent with a recent study implicating the pCA1-NAcc pathway in mediating discrimination of social stimuli (Okuyama et al. 2016). Whether this pathway or other pCA1 projections to prefrontal cortex, hypothalamus or amygdala relay Oxtr dependent computations underlying social recognition in anterior hippocampus to guide social behavior remains to be determined. Our findings that aCA2/CA3 projections to aCA1 mediate discrimination of non-social, but not social, stimuli are consistent with the role of aCA1 in object recognition (Cohen et al. 2013; Cohen and Stackman 2015). Thus, aCA2/CA3 may serve as a divergent point that segregates pattern separation computations to downstream targets depending on the modality of the stimulus. This differential routing may be dependent on engagement of oxytocin signaling in microcircuits in aCA2/CA3, or differences in projection patterns of Oxtr expressing aCA2/CA3 neurons to aCA1 and pCA1.

In summary, our studies begin to illuminate the circuit mechanisms and neural pathways by which hippocampal Oxtrs contribute to social recognition. Oxtrs appear to recruit basic circuit mechanisms supporting pattern separation such as population-based coding to minimize interference between similar social memories. These cognitive computations are relayed from the

anterior to posterior hippocampus via a pathway to pCA1 to guide social behavior. Thus, disruptions in DG-CA2/CA3 circuitry may contribute to social memory impairments seen in autism and other psychiatric disorders (Allsop et al. 2014; Pasciuto et al. 2015; Dudek et al. 2016; Piskorowski et al. 2016).

6.2 Future Directions

6.2.1 Mapping the inputs of Oxtr+ neurons in the hippocampus.

The presence of specific ensembles of neurons in the hippocampus that are privileged to express Oxtrs begs the question of whether these cells receive inputs in a distribution pattern that differs from non-Oxtr expressing cells. For example, a compelling possibility is that Oxtr+ cells in CA2/CA3 receive preferential input from oxytocin-producing neurons in the PVN, rather than from the DG or entorhinal cortex. One way to resolve this question is to perform rabies tracing of inputs onto Oxtr+ cells. This can be accomplished by the strategies developed in Ed Callaway's lab (Wickersham et al. 2007; Sun et al. 2014). Briefly an Oxtr-Cre driver line can be crossed with a floxed TVA line to selectively drive expression of TVA in Oxtr cells. Then, adult mice can be injected in CA2/CA3 with a DIO-AAV helper virus that drives the expression of a Glycoprotein. Three weeks later, psuedotyped G-deleted rabies virus can be injected into the same site. In this manner, retrograde labeling is achieved specifically in Oxtr+ cells by restricting the expression of a glycoprotein that is needed for transsynaptic retrograde trafficking.

6.2.2 In vivo imaging of Oxtr+ neurons in the hippocampus.

Our studies did not show evidence of global remapping of social stimuli in $CA2/3_{distal}$. We had observed an effect only in $CA2/3_{proximal}$, where global remapping is thought to be more robust. However, this result does not necessarily mean that $CA2/3_{distal}$ does not remap in response to social stimuli, especially given prior evidence from *in vivo* that CA2 neurons undergo global remapping

when mice are exposed to social stimuli. catFISH as a technique may simply lack the resolution to detect such an effect. Here I propose performing calcium imaging of $CA2/3_{distal}$ ensembles during exposure to familiar and novel social stimuli to determine the extent to which populations encoding both stimuli overlap. If familiar and novel social stimuli seem to be separable at the level of $CA2/3_{distal}$ population dynamics, I propose utilizing the *Oxtr f/f* mice and co-injecting Camkii-Cre-GFP with DIO-GCaMP6 in order to image population dynamics in the absence of $CA2/3_{distal}$ oxytocin receptors. These *in vivo* experiments may shed more light on the results observed in Chapter 3.

6.2.3 Relating hippocampal oxytocin receptors to aggression and dominance.

Previous studies have implicated a role for hippocampal subregions in rodent models of aggression and dominance. For example, removal of an alpha male from co-housed animals decreases adult hippocampal neurogenesis (Opendak et al. 2016) and potentiates the activity of hippocampal subregions in subordinate animals that subsequently ascend in rank (Williamson, Klein et al., BioRxiv, 2018). Additionally, CA2 is a locus for the expression of aggressive behaviors such as attacking and mounting, which are central to the assertion of dominance, in a vasopressin-dependent manner (Pagani et al. 2015). While oxytocin has previously been implicated in aggression, whether or not Oxtrs in the hippocampus are specifically involved is not known. Given that hippocampal Oxtr deletion results in social amnesia, and mice are more likely to be aggressive with animals they perceive as novel, there may be an interesting link between hippocampal Oxtrs and aggression. A number of simple studies could initially determine whether or not hippocampal Oxtrs are involved: pharmacological blockade of Oxtrs or conditional deletion during measures of aggression (attack, mounting) and dominance (tube test). Furthermore, co-housing control animals and those lacking expression of Oxtrs in CA2/3 and determining whether

the presence of Oxtrs in the hippocampus can directly predict the social rank of an animal (are animals lacking hippocampal Oxtrs biased towards a lower rank?). Finally, if behavioral phenotypes are ascertained with these approaches, then performing *in vivo* recordings or calcium imaging of Oxtr neurons in CA2/CA3 may determine whether there are population-level dynamics that can directly predict an animal's rank or likelihood to express aggression.

References

Aimone, J. B., W. Deng and F. H. Gage (2011). "Resolving new memories: a critical look at the dentate gyrus, adult neurogenesis, and pattern separation." Neuron **70**(4): 589-596.

Al-Ayadhi, L. Y. (2005). "Altered oxytocin and vasopressin levels in autistic children in Central Saudi Arabia." Neurosciences (Riyadh) **10**(1): 47-50.

Alenina, N. and F. Klempin (2015). "The role of serotonin in adult hippocampal neurogenesis." Behav Brain Res **277**: 49-57.

Alexander, G. M., S. Farris, J. R. Pirone, C. Zheng, L. L. Colgin and S. M. Dudek (2016). "Social and novel contexts modify hippocampal CA2 representations of space." Nat Commun **7**: 10300.

Allsop, S. A., C. M. Vander Weele, R. Wichmann and K. M. Tye (2014). "Optogenetic insights on the relationship between anxiety-related behaviors and social deficits." Front Behav Neurosci **8**: 241.

Altman, J. (1963). "Autoradiographic investigation of cell proliferation in the brains of rats and cats." Anat Rec **145**: 573-591.

Altman, J. and G. D. Das (1965). "Autoradiographic and histological evidence of postnatal hippocampal neurogenesis in rats." J Comp Neurol **124**(3): 319-335.

Amaral, D. G., H. E. Scharfman and P. Lavenex (2007). "The dentate gyrus: fundamental neuroanatomical organization (dentate gyrus for dummies)." Prog Brain Res **163**: 3-22.

Amit, D. J., H. Gutfreund and H. Sompolinsky (1987). "Information storage in neural networks with low levels of activity." Phys Rev A Gen Phys **35**(5): 2293-2303.

Anagnostou, E., L. Soorya, W. Chaplin, J. Bartz, D. Halpern, S. Wasserman, A. T. Wang, L. Pepa, N. Tanel, A. Kushki and E. Hollander (2012). "Intranasal oxytocin versus placebo in the treatment of adults with autism spectrum disorders: a randomized controlled trial." Mol Autism **3**(1): 16.

Andari, E., J. R. Duhamel, T. Zalla, E. Herbrecht, M. Leboyer and A. Sirigu (2010). "Promoting social behavior with oxytocin in high-functioning autism spectrum disorders." Proc Natl Acad Sci U S A **107**(9): 4389-4394.

Anthony, T. E., N. Dee, A. Bernard, W. Lerchner, N. Heintz and D. J. Anderson (2014). "Control of stress-induced persistent anxiety by an extra-amygdala septohypothalamic circuit." Cell **156**(3): 522-536.

Aoki, Y., Y. Nishimura, T. Hondrich, R. Nakayama, H. Igata, T. Sasaki and Y. Ikegaya (2017). "Selective attenuation of electrophysiological activity of the dentate gyrus in a social defeat mouse model." J Physiol Sci **67**(4): 507-513.

Aqrabawi, A. J. and J. C. Kim (2018). "Topographic Organization of Hippocampal Inputs to the Anterior Olfactory Nucleus." Front Neuroanat **12**: 12.

Aschauer, D. F., S. Kreuz and S. Rumpel (2013). "Analysis of transduction efficiency, tropism and axonal transport of AAV serotypes 1, 2, 5, 6, 8 and 9 in the mouse brain." PLoS One **8**(9): e76310.

Bagot, R. C., E. M. Parise, C. J. Pena, H. X. Zhang, I. Maze, D. Chaudhury, B. Persaud, R. Cachope, C. A. Bolanos-Guzman, J. F. Cheer, K. Deisseroth, M. H. Han and E. J. Nestler (2015). "Corrigendum: Ventral hippocampal afferents to the nucleus accumbens regulate susceptibility to depression." Nat Commun **6**: 7626.

Bakker, A., C. B. Kirwan, M. Miller and C. E. Stark (2008). "Pattern separation in the human hippocampal CA3 and dentate gyrus." Science **319**(5870): 1640-1642.

Bargmann, W. and E. Scharrer (1951). "The site of origin of the hormones of the posterior pituitary." Am Sci **39**(2): 255-259.

Barnes, C. A., B. L. McNaughton, S. J. Mizumori, B. W. Leonard and L. H. Lin (1990). "Comparison of spatial and temporal characteristics of neuronal activity in sequential stages of hippocampal processing." Prog Brain Res **83**: 287-300.

Bauman, M. and T. L. Kemper (1985). "Histoanatomic observations of the brain in early infantile autism." Neurology **35**(6): 866-874.

Bauman, M. L., T. L. Kemper and D. M. Arin (1995). "Pervasive neuroanatomic abnormalities of the brain in three cases of Rett's syndrome." Neurology **45**(8): 1581-1586.

Beadle, J. N., D. Tranel, N. J. Cohen and M. C. Duff (2013). "Empathy in hippocampal amnesia." Front Psychol **4**: 69.

Bender, F., M. Gorbati, M. C. Cadavieco, N. Denisova, X. Gao, C. Holman, T. Korotkova and A. Ponomarenko (2015). "Theta oscillations regulate the speed of locomotion via a hippocampus to lateral septum pathway." Nat Commun **6**: 8521.

Berron, D., H. Schutze, A. Maass, A. Cardenas-Blanco, H. J. Kuijf, D. Kumaran and E. Duzel (2016). "Strong Evidence for Pattern Separation in Human Dentate Gyrus." J Neurosci **36**(29): 7569-7579.

Besnard, A. and A. Sahay (2016). "Adult Hippocampal Neurogenesis, Fear Generalization, and Stress." Neuropsychopharmacology **41**(1): 24-44.

Boehringer, R., D. Polygalov, A. J. Y. Huang, S. J. Middleton, V. Robert, M. E. Wintzer, R. A. Piskorowski, V. Chevaleyre and T. J. McHugh (2017). "Chronic Loss of CA2 Transmission Leads to Hippocampal Hyperexcitability." Neuron **94**(3): 642-655 e649.

Brady, J. V. and W. J. Nauta (1953). "Subcortical mechanisms in emotional behavior: affective changes following septal forebrain lesions in the albino rat." J Comp Physiol Psychol **46**(5): 339-346.

Bredewold, R., J. K. Schiavo, M. van der Hart, M. Verreij and A. H. Veenema (2015). "Dynamic changes in extracellular release of GABA and glutamate in the lateral septum during social play behavior in juvenile rats: Implications for sex-specific regulation of social play behavior." Neuroscience **307**: 117-127.

Burd, G. D. and F. Nottebohm (1985). "Ultrastructural characterization of synaptic terminals formed on newly generated neurons in a song control nucleus of the adult canary forebrain." J Comp Neurol **240**(2): 143-152.

Busnelli, M., E. Bulgheroni, M. Manning, G. Kleinau and B. Chini (2013). "Selective and potent agonists and antagonists for investigating the role of mouse oxytocin receptors." J Pharmacol Exp Ther **346**(2): 318-327.

Calfa, G., M. Volosin and V. A. Molina (2006). "Glucocorticoid receptors in lateral septum are involved in the modulation of the emotional sequelae induced by social defeat." Behav Brain Res **172**(2): 324-332.

Cameron, H. A., C. S. Woolley, B. S. McEwen and E. Gould (1993). "Differentiation of newly born neurons and glia in the dentate gyrus of the adult rat." Neuroscience **56**(2): 337-344.

Carey, Benedict. "H.M., an Unforgettable Amnesiac, Dies at 82." *New York Times* 4 Dec. 2008: A1. *New York Times*. Web. 1 March 2018.

Cenquizca, L. A. and L. W. Swanson (2007). "Spatial organization of direct hippocampal field CA1 axonal projections to the rest of the cerebral cortex." Brain Res Rev **56**(1): 1-26.

Chevaleyre, V. and S. A. Siegelbaum (2010). "Strong CA2 pyramidal neuron synapses define a powerful disynaptic cortico-hippocampal loop." Neuron **66**(4): 560-572.

Chiang, M. C., A. J. Y. Huang, M. E. Wintzer, T. Ohshima and T. J. McHugh (2018). "A role for CA3 in social recognition memory." Behav Brain Res.

Choe, H. K., M. D. Reed, N. Benavidez, D. Montgomery, N. Soares, Y. S. Yim and G. B. Choi (2015). "Oxytocin Mediates Entrainment of Sensory Stimuli to Social Cues of Opposing Valence." Neuron **87**(1): 152-163.

Ciocchi, S., J. Passecker, H. Malagon-Vina, N. Mikus and T. Klausberger (2015). "Brain computation. Selective information routing by ventral hippocampal CA1 projection neurons." Science **348**(6234): 560-563.

Clarke, A. and S. E. File (1982). "Selective neurotoxin lesions of the lateral septum: changes in social and aggressive behaviours." Pharmacol Biochem Behav **17**(4): 623-628.

Clelland, C. D., M. Choi, C. Romberg, G. D. Clemenson, Jr., A. Fragniere, P. Tyers, S. Jessberger, L. M. Saksida, R. A. Barker, F. H. Gage and T. J. Bussey (2009). "A functional role for adult hippocampal neurogenesis in spatial pattern separation." Science **325**(5937): 210-213.

Cohen, S. J., A. H. Munchow, L. M. Rios, G. Zhang, H. N. Asgeirsdottir and R. W. Stackman, Jr. (2013). "The rodent hippocampus is essential for nonspatial object memory." Curr Biol **23**(17): 1685-1690.

Cohen, S. J. and R. W. Stackman, Jr. (2015). "Assessing rodent hippocampal involvement in the novel object recognition task. A review." Behav Brain Res **285**: 105-117.

Colgin, L. L., E. I. Moser and M. B. Moser (2008). "Understanding memory through hippocampal remapping." Trends Neurosci **31**(9): 469-477.

Cook-Snyder, D. R., A. Jones and L. G. Reijmers (2015). "A retrograde adeno-associated virus for collecting ribosome-bound mRNA from anatomically defined projection neurons." Front Mol Neurosci **8**: 56.

Crawley, J. N., T. Chen, A. Puri, R. Washburn, T. L. Sullivan, J. M. Hill, N. B. Young, J. J. Nadler, S. S. Moy, L. J. Young, H. K. Caldwell and W. S. Young (2007). "Social approach behaviors in oxytocin knockout mice: comparison of two independent lines tested in different laboratory environments." Neuropeptides **41**(3): 145-163.

Cservenak, M., V. Kis, D. Keller, D. Dimen, L. Menyhart, S. Olah, E. R. Szabo, J. Barna, E. Renner, T. B. Usdin and A. Dobolyi (2017). "Maternally involved galanin neurons in the preoptic area of the rat." Brain Struct Funct **222**(2): 781-798.

Cui, Z., C. R. Gerfen and W. S. Young, 3rd (2013). "Hypothalamic and other connections with dorsal CA2 area of the mouse hippocampus." J Comp Neurol **521**(8): 1844-1866.

da Silveira, L. T., C. M. Junta, N. Monesi, G. R. de Oliveira-Pelegrin, G. A. Passos and M. J. Rocha (2007). "Time course of c-fos, vasopressin and oxytocin mRNA expression in the hypothalamus following long-term dehydration." Cell Mol Neurobiol **27**(5): 575-584.

Daenen, E. W., G. Wolterink, M. A. Gerrits and J. M. Van Ree (2002). "The effects of neonatal lesions in the amygdala or ventral hippocampus on social behaviour later in life." Behav Brain Res **136**(2): 571-582.

Dager, S. R., L. Wang, S. D. Friedman, D. W. Shaw, J. N. Constantino, A. A. Artru, G. Dawson and J. G. Csernansky (2007). "Shape mapping of the hippocampus in young children with autism spectrum disorder." AJNR Am J Neuroradiol **28**(4): 672-677.

Danielson, N. B., P. Kaifosh, J. D. Zaremba, M. Lovett-Barron, J. Tsai, C. A. Denny, E. M. Balough, A. R. Goldberg, L. J. Drew, R. Hen, A. Losonczy and M. A. Kheirbek (2016). "Distinct Contribution of Adult-Born Hippocampal Granule Cells to Context Encoding." Neuron **90**(1): 101-112.

Davidson, P. S., H. Drouin, D. Kwan, M. Moscovitch and R. S. Rosenbaum (2012). "Memory as social glue: close interpersonal relationships in amnesic patients." Front Psychol **3**: 531.

Deng, W., J. B. Aimone and F. H. Gage (2010). "New neurons and new memories: how does adult hippocampal neurogenesis affect learning and memory?" Nat Rev Neurosci **11**(5): 339-350.

DeVito, L. M., R. Konigsberg, C. Lykken, M. Sauvage, W. S. Young, 3rd and H. Eichenbaum (2009). "Vasopressin 1b receptor knock-out impairs memory for temporal order." J Neurosci **29**(9): 2676-2683.

Dölen, G. (2015). "Autism: Oxytocin, serotonin, and social reward." Soc Neurosci **10**(5): 450-465.

Dölen, G. (2015). "Oxytocin: parallel processing in the social brain?" J Neuroendocrinol **27**(6): 516-535.

Dölen, G., A. Darvishzadeh, K. W. Huang and R. C. Malenka (2013). "Social reward requires coordinated activity of nucleus accumbens oxytocin and serotonin." Nature **501**(7466): 179-184.

Drew, L. J., M. A. Kheirbek, V. M. Luna, C. A. Denny, M. A. Cloidt, M. V. Wu, S. Jain, H. E. Scharfman and R. Hen (2016). "Activation of local inhibitory circuits in the dentate gyrus by adult-born neurons." Hippocampus **26**(6): 763-778.

Dubrovsky, B., J. Harris, K. Gijsbers and A. Tatarinov (2002). "Oxytocin induces long-term depression on the rat dentate gyrus: possible ATPase and ectoprotein kinase mediation." Brain Res Bull **58**(2): 141-147.

Dudek, S. M., G. M. Alexander and S. Farris (2016). "Rediscovering area CA2: unique properties and functions." Nat Rev Neurosci **17**(2): 89-102.

Eriksson, P. S., E. Perfilieva, T. Bjork-Eriksson, A. M. Alborn, C. Nordborg, D. A. Peterson and F. H. Gage (1998). "Neurogenesis in the adult human hippocampus." Nat Med **4**(11): 1313-1317.

Ernst, A., K. Alkass, S. Bernard, M. Salehpour, S. Perl, J. Tisdale, G. Possnert, H. Druid and J. Frisen (2014). "Neurogenesis in the striatum of the adult human brain." Cell **156**(5): 1072-1083.

Fanselow, M. S. and H. W. Dong (2010). "Are the dorsal and ventral hippocampus functionally distinct structures?" Neuron **65**(1): 7-19.

Felix-Ortiz, A. C., A. Beyeler, C. Seo, C. A. Leppla, C. P. Wildes and K. M. Tye (2013). "BLA to vHPC inputs modulate anxiety-related behaviors." Neuron **79**(4): 658-664.

Felix-Ortiz, A. C. and K. M. Tye (2014). "Amygdala inputs to the ventral hippocampus bidirectionally modulate social behavior." J Neurosci **34**(2): 586-595.

Ferguson, J. N., J. M. Aldag, T. R. Insel and L. J. Young (2001). "Oxytocin in the medial amygdala is essential for social recognition in the mouse." J Neurosci **21**(20): 8278-8285.

Ferguson, J. N., L. J. Young, E. F. Hearn, M. M. Matzuk, T. R. Insel and J. T. Winslow (2000). "Social amnesia in mice lacking the oxytocin gene." Nat Genet **25**(3): 284-288.

Ferrero, D. M., L. M. Moeller, T. Osakada, N. Horio, Q. Li, D. S. Roy, A. Cichy, M. Spehr, K. Touhara and S. D. Liberles (2013). "A juvenile mouse pheromone inhibits sexual behaviour through the vomeronasal system." Nature **502**(7471): 368-371.

Finlay, J. M., G. A. Dunham, A. M. Isherwood, C. J. Newton, T. V. Nguyen, P. C. Reppar, I. Snitkovski, S. A. Paschall and R. W. Greene (2015). "Effects of prefrontal cortex and hippocampal NMDA NR1-subunit deletion on complex cognitive and social behaviors." Brain Res **1600**: 70-83.

Frankland, P. W., V. Cestari, R. K. Filipkowski, R. J. McDonald and A. J. Silva (1998). "The dorsal hippocampus is essential for context discrimination but not for contextual conditioning." Behav Neurosci **112**(4): 863-874.

Freeman, S. M., K. Inoue, A. L. Smith, M. M. Goodman and L. J. Young (2014). "The neuroanatomical distribution of oxytocin receptor binding and mRNA in the male rhesus macaque (Macaca mulatta)." Psychoneuroendocrinology **45**: 128-141.

Garrett, L., J. Zhang, A. Zimprich, K. M. Niedermeier, H. Fuchs, V. Gailus-Durner, M. Hrabe de Angelis, D. Vogt Weisenhorn, W. Wurst and S. M. Holter (2015). "Conditional Reduction of Adult Born Doublecortin-Positive Neurons Reversibly Impairs Selective Behaviors." Front Behav Neurosci **9**: 302.

Glasper, E. R. and E. Gould (2013). "Sexual experience restores age-related decline in adult neurogenesis and hippocampal function." Hippocampus **23**(4): 303-312.

Goldman, S. A. and F. Nottebohm (1983). "Neuronal production, migration, and differentiation in a vocal control nucleus of the adult female canary brain." Proc Natl Acad Sci U S A **80**(8): 2390-2394.

GoodSmith, D., X. Chen, C. Wang, S. H. Kim, H. Song, A. Burgalossi, K. M. Christian and J. J. Knierim (2017). "Spatial Representations of Granule Cells and Mossy Cells of the Dentate Gyrus." Neuron **93**(3): 677-690 e675.

Gould, E., B. S. McEwen, P. Tanapat, L. A. Galea and E. Fuchs (1997). "Neurogenesis in the dentate gyrus of the adult tree shrew is regulated by psychosocial stress and NMDA receptor activation." J Neurosci **17**(7): 2492-2498.

Gould, E., A. J. Reeves, M. Fallah, P. Tanapat, C. G. Gross and E. Fuchs (1999). "Hippocampal neurogenesis in adult Old World primates." Proc Natl Acad Sci U S A **96**(9): 5263-5267.

Gould, E., P. Tanapat, B. S. McEwen, G. Flugge and E. Fuchs (1998). "Proliferation of granule cell precursors in the dentate gyrus of adult monkeys is diminished by stress." Proc Natl Acad Sci U S A **95**(6): 3168-3171.

Green, S. A., J. D. Rudie, N. L. Colich, J. J. Wood, D. Shirinyan, L. Hernandez, N. Tottenham, M. Dapretto and S. Y. Bookheimer (2013). "Overreactive brain responses to sensory stimuli in youth with autism spectrum disorders." J Am Acad Child Adolesc Psychiatry **52**(11): 1158-1172.

Groen, W., M. Teluij, J. Buitelaar and I. Tendolkar (2010). "Amygdala and hippocampus enlargement during adolescence in autism." J Am Acad Child Adolesc Psychiatry **49**(6): 552-560.

Gu, Y., M. Arruda-Carvalho, J. Wang, S. R. Janoschka, S. A. Josselyn, P. W. Frankland and S. Ge (2012). "Optical controlling reveals time-dependent roles for adult-born dentate granule cells." Nat Neurosci **15**(12): 1700-1706.

Guastella, A. J., S. L. Einfeld, K. M. Gray, N. J. Rinehart, B. J. Tonge, T. J. Lambert and I. B. Hickie (2010). "Intranasal oxytocin improves emotion recognition for youth with autism spectrum disorders." Biol Psychiatry **67**(7): 692-694.

Guzowski, J. F. and P. F. Worley (2001). "Cellular compartment analysis of temporal activity by fluorescence in situ hybridization (catFISH)." Curr Protoc Neurosci **Chapter 1**: Unit 1 8.

Hammock, E. A. and P. Levitt (2013). "Oxytocin receptor ligand binding in embryonic tissue and postnatal brain development of the C57BL/6J mouse." Front Behav Neurosci **7**: 195.

Harden, S. W. and C. J. Frazier (2016). "Oxytocin depolarizes fast-spiking hilar interneurons and induces GABA release onto mossy cells of the rat dentate gyrus." Hippocampus **26**(9): 1124-1139.

Hattori, R., K. V. Kuchibhotla, R. C. Froemke and T. Komiyama (2017). "Functions and dysfunctions of neocortical inhibitory neuron subtypes." Nat Neurosci **20**(9): 1199-1208.

Hayut, I., E. E. Fanselow, B. W. Connors and D. Golomb (2011). "LTS and FS inhibitory interneurons, short-term synaptic plasticity, and cortical circuit dynamics." PLoS Comput Biol **7**(10): e1002248.

Hidema, S., T. Fukuda, Y. Hiraoka, H. Mizukami, R. Hayashi, A. Otsuka, S. Suzuki, S. Miyazaki and K. Nishimori (2016). "Generation of Oxtr cDNA(HA)-Ires-Cre Mice for Gene Expression in an Oxytocin Receptor Specific Manner." J Cell Biochem **117**(5): 1099-1111.

Hitti, F. L. and S. A. Siegelbaum (2014). "The hippocampal CA2 region is essential for social memory." Nature **508**(7494): 88-92.

Hoyle, C. H. (1999). "Neuropeptide families and their receptors: evolutionary perspectives." Brain Res **848**(1-2): 1-25.

Hu, H., J. Gan and P. Jonas (2014). "Interneurons. Fast-spiking, parvalbumin(+) GABAergic interneurons: from cellular design to microcircuit function." Science **345**(6196): 1255263.

Hung, L. W., S. Neuner, J. S. Polepalli, K. T. Beier, M. Wright, J. J. Walsh, E. M. Lewis, L. Luo, K. Deisseroth, G. Dölen and R. C. Malenka (2017). "Gating of social reward by oxytocin in the ventral tegmental area." Science **357**(6358): 1406-1411.

Ikrar, T., N. Guo, K. He, A. Besnard, S. Levinson, A. Hill, H. K. Lee, R. Hen, X. Xu and A. Sahay (2013). "Adult neurogenesis modifies excitability of the dentate gyrus." Front Neural Circuits **7**: 204.

Insel, T. R. and T. J. Hulihan (1995). "A gender-specific mechanism for pair bonding: oxytocin and partner preference formation in monogamous voles." Behav Neurosci **109**(4): 782-789.

Ishizuka, N., J. Weber and D. G. Amaral (1990). "Organization of intrahippocampal projections originating from CA3 pyramidal cells in the rat." J Comp Neurol **295**(4): 580-623.

Ito, W., M. Chehab, S. Thakur, J. Li and A. Morozov (2011). "BDNF-restricted knockout mice as an animal model for aggression." Genes Brain Behav **10**(3): 365-374.

Jeltsch, H., F. Bertrand, C. Lazarus and J. C. Cassel (2001). "Cognitive performances and locomotor activity following dentate granule cell damage in rats: role of lesion extent and type of memory tested." Neurobiol Learn Mem **76**(1): 81-105.

Jimenez, J. C., K. Su, A. R. Goldberg, V. M. Luna, J. S. Biane, G. Ordek, P. Zhou, S. K. Ong, M. A. Wright, L. Zweifel, L. Paninski, R. Hen and M. A. Kheirbek (2018). "Anxiety Cells in a Hippocampal-Hypothalamic Circuit." Neuron **97**(3): 670-683 e676.

Jinde, S., V. Zsiros, Z. Jiang, K. Nakao, J. Pickel, K. Kohno, J. E. Belforte and K. Nakazawa (2012). "Hilar mossy cell degeneration causes transient dentate granule cell hyperexcitability and impaired pattern separation." Neuron **76**(6): 1189-1200.

Jinde, S., V. Zsiros and K. Nakazawa (2013). "Hilar mossy cell circuitry controlling dentate granule cell excitability." Front Neural Circuits **7**: 14.

Jung, M. W. and B. L. McNaughton (1993). "Spatial selectivity of unit activity in the hippocampal granular layer." Hippocampus **3**(2): 165-182.

Jung, M. W., S. I. Wiener and B. L. McNaughton (1994). "Comparison of spatial firing characteristics of units in dorsal and ventral hippocampus of the rat." J Neurosci **14**(12): 7347-7356.

Kaplan, M. S. and J. W. Hinds (1977). "Neurogenesis in the adult rat: electron microscopic analysis of light radioautographs." Science **197**(4308): 1092-1094.

Kasahara, Y., Y. Takayanagi, T. Kawada, K. Itoi and K. Nishimori (2007). "Impaired thermoregulatory ability of oxytocin-deficient mice during cold-exposure." Biosci Biotechnol Biochem **71**(12): 3122-3126.

Kay, K., M. Sosa, J. E. Chung, M. P. Karlsson, M. C. Larkin and L. M. Frank (2016). "A hippocampal network for spatial coding during immobility and sleep." Nature **531**(7593): 185-190.

Kempermann, G., H. G. Kuhn and F. H. Gage (1997). "More hippocampal neurons in adult mice living in an enriched environment." Nature **386**(6624): 493-495.

Kesner, R. P. (2007). "Behavioral functions of the CA3 subregion of the hippocampus." Learn Mem **14**(11): 771-781.

Kheirbek, M. A., L. J. Drew, N. S. Burghardt, D. O. Costantini, L. Tannenholz, S. E. Ahmari, H. Zeng, A. A. Fenton and R. Hen (2013). "Differential control of learning and anxiety along the dorsoventral axis of the dentate gyrus." Neuron **77**(5): 955-968.

Kheirbek, M. A., L. Tannenholz and R. Hen (2012). "NR2B-dependent plasticity of adult-born granule cells is necessary for context discrimination." J Neurosci **32**(25): 8696-8702.

Kirk, R. A., S. N. Redmon and R. P. Kesner (2017). "The ventral dentate gyrus mediates pattern separation for reward value." Behav Neurosci **131**(1): 42-45.

Kjelstrup, K. G., F. A. Tuvnes, H. A. Steffenach, R. Murison, E. I. Moser and M. B. Moser (2002). "Reduced fear expression after lesions of the ventral hippocampus." Proc Natl Acad Sci U S A **99**(16): 10825-10830.

Knierim, J. J. and J. P. Neunuebel (2016). "Tracking the flow of hippocampal computation: Pattern separation, pattern completion, and attractor dynamics." Neurobiol Learn Mem **129**: 38-49.

Kogan, J. H., P. W. Frankland and A. J. Silva (2000). "Long-term memory underlying hippocampus-dependent social recognition in mice." Hippocampus **10**(1): 47-56.

Kohara, K., M. Pignatelli, A. J. Rivest, H. Y. Jung, T. Kitamura, J. Suh, D. Frank, K. Kajikawa, N. Mise, Y. Obata, I. R. Wickersham and S. Tonegawa (2014). "Cell type-specific genetic and optogenetic tools reveal hippocampal CA2 circuits." Nat Neurosci **17**(2): 269-279.

Kuhn, H. G., H. Dickinson-Anson and F. H. Gage (1996). "Neurogenesis in the dentate gyrus of the adult rat: age-related decrease of neuronal progenitor proliferation." J Neurosci **16**(6): 2027-2033.

Lacefield, C. O., V. Itskov, T. Reardon, R. Hen and J. A. Gordon (2012). "Effects of adult-generated granule cells on coordinated network activity in the dentate gyrus." Hippocampus **22**(1): 106-116.

Lagace, D. C., M. H. Donovan, N. A. DeCarolis, L. A. Farnbauch, S. Malhotra, O. Berton, E. J. Nestler, V. Krishnan and A. J. Eisch (2010). "Adult hippocampal neurogenesis is functionally important for stress-induced social avoidance." Proc Natl Acad Sci U S A **107**(9): 4436-4441.

Le Duigou, C., J. Simonnet, M. T. Telenczuk, D. Fricker and R. Miles (2014). "Recurrent synapses and circuits in the CA3 region of the hippocampus: an associative network." Front Cell Neurosci **7**: 262.

Lee, H., C. Wang, S. S. Deshmukh and J. J. Knierim (2015). "Neural Population Evidence of Functional Heterogeneity along the CA3 Transverse Axis: Pattern Completion versus Pattern Separation." Neuron **87**(5): 1093-1105.

Lee, H. J., H. K. Caldwell, A. H. Macbeth, S. G. Tolu and W. S. Young, 3rd (2008). "A conditional knockout mouse line of the oxytocin receptor." Endocrinology **149**(7): 3256-3263.

Lee, H. J., A. H. Macbeth, J. H. Pagani and W. S. Young, 3rd (2009). "Oxytocin: the great facilitator of life." Prog Neurobiol **88**(2): 127-151.

Lee, S. E., S. B. Simons, S. A. Heldt, M. Zhao, J. P. Schroeder, C. P. Vellano, D. P. Cowan, S. Ramineni, C. K. Yates, Y. Feng, Y. Smith, J. D. Sweatt, D. Weinshenker, K. J. Ressler, S. M. Dudek and J. R. Hepler (2010). "RGS14 is a natural suppressor of both synaptic plasticity in CA2 neurons and hippocampal-based learning and memory." Proc Natl Acad Sci U S A **107**(39): 16994-16998.

Leuner, B., J. M. Caponiti and E. Gould (2012). "Oxytocin stimulates adult neurogenesis even under conditions of stress and elevated glucocorticoids." Hippocampus **22**(4): 861-868.

Li, Y., A. Mathis, B. F. Grewe, J. A. Osterhout, B. Ahanonu, M. J. Schnitzer, V. N. Murthy and C. Dulac (2017). "Neuronal Representation of Social Information in the Medial Amygdala of Awake Behaving Mice." Cell **171**(5): 1176-1190 e1117.

Lin, D., M. P. Boyle, P. Dollar, H. Lee, E. S. Lein, P. Perona and D. J. Anderson (2011). "Functional identification of an aggression locus in the mouse hypothalamus." Nature **470**(7333): 221-226.

Lin, Y. T., C. C. Chen, C. C. Huang, K. Nishimori and K. S. Hsu (2017). "Oxytocin stimulates hippocampal neurogenesis via oxytocin receptor expressed in CA3 pyramidal neurons." Nat Commun **8**(1): 537.

Lin, Y. T., T. Y. Hsieh, T. C. Tsai, C. C. Chen, C. C. Huang and K. S. Hsu (2018). "Conditional Deletion of Hippocampal CA2/CA3a Oxytocin Receptors Impairs the Persistence of Long-Term Social Recognition Memory in Mice." J Neurosci **38**(5): 1218-1231.

Liu, X., S. Ramirez, P. T. Pang, C. B. Puryear, A. Govindarajan, K. Deisseroth and S. Tonegawa (2012). "Optogenetic stimulation of a hippocampal engram activates fear memory recall." Nature **484**(7394): 381-385.

Lorente de Nó, R (1934). "Studies on the structure of the cerebral cortex. II. Continuation of the study of the ammonic system." J. Psychol. Neurol. 46: 113-177.

Lukas, M., I. Toth, A. H. Veenema and I. D. Neumann (2013). "Oxytocin mediates rodent social memory within the lateral septum and the medial amygdala depending on the relevance of the social stimulus: male juvenile versus female adult conspecifics." Psychoneuroendocrinology **38**(6): 916-926.

Luo, A. H., P. Tahsili-Fahadan, R. A. Wise, C. R. Lupica and G. Aston-Jones (2011). "Linking context with reward: a functional circuit from hippocampal CA3 to ventral tegmental area." Science **333**(6040): 353-357.

Macbeth, A. H., H. J. Lee, J. Edds and W. S. Young, 3rd (2009). "Oxytocin and the oxytocin receptor underlie intrastrain, but not interstrain, social recognition." Genes Brain Behav **8**(5): 558-567.

Malberg, J. E., A. J. Eisch, E. J. Nestler and R. S. Duman (2000). "Chronic antidepressant treatment increases neurogenesis in adult rat hippocampus." J Neurosci **20**(24): 9104-9110.

Mankin, E. A., G. W. Diehl, F. T. Sparks, S. Leutgeb and J. K. Leutgeb (2015). "Hippocampal CA2 activity patterns change over time to a larger extent than between spatial contexts." Neuron **85**(1): 190-201.

Marlin, B. J. and R. C. Froemke (2017). "Oxytocin modulation of neural circuits for social behavior." Dev Neurobiol **77**(2): 169-189.

Marlin, B. J., M. Mitre, A. D'Amour J, M. V. Chao and R. C. Froemke (2015). "Oxytocin enables maternal behaviour by balancing cortical inhibition." Nature **520**(7548): 499-504.

Marr, D. (1971). "Simple memory: a theory for archicortex." Philos Trans R Soc Lond B Biol Sci **262**(841): 23-81.

McAvoy, K. M., K. N. Scobie, S. Berger, C. Russo, N. Guo, P. Decharatanachart, H. Vega-Ramirez, S. Miake-Lye, M. Whalen, M. Nelson, M. Bergami, D. Bartsch, R. Hen, B. Berninger and A. Sahay (2016). "Modulating Neuronal Competition Dynamics in the Dentate Gyrus to Rejuvenate Aging Memory Circuits." Neuron **91**(6): 1356-1373.

McClelland, J. L. and N. H. Goddard (1996). "Considerations arising from a complementary learning systems perspective on hippocampus and neocortex." Hippocampus **6**(6): 654-665.

McGlinchey, E. M. and G. Aston-Jones (2018). "Dorsal Hippocampus Drives Context-Induced Cocaine Seeking via Inputs to Lateral Septum." Neuropsychopharmacology **43**(5): 987-1000.

McHugh, T. J., M. W. Jones, J. J. Quinn, N. Balthasar, R. Coppari, J. K. Elmquist, B. B. Lowell, M. S. Fanselow, M. A. Wilson and S. Tonegawa (2007). "Dentate gyrus NMDA receptors mediate rapid pattern separation in the hippocampal network." Science **317**(5834): 94-99.

McNaughton, B.L. and Morris, R.G.M. (1987). "Hippocampal synaptic enhancement and information storage within a distributed memory system. Trends Neurosci. **10**: 408-415.

Mesic, I., Y. F. Guzman, A. L. Guedea, V. Jovasevic, K. A. Corcoran, K. Leaderbrand, K. Nishimori, A. Contractor and J. Radulovic (2015). "Double Dissociation of the Roles of Metabotropic Glutamate Receptor 5 and Oxytocin Receptor in Discrete Social Behaviors." Neuropsychopharmacology **40**(10): 2337-2346.

Miles, R. and R. K. Wong (1983). "Single neurones can initiate synchronized population discharge in the hippocampus." Nature **306**(5941): 371-373.

Miles, R. and R. K. Wong (1986). "Excitatory synaptic interactions between CA3 neurones in the guinea-pig hippocampus." J Physiol **373**: 397-418.

Miller, M., K. L. Bales, S. L. Taylor, J. Yoon, C. M. Hostetler, C. S. Carter and M. Solomon (2013). "Oxytocin and vasopressin in children and adolescents with autism spectrum disorders: sex differences and associations with symptoms." Autism Res **6**(2): 91-102.

Mitre, M., B. J. Marlin, J. K. Schiavo, E. Morina, S. E. Norden, T. A. Hackett, C. J. Aoki, M. V. Chao and R. C. Froemke (2016). "A Distributed Network for Social Cognition Enriched for Oxytocin Receptors." J Neurosci **36**(8): 2517-2535.

Modahl, C., L. Green, D. Fein, M. Morris, L. Waterhouse, C. Feinstein and H. Levin (1998). "Plasma oxytocin levels in autistic children." Biol Psychiatry **43**(4): 270-277.

Montagrin, A., C. Saiote and D. Schiller (2017). "The social hippocampus." Hippocampus.

Morris, A. M., J. C. Churchwell, R. P. Kesner and P. E. Gilbert (2012). "Selective lesions of the dentate gyrus produce disruptions in place learning for adjacent spatial locations." Neurobiol Learn Mem **97**(3): 326-331.

Moser, M. B., E. I. Moser, E. Forrest, P. Andersen and R. G. Morris (1995). "Spatial learning with a minislab in the dorsal hippocampus." Proc Natl Acad Sci U S A **92**(21): 9697-9701.

Nakajima, M., A. Gorlich and N. Heintz (2014). "Oxytocin modulates female sociosexual behavior through a specific class of prefrontal cortical interneurons." Cell **159**(2): 295-305.

Nakashiba, T., J. D. Cushman, K. A. Pelkey, S. Renaudineau, D. L. Buhl, T. J. McHugh, V. Rodriguez Barrera, R. Chittajallu, K. S. Iwamoto, C. J. McBain, M. S. Fanselow and S. Tonegawa (2012). "Young dentate granule cells mediate pattern separation, whereas old granule cells facilitate pattern completion." Cell **149**(1): 188-201.

Neunuebel, J. P. and J. J. Knierim (2012). "Spatial firing correlates of physiologically distinct cell types of the rat dentate gyrus." J Neurosci **32**(11): 3848-3858.

Neunuebel, J. P. and J. J. Knierim (2014). "CA3 retrieves coherent representations from degraded input: direct evidence for CA3 pattern completion and dentate gyrus pattern separation." Neuron **81**(2): 416-427.

Niibori, Y., T. S. Yu, J. R. Epp, K. G. Akers, S. A. Josselyn and P. W. Frankland (2012). "Suppression of adult neurogenesis impairs population coding of similar contexts in hippocampal CA3 region." Nat Commun **3**: 1253.

Nottebohm, F. (1985). "Neuronal replacement in adulthood." Ann N Y Acad Sci **457**: 143-161.

O'Keefe, J. (1976). "Place units in the hippocampus of the freely moving rat." Exp Neurol **51**(1): 78-109.

O'Keefe, J. and J. Dostrovsky (1971). "The hippocampus as a spatial map. Preliminary evidence from unit activity in the freely-moving rat." Brain Res **34**(1): 171-175.

O'Reilly, R. C. and J. L. McClelland (1994). "Hippocampal conjunctive encoding, storage, and recall: avoiding a trade-off." Hippocampus **4**(6): 661-682.

Oettl, L. L., N. Ravi, M. Schneider, M. F. Scheller, P. Schneider, M. Mitre, M. da Silva Gouveia, R. C. Froemke, M. V. Chao, W. S. Young, A. Meyer-Lindenberg, V. Grinevich, R. Shusterman and W. Kelsch (2016). "Oxytocin Enhances Social Recognition by Modulating Cortical Control of Early Olfactory Processing." Neuron **90**(3): 609-621.

Ohara, S., S. Sato, K. Tsutsui, M. P. Witter and T. Iijima (2013). "Organization of multisynaptic inputs to the dorsal and ventral dentate gyrus: retrograde trans-synaptic tracing with rabies virus vector in the rat." PLoS One **8**(11): e78928.

Okuyama, T., T. Kitamura, D. S. Roy, S. Itohara and S. Tonegawa (2016). "Ventral CA1 neurons store social memory." Science **353**(6307): 1536-1541.

Opendak, M., B. A. Briones and E. Gould (2016). "Social behavior, hormones and adult neurogenesis." Front Neuroendocrinol **41**: 71-86.

Opendak, M., L. Offit, P. Monari, T. J. Schoenfeld, A. N. Sonti, H. A. Cameron and E. Gould (2016). "Lasting Adaptations in Social Behavior Produced by Social Disruption and Inhibition of Adult Neurogenesis." J Neurosci **36**(26): 7027-7038.

Owen, S. F., S. N. Tuncdemir, P. L. Bader, N. N. Tirko, G. Fishell and R. W. Tsien (2013). "Oxytocin enhances hippocampal spike transmission by modulating fast-spiking interneurons." Nature **500**(7463): 458-462.

Padilla-Coreano, N., S. S. Bolkan, G. M. Pierce, D. R. Blackman, W. D. Hardin, A. L. Garcia-Garcia, T. J. Spellman and J. A. Gordon (2016). "Direct Ventral Hippocampal-Prefrontal Input Is Required for Anxiety-Related Neural Activity and Behavior." Neuron **89**(4): 857-866.

Pagani, J. H., M. Zhao, Z. Cui, S. K. Avram, D. A. Caruana, S. M. Dudek and W. S. Young (2015). "Role of the vasopressin 1b receptor in rodent aggressive behavior and synaptic plasticity in hippocampal area CA2." Mol Psychiatry **20**(4): 490-499.

Paller, K. A., C. Ranganath, B. Gonsalves, K. S. LaBar, T. B. Parrish, D. R. Gitelman, M. M. Mesulam and P. J. Reber (2003). "Neural correlates of person recognition." Learn Mem **10**(4): 253-260.

Park, E., D. Dvorak and A. A. Fenton (2011). "Ensemble place codes in hippocampus: CA1, CA3, and dentate gyrus place cells have multiple place fields in large environments." PLoS One **6**(7): e22349.

Parker, K. J., J. P. Garner, R. A. Libove, S. A. Hyde, K. B. Hornbeak, D. S. Carson, C. P. Liao, J. M. Phillips, J. F. Hallmayer and A. Y. Hardan (2014). "Plasma oxytocin concentrations and OXTR polymorphisms predict social impairments in children with and without autism spectrum disorder." Proc Natl Acad Sci U S A **111**(33): 12258-12263.

Parker, K. J., O. Oztan, R. A. Libove, R. D. Sumiyoshi, L. P. Jackson, D. S. Karhson, J. E. Summers, K. E. Hinman, K. S. Motonaga, J. M. Phillips, D. S. Carson, J. P. Garner and A. Y. Hardan (2017). "Intranasal oxytocin treatment for social deficits and biomarkers of response in children with autism." Proc Natl Acad Sci U S A **114**(30): 8119-8124.

Pasciuto, E., S. C. Borrie, A. K. Kanellopoulos, A. R. Santos, E. Cappuyns, L. D'Andrea, L. Pacini and C. Bagni (2015). "Autism Spectrum Disorders: Translating human deficits into mouse behavior." Neurobiol Learn Mem **124**: 71-87.

Paton, J. A. and F. N. Nottebohm (1984). "Neurons generated in the adult brain are recruited into functional circuits." Science **225**(4666): 1046-1048.

Pearson-Leary, J., D. Eacret, R. Chen, H. Takano, B. Nicholas and S. Bhatnagar (2017). "Inflammation and vascular remodeling in the ventral hippocampus contributes to vulnerability to stress." Transl Psychiatry **7**(6): e1160.

Pena, R.R., A.R. Pereira-Caixeta, M.F.D. Moraes and G.S. Pereira (2014). "Anisomycin administered in the olfactory bulb and dorsal hippocampus impaired social recognition memory in different time points." Brain Res. Bull. 109: 151-157.

Piatti, V. C., L. A. Ewell and J. K. Leutgeb (2013). "Neurogenesis in the dentate gyrus: carrying the message or dictating the tone." Front Neurosci **7**: 50.

Pirnik, Z., B. Mravec and A. Kiss (2004). "Fos protein expression in mouse hypothalamic paraventricular (PVN) and supraoptic (SON) nuclei upon osmotic stimulus: colocalization with vasopressin, oxytocin, and tyrosine hydroxylase." Neurochem Int **45**(5): 597-607.

Pisansky, M. T., L. R. Hanson, Gottesman, II and J. C. Gewirtz (2017). "Oxytocin enhances observational fear in mice." Nat Commun **8**(1): 2102.

Piskorowski, R. A., K. Nasrallah, A. Diamantopoulou, J. Mukai, S. I. Hassan, S. A. Siegelbaum, J. A. Gogos and V. Chevaleyre (2016). "Age-Dependent Specific Changes in Area CA2 of the Hippocampus and Social Memory Deficit in a Mouse Model of the 22q11.2 Deletion Syndrome." Neuron **89**(1): 163-176.

Quintana, D.S., J. Rokicki, D. van der Meer, D. Alnaes, T. Kaufmann, A.C. Palomera, I. Dieset, O.A. Andreassen, and L.T. Westlyle (2017). "Oxytocin gene networks in the human brain: A gene expression and large-scale fMRI meta-analysis study." BioRxiv.

Rametti, G., C. Junque, P. Vendrell, R. Catalan, R. Penades, N. Bargallo and M. Bernardo (2009). "Hippocampal underactivation in an fMRI study of word and face memory recognition in schizophrenia." Eur Arch Psychiatry Clin Neurosci **259**(4): 203-211.

Ramirez, S., X. Liu, P. A. Lin, J. Suh, M. Pignatelli, R. L. Redondo, T. J. Ryan and S. Tonegawa (2013). "Creating a false memory in the hippocampus." Science **341**(6144): 387-391.

Ramirez, S., X. Liu, C. J. MacDonald, A. Moffa, J. Zhou, R. L. Redondo and S. Tonegawa (2015). "Activating positive memory engrams suppresses depression-like behaviour." Nature **522**(7556): 335-339.

Ramón y Cajal, S. (1928). Degeneration and regeneration of the nervous system. Oxford, England: Clarendon Press.

Redondo, R. L., J. Kim, A. L. Arons, S. Ramirez, X. Liu and S. Tonegawa (2014). "Bidirectional switch of the valence associated with a hippocampal contextual memory engram." Nature **513**(7518): 426-430.

Ripamonti, S., M. C. Ambrozkiewicz, F. Guzzi, M. Gravati, G. Biella, I. Bormuth, M. Hammer, L. P. Tuffy, A. Sigler, H. Kawabe, K. Nishimori, M. Toselli, N. Brose, M. Parenti and J. Rhee (2017). "Transient oxytocin signaling primes the development and function of excitatory hippocampal neurons." Elife **6**.

Risold, P. Y. and L. W. Swanson (1997). "Connections of the rat lateral septal complex." Brain Res Brain Res Rev **24**(2-3): 115-195.

Robinson, N. T. M., J. B. Priestley, J. W. Rueckemann, A. D. Garcia, V. A. Smeglin, F. A. Marino and H. Eichenbaum (2017). "Medial Entorhinal Cortex Selectively Supports Temporal Coding by Hippocampal Neurons." Neuron **94**(3): 677-688 e676.

Sahay, A., K. N. Scobie, A. S. Hill, C. M. O'Carroll, M. A. Kheirbek, N. S. Burghardt, A. A. Fenton, A. Dranovsky and R. Hen (2011). "Increasing adult hippocampal neurogenesis is sufficient to improve pattern separation." Nature **472**(7344): 466-470.

Santoro, A. (2013). "Reassessing pattern separation in the dentate gyrus." Front Behav Neurosci **7**: 96.

Sartor, G. C. and G. S. Aston-Jones (2012). "A septal-hypothalamic pathway drives orexin neurons, which is necessary for conditioned cocaine preference." J Neurosci **32**(13): 4623-4631.

Scharfman, H. E. and H. L. Bernstein (2015). "Potential implications of a monosynaptic pathway from mossy cells to adult-born granule cells of the dentate gyrus." Front Syst Neurosci **9**: 112.

Schmidt, B., D. F. Marrone and E. J. Markus (2012). "Disambiguating the similar: the dentate gyrus and pattern separation." Behav Brain Res **226**(1): 56-65.

Schoenfeld, T. J. and E. Gould (2012). "Stress, stress hormones, and adult neurogenesis." Exp Neurol **233**(1): 12-21.

Schumann, C. M., J. Hamstra, B. L. Goodlin-Jones, L. J. Lotspeich, H. Kwon, M. H. Buonocore, C. R. Lammers, A. L. Reiss and D. G. Amaral (2004). "The amygdala is enlarged in children but not adolescents with autism; the hippocampus is enlarged at all ages." J Neurosci **24**(28): 6392-6401.

Senzai, Y. and G. Buzsaki (2017). "Physiological Properties and Behavioral Correlates of Hippocampal Granule Cells and Mossy Cells." Neuron **93**(3): 691-704 e695.

Sheehan, T. P., R. A. Chambers and D. S. Russell (2004). "Regulation of affect by the lateral septum: implications for neuropsychiatry." Brain Res Brain Res Rev **46**(1): 71-117.

Shin, S., H. Pribiag, V. Lilascharoen, D. Knowland, X. Y. Wang and B. K. Lim (2018). "Drd3 Signaling in the Lateral Septum Mediates Early Life Stress-Induced Social Dysfunction." Neuron **97**(1): 195-208 e196.

Sloviter, R. S. and B. P. Damiano (1981). "On the relationship between kainic acid-induced epileptiform activity and hippocampal neuronal damage." Neuropharmacology **20**(11): 1003-1011.

Smith, A. S., S. K. Williams Avram, A. Cymerblit-Sabba, J. Song and W. S. Young (2016). "Targeted activation of the hippocampal CA2 area strongly enhances social memory." Mol Psychiatry **21**(8): 1137-1144.

Snyder, J. S., A. Soumier, M. Brewer, J. Pickel and H. A. Cameron (2011). "Adult hippocampal neurogenesis buffers stress responses and depressive behaviour." Nature **476**(7361): 458-461.

Soloff, M. S., M. Alexandrova and M. J. Fernstrom (1979). "Oxytocin receptors: triggers for parturition and lactation?" Science **204**(4399): 1313-1315.

Sorrells, S. F., M. F. Paredes, A. Cebrian-Silla, K. Sandoval, D. Qi, K. W. Kelley, D. James, S. Mayer, J. Chang, K. I. Auguste, E. F. Chang, A. J. Gutierrez, A. R. Kriegstein, G. W. Mathern, M. C. Oldham, E. J. Huang, J. M. Garcia-Verdugo, Z. Yang and A. Alvarez-Buylla (2018). "Human hippocampal neurogenesis drops sharply in children to undetectable levels in adults." Nature **555**(7696): 377-381.

Spalding, K. L., O. Bergmann, K. Alkass, S. Bernard, M. Salehpour, H. B. Huttner, E. Bostrom, I. Westerlund, C. Vial, B. A. Buchholz, G. Possnert, D. C. Mash, H. Druid and J. Frisen (2013). "Dynamics of hippocampal neurogenesis in adult humans." Cell **153**(6): 1219-1227.

Stevenson, E. L. and H. K. Caldwell (2014). "Lesions to the CA2 region of the hippocampus impair social memory in mice." Eur J Neurosci **40**(9): 3294-3301.

Stranahan, A. M., D. Khalil and E. Gould (2006). "Social isolation delays the positive effects of running on adult neurogenesis." Nat Neurosci **9**(4): 526-533.

Strange, B. A., M. P. Witter, E. S. Lein and E. I. Moser (2014). "Functional organization of the hippocampal longitudinal axis." Nat Rev Neurosci **15**(10): 655-669.

Sun, J., M. A. Bonaguidi, H. Jun, J. U. Guo, G. J. Sun, B. Will, Z. Yang, M. H. Jang, H. Song, G. L. Ming and K. M. Christian (2015). "A septo-temporal molecular gradient of sfrp3 in the dentate gyrus differentially regulates quiescent adult hippocampal neural stem cell activation." Mol Brain **8**: 52.

Sun, W., A. Winseck, S. Vinsant, O. H. Park, H. Kim and R. W. Oppenheim (2004). "Programmed cell death of adult-generated hippocampal neurons is mediated by the proapoptotic gene Bax." J Neurosci **24**(49): 11205-11213.

Sun, Y., A. Q. Nguyen, J. P. Nguyen, L. Le, D. Saur, J. Choi, E. M. Callaway and X. Xu (2014). "Cell-type-specific circuit connectivity of hippocampal CA1 revealed through Cre-dependent rabies tracing." Cell Rep **7**(1): 269-280.

Swanson, L. W., P. E. Sawchenko and W. M. Cowan (1981). "Evidence for collateral projections by neurons in Ammon's horn, the dentate gyrus, and the subiculum: a multiple retrograde labeling study in the rat." J Neurosci **1**(5): 548-559.

Sweeney, P. and Y. Yang (2015). "An excitatory ventral hippocampus to lateral septum circuit that suppresses feeding." Nat Commun **6**: 10188.

Takamura, N., S. Nakagawa, T. Masuda, S. Boku, A. Kato, N. Song, Y. An, Y. Kitaichi, T. Inoue, T. Koyama and I. Kusumi (2014). "The effect of dopamine on adult hippocampal neurogenesis." Prog Neuropsychopharmacol Biol Psychiatry **50**: 116-124.

Takayanagi, Y., M. Yoshida, I. F. Bielsky, H. E. Ross, M. Kawamata, T. Onaka, T. Yanagisawa, T. Kimura, M. M. Matzuk, L. J. Young and K. Nishimori (2005). "Pervasive social deficits, but normal parturition, in oxytocin receptor-deficient mice." Proc Natl Acad Sci U S A **102**(44): 16096-16101.

Talani, G., F. Biggio, V. Licheri, V. Locci, G. Biggio and E. Sanna (2016). "Isolation Rearing Reduces Neuronal Excitability in Dentate Gyrus Granule Cells of Adolescent C57BL/6J Mice: Role of GABAergic Tonic Currents and Neurosteroids." Front Cell Neurosci **10**: 158.

Tashiro, A., V. M. Sandler, N. Toni, C. Zhao and F. H. Gage (2006). "NMDA-receptor-mediated, cell-specific integration of new neurons in adult dentate gyrus." Nature **442**(7105): 929-933.

Tavares, R. M., A. Mendelsohn, Y. Grossman, C. H. Williams, M. Shapiro, Y. Trope and D. Schiller (2015). "A Map for Social Navigation in the Human Brain." Neuron **87**(1): 231-243.

Thompson, C. L., S. D. Pathak, A. Jeromin, L. L. Ng, C. R. MacPherson, M. T. Mortrud, A. Cusick, Z. L. Riley, S. M. Sunkin, A. Bernard, R. B. Puchalski, F. H. Gage, A. R. Jones, V. B. Bajic, M. J. Hawrylycz and E. S. Lein (2008). "Genomic anatomy of the hippocampus." Neuron **60**(6): 1010-1021.

Tonegawa, S., X. Liu, S. Ramirez and R. Redondo (2015). "Memory Engram Cells Have Come of Age." Neuron **87**(5): 918-931.

Treves, A. and E. T. Rolls (1992). "Computational constraints suggest the need for two distinct input systems to the hippocampal CA3 network." Hippocampus **2**(2): 189-199.

Treves, A. and E. T. Rolls (1994). "Computational analysis of the role of the hippocampus in memory." Hippocampus **4**(3): 374-391.

Trinkler, I., J. A. King, C. F. Doeller, M. D. Rugg and N. Burgess (2009). "Neural bases of autobiographical support for episodic recollection of faces." Hippocampus **19**(8): 718-730.

Tronel, S., L. Belnoue, N. Grosjean, J. M. Revest, P. V. Piazza, M. Koehl and D. N. Abrous (2012). "Adult-born neurons are necessary for extended contextual discrimination." Hippocampus **22**(2): 292-298.

Tzeng, W. Y., H. H. Wu, C. Y. Wang, J. C. Chen, L. Yu and C. G. Cherng (2016). "Sex Differences in Stress and Group Housing Effects on the Number of Newly Proliferated Cells and Neuroblasts in Middle-Aged Dentate Gyrus." Front Behav Neurosci **10**: 249.

van Praag, H., B. R. Christie, T. J. Sejnowski and F. H. Gage (1999). "Running enhances neurogenesis, learning, and long-term potentiation in mice." Proc Natl Acad Sci U S A **96**(23): 13427-13431.

van Wimersma Greidanus, T.B. and C. Maigret (1996). "The role of limbic vasopressin and oxytocin in social recognition." Brain Res. 713(1-2): 153-159.

Veenema, A. H., D. I. Beiderbeck, M. Lukas and I. D. Neumann (2010). "Distinct correlations of vasopressin release within the lateral septum and the bed nucleus of the stria terminalis with the display of intermale aggression." Horm Behav **58**(2): 273-281.

Vouimba, R. M., R. Garcia and R. Jaffard (1998). "Opposite effects of lateral septal LTP and lateral septal lesions on contextual fear conditioning in mice." Behav Neurosci **112**(4): 875-884.

Wang, H., F. Duclot, Y. Liu, Z. Wang and M. Kabbaj (2013). "Histone deacetylase inhibitors facilitate partner preference formation in female prairie voles." Nat Neurosci **16**(7): 919-924.

Watanabe, T., M. Kuroda, H. Kuwabara, Y. Aoki, N. Iwashiro, N. Tatsunobu, H. Takao, Y. Nippashi, Y. Kawakubo, A. Kunimatsu, K. Kasai and H. Yamasue (2015). "Clinical and neural effects of six-week administration of oxytocin on core symptoms of autism." Brain **138**(Pt 11): 3400-3412.

Weeden, C. S., J. M. Roberts, A. M. Kamm and R. P. Kesner (2015). "The role of the ventral dentate gyrus in anxiety-based behaviors." Neurobiol Learn Mem **118**: 143-149.

Wersinger, S. R., E. I. Ginns, A. M. O'Carroll, S. J. Lolait and W. S. Young, 3rd (2002). "Vasopressin V1b receptor knockout reduces aggressive behavior in male mice." Mol Psychiatry **7**(9): 975-984.

West, M. J., L. Slomianka and H. J. Gundersen (1991). "Unbiased stereological estimation of the total number of neurons in thesubdivisions of the rat hippocampus using the optical fractionator." Anat Rec **231**(4): 482-497.

Wickersham, I. R., D. C. Lyon, R. J. Barnard, T. Mori, S. Finke, K. K. Conzelmann, J. A. Young and E. M. Callaway (2007). "Monosynaptic restriction of transsynaptic tracing from single, genetically targeted neurons." Neuron **53**(5): 639-647.

Williamson, C.M., I.S. Klein, W. Lee and J.P. Curley (2018). "Immediate early gene activation throughout the brain is associated with dynamic changes in social context." BioRxiv.

Winslow, J. T., E. F. Hearn, J. Ferguson, L. J. Young, M. M. Matzuk and T. R. Insel (2000). "Infant vocalization, adult aggression, and fear behavior of an oxytocin null mutant mouse." Horm Behav **37**(2): 145-155.

Wintzer, M. E., R. Boehringer, D. Polygalov and T. J. McHugh (2014). "The hippocampal CA2 ensemble is sensitive to contextual change." J Neurosci **34**(8): 3056-3066.

Witter, M. P. (2007). "Intrinsic and extrinsic wiring of CA3: indications for connectional heterogeneity." Learn Mem **14**(11): 705-713.

Xia, L., S. K. Nygard, G. G. Sobczak, N. J. Hourguettes and M. R. Bruchas (2017). "Dorsal-CA1 Hippocampal Neuronal Ensembles Encode Nicotine-Reward Contextual Associations." Cell Rep **19**(10): 2143-2156.

Yassa, M. A. and C. E. Stark (2011). "Pattern separation in the hippocampus." Trends Neurosci **34**(10): 515-525.

Yoshida, M., Y. Takayanagi, K. Inoue, T. Kimura, L. J. Young, T. Onaka and K. Nishimori (2009). "Evidence that oxytocin exerts anxiolytic effects via oxytocin receptor expressed in serotonergic neurons in mice." J Neurosci **29**(7): 2259-2271.

Young, W. S., J. Li, S. R. Wersinger and M. Palkovits (2006). "The vasopressin 1b receptor is prominent in the hippocampal area CA2 where it is unaffected by restraint stress or adrenalectomy." Neuroscience **143**(4): 1031-1039.

Zhang, L. and V. S. Hernandez (2013). "Synaptic innervation to rat hippocampus by vasopressin-immuno-positive fibres from the hypothalamic supraoptic and paraventricular nuclei." Neuroscience **228**: 139-162.

Zhang, T. Y., C. L. Keown, X. Wen, J. Li, D. A. Vousden, C. Anacker, U. Bhattacharyya, R. Ryan, J. Diorio, N. O'Toole, J. P. Lerch, E. A. Mukamel and M. J. Meaney (2018). "Environmental enrichment increases transcriptional and epigenetic differentiation between mouse dorsal and ventral dentate gyrus." Nat Commun **9**(1): 298.

Zhao, C., B. Eisinger and S. C. Gammie (2013). "Characterization of GABAergic neurons in the mouse lateral septum: a double fluorescence in situ hybridization and immunohistochemical study using tyramide signal amplification." PLoS One **8**(8): e73750.

Zhao, C., E. M. Teng, R. G. Summers, Jr., G. L. Ming and F. H. Gage (2006). "Distinct morphological stages of dentate granule neuron maturation in the adult mouse hippocampus." J Neurosci **26**(1): 3-11.

Zhao, M., Y. S. Choi, K. Obrietan and S. M. Dudek (2007). "Synaptic plasticity (and the lack thereof) in hippocampal CA2 neurons." J Neurosci **27**(44): 12025-12032.

Zinn, C.G., N. Clairis, L.E.S. Cavalcente, C.R.G Furini, J de Carvalho Myskiw and I. Izquierdo (2016). "Major neurotransmitter systems in dorsal hippocampus and basolateral amygdala control social recognition memory." PNAS. 113(33); E4914-E4919.

Zoicas, I., D. A. Slattery and I. D. Neumann (2014). "Brain oxytocin in social fear conditioning and its extinction: involvement of the lateral septum." Neuropsychopharmacology **39**(13): 3027-3035.

Zou, D., L. Chen, D. Deng, D. Jiang, F. Dong, C. McSweeney, Y. Zhou, L. Liu, G. Chen, Y. Wu and Y. Mao (2016). "DREADD in parvalbumin interneurons of the dentate gyrus modulates anxiety, social interaction and memory extinction." Curr Mol Med **16**(1): 91-102.

Page intentionally left blank.

Appendix 1

(Raam *et al.*, 2017)

nature COMMUNICATIONS

ARTICLE

DOI: 10.1038/s41467-017-02173-0 OPEN

Hippocampal oxytocin receptors are necessary for discrimination of social stimuli

Tara Raam[1,2,3,4], Kathleen M. McAvoy[1,2,3], Antoine Besnard[1,2,3], Alexa Veenema[5] & Amar Sahay[1,2,3,4,6]

Oxytocin receptor (Oxtr) signaling in neural circuits mediating discrimination of social stimuli and affiliation or avoidance behavior is thought to guide social recognition. Remarkably, the physiological functions of Oxtrs in the hippocampus are not known. Here we demonstrate using genetic and pharmacological approaches that Oxtrs in the anterior dentate gyrus (aDG) and anterior CA2/CA3 (aCA2/CA3) of mice are necessary for discrimination of social, but not non-social, stimuli. Further, Oxtrs in aCA2/CA3 neurons recruit a population-based coding mechanism to mediate social stimuli discrimination. Optogenetic terminal-specific attenuation revealed a critical role for aCA2/CA3 outputs to posterior CA1 for discrimination of social stimuli. In contrast, aCA2/CA3 projections to aCA1 mediate discrimination of non-social stimuli. These studies identify a role for an aDG-CA2/CA3 axis of *Oxtr* expressing cells in discrimination of social stimuli and delineate a pathway relaying social memory computations in the anterior hippocampus to the posterior hippocampus to guide social recognition.

[1] Center for Regenerative Medicine, Massachusetts General Hospital, Boston, MA 02114, USA. [2] Harvard Stem Cell Institute, Cambridge, MA 02138, USA. [3] Department of Psychiatry, Massachusetts General Hospital, Harvard Medical School, Boston, MA 02114, USA. [4] Program in Neuroscience, Harvard Medical School, Boston, MA 02115, USA. [5] Department of Psychology, Michigan State University, East Lansing, MI 48824, USA. [6] Broad Institute of Harvard and MIT, Cambridge, MA 02142, USA. Correspondence and requests for materials should be addressed to A.S. (email: asahay@mgh.harvard.edu)

Social recognition in mammals is a complex biological process that necessitates, in part, communication between neural circuits subserving discrimination of socially relevant stimuli and those mediating expression of affiliation or avoidance. Alterations in circuits underlying social discrimination or social interaction or the pathways that link these circuits may underlie social recognition deficits seen in autism spectrum disorders and other psychiatric disorders[1–3]. One general mechanism by which distinct behaviors such as reward seeking, social exploration, and discrimination of social stimuli are orchestrated is through the actions of neuromodulators such as oxytocin (OT)[4–7]. Although a growing number of studies have begun to shed light on OT receptor (Oxtr) signaling in the nucleus accumbens, piriform cortex, lateral septum (LS), prefrontal cortex, and ventral tegmental area in social interaction[8–17], the role of hippocampal Oxtrs in social memory processing is not known.

Evidence from classical lesion studies and more recently, from optogenetic and genetic manipulations implicates the anterior and posterior hippocampus in social memory processing[18–24]. Genetic silencing of anterior CA2 (aCA2) population of neurons or excitotoxic lesions of aCA2/CA3[19,22,23] impairs social recognition memory, whereas optogenetic activation of hypothalamic inputs onto aCA2 promotes social memory[24]. Basolateral amygdala inputs to the posterior hippocampus modulate social interaction[20] and posterior CA1 (pCA1) via its projections to the nucleus accumbens is both necessary and sufficient to mediate discrimination of social, but not non-social, stimuli[25]. As aCA2/CA3 projects to aCA1, dorsolateral septum (DLS) and pCA1, it is not clear which of these projections relay social memory computations from aCA2/CA3 to brain regions such as the NAcc and prefrontal cortex that subserve social behavior[9–16,26]. Furthermore, because aCA1 is also important for novel object recognition[27,28], it is unclear whether aCA2/CA3 projections to aCA1 mediate discrimination of both social and non-social stimuli.

Radioligand binding studies, knock-in reporter mice and immunohistochemistry studies have begun to illuminate the distribution of Oxtrs in the hippocampus with varying degrees of resolution[24,29–32]. In mice, *Oxtr* expression has been reported in polymorphic layer of dentate gyrus (DG), and CA2 and CA3, although the precise identity of *Oxtr*-expressing cell types is poorly characterized. Pioneering studies relying on injection of anti-OT (OT) sera into the posterior hippocampus suggested a role for OT in social exploration[33]. Partial genetic deletion of *Oxtr* in the forebrain during the postnatal period impaired discrimination of intrastrain, but not inter-strain, social recognition suggesting a role for forebrain Oxtrs in fine discrimination of social stimuli[34]. However, whether this phenotype is due to loss of Oxtr signaling in the hippocampus, LS, ventral pallidum, or other brain regions is not known[34,35].

Studies of contextual discrimination have demonstrated that the aDG-CA3 circuit is critical for resolving interference between similar memories[36,37]. One circuit mechanism utilized to minimize interference between similar memories is population-based encoding of similar inputs in non-overlapping ensembles of neurons. Such a mechanism is thought to support pattern separation, as it facilitates transformation of similar inputs into divergent outputs[38–46]. Although population-based coding in aDG-CA3 has been demonstrated to underlie discrimination of similar contexts or navigation of similar environments[43,44,47–51], it remains unclear whether this mechanism is also used for discrimination of social stimuli. Consistent with this notion, in vivo recordings in CA2 in rats reveal global remapping of place fields in response to presentation of a familiar or novel social stimulus in a context[21]. As Oxtr signaling enhances signal-to-noise processing in both mice and rats[15,52,53], Oxtrs are well positioned to modulate DG-CA3 encoding functions under conditions in which OT is released (e.g., when processing social information). Based on these observations, we hypothesized that Oxtrs in aDG-CA2/CA3 contribute to discrimination of social stimuli.

Here we demonstrate using genetic and pharmacological approaches that *Oxtrs* in the aDG-CA2/CA3 circuit are necessary for discrimination of social, but not non-social (object), stimuli. We show using cellular compartment analysis of temporal activity by fluorescence in situ hybridization (catFISH)[54,55] that Oxtrs in aCA2/CA3 neurons recruit a population-based coding mechanism to mediate discrimination of social stimuli. Optogenetic terminal-specific attenuation studies revealed a critical role for aCA2/CA3 outputs to pCA1, but not aCA1, for discrimination of social stimuli. In contrast, aCA2/CA3 projections to aCA1 mediate discrimination of non-social stimuli. Together these studies identify a role for a aDG-CA2/CA3 axis of Oxtr-expressing cells in discrimination of social stimuli and delineate a pathway by which computations underlying social information processing are relayed from anterior hippocampus to the posterior hippocampus, to guide social recognition.

Results

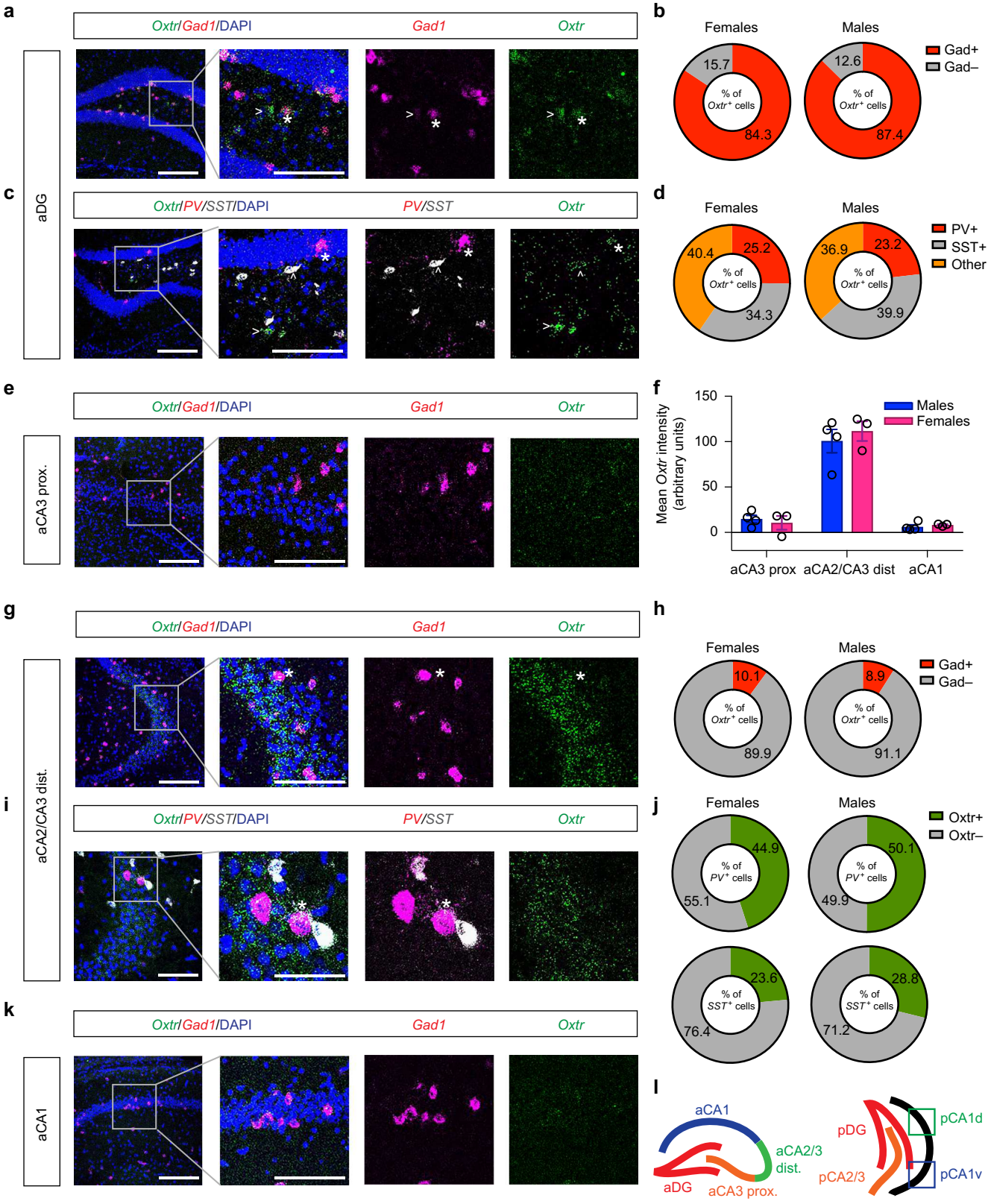
Characterization of *Oxtr* expression in the hippocampus. To comprehensively map the expression of *Oxtr* in the hippocampus, we performed multiplex FISH using riboprobes directed against *Oxtr*, glutamate decarboxylase 1 (*Gad1)*, a marker for GABAergic inhibitory neurons, and markers of interneuron subpopulations, Parvalbumin (*PV*), and Somatostatin (*SST)* in age-matched male and female mice. Within anterior DG (aDG), *Oxtr* expression colocalized primarily with *Gad1* (84.3% in females and 87.4% in males), indicating the identity of these neurons primarily as inhibitory interneurons (Fig. 1a, b). A small population of $Oxtr^+$ cells in the hilus did not colocalize with *Gad1* (Fig. 1a), suggesting that these cells are most likely excitatory mossy cells. Oxtr expression was absent from $Gad1^-$ cells in the granule cell layer of the DG, indicating that *Oxtr* is not expressed in dentate granule neurons. Analysis of *Oxtr*, *PV*, and *SST* expression in aDG showed greater colocalization of *Oxtr* with *SST* than with *PV* (Fig. 1c, d). Further, a large percentage of *Oxtr* cells in aDG were negative for both *PV* and *SST*, indicating the presence of additional subclasses of $Oxtr^+$ interneurons that are not captured in *PV*- and *SST*-only expressing populations.

Next we analyzed *Oxtr* expression within anterior CA subfields as follows: $aCA3_{proximal}$, $aCA2/CA3_{distal}$, and aCA1 (schematic shown in Fig. 1l). Quantification of *Oxtr* intensity revealed enrichment of *Oxtr* expression in the $aCA2/CA3_{distal}$ region while *Oxtr* levels in $aCA3_{proximal}$ and aCA1 were comparable to that of background (Fig. 1e, f, g, k). Colocalization analysis of *Oxtr* and *Gad1* in $aCA2/CA3_{distal}$ subregion revealed low overlap (10.1% in females and 8.9% in males, Fig. 1g, h), suggesting that the vast majority of *Oxtr*-expressing cells in $aCA2/CA3_{distal}$ are excitatory. Assessment of overlap between *Oxtr*, *PV*, and *SST* in $aCA2/CA3_{distal}$ revealed a larger fraction of *PV*+*Oxtr*+ cells than SST+*Oxtr*+ cells (Fig. 1i, j). We did not detect sexual dimorphism in *Oxtr* expression within any subregion of the anterior hippocampus.

Within the posterior hippocampus, we observed dense *Oxtr* expression in pDG (Supplementary Fig. 1a). In contrast to aDG where the majority of *Oxtr* cells were GABA-ergic interneurons, >50% of *Oxtr*-expressing cells in pDG were $Gad1^-$ putative mossy cells (Supplementary Fig. 1a, b). $Oxtr^+$ dentate granule neurons were not observed in pDG. Similar to aDG, further characterization of *Oxtr*+ cells revealed a mixed population of

PV$^+$ and *SST*$^+$ cells, with a larger fraction of *Oxtr*+ cells colocalizing with *SST* than with *PV* (Supplementary Fig. 1c, d).

Next we analyzed *Oxtr* expression within posterior CA subfields (pCA2/3 and the dorsal and ventral segments of pCA1, schematic shown in Fig. 1l). We observed enriched expression of *Oxtr* in pCA2/3 and pCA1v; however, *Oxtr* expression was comparable to the background in pCA1d (Supplementary Fig. 1e, i, j, k). Within pCA2/3, *Oxtr* is predominantly expressed in excitatory neurons of the pyramidal cell layer, with 15–20% overlap between *Oxtr* and *Gad1* (Supplementary Fig. 1e, f). Similar to aCA2/CA3$_{distal}$, these cells are a mixed population of *PV*- and *SST*-expressing cells, with a



larger fraction of *PV*+ cells expressing *Oxtr* than *SST*+ cells (Supplementary Fig. 1g, h). In contrast to negligible *Oxtr* expression in aCA1, *Oxtr* expression was dense in the pyramidal layer of the ventral segment of pCA1 (Supplementary Fig. 1k, l). A small fraction of *Oxtr*+ cells colocalized with *Gad1*, with a larger fraction of PV^+ cells that were *Oxtr*+ than *SST*+ cells (Supplementary Fig. 1m,n). We did not detect any sexual dimorphism in *Oxtr* expression within any subregion of posterior hippocampus.

aDG hilar Oxtrs are necessary for social discrimination. To determine the behavioral contributions of *Oxtr* in aDG hilar neurons, we utilized a conditional knockout mouse line of the Oxtr, $Oxtr^{f/f}$[35], which permits Cre recombinase-dependent deletion of *Oxtr*. We employed an AAV_9 Cre-expressing virus expressed under the control of a human Synapsin promoter, in order to target both inhibitory interneurons and excitatory mossy cells in aDG (Fig. 2a, b). Although previous reports indicate that the AAV_9 serotype is anterogradely transported from some cell types, we did not observe any transport to CA3/CA2[56,57] (Supplementary Fig. 2a) or retrograde trafficking to brain regions projecting to the DG (Supplementary Fig. 2b–e), as has also been previously reported with high titre AAV_9 viruses[58]. In order to determine viral mediated recombination of *Oxtrs*, we quantified the percentage of DAPI+cells expressing *Oxtr* messenger RNA in aDG hilar neurons of $Oxtr^{+/+}$ vs. $Oxtr^{f/f}$ mice injected with AAV_9-hSyn-Cre. *Oxtr*+ cells comprised 11% of all DAPI+ cells in $Oxtr^{+/+}$ mice and 6% of all DAPI+ cells in $Oxtr^{f/f}$ mice, demonstrative of *Oxtr* recombination (Supplementary Fig. 2f, g).

Bilateral infection of Cre-expressing virus in aDG resulted in an increased number of *c-fos*-expressing dentate granule neurons following exposure to a social stimulus, suggesting a loss of inhibition onto dentate granule neurons (unpaired *t*-test, green fluorescent protein (GFP) vs. Cre: $p = 0.0158$, Fig. 2c). aDG *Oxtr* deletion did not significantly affect performance in tests of object exploration, novel object recognition, or social exploration (Fig. 2d–f). Habituation to a social stimulus was modestly impaired (trend, two-way analysis of variance (ANOVA), interaction: $F_{(2,30)} = 2.613$, $p = 0.0899$). However, aDG *Oxtr* deletion resulted in a robust deficit in the social discrimination task. Whereas control animals strongly preferred a novel animal to a familiar animal, Cre-injected animals did not show a preference (two-way ANOVA, treatment: $F_{(1,15)} = 0.8955$, $p = 0.3590$, stimulus: $F_{(1,15)} = 25.78$, $p = 0.0001$, interaction: $F_{(1,15)} = 10.32$, $p = 0.0058$; Multiple comparisons, Familiar vs. Novel, GFP: $p < 0.0001$, Cre: $p = 0.5294$, Fig. 2g). Discrimination ratios were significantly lower in Cre animals than in GFP animals (unpaired *t*-test, GFP vs Cre: $p = 0.0036$, Fig. 2g). Unilateral injection of Cre into aDG was insufficient to reproduce this effect (GFP $n = 11$, Cre $n = 7$, unpaired *t*-test GFP vs. Cre: $p = 0.2976$). Deletion of Oxtrs in aDG did not affect measures of innate anxiety in the open field test (OFT) or elevated plus maze (EPM) (Supplementary Fig. 3a–c). Together, these data demonstrate a critical role for Oxtrs in the aDG in mediating discrimination of social, but not non-social, stimuli.

$aCA2/CA3_{distal}$ Oxtrs are necessary for social discrimination. As CA2/CA3 is the primary output of the DG and *Oxtrs* are densely expressed in $aCA2/CA3_{distal}$, we next sought to assess the contributions of Oxtr in $aCA2/CA3_{distal}$ to object and social recognition. We preferentially targeted the principal layer of $aCA2/CA3_{distal}$ of $Oxtr^{f/f}$ mice by employing a virus that drives expression of Cre-recombinase under a CamKIIα promoter (Fig. 3a, b). Cre virus was expressed predominantly in pyramidal neurons (92.8%) and a small percentage of GABA-ergic interneurons (7.3%) (Supplementary Fig. 5b). We did not observe any retrograde or anterograde transport of Cre virus to inputs or outputs of $aCA2/CA3_{distal}$ in sections immunolabeled for GFP (Supplementary Fig. 4a–c). To determine recombination of *Oxtrs* in $aCA2/CA3_{distal}$, we quantified the percentage of DAPI+ cells expressing *Oxtr* mRNA in $aCA2/CA3_{distal}$ of $Oxtr^{+/+}$ vs. $Oxtr^{f/f}$ mice injected with AAV_9-CamKIIα-Cre. *Oxtr*+ cells comprised 50% of all DAPI+ cells in $Oxtr^{+/+}$ mice and 25% of all DAPI+ cells in $Oxtr^{f/f}$ mice (Supplementary Fig. 4d, e). Interestingly, although we observed fewer total DAPI+ cells that were positive for *Oxtr* in $Oxtr^{f/f}$ mice, we observed larger *Oxtr* puncta in cells that retained *Oxtr* mRNA, suggestive of potential redistribution of transcripts.

Oxtr deletion in $aCA2/CA3_{distal}$ neurons did not affect object exploration, novel object recognition, or social exploration (Fig. 3c–e). However, although control virus (GFP) injected mice habituated to the familiar animal over trials 1 through 3, Cre-injected animals failed to show this habituation (two-way ANOVA, treatment: $F_{(1,15)} = 0.2574$, $p = 0.6193$, trial: $F_{(2,30)} = 0.6646$, $p = 0.5219$, interaction: $F_{(2,30)} = 6.282$, $p = 0.0053$; Multiple comparisons, Trial 1 vs. Trial 3, GFP: $p < 0.05$, Cre: $p > 0.05$, Fig. 3f). Furthermore, control animals demonstrated a strong preference for the novel animal, whereas Cre-injected animals failed to show a preference (two-way ANOVA, treatment: $F_{(1,15)} = 0.00185$, $p = 0.9663$, stimulus: $F_{(1,15)} = 19.98$, $p = 0.0004$, interaction: $F_{(1,15)} = 5.597$, $p = 0.0319$; Multiple comparisons, Familiar vs. Novel, GFP: $p = 0.0009$, Cre: $p = 0.2439$, Fig. 3f). In addition, discrimination ratios were significantly lower in Cre animals than in GFP animals (unpaired *t*-test, GFP vs. Cre: $p = 0.0038$, Fig. 3f). Deletion of *Oxtrs* in $aCA2/CA3_{distal}$ did not

Fig. 1 Characterization of *Oxtr* expression in anterior hippocampus. **a** Representative low-magnification (left) and high-magnification (right) images of *Oxtr* and *Gad1* mRNA expression in anterior DG by FISH ($n = 4$ males, 3 females). Asterisk (*) denotes $Oxtr^+/Gad1^+$ interneuron. Arrowhead (>) denotes $Oxtr^+/GAD1^-$ mossy cell. Scale bar, 100 μm. Inset scale bar, 50 μm. **b** Quantification of *Gad1* and *Oxtr* colocalization for males and females, expressed as a percentage of $Gad1^+$ cells over total $Oxtr^+$ cells. **c** Representative images of low-magnification (left) and high-magnification (right) images of *Oxtr*, *PV*, and *SST* mRNA expression in anterior DG by FISH ($n = 4$ males, 3 females). Asterisk (*) denotes $PV^+/Oxtr^+$ interneuron. Right-facing arrowhead (>) denotes $Oxtr^+$ mossy cell. Upward facing arrowhead (^) denotes $Oxtr^+/SST^+$ interneuron. Scale bar, 100 μm. Inset scale bar, 50 μm. **d** Quantification of *Oxtr* colocalization with *PV* and *SST*, expressed as a percentage of total *Oxtr* cells. **e** Representative low-magnification (left) and high-magnification (right) images of *Oxtr* and *Gad1* mRNA expression in $aCA3_{proximal}$ by FISH ($n = 4$ males, 3 females). Scale bar, 100 μm. Inset scale bar, 50 μm. **f** Quantification of mean *Oxtr* intensity for CA regions expressed in arbitrary units, normalized for background. **g** Representative low-magnification (left) and high-magnification (right) images of *Oxtr* and *Gad1* mRNA expression in $aCA2/CA3_{distal}$ by FISH ($n = 4$ males, 3 females). Asterisk (*) denotes $Oxtr^+/GAD1^+$ interneuron. Scale bar, 100 μm. Inset scale bar, 50 μm. **h** Quantification of *Gad1* and *Oxtr* colocalization in $aCA2/CA3_{distal}$ for males and females, expressed as a percentage of $Gad1^+$ cells over $Oxtr^+$ cells. **i** Representative images of *Oxtr*, *PV*, and *SST* mRNA expression in $aCA2/CA3_{distal}$ by FISH ($n = 4$ males, 3 females). Asterisk (*) denotes $PV^+/Oxtr^+$ interneuron. Scale bar, 50 μm. Inset scale bar, 25 μm. **j** Quantification of *Oxtr* colocalization with *PV* and *SST* in $aCA2/CA3_{distal}$, expressed as a percentage of total *PV* cells (top) or *SST* cells (bottom). **k** Representative low-magnification (left) and high-magnification (right) images of *Oxtr* and *Gad1* mRNA expression in aCA1 by FISH ($n = 4$ males, 3 females). Scale bar, 100 μm. Inset scale bar, 50 μm. **l** Schematic of anterior and posterior hippocampal subregions boundaries

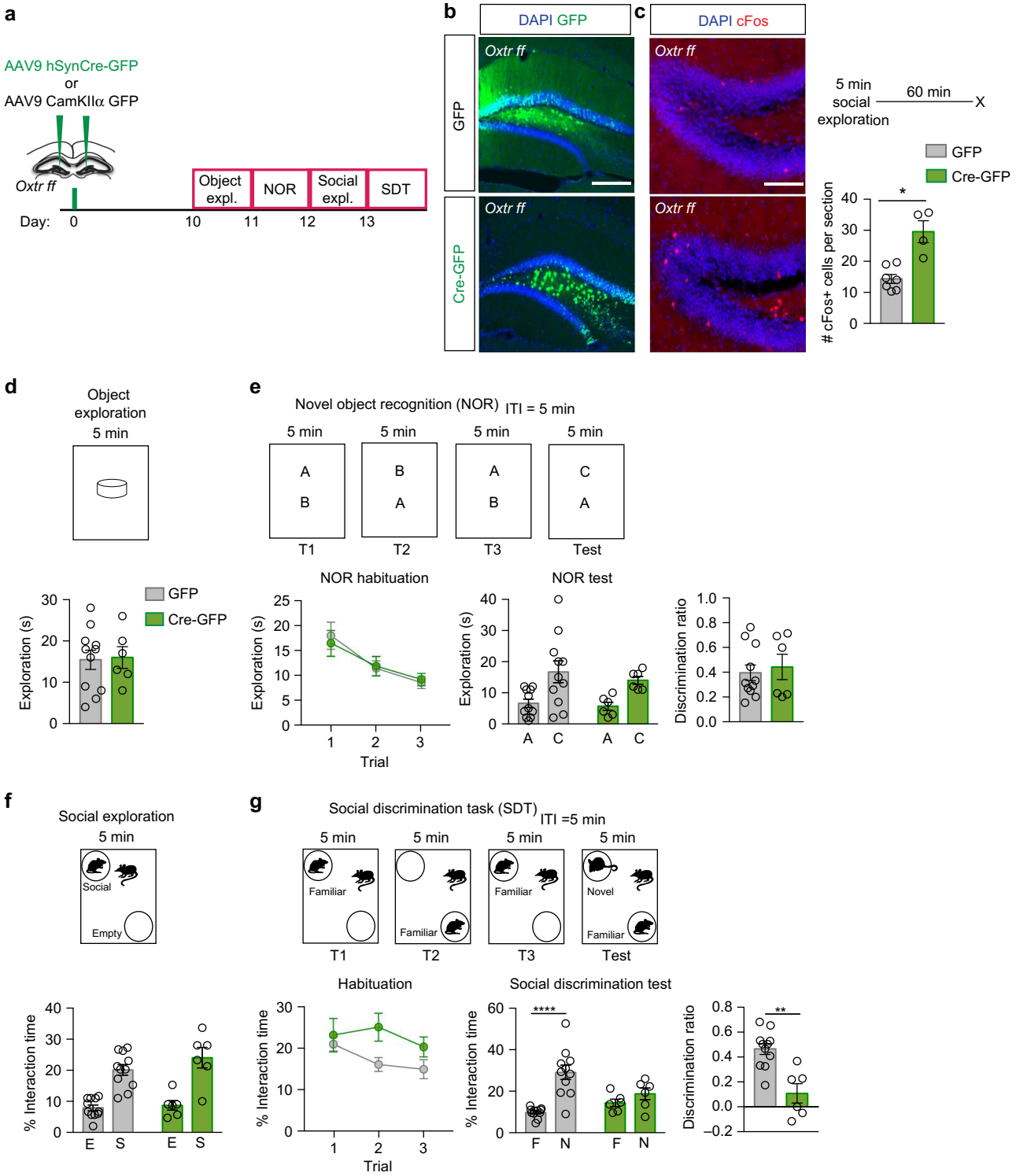


Fig. 2 Viral recombination of *Oxtr* in anterior DG hilar neurons impairs discrimination of social, but not non-social, stimuli. **a** Schematic illustrating viral injection and behavioral testing timeline. **b** Representative images of Cre and GFP virus infection in aDG. Scale bar, 200 μm. **c** Representative images and quantifications of cFos immunoreactivity in granule cell layer of aDG (GFP: $n = 7$, Cre: $n = 4$). Scale bar, 75 μm. **d** Behavioral schematic (top) and quantification (bottom) of single object exploration (GFP: $n = 11$, Cre: $n = 6$). **e** Behavioral schematic (top) and quantification (bottom) of novel objection recognition (GFP: $n = 11$, Cre: $n = 6$). Quantifications are displayed as Habituation (trials 1-3), Test (trial 4), and discrimination ratio (trial 4). **f** Behavioral schematic (top) and quantification (bottom) of social exploration test (GFP: $n = 11$, Cre: $n = 6$). **g** Behavioral schematic (top) and quantification (bottom) of social discrimination task (GFP: $n = 11$, Cre: $n = 6$). Quantifications are displayed as Habituation (trials 1-3), Test (trial 4), and discrimination ratio (trial 4). All data are displayed as mean ± SEM

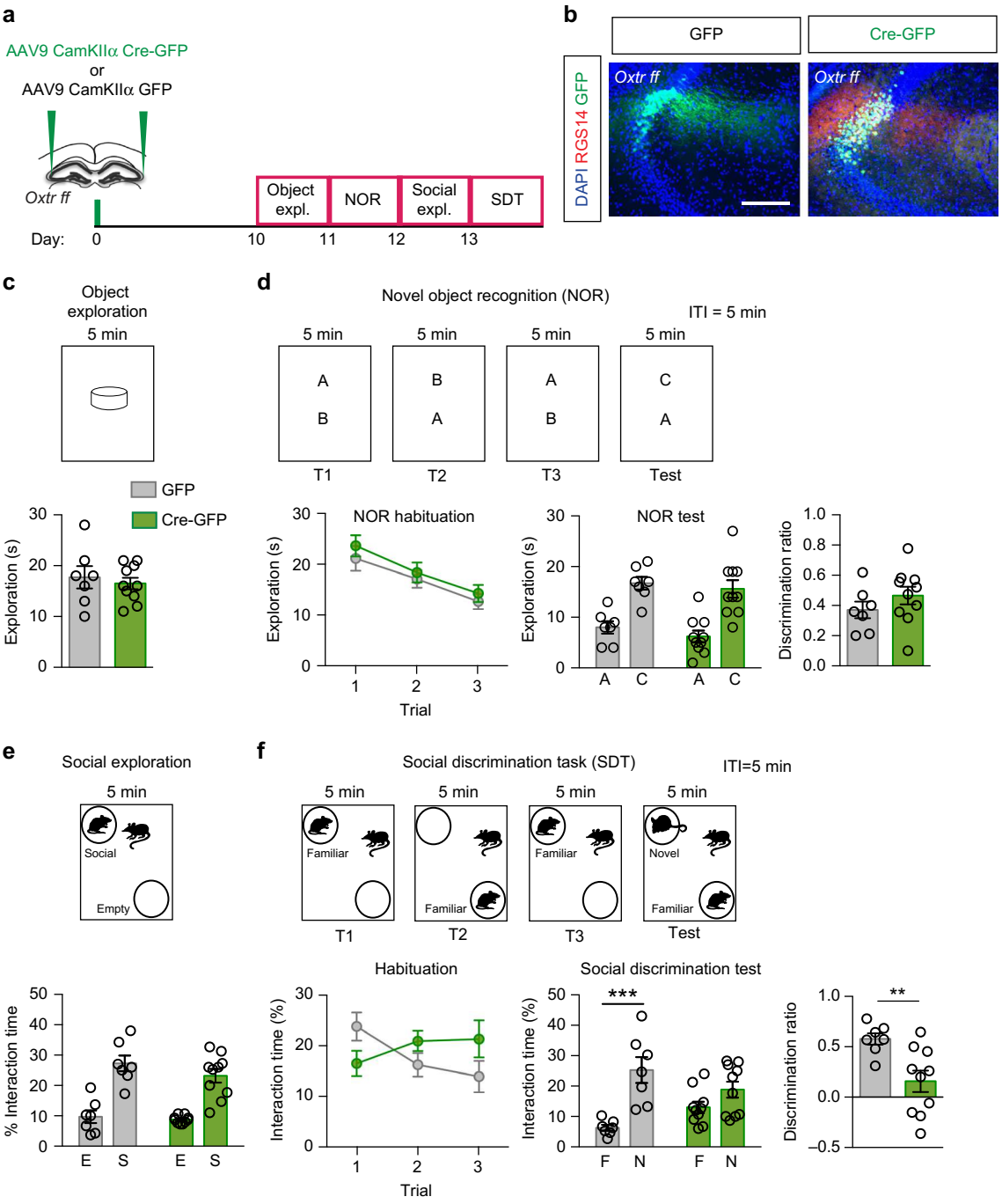


Fig. 3 Viral recombination of *Oxtr* in aCA2/CA3$_{distal}$ impairs discrimination of social, but not non-social, stimuli. **a** Schematic illustrating viral injection and behavioral testing timeline. **b** Representative images of Cre and GFP virus infection in aCA2/CA3. Scale bar, 200 µm. **c** Behavioral schematic (top) and quantification (bottom) of single object exploration (GFP: $n = 7$, Cre: $n = 10$). **d** Behavioral schematic (top) and quantification (bottom) of novel objection recognition (GFP: $n = 7$, Cre: $n = 10$). Quantifications are displayed as Habituation (trials 1-3), Test (trial 4), and discrimination ratio (trial 4). **e** Behavioral schematic (top) and quantification (bottom) of social exploration test (GFP: $n = 7$, Cre: $n = 10$). **f** Behavioral schematic (top) and quantification (bottom) of social discrimination task (GFP: $n = 7$, Cre: $n = 10$). Quantifications are displayed as Habituation (trials 1-3), Test (trial 4), and discrimination ratio (trial 4). All data are displayed as mean ± SEM

affect measures of innate anxiety in the open field (Supplementary Fig. 5a, c). Interestingly, in the EPM, we observed a decrease in time spent in the center, a decision-making point in the maze, at the expense of time spent in the closed arm, but not time spent in open arms (Supplementary Fig. 5a, d).

To distinguish between the potential contribution of Oxtrs to habituation (or acquisition) vs. retrieval in the social discrimination task, we employed pharmacological blockade of Oxtrs in vivo only during the retrieval phase of this task. Adult male C57BL/6J mice received a bilateral guide cannulae placed over aCA2/CA3 10 days before behavior (Supplementary Fig. 6a, b). Following habituation and acquisition, we infused sterile saline or Oxtr antagonist, Oxtr-A, (L-368,899 Hydrochloride, Tocris) bilaterally into aCA2/CA3$_{distal}$ after Trial 3 and immediately before Trial 4. Under conditions in which subjects have sufficiently encoded the familiar stimulus, acute blockade of Oxtrs during retrieval was

sufficient to impair discrimination of social stimuli (two-way ANOVA, treatment: $F_{(1,5)} = 2.373$, $p = 0.1841$, stimulus, $F_{(1,5)} = 1.509$, $p = 0.2739$, interaction, group × stimulus: $F_{(1,5)} = 9.802$, $p = 0.0259$; paired *t*-test Familiar vs. Novel, Saline: $p = 0.0148$, Oxtr-A: $p = 0.1672$, Supplementary Fig. 6c). Similarly, discrimination ratios were significantly lower during Oxtr-A infusion than during saline infusion (paired *t*-test, $p = 0.0109$, Supplementary Fig. 6c).

Together, these experiments suggest through genetic deletion that Oxtrs in aCA2/CA3$_{distal}$ are critical for social discrimination, but not object discrimination. Furthermore, our pharmacological blockade studies suggest that Oxtr function is necessary during the retrieval window to mediate discrimination of social stimuli.

aCA2/CA3$_{distal}$ Oxtrs mediate population-based social coding. The DG-CA3 circuit recruits population-based coding to encode similar memories in non-overlapping ensembles, thereby minimizing interference between similar memories during storage. Such a mechanism has been shown to underlie navigation and discrimination of similar contexts[43,44,47–51], and has been more recently shown in CA2 of rats in response to social stimuli[21]. We asked whether Oxtrs in aCA2/CA3$_{distal}$ recruit population based coding mechanisms to distinguish between similar social stimuli by utilizing catFISH in combination with viral deletion of *Oxtrs* in aCA2/CA3$_{distal}$. This approach allows us to visualize ensembles of neurons activated in response to social stimuli at distinct temporal windows based on sub-cellular localization of *cFos* mRNA transcripts in either the nucleus or the cytoplasm[54,55] (Fig. 4a, b and Supplementary Fig. 7). Adult male *Oxtr$^{f/f}$* mice were injected with AAV CamKIIα-GFP or CamKIIα-Cre-GFP in aCA2/CA3$_{distal}$ 1 week before exposure to two social stimuli: re-exposure to a single mouse (A–A), or new exposure to a novel mouse (A–B) (four groups in total, Fig. 4c). Analysis of cellular ensembles in CA3$_{proximal}$ of control animals revealed higher percentage overlap (cells positive for both nuclear and cytoplasmic *cFos* transcript are indicative of reactivation) in the A–A condition relative to the A–B condition. In contrast, Cre-injected animals exhibited comparable levels of re-activation (overlap) in A–A and A–B conditions (two-way ANOVA, treatment: $F_{(1,15)} = 0.1703$, $p = 0.6856$, exposure: $F_{(1,15)} = 3.335$, $p = 0.0878$, interaction: $F_{(1,15)} = 5.917$, $p = 0.0280$; Multiple comparisons, AA vs AB, GFP: $p = 0.0145$, Cre: $p > 0.9999$, Fig. 4d). Interestingly, analysis of sub-cellular transcript localization in CA3$_{distal}$ of controls and experimental groups revealed comparable levels of ensemble reactivation in response to A–A and A–B conditions (Fig. 4f), consistent with reports that CA3$_{proximal}$ and CA3$_{distal}$ are functionally distinct[45,46,49]. We did not observe differences in the total number of activated cells for either CA3$_{proximal}$ or CA3$_{distal}$ (Fig. 4e, g and Supplementary Fig.7).

Roles of aCA2/CA3 distal outputs in social discrimination. Social information processed in aCA2/CA3$_{distal}$ may be relayed via projections to aCA1, DLS, and/or pCA1 to subcortical and prefrontal circuits, to guide social behavior[59–61] (Supplementary Figs. 8 and 10). To begin to understand how Oxtr-dependent computations underlying social recognition performed in aCA2/CA3$_{distal}$ are relayed out of the anterior hippocampus to limbic circuits that mediate social behavior, we utilized in vivo terminal-specific optogenetic silencing to attenuate aCA2/CA3$_{distal}$ outputs to these three downstream targets. We first targeted the pathway from aCA2/CA3$_{distal}$ to aCA1. We injected AAV$_5$-CamKIIα-eNpHR-EYFP or AAV$_5$-CamKIIα-EYFP bilaterally into aCA2/CA3$_{distal}$ of adult male mice. Three weeks post injection, bilateral optogenetic implants were placed above aCA1. Mice were then tested for both object behavior and social behavior (Fig. 5a–d). Optogenetic illumination of aCA2/CA3$_{distal}$ terminals in aCA1 in the test phase of novel object recognition task robustly impaired discrimination between familiar and novel object in NpHR animals relative to controls (two-way ANOVA, treatment: $F_{(1,14)} = 3.783$, $p = 0.0721$, object: $F_{(1,14)} = 28.67$, $p = 0.0001$, interaction: $F_{(1,14)} = 15.88$, $p = 0.0014$; Multiple comparisons, Object A vs. C, EYFP: $p < 0.0001$, NpHR: $p = 0.6985$, Fig. 5d). Discrimination ratios of NpHR mice were significantly lower than controls (unpaired *t*-test $p = 0.0029$, Fig. 5d). We did not observe any effects on object exploration, social exploration, or discrimination of social stimuli (Fig. 5c, e, f). These data suggest that aCA2/CA3$_{distal}$ outputs to aCA1 are critical for object recognition but are dispensable for discrimination of social stimuli.

We next asked whether aCA2/CA3$_{distal}$ outputs to the DLS mediate social discrimination[12,14,59,60]. AAV$_5$-CamKIIα-eNpHR-EYFP or AAV$_5$-CamKIIα-EYFP viruses were bilaterally injected into aCA2/CA3$_{distal}$ of adult male mice and bilateral optogenetic implants were placed above the DLS (Supplementary Fig. 9a, b). Optogenetic attenuation of terminals was confirmed by quantifying the number of cFos+cells in the termination area (unpaired *t*-test, $p = 0.0006$, Supplementary Fig. 9c). We observed a modest enhancement in social discrimination (two-way ANOVA, treatment: $F_{(1,30)} = 0.2753$, $p = 0.6037$, stimulus: $F_{(1,30)} = 52.65$, $p < 0.0001$, interaction: $F_{(1,30)} = 4.861$, $p = 0.0353$; Multiple comparisons, Familiar vs. Novel, EYFP: $p = 0.0018$, NpHR: $p < 0.0001$, Supplementary Fig. 9g). Discrimination ratios were significantly higher for NpHR animals than control animals (unpaired *t*-test, $p = 0.0121$, Supplementary Fig. 9g). We did not observe any effects on single object exploration, NOR, or social exploration (Supplementary Fig. 9d, e, f). These data suggest that attenuation of aCA2/CA3$_{distal}$-DLS projections may modestly promote discrimination of social stimuli.

Recent studies have demonstrated a role for pCA1-NAcc circuit in social discrimination[25]. We observed direct outputs from aCA2/CA3$_{distal}$ to the dorsal segment of pCA1 (Fig. 6b)[62] and confirmed the colocalization of these terminals with the CA1 marker, WFS1 (Supplementary Fig. 10). We attenuated these outputs by injecting AAV$_5$-CamKIIα-eNpHR-EYFP or AAV$_5$-CamKIIα-EYFP into bilateral aCA2/CA3$_{distal}$ of adult male mice and placing a bilateral optogenetic implant above pCA1 (Fig. 6a). Effective silencing was confirmed by quantifying the number of cFos+cells in pCA1 below the optogenetic implant (unpaired *t*-test, $p = 0.0223$, Fig. 6c). Optogenetic attenuation of aCA2/CA3$_{distal}$ terminals in pCA1 did not affect performance in tests of single object exploration, novel object recognition, or social exploration (Fig. 6d–f). In contrast, optogenetic illumination of aCA2/CA3$_{distal}$ terminals in pCA1 in the test phase of social discrimination task markedly impaired discrimination in NpHR animals as compared with controls (two-way ANOVA, treatment: $F_{(1,12)} = 0.82$, $p = 0.3830$, stimulus: $F_{(1,12)} = 64.71$, $p < 0.0001$, interaction: $F_{(1,12)} = 13.4$, $p = 0.0033$; Multiple comparison, Familiar vs. Novel, EYFP: $p < 0.0001$, NpHR: $p = 0.0184$, Fig. 6g). Discrimination ratios were also significantly lower for NpHR animals as compared with controls (unpaired *t*-test, $p = 0.0006$, Fig. 6g). Together, these data suggest that aCA2/CA3$_{distal}$ projections to pCA1 relay social information to subcortical and prefrontal circuits to guide social behavior.

Discussion

Social recognition, the ability to recognize and distinguish between conspecifics is essential to the formation and stability of social interactions across species. As such, it is not surprising that cortical and subcortical circuits must communicate to support efficient social recognition. Remarkably, despite studies

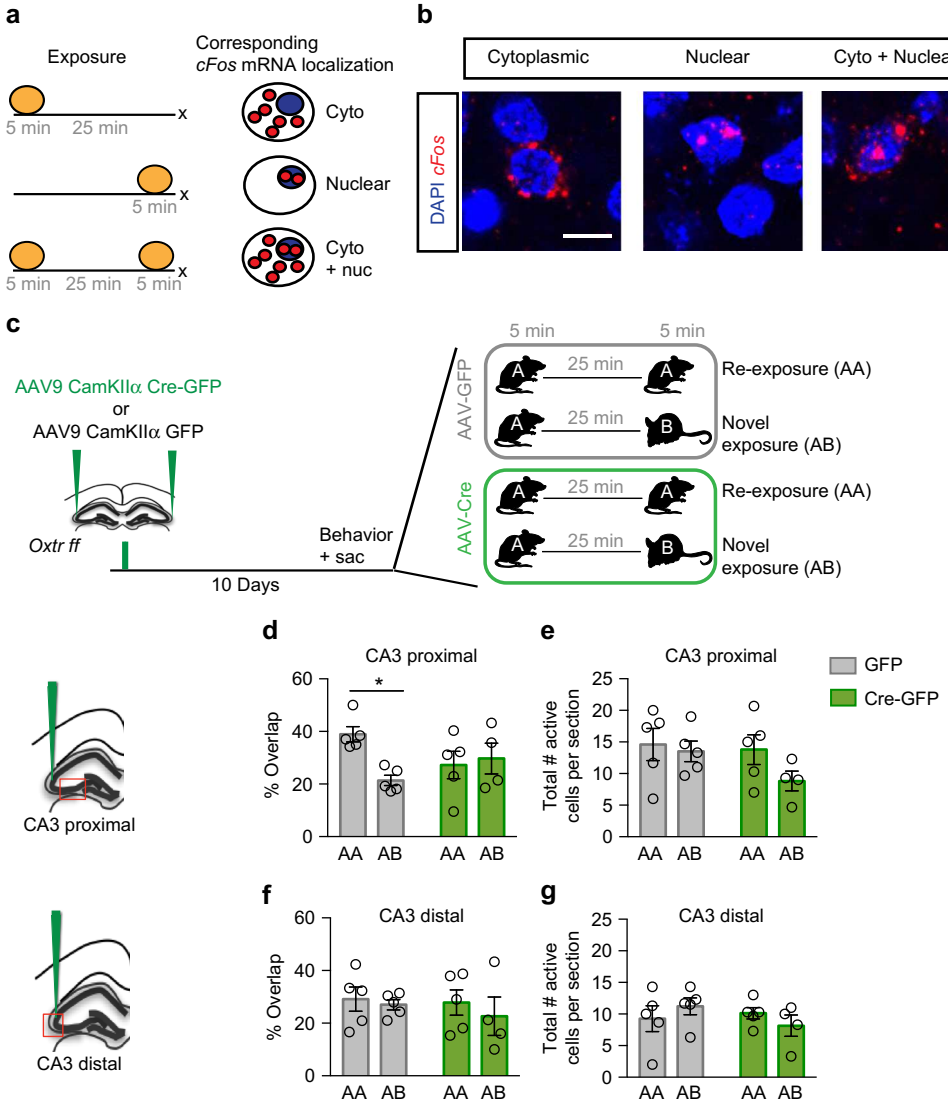


Fig. 4 Viral recombination of *Oxtr* in aCA2/CA3$_{distal}$ impairs population based coding of social stimuli. **a** Schematic illustrating conceptual design of catFISH using *c-fos* intronic and full-length mRNA localization as readouts for ensembles of neurons activated at distinct behavioral windows. **b** Representative images of CA3 pyramidal neurons exhibiting cytoplasmic, nuclear, or cytoplasmic and nuclear localization of *c-fos* mRNA transcripts. Scale bar, 10 µm. **c** Schematic illustrating viral injection and behavioral exposure timelines (GFP AA: $n = 5$, GFP AB: $n = 5$, Cre AA: $n = 5$, Cre AB: $n = 4$). **d**, **f** Percent overlap between ensembles of neurons encoding first and second stimulus for CA3$_{proximal}$ (top) and CA3$_{distal}$ (bottom), respectively. **e**, **g** Total number of active cells per section for CA3$_{proximal}$ (top) and CA3$_{distal}$ (bottom), respectively. All data are displayed as mean ± SEM

implicating Oxtrs in different brain regions in social recognition, the role of Oxtrs in the hippocampus has remained unaddressed. Here we identify a role for a aDG-CA2/CA3 axis of Oxtr-expressing cells in discrimination of social, but not non-social, stimuli. Further, Oxtr deletion in aDG and aCA2/CA3$_{distal}$ did not affect object behaviors or social interaction suggesting a specific role for Oxtrs in fine discrimination of social stimuli, consistent with phenotype of mice lacking Oxtrs in the forebrain[34]. Our findings are consistent with a general role of the aDG-CA3 circuit of the hippocampus in resolving interference between similar memories[37,61,63,64]. The lack of an effect of Oxtr deletion in aDG-CA2/CA3 in object recognition suggests that the same aDG-CA2/CA3 memory circuit scaffold has been co-opted by an ancient evolutionarily conserved neuromodulatory system, OT-Oxtr, to permit encoding when OT is released (such as during encounter of social stimuli)[13].

Recent studies have suggested that CA2 links social information with space or contextual information[21]. However, whether CA3 exhibits population-based coding in response to similar social stimuli or whether Oxtr engages such population-based coding mechanisms to promote social discrimination is not known. Using catFISH based ensemble imaging we found that the CA3$_{proximal}$, but not CA3$_{distal}$, subregion exhibits population-based coding when mice encountered similar, but not the same, social stimuli. The lack of population-based coding in CA3$_{distal}$ may be explained by changes in firing rate that are not detectable with catFISH. Caveats notwithstanding, these findings are consistent with growing evidence that under conditions of high input similarity (as is the case here with mice of the same genetic background) CA3$_{proximal}$, but not CA3$_{distal}$, performs population-based coding[45,46,49]. Preferential removal of Oxtrs of aCA2/CA3 pyramidal neurons impaired population based coding in CA3$_{proximal}$, suggesting that OT recruits basic circuit mechanisms normally used by CA3$_{proximal}$ to support orthogonalization of similar inputs into divergent outputs (pattern separation) to minimize overlap between social stimuli. These findings are

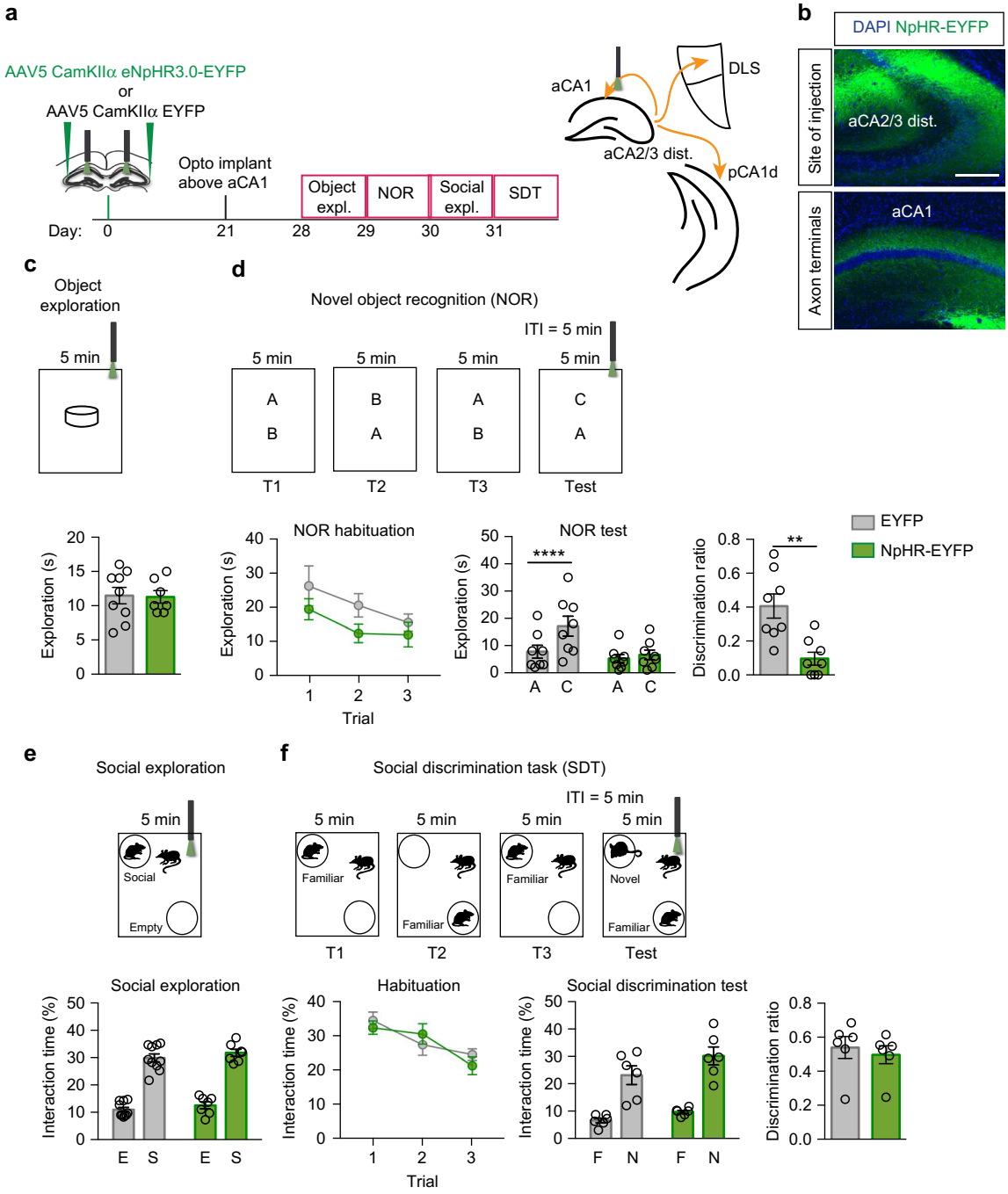


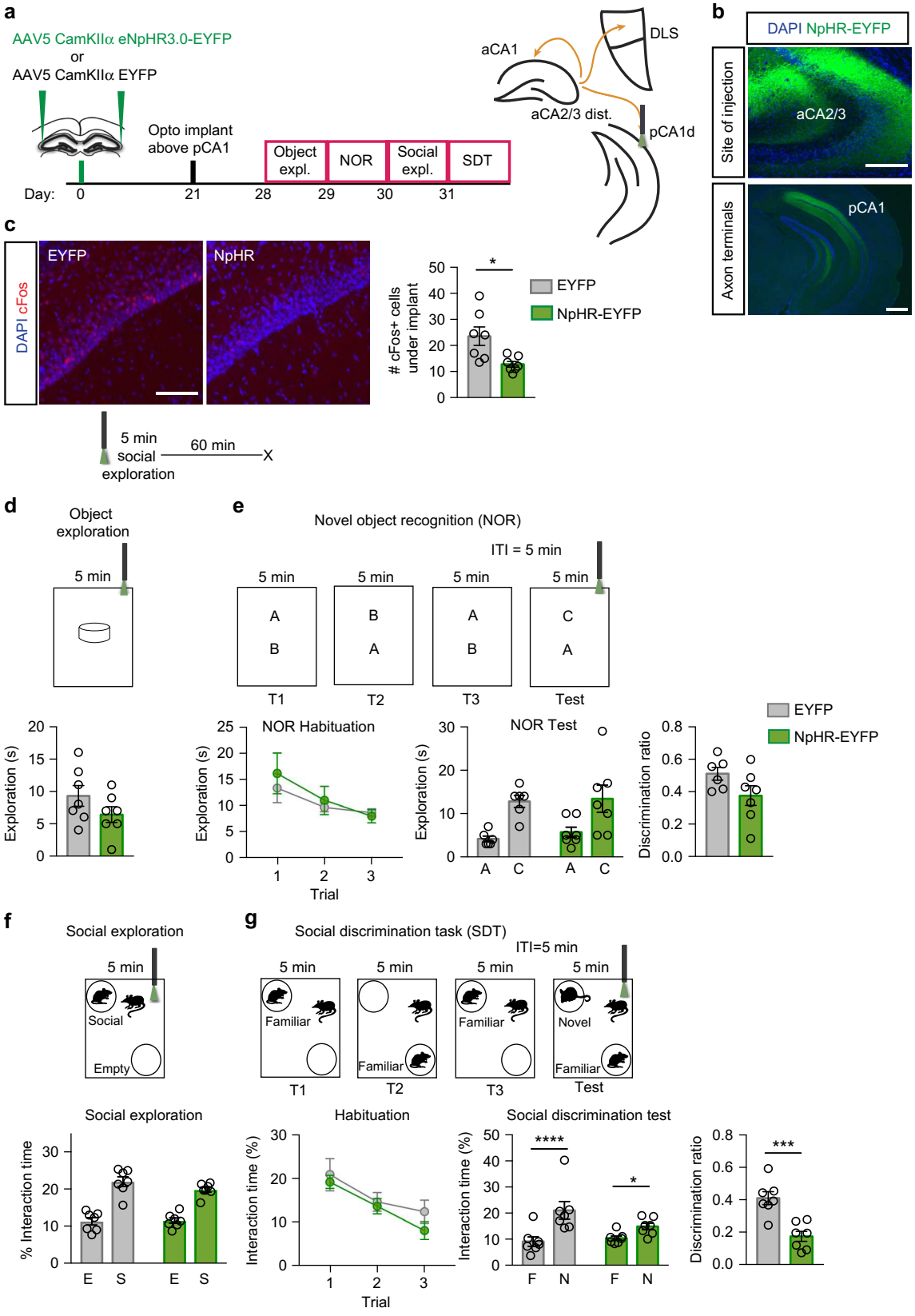
Fig. 5 Optogenetic attenuation of aCA2/CA3$_{distal}$ outputs to aCA1 impairs discrimination of object, but not social stimuli. **a** Schematic illustrating viral injection, optogenetic implants and behavioral testing timeline. **b** Representative images of site of injection of eNpHR3.0 virus in aCA2/CA3$_{distal}$ cell bodies (top) and corresponding axon terminals in aCA1 (bottom). Scale bar, 200 µm. **c** Behavioral schematic (top) and quantification (bottom) of single object exploration (EYFP: $n = 9$, NpHR: $n = 7$). **d** Behavioral schematic (top) and quantification (bottom) of novel objection recognition (EYFP: $n = 8$, NpHR: $n = 8$). Quantifications are displayed as Habituation (trials 1-3), Test (trial 4), and discrimination ratio (trial 4). Laser was on during trial 4 only. **e** Behavioral schematic (top) and quantification (bottom) of social exploration test (EYFP: $n = 10$, NpHR: $n = 7$). **f** Behavioral schematic (top) and quantification (bottom) of social discrimination task (EYFP: $n = 6$, NpHR: $n = 6$). Quantifications are displayed as Habituation (trials 1-3), Test (trial 4), and discrimination ratio (trial 4). Laser was on during trial 4 only. All data are displayed as mean ± SEM

consistent with previous reports that identify functional heterogeneity among CA3 subregions, with CA3$_{proximal}$ behaving as a pattern separator, much similar to the DG, and CA3$_{distal}$, strongly influenced by its auto-associative networks, functioning as a pattern completion network[45,46,49,65]. However, that we see a disruption in population based coding in CA3$_{proximal}$, despite low Oxtr expression in this region, suggests a role for local microcircuits within CA3 that communicate social information mediated by OT signaling in aCA2/CA3$_{distal}$ to pattern separation networks in CA3$_{proximal}$.

Oxtrs in the auditory and piriform cortices and hippocampus have been shown to enhance signal-to-noise processing through the modulation of excitatory and inhibitory neurons[15,52,53,66]. Interestingly, we observed increased activation of the DG

following recombination of Oxtr in the hilus, suggestive of decreased sparseness, and reminiscent of potentiated social stimulus-induced DG activation in mice lacking OT[67]. Clarification of the functions of Oxtr in aCA2 or aCA3 excitatory neurons and within distinct GABAergic populations (SST, PV, and other subtypes) and non-GABAergic (presumably mossy cells) cells in the hilus will further edify the contributions of Oxtrs to DG-CA2/CA3 circuit properties.

Our optogenetic terminal-specific attenuation studies revealed a critical role for aCA2/CA3 outputs to pCA1, but not aCA1, for



discrimination of social stimuli. The modest levels of discrimination of social stimuli that were persistent following optogenetic attenuation of aCA2/CA3 projections to pCA1 may reflect insufficient illumination of the large termination zone in pCA1d, incomplete silencing, and/or lack of targeting just the Oxtr-expressing neurons in aCA2/3. Nevertheless, these results are consistent with a recent study implicating the pCA1-NAcc pathway in mediating discrimination of social stimuli. Whether this pathway or other pCA1 projections to prefrontal cortex, hypothalamus, or amygdala relay Oxtr-dependent computations underlying social recognition in anterior hippocampus to guide social behavior remains to be determined. Our findings that aCA2/CA3 projections to aCA1 mediate discrimination of non-social, but not social, stimuli are consistent with the role of aCA1 in object recognition[27,28]. Thus, social and non-social information maybe differentially routed out of aCA2/CA3 to aCA1 or pCA1. Differential routing may be dependent on engagement of OT signaling in microcircuits in aCA2/CA3 or differences in projection patterns of Oxtr-expressing aCA2/CA3 neurons to aCA1 and pCA1.

In summary, our studies begin to illuminate the circuit mechanisms and neural pathways by which hippocampal Oxtrs contribute to social recognition. Oxtrs appear to recruit basic circuit mechanisms supporting pattern separation such as population based coding to minimize interference between similar social memories. These cognitive computations are relayed from the anterior to posterior hippocampus via an aCA2/CA3-pCA1 pathway to guide social behavior. Thus, disruptions in DG-CA2/CA3 circuitry may contribute to social memory impairments seen in autism and other psychiatric disorders[1–3,68–70].

Methods

Mouse lines and animal care. Two strains of mice were used in these experiments. Multiplex FISH and optogenetic terminal-specific silencing experiments were carried out in C57Bl/6J mice. Oxtr conditional knockout mice ($Oxtr^{f/f}$) rederived at Jackson Labs were utilized for viral-mediated recombination of Oxtrs[35](Jackson Laboratories stock 008471). All experiments were carried out in adult male mice (8 weeks old). All mice were housed three to five per cage in standard laboratory conditions under a 12 h light–dark cycle (0700–1700 h) with ad libitum access to food and water. Behavioral testing occurred during the light cycle. All experiments were carried out in accordance with procedures approved by the Institutional Animal Care and Use Committee at the Massachusetts General Hospital in accordance with NIH guidelines.

Multiplex fluorescence in situ hybridization. FISH was carried out using ACDBio RNAscope multiplex fluorescence assay. Probes were obtained as following: C1: *PV* (Mm-Pvalb: 421931), *Cre* (CRE: 312281), C2: *Oxtr* (Mm-Oxtr-C2: 402651-C2), C3: *Gad1* (Mm-Gad1-C3: 400951-C3), and *SST* (Mm-Sst-C3: 404631-C3). Brain tissue was obtained from age-matched 8-10 week-old male and female C57BL/6J mice and immediately fresh-frozen in optimal cutting temperature (OCT) medium on dry ice. For the assessment of Oxtr knockout, $Oxtr^{+/+}$ and $Oxtr^{f/f}$ mice were injected in aDG or aCA2/CA3 with AAV-CRE (AAV-hSyn Cre-GFP, diluted 1 : 100, 0.3 µl bilaterally, in aDG and AAV_9-CamKII-Cre-GFP 1 : 5 dilution, 0.3 µl bilaterally in aCA2.3). Twenty-micrometer sections were obtained using a cryostat (Leica, Germany) and stored at − 80 °C. Before RNAscope protocol, sections were incubated at − 20 °C for 1 h. RNAscope protocol was followed as indicated in user manual with adjustments as mentioned here. Briefly, sections were fixed with 4% chilled paraformaldehyde (PFA) for 30 or 60 min and rinsed in 1 × phosphate-buffered saline (PBS) for 5 min. Sections were then dehydrated in four 5 min dehydration steps in 50%, 75%, 100%, and 100% ethanol, respectively. Tissue was digested with Protease III for 30 min at room temperature and rinsed in 1 × PBS. *Oxtr* and *Gad1* probes were diluted 1 : 50 in probe diluent and pipetted onto each slide. *Oxtr* and *SST* probes were diluted 1 : 50 in *PV* C1 probe and pipetted onto each slide. For assessment of OxtR knockout, *Oxtr* probe was diluted 1 : 50 in *Cre* C1 probe. Probe hybridization took place for 2 h at 40 °C and slides were then rinsed in 1 × wash buffer. Sections were then incubated at 40 °C in Amp1 for 30 min, Amp 2 for 15 min, Amp3 for 30 min, and Amp4 for 15 min, with 1 × Wash Buffer rinses between each incubation. Sections were finally mounted with DAPI (4',6-diamidino-2-phenylindole) Fluoromount and stored at − 20 °C.

Adeno-associated viruses (AAV). AAV_5-CaMKIIα-eYFP (6×10^{12} particles per mL) and AAV_5-CaMKIIα-eNpHR3.0-eYFP (3×10^{12} particles per mL) viruses were generated by and obtained from the University of North Carolina Vector Core (Chapel Hill, NC). AAV_9-CamKIIα-Cre-GFP (1.07×10^{13} particles per mL), AAV_9-CamKIIα-GFP (6.27×10^{13} particles per mL) and AAV_9-hSyn-Cre-GFP (11.7×10^{13} particles per mL) were generated by and obtained from the University of Pennsylvania Vector Core (Philadelphia, Pennsylvania).

Stereotactic surgery. Viral injections: adult mice (8 weeks old) were maintained under standard housing conditions. Mice were given carprofen (5 mg kg^{-1} subcutaneously) before surgery and 24 h later to minimize discomfort. Mice were anesthetized with ketamine and xylazine (10 and 1.6 mg mL^{-1}, intraperitoneally (i.p.)) and placed in a stereotaxic frame (Stoelting). Small holes were drilled at each injection location and injected with a Hamilton microsyringe at a rate of 0.1 µl min^{-1}. For aDG KO experiment, 0.2 µl 1 : 1,000 AAV9-hSyn-Cre-GFP or 1 : 50 AAV9-CamKIIα-GFP was injected bilaterally (AP − 1.9 mm, ML ± 1.1 mm, DV − 2.6 mm from Bregma) into *Oxtr f/f* mice. For $aCA2/CA3_{distal}$KO experiments, 0.3 µl 1:50 AAV9-CamKIIα-Cre-GFP or 1 : 50 AAV9-CamKIIα-GFP was injected bilaterally (AP − 1.9 mm, ML ± 2.55 mm, DV − 2.3 mm from Bregma) into *Oxtr f/f* mice. For optogenetic silencing experiments, 0.3 µl undiluted AAV5-CaMKIIα-eNpHR3.0-eYFP or AAV5-CaMKIIα-eYFP was injected bilaterally into $aCA2/CA3_{distal}$. After completion of the injection, the needle was left on the site of injection for 5 min, raised 0.2 mm, and left on the site for an additional 5 min, to allow diffusion of virus at the injection site and then slowly withdrawn. The skin incision was closed carefully using nylon sutures. Animals were monitored during recovery.

Optogenetic implants: mice were surgically implanted with fiber optic cannulas 3–4 weeks following injection of AAV5-CaMKIIα-eYFP or AAV5-CaMKIIα-eNpHR3.0-eYFP and behavioral experiments started 1 week after surgery. Mice were implanted bilaterally with chronically dwelling optical fibers targeted to the anterior CA1 (AP − 1.9 mm, ML ± 1.5 mm, DV − 1.2 mm from Bregma), pCA1 (AP − 3.35 mm, ML ± 3.1 mm, DV − 1.7 mm from Bregma), or DLS (AP + 1.15 mm, ML ± 1.0 mm angle ± 10°, DV − 2.5 mm from Bregma). Optical fibers were secured with one cranial screw and dental cement. After surgery, mice were returned to their home cage and monitored until recovery from surgery.

Construction of optical fibers. Two hundred micrometer core, 0.37 numerical aperture multimode fiber (ThorLabs) was threaded through and glued with epoxy to a 230 µm core stainless steel or zirconia multimode ferrule (Fiber Instrument Sales and Precision Fiber Products), polished, and cut for implantation. Optical patch cables were generated the same way, with the free end connected to a multimode FC ferrule assembly for connecting to a 1 × 2 Optical rotary joint (Doric lenses). The other end of the rotary joint was connected via a patch cable to a 561 nm laser diode (OEM laser systems) via a non-contact style laser to fiber coupler (OZ optics).

In vivo laser delivery. Age-matched, genotyped-matched male mice (3–4 months old) were used for all behavioral experiments. Mice were kept in a quiet room for at least 1 h before testing. Behavioral tests took place under bright lighting conditions (700 lux) and performed in the following order: single object exploration (day 1), novel object recognition (day 2), social exploration (day 3), and social discrimination (day 4). Before each experiment, mice were bilaterally attached to the patch cables via a zirconia sleeve and allowed to recover for 2–3 min in a transition

Fig. 6 Optogenetic attenuation of $aCA2/CA3_{distal}$ outputs to pCA1 impairs discrimination of social, but not non-social, stimuli. **a** Schematic illustrating viral injection, optogenetic implants and behavioral testing timeline. **b** Representative images of site of injection of eNpHR3.0 virus in $aCA2/CA3_{distal}$ cell bodies (top) and corresponding axon terminals in pCA1 (bottom). Scale bars, 200 µm (top) and 500 µm (bottom). **c** Representative images and quantifications of cFos immunoreactivity in pyramidal layer of pCA1 during optogenetic silencing (EYFP: $n = 7$, NpHR: $n = 7$). Scale bar, 100 µm. **d** Behavioral schematic (top) and quantification (bottom) of single object exploration (EYFP: $n = 7$, NpHR: $n = 7$). **e** Behavioral schematic (top) and quantification (bottom) of novel objection recognition (EYFP: $n = 6$, NpHR: $n = 7$). Quantifications are displayed as Habituation (trials 1-3), Test (trial 4), and discrimination ratio (trial 4). Laser was on during trial 4 only. **f** Behavioral schematic (top) and quantification (bottom) of social exploration test (EYFP: $n = 6$, NpHR: $n = 7$). **g** Behavioral schematic (top) and quantification (bottom) of social discrimination task (EYFP: $n = 6$, NpHR: $n = 7$). Quantifications are displayed as Habituation (trials 1-3), Test (trial 4), and discrimination ratio (trial 4). Laser was on during trial 4 only. All data are displayed as mean ± SEM

cage similar to their home cage. The patch cables were interfaced to an FC/PC rotary joint (Doric lenses), which was attached on the other end to a laser diode (561 nm). The light power at the end of the fiber tip was 10–15 mW. At the end of each behavioral experiment (5–7 weeks following viral surgery), mice were analyzed for viral and fiber optics placement and mis-targeted animals were excluded from the analysis. In aCA2/CA3-CA1 attenuation experiment, animal numbers varied across behavioral tasks because of loss of optogenetic implants during course of testing and two behavioral cohorts were utilized, with the second cohort being used for a context-updating task instead of social discrimination after social exploration. Randomly selected videos were scored by two different investigators.

Single object exploration. Mice were placed an arena filled with bedding (45 cm long, 15 cm high and 30 cm wide) with a single novel object for 5 min. Sessions were video-recorded and videos were manually scored for object exploration (when an animal's snout was 2 cm or less from the object) by an investigator blind to animal treatment identity. For optogenetic experiments, light of 561 nm was turned on for the full duration of the session.

Novel object recognition. Mice were placed in an arena filled with bedding (45 cm long, 15 cm high and 30 cm wide) with two distinct objects (A and B) for three 5 min sessions, with a 5 min intertrial interval. Mice habituated to the objects during the three training sessions and one of the objects was subsequently replaced with a novel object (C) in session four. Objects were counterbalanced across subjects and object positions were counterbalanced across trials. The objects that were selected for testing elicited comparable levels of exploration based on exploration levels in pilot experiments. Sessions were video-recorded and videos were manually scored for object exploration (when an animal's snout was 2 cm or less from the object) by an investigator blind to object identity and animal treatment identity. For optogenetic experiments, light of 561 nm was turned on only during trial 4.

Social exploration. Mice were placed in an open plexiglass arena (41 cm × 41 cm, Kinder Scientific) for 5 min with two pencil-wire cups placed on opposing corners of the arena. Habituation to the chamber took place one day before the start of behavioral testing. One cup remained empty, whereas the other contained a novel adult male C57Bl/6J mouse. Sessions were video-recorded and videos were manually scored for exploration of the social cup and empty cup (direct snout-to-cup contact, with at least two paws on the ground—time spent climbing on the cup was not included) by an investigator blind to animal treatment identity. Stimulus mice were trained to sit in pencil-wire cups for three 15 min sessions several days before behavioral testing. For optogenetic experiments, light of 561 nm was turned on for the full duration of the session.

Social recognition (habituation and discrimination). The same plexiglass arena and pencil-wire cup set-up as described for social exploration was used. Mice were placed in the arena for three 5 min sessions with an empty cup and a novel adult male C57Bl/6J mouse, with a 5 min intertrial interval. Mice habituated to the stimulus during the first three sessions, rendering it "familiar." During trial 4, a novel adult male mouse was placed in the opposing cup and subjects were tested for discrimination between the novel and familiar mouse. Social stimuli were counterbalanced across subjects and the position of the familiar social stimulus was counterbalanced across trials. Sessions were video-recorded and videos were manually scored for interaction with the novel vs familiar mouse (direct snout-to-cup contact, with at least two paws on the ground—time spent climbing on the cup was not included) by an investigator blind to animal treatment identity. Stimulus mice were trained to sit in pencil-wire cups for three 15 min sessions several days before behavioral testing. For optogenetic experiments, light of 561 nm was turned on only during trial 4. Videos were scored by two different investigators.

aDG genetic deletion cohorts. For Fig. 2 and the corresponding Supplementary Fig. 3, number of animals is variable across behaviors, because two different cohorts were used. The first cohort ($n = 7$, 4) was used for all behaviors and cFos analysis. The second cohort ($n = 4$, 2) was used to increase the N for the four behaviors in the main Figure, but was not used for anxiety (OFT and EPM) or cFos analysis.

catFISH assay. The catFISH assay was performed as previously described[47]. Briefly, adult male *Oxtr f/f* mice received bilateral stereotactic injections of AAV9-CamKIIα-Cre-GFP diluted at 1 : 50 into aCA2/CA3$_{distal}$ 10 days before behavior, as described above. Animals experienced two 5 min behavioral episodes 25 min apart and brains were isolated and flash frozen in isopentane on dry ice immediately after the second episode. An intronic *c-fos* probe containing the entire first intron of the Fos gene[54] (generous gift of Dr. Dayu Lin) and a full-length *c-fos* cRNA probe were used to detect nuclear and cytoplasmic c-fos transcripts, respectively. Nuclear c-fos was defined as puncta colocalizing with DAPI labeling, whereas cytoplasmic labeling was defined as c-fos-positive labeling surrounding the nucleus. CA3$_{proximal}$ comprised an region of interest (ROI) with a volume of 788,546 cubic micrometers per section and contained on average 521.67 DAPI$^+$ cells ($n = 3$). CA3distal comprised an ROI with a volume of 1,216,503 cubic micrometers per section and contained an average of 554.67 DAPI$^+$ cells ($n = 3$). CA2 was not quantified due to too few cFos$^+$ foci for analysis (on average two cFos$^+$ cells per section). Representative images of each condition are included in.

Histology and immunohistochemistry. Mice were anesthetized with ketamine (100 mg kg^{-1} i.p.) and xylazine (3 mg kg^{-1} i.p.), and transcardially perfused with 10 mM PBS, pH 7.5 at 4 °C, followed by a fixative solution containing 4% PFA in PBS. Brains were post-fixed in 4% PFA overnight at 4 °C and cryo-protected for 72 h in 30% sucrose at 4 °C before freezing in OCT on dry ice. Coronal sections were obtained at 35 µm using a cryostat (Leica, Germany) in six matched sets. Sections were stored in 1 × PBS with 0.01% Azide at 4 °C. Floating sections were used to perform immunohistochemical labeling. Briefly, sections were washed in 1 × PBS, incubated for 15 min at room temperature in 1 × PBS containing 0.3% Triton X-100, blocked in 1 × PBS containing 0.3% Triton X-100 and 10% Normal donkey serum for 1 h at room temperature, and incubated in primary antibodies in blocking buffer with shaking overnight at 4 °C. Primary antibodies were used as follows: GFP (rabbit anti-GFP, Life Technologies A11122, 1 : 500, Antibodyregistry.org: AB_221569); goat anti-GFP, Novus Biologicals, NB100-1770, 1 : 500, (Antibodyregistry.org: AB_10128178), cFos (Rabbit, Santa Cruz, 1 : 2,000, Santa Cruz SC52, Antibodyregistry.org: AB_2106783), RGS14 (Mouse, UC Davis/NIH NeuroMab, 1 : 400). The following day, sections were washed three times in 1 × PBS and incubated with fluorescent-label-coupled secondary antibodies (Jackson Immunoresearch, Donkey anti-Rabbit, Goat, or Mouse, 488-, Cy3-, or Cy5-coupled, 1 : 500) for 2 h at room temperature.

cFos and perfusion. Mice were exposed to a novel social stimulus in a novel arena filled with bedding for 5 min and promptly returned to home cage. Mice were then anesthetized with ketamine (100 mg kg^{-1} i.p.) and xylazine (3 mg kg^{-1} i.p.), and transcardially perfused 60 min post exposure, as described above in "Histology and immunohistochemistry." For optogenetic silencing cFos experiments, mice were given 3–5 min to acclimate after being bilaterally attached to a laser patch cord, before the laser was turned on and social exposure began.

Image acquisition and analysis. For RNAscope multiplex FISH: × 20, × 40, or × 60 confocal z-stack images were obtained with a Nikon A1R Si confocal laser. Images were acquired at 1,024 resolution as 10 µm z-stacks with a step size of 2 µm. For colocalization analysis, cells were manually identified as *Oxtr*$^+$, *Gad1*$^+$, *SST*$^+$, and/or *PV*$^+$ or double positive, and expressed as a percentage of *Oxtr*$^+$ cells (for DG) or as a percentage of *SST*$^+$, or *PV*$^+$ cells (for CA2/CA3). For *Oxtr* knockdown analysis, all DAPI nuclei per image were counted (for DG injections: cells in the hilus, excluding granule cell layer and CA3, were counted, whereas for CA2/CA3 injections cells in the CA2/CA3 principal cell layer were counted), and cells were manually identified as *Oxtr*$^+$, *Cre*$^+$, and/or *OxtR*$^+$*CRE*$^+$ double positive. The *Oxtr*$^+$ population was expressed as a percentage of total DAPI cells. For *Oxtr* mean intensity calculated for CA regions, mean intensity was measured for the region comprised by the principal layer. A similar sized region from background area was measured for intensity and subtracted from mean *Oxtr* intensity, in order to control for differences in background.

For cFos analysis: × 10 bilateral images were acquired using a Nikon epifluorescence microscope. cFos+ cells were manually quantified as those with intensity higher than background in the aDG granule cell layer, pCA1 pyramidal cell layer directly under the implant, and DLS. For aDG, both blades were assessed. Data were expressed as # cFos+ cells per section. All quantifications and analyses were completed by an experimenter blind to treatment condition.

For catFISH: confocal z-stack images using a × 60 oil objective (1.0 µm step size) were acquired along the aCA2/CA3 pyramidal layer using a Nikon A1R Si confocal laser, a TiE inverted research microscope, and NIS Elements software. Image analysis was performed with NIS Elements software. Four to eight hemisections were scanned per mouse. Images were manually counted for c-fos transcript labeling. Data are presented as cells/section. Quantifications were performed by an investigator blind to treatment condition and two different investigators. Details of OFT, EPM, and pharmacological blockade of Oxtrs can be found in Supplementary Note 1.

Statistics. Statistical analysis was carried out using GraphPad Prism v7 software. Data (mean ± SEM) were analyzed using paired or unpaired two-tailed Student's t-test, to compare two groups. Behavioral data were analyzed using mixed factor two-way ANOVA with repeated measure followed by Bonferroni's multiple comparisons test when the interaction, p-value was < 0.05. Detailed statistical analyses can be found in Supplementary Table 1. In all cases, significance was set at $p < 0.05$.

Data availability. All relevant data are available from the authors.

Received: 9 May 2017 Accepted: 10 November 2017
Published online: 08 December 2017

References

1. Kennedy, D. P. & Adolphs, R. The social brain in psychiatric and neurological disorders. *Trends Cogn. Sci.* **16**, 559–572 (2012).
2. Allsop, S. A., Vander Weele, C. M., Wichmann, R. & Tye, K. M. Optogenetic insights on the relationship between anxiety-related behaviors and social deficits. *Front Behav. Neurosci.* **8**, 241 (2014).
3. Pasciuto, E. et al. Autism spectrum disorders: translating human deficits into mouse behavior. *Neurobiol. Learn. Mem.* **124**, 71–87 (2015).
4. Donaldson, Z. R. & Young, L. J. Oxytocin, vasopressin, and the neurogenetics of sociality. *Science* **322**, 900–904 (2008).
5. Lee, H. J., Macbeth, A. H., Pagani, J. H. & Young, W. S. 3rd Oxytocin: the great facilitator of life. *Prog. Neurobiol.* **88**, 127–151 (2009).
6. Stoop, R. Neuromodulation by oxytocin and vasopressin. *Neuron* **76**, 142–159 (2012).
7. Meyer-Lindenberg, A., Domes, G., Kirsch, P. & Heinrichs, M. Oxytocin and vasopressin in the human brain: social neuropeptides for translational medicine. *Nat. Rev. Neurosci.* **12**, 524–538 (2011).
8. Dumais, K. M. & Veenema, A. H. Vasopressin and oxytocin receptor systems in the brain: sex differences and sex-specific regulation of social behavior. *Front. Neuroendocrinol.*, https://doi.org/10.1016/j.yfrne.2015.04.003 (2015).
9. Lee, H. J., Caldwell, H. K., Macbeth, A. H. & Young, W. S. 3rd Behavioural studies using temporal and spatial inactivation of the oxytocin receptor. *Prog. Brain Res.* **170**, 73–77 (2008).
10. Dolen, G., Darvishzadeh, A., Huang, K. W. & Malenka, R. C. Social reward requires coordinated activity of nucleus accumbens oxytocin and serotonin. *Nature* **501**, 179–184 (2013).
11. Guzman, Y. F. et al. Fear-enhancing effects of septal oxytocin receptors. *Nat. Neurosci.* **16**, 1185–1187 (2013).
12. Guzman, Y. F. et al. Role of oxytocin receptors in modulation of fear by social memory. *Psychopharmacol. (Berl.).* **231**, 2097–2105 (2014).
13. Lukas, M., Toth, I., Veenema, A. H. & Neumann, I. D. Oxytocin mediates rodent social memory within the lateral septum and the medial amygdala depending on the relevance of the social stimulus: male juvenile vs. female adult conspecifics. *Psychoneuroendocrinology* **38**, 916–926 (2013).
14. Mesic, I. et al. Double dissociation of the roles of metabotropic glutamate receptor 5 and oxytocin receptor in discrete social behaviors. *Neuropsychopharmacology* **40**, 2337–2346 (2015).
15. Choe, H. K. et al. Oxytocin mediates entrainment of sensory stimuli to social cues of opposing valence. *Neuron* **87**, 152–163 (2015).
16. Nakajima, M., Gorlich, A. & Heintz, N. Oxytocin modulates female sociosexual behavior through a specific class of prefrontal cortical interneurons. *Cell* **159**, 295–305 (2014).
17. Xiao, L., Priest, M. F., Nasenbeny, J., Lu, T. & Kozorovitskiy, Y. Biased oxytocinergic modulation of midbrain dopamine systems. *Neuron* **95**, 368–384 e365 (2017).
18. Kogan, J. H., Frankland, P. W. & Silva, A. J. Long-term memory underlying hippocampus-dependent social recognition in mice. *Hippocampus* **10**, 47–56 (2000).
19. Finlay, J. M. et al. Effects of prefrontal cortex and hippocampal NMDA NR1-subunit deletion on complex cognitive and social behaviors. *Brain. Res.* **1600**, 70–83 (2015).
20. Felix-Ortiz, A. C. & Tye, K. M. Amygdala inputs to the ventral hippocampus bidirectionally modulate social behavior. *J. Neurosci.* **34**, 586–595 (2014).
21. Alexander, G. M. et al. Social and novel contexts modify hippocampal CA2 representations of space. *Nat. Commun.* **7**, 10300 (2016).
22. Stevenson, E. L. & Caldwell, H. K. Lesions to the CA2 region of the hippocampus impair social memory in mice. *Eur. J. Neurosci.* **40**, 3294–3301 (2014).
23. Hitti, F. L. & Siegelbaum, S. A. The hippocampal CA2 region is essential for social memory. *Nature* **508**, 88–92 (2014).
24. Smith, A. S., Williams Avram, S. K., Cymerblit-Sabba, A., Song, J. & Young, W. S. Targeted activation of the hippocampal CA2 area strongly enhances social memory. *Mol. Psychiatry*, https://doi.org/10.1038/mp.2015.189 (2016).
25. Okuyama, T., Kitamura, T., Roy, D. S., Itohara, S. & Tonegawa, S. Ventral CA1 neurons store social memory. *Science* **353**, 1536–1541 (2016).
26. Sheehan, T. P., Chambers, R. A. & Russell, D. S. Regulation of affect by the lateral septum: implications for neuropsychiatry. *Brain Res. Brain Res. Rev.* **46**, 71–117 (2004).
27. Cohen, S. J. & Stackman, R. W. Jr. Assessing rodent hippocampal involvement in the novel object recognition task. A review. *Behav. Brain. Res.* **285**, 105–117 (2015).
28. Stackman, R. W. Jr., Cohen, S. J., Lora, J. C. & Rios, L. M. Temporary inactivation reveals that the CA1 region of the mouse dorsal hippocampus plays an equivalent role in the retrieval of long-term object memory and spatial memory. *Neurobiol. Learn. Mem.* **133**, 118–128 (2016).
29. Hammock, E. A. & Levitt, P. Oxytocin receptor ligand binding in embryonic tissue and postnatal brain development of the C57BL/6J mouse. *Front. Behav. Neurosci.* **7**, 195 (2013).
30. Hidema, S. et al. Generation of Oxtr cDNA -Ires-Cre mice for gene expression in an oxytocin receptor specific manner. *J. Cell. Biochemi.*, https://doi.org/10.1002/jcb.25393 (2015).
31. Yoshida, M. et al. Evidence that oxytocin exerts anxiolytic effects via oxytocin receptor expressed in serotonergic neurons in mice. *J. Neurosci.* **29**, 2259–2271 (2009).
32. Mitre, M. et al. A distributed network for social cognition enriched for oxytocin receptors. *J. Neurosci.* **36**, 2517–2535 (2016).
33. van Wimersma Greidanus, T. B. & Maigret, C. The role of limbic vasopressin and oxytocin in social recognition. *Brain Res.* **713**, 153–159 (1996).
34. Macbeth, A. H., Lee, H. J., Edds, J. & Young, W. S. 3rd Oxytocin and the oxytocin receptor underlie intrastrain, but not interstrain, social recognition. *Genes. Brain. Behav.* **8**, 558–567 (2009).
35. Lee, H. J., Caldwell, H. K., Macbeth, A. H., Tolu, S. G. & Young, W. S. 3rd A conditional knockout mouse line of the oxytocin receptor. *Endocrinology* **149**, 3256–3263 (2008).
36. McHugh, T. J. et al. Dentate gyrus NMDA receptors mediate rapid pattern separation in the hippocampal network. *Science* **317**, 94–99 (2007).
37. Frankland, P. W., Cestari, V., Filipkowski, R. K., McDonald, R. J. & Silva, A. J. The dorsal hippocampus is essential for context discrimination but not for contextual conditioning. *Behav. Neurosci.* **112**, 863–874 (1998).
38. McNaughton, B. & Morris, R. Hippocampal synaptic enhancement and information storage within a distributed memory system. *Trends Neurosci.* **10**, 408–415 (1987).
39. O'Reilly, R. C. & McClelland, J. L. Hippocampal conjunctive encoding, storage, and recall: avoiding a trade-off. *Hippocampus* **4**, 661–682 (1994).
40. Gilbert, P. E., Kesner, R. P. & Lee, I. Dissociating hippocampal subregions: double dissociation between dentate gyrus and CA1. *Hippocampus* **11**, 626–636 (2001).
41. Rolls, E. T. & Kesner, R. P. A computational theory of hippocampal function, and empirical tests of the theory. *Prog. Neurobiol.* **79**, 1–48 (2006).
42. Bakker, A., Kirwan, C. B., Miller, M. & Stark, C. E. Pattern separation in the human hippocampal CA3 and dentate gyrus. *Science* **319**, 1640–1642 (2008).
43. Neunuebel, J. P. & Knierim, J. J. CA3 retrieves coherent representations from degraded input: direct evidence for CA3 pattern completion and dentate gyrus pattern separation. *Neuron* **81**, 416–427 (2014).
44. Deng, W., Mayford, M. & Gage, F. H. Selection of distinct populations of dentate granule cells in response to inputs as a mechanism for pattern separation in mice. *eLife* **2**, e00312 (2013).
45. GoodSmith, D. et al. Spatial representations of granule cells and mossy cells of the dentate gyrus. *Neuron* **93**, 677–690 e675 (2017).
46. Knierim, J. J. & Neunuebel, J. P. Tracking the flow of hippocampal computation: pattern separation, pattern completion, and attractor dynamics. *Neurobiol. Learn. Mem.* **129**, 38–49 (2016).
47. McAvoy, K. M. et al. Modulating neuronal competition dynamics in the dentate gyrus to rejuvenate aging memory circuits. *Neuron* **91**, 1356–1373 (2016).
48. Leutgeb, J. K., Leutgeb, S., Moser, M. B. & Moser, E. I. Pattern separation in the dentate gyrus and CA3 of the hippocampus. *Science* **315**, 961–966 (2007).
49. Lee, H., Wang, C., Deshmukh, S. S. & Knierim, J. J. Neural population evidence of functional heterogeneity along the CA3 transverse axis: pattern completion vs. pattern separation. *Neuron* **87**, 1093–1105 (2015).
50. Niibori, Y. et al. Suppression of adult neurogenesis impairs population coding of similar contexts in hippocampal CA3 region. *Nat. Commun.* **3**, 1253 (2012).
51. Colgin, L. L., Moser, E. I. & Moser, M. B. Understanding memory through hippocampal remapping. *Trends Neurosci.* **31**, 469–477 (2008).
52. Marlin, B. J., Mitre, M., D'Amour, J. A., Chao, M. V. & Froemke, R. C. Oxytocin enables maternal behaviour by balancing cortical inhibition. *Nature* **520**, 499–504 (2015).
53. Owen, S. F. et al. Oxytocin enhances hippocampal spike transmission by modulating fast-spiking interneurons. *Nature* **500**, 458–462 (2013).
54. Lin, D. et al. Functional identification of an aggression locus in the mouse hypothalamus. *Nature* **470**, 221–226 (2011).

55. Guzowski, J. F. & Worley, P. F. Cellular compartment analysis of temporal activity by fluorescence in situ hybridization (catFISH). *Curr. Protoc. Neurosci./editorial board, Jacqueline N. Crawley… [et al.]* **Chapter 1**, Unit 1 8, https://doi.org/10.1002/0471142301.ns0108s15 (2001).
56. Cearley, C. N. & Wolfe, J. H. A single injection of an adeno-associated virus vector into nuclei with divergent connections results in widespread vector distribution in the brain and global correction of a neurogenetic disease. *J. Neurosci.* **27**, 9928–9940 (2007).
57. Aschauer, D. F., Kreuz, S. & Rumpel, S. Analysis of transduction efficiency, tropism and axonal transport of AAV serotypes 1, 2, 5, 6, 8 and 9 in the mouse brain. *PLoS ONE* **8**, e76310 (2013).
58. Cook-Snyder, D. R., Jones, A. & Reijmers, L. G. A retrograde adeno-associated virus for collecting ribosome-bound mRNA from anatomically defined projection neurons. *Front. Mol. Neurosci.* **8**, 56 (2015).
59. Risold, P. Y. & Swanson, L. W. Structural evidence for functional domains in the rat hippocampus. *Science* **272**, 1484–1486 (1996).
60. Risold, P. Y. & Swanson, L. W. Connections of the rat lateral septal complex. *Brain Res. Brain Res. Rev.* **24**, 115–195 (1997).
61. Fanselow, M. S. & Dong, H. W. Are the dorsal and ventral hippocampus functionally distinct structures? *Neuron* **65**, 7–19 (2010).
62. Kohara, K. et al. Cell type-specific genetic and optogenetic tools reveal hippocampal CA2 circuits. *Nat. Neurosci.* **17**, 269–279 (2014).
63. Besnard, A. & Sahay, A. Adult hippocampal neurogenesis, fear generalization, and stress. *Neuropsychopharmacology* **41**, 24–44 (2016).
64. Yassa, M. A. & Stark, C. E. Pattern separation in the hippocampus. *Trends Neurosci.* **34**, 515–525 (2011).
65. Sun, Q. et al. Proximodistal heterogeneity of hippocampal CA3 pyramidal neuron intrinsic properties, connectivity, and reactivation during memory recall. *Neuron* **95**, 656–672 e653 (2017).
66. Ripamonti, S. et al. Transient oxytocin signaling primes the development and function of excitatory hippocampal neurons. *eLife* **6**, https://doi.org/10.7554/eLife.22466 (2017).
67. Ferguson, J. N., Aldag, J. M., Insel, T. R. & Young, L. J. Oxytocin in the medial amygdala is essential for social recognition in the mouse. *J. Neurosci.* **21**, 8278–8285 (2001).
68. Piskorowski, R. A. et al. Age-dependent specific changes in area CA2 of the hippocampus and social memory deficit in a mouse model of the 22q11.2 deletion syndrome. *Neuron* **89**, 163–176 (2016).
69. Jones, M. W. & McHugh, T. J. Updating hippocampal representations: CA2 joins the circuit. *Trends Neurosci.* **34**, 526–535 (2011).
70. Dudek, S. M., Alexander, G. M. & Farris, S. Rediscovering area CA2: unique properties and functions. *Nat. Rev. Neurosci.* **17**, 89–102 (2016).

Acknowledgements

We thank members of the Sahay lab for their comments on the manuscript. A.S. acknowledges support from US National Institutes of Health Biobehavioral Research Awards for Innovative New Scientists (BRAINS) 1-R01MH104175, NIH-NIA 1R01AG048908-01, NIH-NIMH 1R01MH111729-01, Ellison Medical Foundation New Scholar in Aging, Whitehall Foundation, Inscopix Decode award, NARSAD Independent Investigator Award, Ellison Family Philanthropic support, Blue Guitar Fund, Harvard NeurodiscoveryCenter/MADRC Center Pilot Grant Award, HSCI Development grant, and HSCI seed grant.

Author contributions

T.R., K.M.M., and A.B. carried out experiments and analyzed data. A.V. contributed reagents and shared resources. T.R. and A.S. co-developed the concept and wrote the manuscript. A.S. conceived and supervised all aspects of the project.

Additional information

Supplementary Information accompanies this paper at https://doi.org/10.1038/s41467-017-02173-0.

Competing interests: The authors declare no competing financial interests.

Reprints and permission information is available online at http://npg.nature.com/reprintsandpermissions/

Publisher's note: Springer Nature remains neutral with regard to jurisdictional claims in published maps and institutional affiliations.

Open Access This article is licensed under a Creative Commons Attribution 4.0 International License, which permits use, sharing, adaptation, distribution and reproduction in any medium or format, as long as you give appropriate credit to the original author(s) and the source, provide a link to the Creative Commons license, and indicate if changes were made. The images or other third party material in this article are included in the article's Creative Commonslicense, unless indicated otherwise in a credit line to the material. If material is not included in the article'sCreative Commons license and your intended use is not permitted by statutory regulation or exceeds the permitted use, you will need to obtain permission directly from the copyright holder. To view a copy of this license, visit http://creativecommons.org/licenses/by/4.0/.

© The Author(s) 2017